PERFORMANCE MODELING AND RISK ANALYSIS

OF TRANSIT VESSEL TRAFFIC IN THE ISTANBUL STRAIT: STUDIES ON

QUEUES WITH MULTIPLE TYPES OF INTERRUPTIONS*

by

ÖZGECAN S. ULUSÇU TÜTÜN

A Dissertation submitted to the

Graduate School-New Brunswick

Rutgers, The State University of New Jersey

in partial fulfillment of the requirements

for the degree of

Doctor of Philosophy

Graduate Program in Industrial and Systems Engineering

written under the direction of

Professor Tayfur Altıok

and approved by

____

____

____

____

New Brunswick, New Jersey

May, 2008

* This work is in part funded by the Laboratory for Port Security at Rutgers University, NSF Grant Number INT-0423262, and TUBITAK, The Scientific and Technological Research Council of Turkey.

ABSTRACT OF THE DISSERTATION

Performance Modeling and Risk Analysis of Transit Vessel Traffic in the Istanbul Strait: Studies on Queues with Multiple Types of Interruptions

By ÖZGECAN S. ULUSÇU TÜTÜN

Dissertation Director:
Professor Tayfur Altıok

The Istanbul Strait, the narrow waterway separating Europe from Asia, holds a strategic importance in maritime transportation as it links the Black Sea to the Mediterranean. It is considered one of the world's most dangerous waterways to navigate. Over 50,000 transit vessels pass through the Strait annually, 20% of which carry dangerous cargo.

In this research, we have developed a mathematical risk analysis model to analyze the risks involved in the transit vessel traffic system in the Istanbul Strait. In the first step of the risk analysis, the transit vessel traffic system is analyzed and a simulation model is developed to mimic and study the system behavior. In addition to vessel traffic and geographical conditions, the current vessel scheduling practices are modeled using a scheduling algorithm. This algorithm is developed through discussions with the Turkish Straits Vessel Traffic Services (VTS) to mimic their decisions on sequencing vessel entrances as well as coordinating vessel traffic in both directions. Furthermore, a

scenario analysis is performed to evaluate the impact of several parameters on the system performance.

Risk analysis is performed by incorporating a probabilistic accident risk model into the simulation model. A mathematical model is developed based on probabilistic arguments and historical data and subject matter expert opinions. We have also performed a scenario analysis to evaluate the characteristics of the accident risk. This analysis allows us to investigate how various factors impact risk. These factors include vessel arrivals, scheduling policies, pilotage, overtaking, and local traffic density. Policy indications are made based on results.

Finally, complexity of the operations at the Strait has motivated us to model congestion at the waterway entrances through queueing analysis. We have developed queueing models subject to various operation-independent interruptions. We have used waiting time arguments and service completion time analysis to approximate the expected waiting time of a vessel in the aforementioned queue for various cases of service interruptions. These cases include the single-class models with non-simultaneous and possibly simultaneous interruptions, the multi-class priority queueing model with k possibly simultaneous class-independent interruptions, and the two-class priority queueing model with k possibly simultaneous class-dependent interruptions.

PREFACE

There are many parties involved in the Istanbul Strait transit vessel traffic including Turkey, the IMO, Russia and other Caspian countries. Each party is trying to look after its own interests in the region. For example, some parties are trying to increase passages trough the Strait. The simulation developed in this research can be used to model such increase in traffic and show its effect on the vessel waiting times. Also, the imbedded risk analysis model can demonstrate the effects of such policy on the accident risk. In addition, the developed scheduling algorithm can be used in the Istanbul Strait or any other narrow waterway such as Panama or Suez canals.

Furthermore, the complexity of the operations at the Strait has motivated us to model congestion at the waterway entrances through queueing analysis. The main contribution is approximating expected waiting times in queues with multiple types of simultaneous interruptions, which has not been done in the literature. The contribution includes single-class and multi-class cases and the case where interruptions are dependent on the classes of customers.

This research is part of the joint project with the Boğaziçi University. It is in part funded by the Laboratory for Port Security at Rutgers University, NSF Grant Number INT-0423262, and TUBITAK, The Scientific and Technological Research Council of Turkey.

ACKNOWLEDGEMENT

My first and sincerest acknowledgment must go to my advisor Tayfur Altıok. I am indebted to him for his guidance and support throughout the years. He has been instrumental in ensuring my academic, professional and moral well being. This work would not have been possible without him.

I would also like to express my gratitude to İlhan Or at Boğaziçi University for his invaluable insight and guidance. Many thanks also to the committee members Melike Baykal-Gürsoy, Maria Boile and Mohsen Jafari.

I am also grateful to my friends and colleagues at Boğaziçi University. In particular, I would like to thank Birnur Özbaş, Alper Almaz, and Tuba Yılmaz. Birnur deserves particular credit for being my partner in crime and putting up with my antics. Many thanks also to Wan Yee Chan for her valuable assistance.

The data for this research were provided by the Turkish Straits Vessel Traffic Services (VTS) and various subject matter experts. I am extremely grateful for their generosity.

A heartfelt thank-you goes to my wonderful family for always being there when I needed them most, and encouraging me when I doubted myself. I treasure them more than anything in the world.

DEDICATION

To my better half Hasan Tütün. Because of him I wake up every day wanting to be a better person. He has been my greatest joy and support in the world for more than nine years. He is the only one in the world who truly knows me and still loves me for all that I am.

To my best friend, companion, partner in life and eternal love…

Quand il me prend dans ses bras
Il me parle tout bas
Je vois la vie en rose...

TABLE OF CONTENTS

LISTS OF TABLES

LIST OF ILLUSTRATIONS

1 INTRODUCTION

Peter Gilles, a French humanist writing in the 16th century, described the Bosporus as a "strait that surpasses all straits, because with one key it opens and closes two worlds, two seas" according to [Freely, 1996]. The two seas that he refers to are the Aegean and the Black Sea, and the two worlds are Europe and Asia, since the Bosporus and the Dardanelles have throughout history been the major crossing-places between the two continents.

The Turkish Straits, which consist of the Istanbul Strait (Bosporus), the Çanakkale Strait (the Dardanelles) and the Sea of Marmara, have for centuries been one of the world's most strategic waterways. As the Black Sea's sole maritime link to the Mediterranean and the open ocean beyond, they are a vital passageway not just for trade but for the projection of military and political power.

The Turkish Straits are distinct among the waterways of the world in their morphological structure and oceanographic characteristics; leading to navigational hazards that are unique to this passageway. The most difficult part of this challenging passage is the Bosporus, which is defined by its extreme narrowness, winding contour and densely populated shores.

Perhaps no other waterway is as fabled as the Bosporus. The earliest myths date back to the second millennium BC. One of these stories tells the myth of Zeus and Io, his mistress whom he changed into a heifer, to hide her from his wife Hera. When Hera found out about the affair, she pursued Io with a relentless gadfly, forcing her to swim the Strait. Thenceforth, the Strait bore the name Bosporus, or "Cow's Ford", commemorating Io.

Jason and the Argonauts, in their quest for the Golden Fleece, barely sailed through the Clashing Rocks, a part of the Bosporus, before the Strait closed behind them. Darius I, the Persian emperor, used pontoons to cross the Bosporus and attack the Greeks. The Byzantine and Ottoman empires were governed from the shores of the Bosporus for over 1,600 years. Today, this narrow passage runs through the heart of Istanbul, home to over 12 million people and some of the world's most celebrated ancient monuments.

The Istanbul Strait is approximately 31 km long, with an average width of 1.5 kilometers. At its narrowest point between Kandilli and Bebek, it measures a mere 698m. It takes several sharp turns, forcing the ships to alter course at least 12 times, sometimes executing turns of up to 80 degrees. Navigation is particularly treacherous at the narrowest point, as the vessels approaching from opposite directions cannot see each other around the bends.

In addition to its winding contour, the unpredictable countervailing currents that may reach 7 knots pose significant danger to ships. Surface currents in the Strait flow from the Black Sea to the Sea of Marmara, but submarine currents 50 feet below the surface run in the opposite direction. Within bays and near point bars, these opposing currents lead to turbulence. The unpredictable climate brings about further danger. During storms with strong southerly winds, the surface currents weaken or reverse in some places, making it even harder to navigate. Not surprisingly, all these elements can easily cause vessels transiting the Strait to veer off course, run aground or collide.

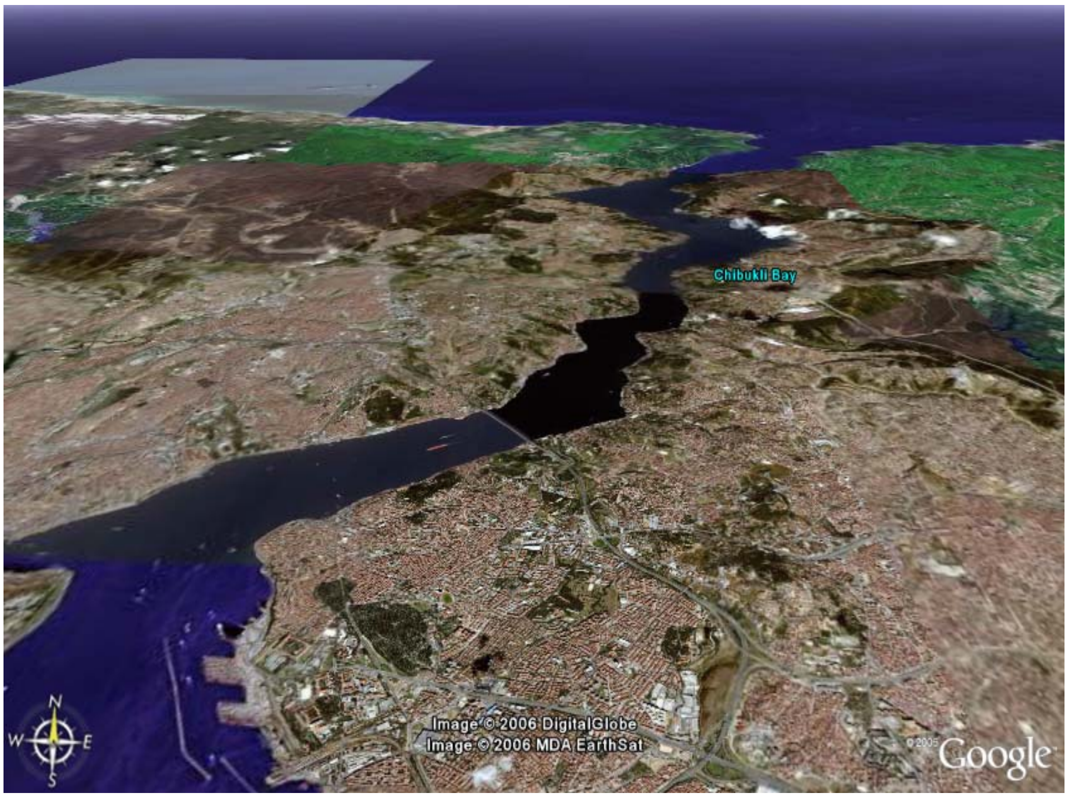

Figure 1.1 Istanbul Strait

The current international legal regime governing the passage of vessels through the Turkish Straits is the 1936 Montreux Convention. Although this instrument provides full authority over the straits to the Turkish government, it asserts that in time of peace, merchant vessels are free to navigate the straits without any formalities. When the Convention was put in place, less than 5,000 vessels used to pass through the Istanbul

Strait annually. Today, the changes in the shipping and navigational circumstances have led to a ten-fold increase in the maritime traffic through the Strait.

Several reasons contributed to this immense increase. The Turkish Straits provide the only maritime link between the Black Sea riparian states and the Mediterranean, forcing these states to rely heavily on the straits for foreign trade. The opening of the Main-Danube canal has linked the Rhine to the Danube, linking the North Sea and Black Sea. Traffic originating from the Volga-Baltic and Volga-Don waterways has also increased in the recent years.

Still, the most alarming increase in traffic is observed in the number of vessels carrying dangerous cargoes. The fall of the Soviet Union in 1991 has led to the emergence of newly independent energy-rich states along the Caspian Sea. Currently, the oil and gas from Azerbaijan, Turkmenistan and Kazakhstan reach the western markets through the Turkish Straits. The maritime traffic will increase substantially since the production is expected to double by 2010. In addition, Russian oil companies are setting new records for production and export. Analysts predict that Russia could be pumping 10 million barrels of crude oil daily by the end of the decade, a significant portion of which is expected to pass through the straits.

During the 1930s, when the Montreux Convention went into force, transport of hazardous materials posed little concern due to the infrequent passages and small vessel sizes. However, the increases in traffic and vessel sizes have raised the likelihood and the severity of accidents. The unusual characteristics of the Bosporus and its climate, coupled with the failure to request pilotage in this treacherous waterway, have led to over 200 accidents in the past decade.

The first major hazardous cargo accident occurred in 1960 when the Greek-flagged M/T World Harmony collided with the Yugoslavian-flagged M/T Peter Zoranic, leading to the death of 20 crew members, severe oil pollution and fire that lasted several weeks, suspending the transit traffic. In 1979, Romanian-flagged Independenta and the Greek freighter M/V Evriyalı collided at the southern entrance of the Strait. 43 crew members died, 64,000 tons of crude oil spilled into the sea and 30,000 tons burned into the atmosphere. In yet another catastrophe, the Greek Cypriot vessels M/T Nassia and M/V Shipbroker collided in the Strait. 29 officers and crewmen perished and 20,000 tons of crude oil burned for five days, suspending the traffic for a week. A potential disaster was averted only because the accident occurred just north of the city.

In order to ensure the safety of navigation, life, property and to protect the environment, the Turkish government adopted unilaterally the 1994 Maritime Traffic Regulations for the Turkish Straits and Marmara Region. Four years later, the rules were revised and the 1998 Reviewed Regulations were adopted. These regulations include extensive provisions for facilitating safe navigation through the straits in order to minimize the likelihood of accidents and pollution. The provisions aim to monitor the vessels with hazardous cargoes, regulate the patterns of ship traffic by establishing new procedures for passage in the straits, and attempt to account for dangerous meteorological and oceanographic conditions by restricting traffic under certain situations.

Even though the number of accidents decreased after the adoption of the regulations, the vulnerability of the straits was evident once again in an incident in 1999. Voganeft-248, a Russian tanker, ran aground and broke apart at the Sea of Marmara entrance of the Strait. Over 800 tons of oil spilled into the sea, and clean-up efforts lasted several months.

The navigational hazards of the Istanbul Strait are real and well known. Although strengthening transit restrictions and safety precautions have decreased the danger, accidents will happen. In 2005, almost 55,000 vessels passed through the Strait, an increase of 16% over the previous year. Inevitably, as the number of vessels transiting the Strait increases dramatically, so will the likelihood of accidents and environmental catastrophes, endangering the only city in the world that stands astride two continents, and its 12 million inhabitants. Therefore, determining accident risks and measures to mitigate these risks becomes of utmost importance. In this dissertation, this is achieved through probabilistic risk analysis.

The goal of this research is to analyze the risks involved in the transit vessel traffic system in the Istanbul Strait. We have developed a detailed mathematical risk analysis model to be used in a risk mitigation process to improve safety in the Strait. In the first step of the risk analysis process, the transit vessel traffic system in the Istanbul Strait is thoroughly analyzed and a simulation model is developed to mimic and study the system.

In addition to transit vessel traffic through the Strait and geographical conditions, the current vessel scheduling practices are modeled using a scheduling algorithm. This algorithm is developed through discussions with the Turkish Straits Vessel Traffic Services (VTS) to mimic their decisions on sequencing vessel entrances as well as giving way to vessel traffic in either direction. Furthermore, a scenario analysis is performed to evaluate the impact of several parameters on the system performance.

Risk analysis of the Strait is performed by incorporating a probabilistic accident risk model into the simulation model. This mathematical model is developed based on probabilistic arguments and utilizes historical accident data and subject matter expert opinions. We have also performed a scenario analysis to evaluate the characteristics of accident risk. This analysis allows us to investigate how changes in various factors impact risk. These factors include vessel arrival rates, scheduling policies, pilotage, overtaking, and local traffic density.

Finally, complexity of the operations at the Istanbul Strait motivated us to model congestion at the waterway entrances through queueing analysis. We have developed single-server queueing models subject to multiple types of operation-independent interruptions. We have used waiting time arguments and service completion time analysis to approximate the expected waiting time of a customer (vessel) in the aforementioned queue for various cases of service interruptions. These cases include the single-class model with non-simultaneous interruptions, the single-class model with possibly simultaneous interruptions, the n-class priority queueing model with k possibly simultaneous class-independent interruptions, and the two-class priority queueing model with k possibly simultaneous class-dependent interruptions.

2 VESSEL TRAFFIC IN THE ISTANBUL STRAIT

More than 50,000 transit vessels in total pass through the Istanbul Strait annually, carrying various cargoes ranging from dry goods to petroleum products. After arriving at the entrances, the vessels may anchor for various reasons including health inspection, loading food or refueling. All vessels, anchored or not, wait in the queue until they are allowed to transit. The Strait is divided into two traffic lanes. The vessels are permitted to enter the Strait one at a time from each entrance. The vessel traffic may be interrupted due to poor visibility, high currents, and other factors such as lane closures caused by vessel accidents or sporting events. Vessels do not stop in the Strait since they may create a high risk situation for other vessels and the environment.

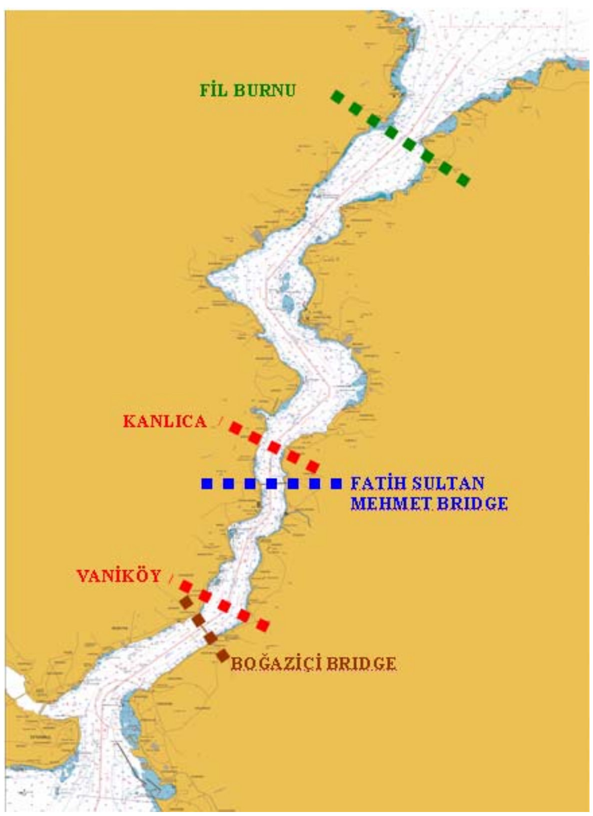

Figure 2.1 Key Locations in the Istanbul Strait

2.1 VESSEL COMPOSITION

The Istanbul Strait is considered one of the most congested maritime traffic regions in the world. Its traffic volume is roughly four times and three times heavier than that of the Panama and Suez canals, respectively. Approximately 55,000 transit vessels pass through the Strait annually.

Turkish authorities categorize transit vessels based on criteria such as vessel size, vessel passage type, vessel draft and the type of cargo.

- Based on the type of cargo they carry, the vessels fall into the following categories:
  - Tankers
  - Dangerous and Hazardous Cargo Carriers
  - LNG & LPG Carriers
  - General Cargo Vessels
  - Passenger Vessels
  - Other

- In terms of length, the vessels are grouped under the following:
  - Less than 50 m.
  - 50-100 m.
  - 100-150 m.
  - 150-200 m.

- ♦ 200-250 m.
- ♦ 250-300 m.
- ♦ 300 m or greater.

- The transit vessels are also categorized as:
  - ♦ Direct-Passing Vessels
  - ♦ Indirect-Passing Vessels

- The final category is the draft size, in which the vessels are grouped under:
  - ♦ 10-15 meters
  - ♦ 15 m or greater. (Deep Draft Vessels)

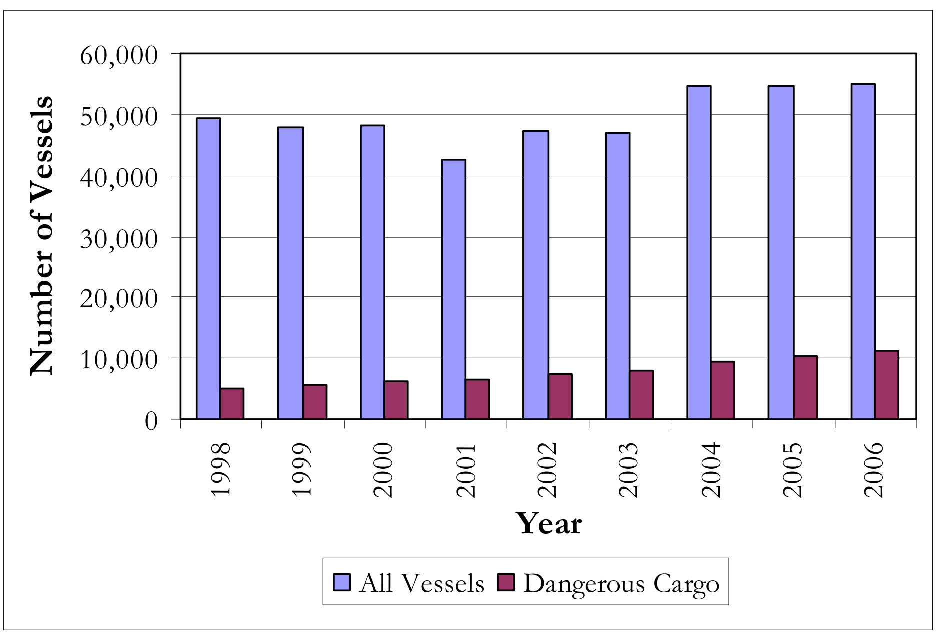

Figure 2.2 Number of vessels carrying dangerous cargo versus all vessels

Figure 2.2 shows the number of all types of vessels navigating through the Istanbul Strait and the total number of vessels carrying dangerous cargo between 1998 and 2006. The historical data through 2004 was obtained from [TUMPA, 2004] and the 2005-2006 data was obtained from the VTS. Between 2003 and 2006, the total number of vessels and the number of vessels carrying dangerous cargo have increased 17% and 40%, respectively.

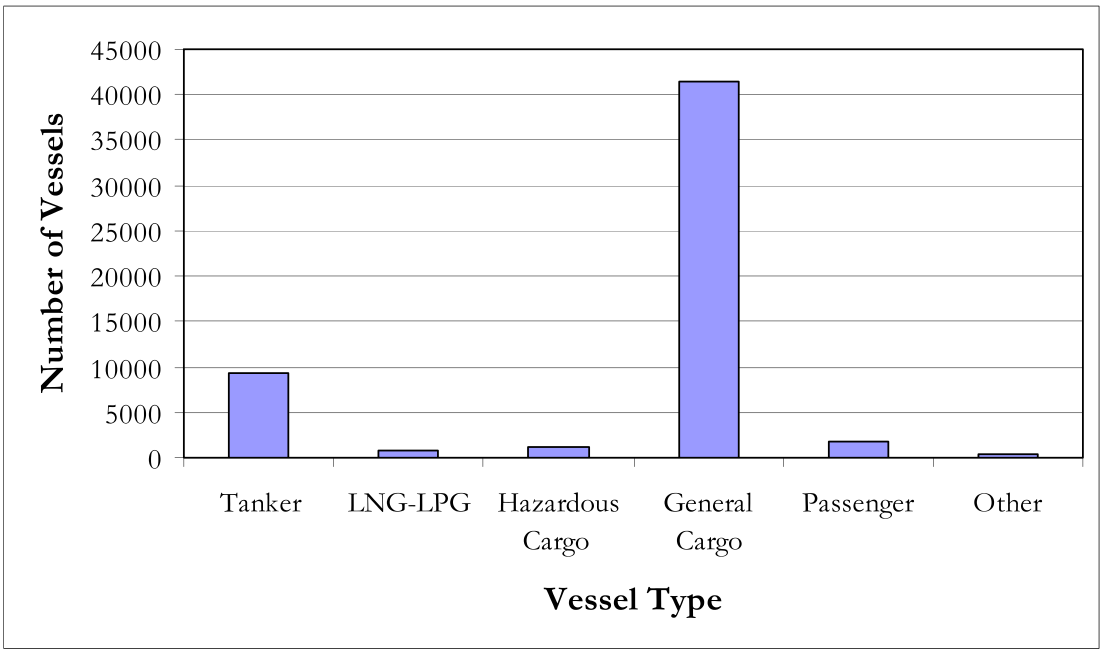

Figure 2.3 Distribution of vessels by type of cargo

Figures 2.3 and 2.4 demonstrate the distribution of transit vessels by cargo type and vessel length in 2006 based on data obtained from the VTS. According to these figures, about 21% of transit vessels carry hazardous materials such as natural gas, agricultural and other chemicals, oil, nuclear waste and derivatives through the Strait. The US Energy Information Administration estimated in [EIA, 2006] that 2.4 million barrels of oil pass through the Strait every day in 2006.

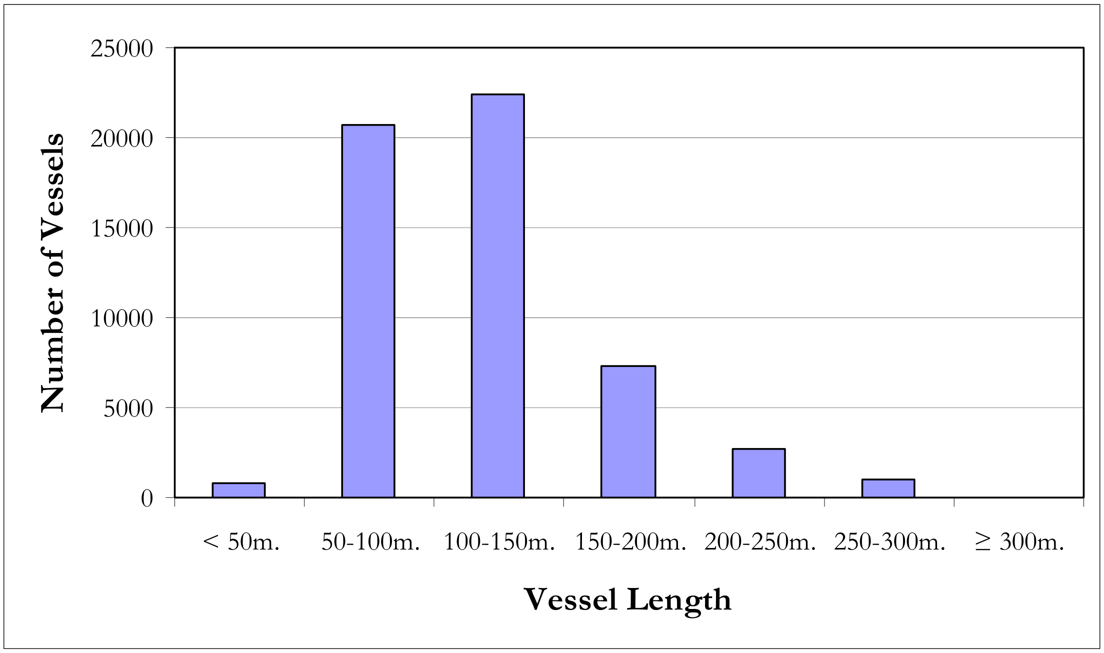

Figure 2.4 Distribution of vessels by vessel length

Figures 2.3 and 2.4 demonstrate the distribution of transit vessels by cargo type and vessel length in 2006 based on data obtained from the VTS. According to these figures, about 21% of transit vessels carry hazardous materials such as natural gas, agricultural and other chemicals, oil, nuclear waste and derivatives through the Strait. The US Energy Information Administration estimated in [EIA, 2006] that 2.4 million barrels of oil pass through the Strait every day in 2006.

About two thirds of the world's oil trade, both crude and refined, is transported by tankers. Tankers have made intercontinental transport possible, as they are low cost, efficient, and flexible. The increase in demand for oil and gas worldwide, the emergence of new energy-rich states in the Caspian Sea region, and the increased production capacity of Russia have led to a significant rise in oil and gas transfer through the Strait.

For example, [Erkaya, 1998] claims that over half of Russia's total oil exports travel through the Istanbul Strait, accounting for about a quarter of the international transit traffic. Traffic through the Strait is expected to increase as Azerbaijan and Kazakhstan augment crude production and exports in the future [EIA, 2006].

In addition, as a result of the technological developments in the shipbuilding industry, vessel sizes passing through the Strait have increased dramatically. For instance, the number of transit vessels exceeding 200 meters in length increased 62% between 1999 and 2006.

In 2006, about 55,000 vessels passed through the Strait, an average of 150 vessels per day. Only 7% of these vessels were more than 200 meters in length, but their presence forced repeated traffic suspensions. According to data obtained from the VTS, the passage of vessels carrying dangerous cargo has forced the Turkish authorities to suspend one-way traffic for 2,627 hours in 2005. Further, the traffic in the Istanbul Strait was suspended in 2005 for 15 days due to severe weather conditions, 43 days due to emergencies, and 10 hours due to sports activities.

In addition to the transit vessels, the daily local vessel traffic volume can reach up to 2,500 according to [Birpınar et al., 2005]. The local traffic consists of the following:

- Ferries
- Intra-city passenger vessels
- Fast ferries

- Passenger boats
- Pleasure crafts
- Fishing boats
- Military vessels
- Tugboats
- Vessels that belong to non-governmental organizations
- Vessels engaged in underwater operations, and survey vessels

2.2 REGULATIONS

The state agencies principally involved with current policy formulation and regulation of the Turkish Straits are Turkey's Prime Ministry Undersecretariat for Maritime Affairs, and the Maritime Department of the Foreign Ministry. Since 1936, these departments have administered the Strait in accordance with the regime set out in the Montreux Convention.

Montreux Convention provides full authority and control over the straits to the Turkish government. However, a crucial exception is articulated in Article 2, which states that "in time of peace, merchant vessels shall enjoy complete freedom of transit and navigation in the straits, by day and by night, under any flag and with any kind of cargo, without any formalities" except sanitary control as stated in [Montreux Conv., 1937]. Further, it adds that "pilotage and towage remain optional".

The convention later asserts in Article 28 that the principle of transit and navigation established under Article 1 shall “continue without limit of time”. This provision is the main point of contention between Turkey and the Black Sea riparian states over Turkey’s right to regulate traffic in the straits.

Even though the Montreux Convention helped establish a reasonable regime for vessel transit in 1936, it did not state any provisions on navigational safety or environmental protection. When the instrument went into force in 1936, only about 4,500 ships passed through the straits annually; and a majority of them were small vessels carrying general cargo. Today, the shipping and navigational circumstances have changed dramatically, leading to an immense increase in maritime traffic. Inevitably, the traffic congestion and the inherent navigational difficulties within the Strait lead to accidents, endangering Istanbul, its inhabitants and the environment.

In an effort to “regulate the maritime traffic scheme in order to ensure the safety of navigation, life and property and to protect the environment in the region”, the Turkish government adopted unilaterally the 1994 Maritime Traffic Regulations for the Turkish Straits and the Marmara Region. The International Maritime Organization (IMO) approved a set of Rules and Regulations on the straits, ratifying most of the measures taken by Turkey.

As a result of severe criticisms from the Black Sea riparian states, especially Russia, and the urging of the IMO, Turkey revised the provisions and adopted the 1998 Revised

Regulations. The regulations aim to monitor the safe passage of vessels carrying dangerous cargo, establish new traffic schemes within the straits, and minimize risk by suspending or restricting traffic under dangerous meteorological conditions.

The most important provision is the implementation of the new Traffic Separation Schemes (TSS), which set new traffic lanes for transiting vessels. The TSS were adopted in compliance with the Reg. 10 of the Convention for Preventing Collision at Sea (COLREGS) and approved by the IMO General Assembly in November 1995. The 1998 Regulations restrict the passage of vessels exceeding 200 meters to daytime. Further, automatic pilots during transit are prohibited.

Vessels approaching the straits are required to provide sailing plans prior to their passage. Vessels are required to submit their sailing plans in compliance with the regulations listed below:

2.2.1 SAILING PLAN 1 (SP 1)

The Sailing Plan 1 is the report that must be submitted by all transit vessels which will pass through the Turkish Straits in order to advise their arrival details. These include:

- Vessel's name
- Date / Time
- Reporting Position

- Maximum maneuvering speed
- Port of departure
- Date, time and point of entry into traffic separation scheme
- Port of destination
- Pilot Request
- Maximum Air Draft
- Type and quantity of the cargo
- Defect / damage / deficiencies / other limitations
- Description of dangerous / nuclear and pollution goods
- Ship's type and size

Table 2.1 shows the regulations regarding Sailing Plan 1 for different vessel types.

Table 2.1 Regulations regarding Sailing Plan 1

<table>
<tr><th>Vessel Type</th><th>Regulation</th></tr>
<tr><td>150-200 m. in length *</td><td rowspan="4">24 hours prior to passage</td></tr>
<tr><td>With a draft between 10-15 meters *</td></tr>
<tr><td>Carrying dangerous cargo **</td></tr>
<tr><td>≥ 500 GT **</td></tr>
<tr><td>200-300 m. in length</td><td rowspan="2">48 hours prior</td></tr>
<tr><td>With a draft over 15 m.</td></tr>
<tr><td>≥ 300 m. in length</td><td rowspan="3">72 hours prior ***</td></tr>
<tr><td>Carrying nuclear cargo or nuclear waste</td></tr>
<tr><td>Propelled by nuclear power</td></tr>
</table>

* These are called "vessels restricted in their ability to maneuver in TSS"
** These vessels, about to depart from ports in the Sea of Marmara, and heading north, should submit an SP 1 report at least 6 hours prior to their departure.
*** These types of vessels should provide information regarding their characteristics and cargo to the Administration during the planning stage of their trip.

2.2.2 SAILING PLAN 2 (SP 2)

In addition to the Sailing Plan 1, vessels listed in Table 2.2 are required to submit another report called Sailing Plan 2 (SP 2), which provides further details to the authorities.

Table 2.2 Regulations regarding Sailing Plan 2

Vessel Type	Regulation
Already submitted SP 1	2 hours (or 20 miles) prior to entering the straits
Warships	
State-owned (not used for commercial purposes)	
≥ 300 m. in length	72 hours prior
Carrying nuclear cargo or nuclear waste	
Propelled by nuclear power	

The other rules and regulations regarding safe passage of the transiting vessels are categorized below.

2.2.3 SPEED

The navigational speed limit at the Strait is 10 nautical miles, unless a higher speed is needed to maintain good steerage.

2.2.4 DISTANCE BETWEEN VESSELS

Transiting vessels must maintain a minimum following distance of 8 cables (1.09 miles) while passing through the Strait. This may be increased by the authorities based on the type of the vessels.

The passage of vessels carrying dangerous or hazardous cargo is regulated under Reg. 25 letter d, which states that when a northbound (southbound) vessel >150m carrying dangerous cargo enters the Strait, no northbound (southbound) vessel with the same characteristics is permitted until the former vessel reaches Fil Burnu (Boğaziçi Bridge).

2.2.5 AIR DRAFT

Due to two suspension bridges crossing the Istanbul Strait, the maximum air draft is limited to 58 meters. Transiting vessels with air drafts of 54 to 58 meters have to be escorted by tugboats.

2.2.6 ANCHORING AND LEAVING THE ANCHORAGE

Direct-passing vessels may anchor for up to 48 hours without a Free Pratique. In [EyeforTransport, 2007], Free Pratique is defined as the permission granted by local medical authorities, denoting that the vessel has a clean Bill of Health so that people may embark and disembark.

2.2.7 OVERTAKING

Overtaking is forbidden unless absolutely necessary. It is not allowed between the Vaniköy and Kanlıca points under any circumstances.

2.2.8 TEMPORARY TRAFFIC SUSPENSIONS

- Traffic in the Strait may temporarily be suspended in case of force majeure situations, collision, grounding, fire, public security, pollution, surface or underwater construction, and the existence of navigational dangers.
- The incoming traffic is suspended when a vessel with a length of 200 to 300 meters passes through the Strait.
- The traffic is suspended in both directions when a vessel exceeding 300 meters in length transits the Strait.

2.2.9 SURFACE CURRENTS

Table 2.3 below depicts the conditions regarding the safe passage of vessels under various surface currents:

Table 2.3 Regulations regarding Surface Currents

	Vessels are not allowed to enter the Istanbul Strait if…	
Condition	**Vessel Type**	**Speed**
Surface current > 4 knots, or Reverse currents observed	Vessels with dangerous cargo	< 10 knots
	Large vessels	
	Deep draft vessels	
Surface current > 6 knots, or Reverse currents observed	Vessels with dangerous cargo	Any
	Large vessels	
	Deep draft vessels	

2.2.10 RESTRICTED VISIBILITY

The passage of vessels may be restricted under certain visibility conditions to ensure safe navigation:

Table 2.4 Regulations regarding Visibility Conditions

Visibility Condition	**Regulation**
≤ 2 miles	All vessels should keep their radar running.
	Vessels with 2 radars shall designate one for the pilot.
≤ 1 mile	Vessel traffic allowed in one direction only.
	Vessels with dangerous/hazardous cargo, large vessels and deep draft vessels shall not enter to the Strait.
≤ 0.5 mile	Vessel traffic suspended in both directions

On December 30, 2003, the Turkish Government introduced in the Turkish Straits a Vessel Traffic Service (VTS), thus completing the legal framework in force to improve the safety of navigation, protection of life and environment. The VTS is in charge of providing the necessary navigational assistance and monitoring the safe passage of vessels.

Complementing the Montreux Convention and the 1998 Regulations are three major legal instruments for regulating transit vessel traffic in the straits; namely The International Convention of Safety of Life at Sea [SOLAS, 1974], the Convention on the International Regulations for Preventing Collisions at Sea [COLREGS, 1972], and the International Convention on Standards of Training, Certification and Watch keeping for Seafarers [STCW, 1978].

SOLAS establishes minimum standards for ensuring that a ship is fit for international transport on the oceans. COLREGS, on the other hand, sets forth detailed rules on the operation of vessels, including safe speeds, right of way, actions to avoid collisions, signaling, fishing vessels and provisions for traffic separation schemes. STCW entails basic requirements for training, certification and watch keeping to be used by seafarers.

2.2.11 STORM

According to the regulations, northbound vessels less than 150 meters in length are not allowed to enter the Strait when there is a storm in the Black Sea.

2.3 LITERATURE REVIEW ON ANALYSIS OF WATERWAYS

Although a significant number of studies involving risk analysis and modeling of accidents exist in the literature, the research conducted on modeling and performance analysis of narrow waterways is scarce. Some of the studies published on the topic are discussed below:

A SLAM model of the Suez Canal traffic flow is reported in [Clark et al., 1983]. The authors propose an experimental traffic control scheme and present the results and discussion of the test performed. A method for analysis of systems with multiple response variables is discussed and illustrated.

[Rosselli et al., 1994] and [Bronzini, 1995] consider an existing simulation model developed originally by the US Army Corps of Engineers for use on the US inland waterway system, and extend it to study the Panama Canal. The objective is to predict the transit capacities of the various Panama Canal alternatives in the future.

In another study, [Golkar et al., 1998] presents the Panama Canal Simulation Model (PCSM) developed by the SABRE group for the Panama Canal Commission. The model is built to measure Canal's capacity under different operating conditions.

Another simulation model of the Panama Canal is presented in [Franzese et al., 2004]. The objective is to help the Panama Canal Authority design a strategic planning tool. The authors incorporate vessel arrivals, traffic rules and vessel sequencing components into the model created using the Arena simulation software. Performance analysis of current and future alternatives of the system is performed using several performance measures such as waiting times, transit times, queue lengths and locks' utilization rates.

A simulation model of the transit traffic in the Istanbul Strait is presented in [Köse et al., 2003]. Specifically, the focus is on the variation of waiting times resulting from different transit vessel arrival frequencies. The results of the simulation model, and the effects of probable increase in maritime traffic due to new oil pipelines, are discussed.

[Merrick et al., 2003] proposes a simulation model to estimate the number of vessel interactions in the current San Francisco Bay system and their increases caused by three alternative expansion plans. The simulation outputs are in the form of geographic profiles showing the frequency of vessel interactions across the study area, thus representing the level of congestion for each alternative and the current ferry system. The increase in the number of situations where ferries are exposed to adverse conditions is evaluated by comparing the outputs.

[Biles et al., 2004] describes the integration of geographic information systems (GIS) with simulation modeling of traffic flow on inland waterways. They present two special cases: the AutoMod modeling of barge traffic on the Ohio River, and the Arena modeling of the transit vessels through the Panama Canal.

The simulation study of the transit maritime traffic in the Istanbul Strait presented in [Özbaş, 2005], focuses on the modeling of the entrance procedures based on vessel types and lengths, prioritization of vessels, pilotage and tugboat services. This model incorporates the former application scheme of rules and regulations for vessel entrance. All vessel arrivals are assumed to be exponential and obtained from the 1999 data along with the vessel profile ratios. A scenario analysis is performed to evaluate the importance of vessel profile, arrival rate, priority of vessels, and support services on the performance measure.

[Almaz et al., 2006] and [Almaz, 2006] present a functional simulation model of the maritime transit traffic in the Istanbul Strait. The objective is to perform scenario analysis to analyze the effectiveness of various policies and decisions related to the transit traffic in the Istanbul Strait. The impacts of the type and frequency of transit vessels as well as various natural factors and resources on the system are also investigated. For this purpose, the rules and regulations, the transit vessel profiles, pilotage and tugboat services, meteorological and geographical conditions are considered in the simulation model.

In addition to modeling and performance analysis, we also develop a scheduling algorithm for the vessel entries in the Istanbul Strait. Even though numerous articles have been published on maritime vessel and fleet scheduling in the last 40 years, the specific literature on the vessel entrance scheduling into a narrow waterway is scarce.

[Norman, 1973] presents an algorithm for scheduling vessel transits through the Panama Canal. The performance of the proposed scheduling algorithm is evaluated by comparing measures such as lock dead times, transit times, delay times, and lock securing times obtained from the algorithm to their observed values.

[Petersen and Taylor, 1988] considers the problem of real time scheduling of vessels through the Welland Canal. The problem is formulated as a combination of a linear programming model and a heuristic, which is solved using a dynamic programming approach.

2.4 MODELING OF THE TRANSIT VESSEL TRAFFIC

We have developed a high-fidelity simulation model representing the vessel traffic in the Istanbul Strait using the Arena simulation tool©. The simulation model is developed mainly for Risk Analysis and mitigation purposes. In addition, it is utilized to investigate the effect of various system attributes such as arrival frequency, number of pilots and number of tugboats on the system performance as well as to test the performance of the scheduling algorithm we have developed for use by the VTS Authorities.

The model includes transit vessels along with local traffic and other vessels. The various components and aspects of the model are explained in detail in the following sections.

© ARENA is a trademark of Rockwell software.

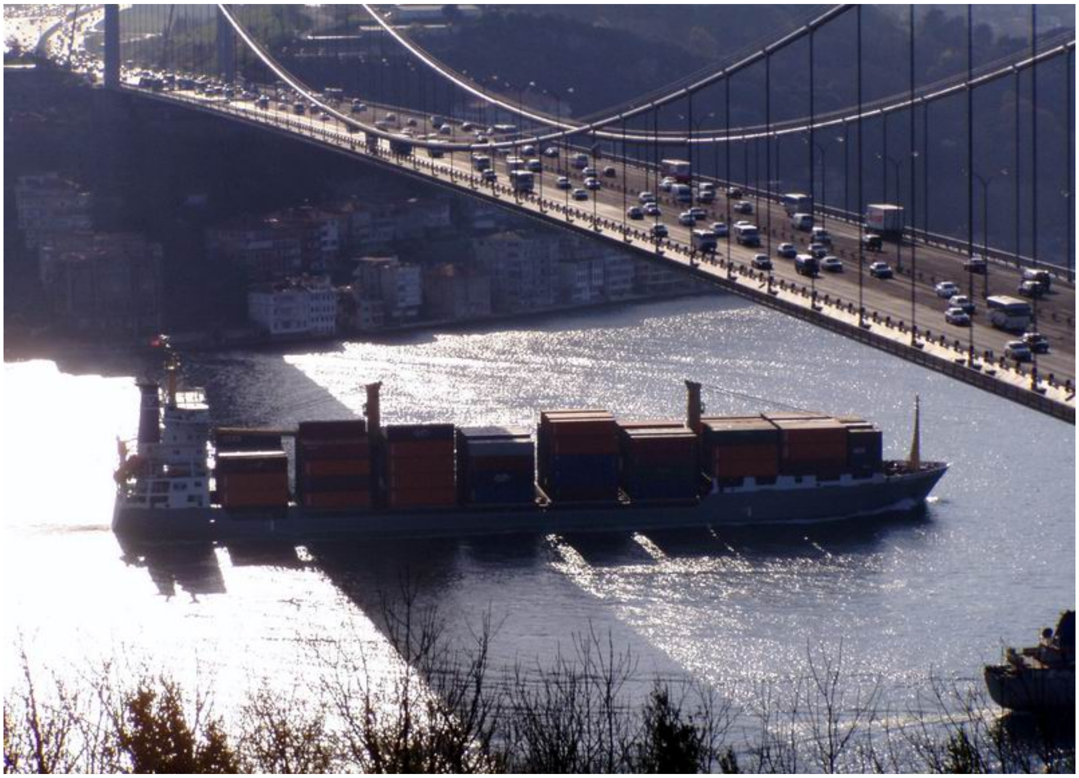

Figure 2.5 Fatih Sultan Mehmet Bridge - the narrowest part of the Strait

2.4.1 VESSEL ARRIVALS

The entities representing different types of vessels are generated according to Sailing Plan 2 (SP2) submitted by approaching vessels. Vessels are created based on cargo type and vessel length categories presented in section 2.1. In other words, every combination of vessel length and cargo type is generated using a unique arrival process deciphered from the arrival data. The inter-arrival time distributions are different for northbound and southbound vessels. Therefore, two separate submodels are used to model southbound and northbound vessel arrivals.

When there is a storm in the Black Sea, the southbound inter-arrival distributions are modified to account for the decrease in the traffic before and during the storm, as well as the increased traffic volume following the storm.

Upon arrival, all vessels are assigned the following attributes based on prior data:

- Vessel Length
- Vessel Class
- Speed
- Age
- Flag
- Tugboat Request Indicator
- Pilot Request Indicator
- Anchorage Indicator
- Anchorage Duration
- Stopover Indicator

The distributions used for the above attributes are unique for each type of vessel of a certain length. Indicator values for tugboat request, pilot request, anchorage and stopover are computed according to the corresponding data. Following its creation, a vessel entity is sent to the anchorage area if its *Anchorage Indicator* equals 1, to wait for its *Anchorage Duration*. After it leaves the anchorage area the entity joins the queue of its *Vessel Class*. The vessel classes that the entities are grouped under for scheduling purposes are shown in Table 2.5. Each vessel waits until one of the entities representing the daytime or nighttime schedulers removes it from the queue.

Table 2.5 Vessel classes for scheduling purposes

		Type				
Length (m.)	Draft (m.)	Tanker	Carrying Dangerous Cargo	LNG-LPG	Dry Cargo	Passenger Vessels
< 50	< 15	Class E	Class E	Class B	Class D	Class P
50 - 100	< 15	Class E	Class E	Class B	Class D	Class P
100 - 150	< 15	Class C	Class C	Class B	Class D	Class P
150 - 200	< 15	Class C	Class C	Class C	Class C	Class P
200 - 250	< 15	Class A	Class A	Class A	Class C	Class P
250 - 300	> 15	Class A	Class A	Class A	Class C	Class P
> 300	> 15	Class T6	Class T6	Class T6	Class T6	Class T6

2.4.2 RESOURCES

When a vessel is removed from the queue, it seizes the necessary resources to enter the Strait based on its indicator attributes. These resources are pilots and tugboats, which are grouped into two categories: northbound and southbound. If there are no resources available, a vessel requesting resources is not removed from the queue. Once a vessel seizes all resources it needs, it enters the Strait.

The seized resources are released by the vessel when it completes its passage. The released resources are then designated to be available in the opposite direction. During the daytime, the transit traffic is allowed in one direction only. The pilots are taxied back to the direction of the one-way traffic every time the number of available pilots on the opposite direction reaches a particular threshold such as five. The number of pilots reserved by the scheduled vessels is also checked. If it is less than five, then only that many pilots are taxied back.

On the other hand, when a pilot is released by a vessel during nighttime, the number of available pilots in the opposite direction is checked to see whether it is five more than half of the total pilot capacity. If so, the released pilot and four others are taxied back to the opposite entrance.

Further, the tugboats return one by one if there are less than two tugboats available in the direction of the one-way traffic and more than two in the opposite direction.

The above particular numbers are some thresholds used to achieve some type of balanced resource allocation in the current operation.

2.4.3 VESSEL SCHEDULING

Turkish Straits Vessel Traffic Services (VTS) schedules vessels entering the Strait based on their waiting times, and priorities. In addition, the regulations in place, the number of vessels in both directions and the number of available pilots play a role in the scheduling decisions. We have tried to develop a mathematical formulation of the current scheduling practice at the VTS. The fundamental philosophy is to schedule the vessels with longer waiting times first while giving priority to large vessels carrying dangerous cargo.

Even though all the operators at the VTS schedule vessels based on the same factors, since the process is not in a standard algorithmic format, it may differ from operator to operator. By developing a scheduling algorithm, we have also intended to provide a standard method for the VTS to schedule transit vessels.

Vessels belonging to Class T6 and Class A may pass through the Strait only during daytime. Therefore, different scheduling policies are used for daytime and nighttime vessel traffic.

2.4.3.1 DAYTIME SCHEDULE

The passage of Class T6 vessels are subject to special permissions from the authorities. When a Class T6 vessel enters the Strait, traffic in both directions is suspended during its passage as mentioned in Section 2.2. On the other hand, when a Class A vessel enters the Strait, only the incoming traffic (opposite direction) is suspended. Also, according to the rules set by the VTS, in a given day the daytime traffic is suspended at most once in each direction.

In order to comply with the regulation concerning the required distance between vessels, Class A vessels enter the Strait every 75 and 90 minutes from north and south entrances, respectively. However, Class C vessels may follow each other with 30-minute intervals. Furthermore, Class D, E, and P vessels may enter every 10 minutes. A typical schedule of vessels entering the Strait during daytime is given in Figures 2.6 and 2.7 for northbound and southbound traffic, respectively.

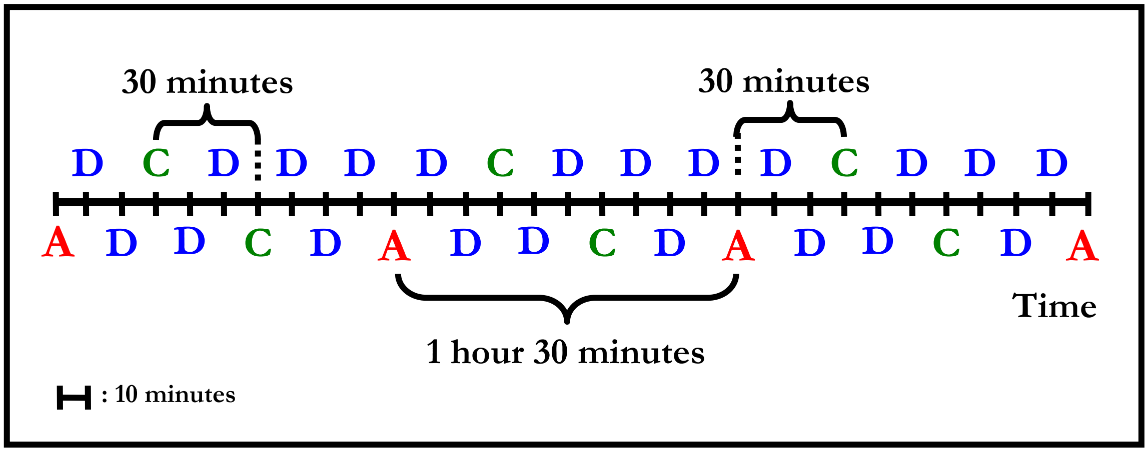

Figure 2.6 A typical schedule of northbound vessels entering the Strait

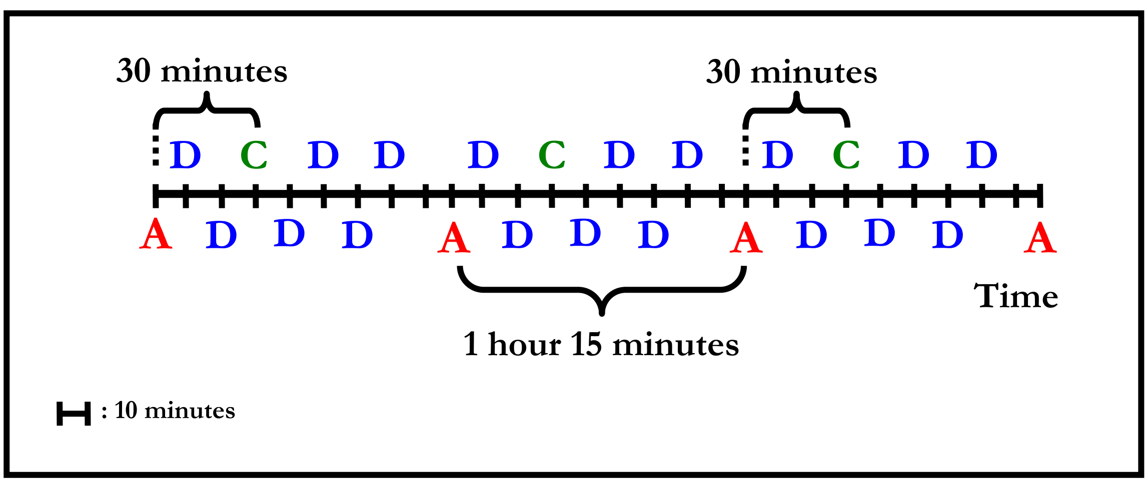

Figure 2.7 A typical schedule of southbound vessels entering the Strait

Since Class T6 and Class A vessels can only pass through the Strait during daytime, the total number of these vessels passing in a day is contingent upon the daytime duration. This duration is seasonal and changes throughout the year.

As a result of our collaboration with the VTS, we have incorporated their limitations and arguments, and developed a scheduling algorithm to plan the daytime traffic in the Istanbul Strait. The objective is to answer the following questions for any given day:

- Which direction should be opened to traffic first?
- How many northbound and southbound Class T6 and Class A vessels will pass?
- How many Class C, P, D, and E vessels will pass between scheduled Class A vessels?

In the section below, we present an algorithmic view of the scheduling decisions in the Istanbul VTS.

DAY TIME VESSEL SCHEDULING ALGORITHM

Since Class T6 and Class A vessels can only pass through the Istanbul Strait during daytime, the VTS gives these types of vessels priority in daytime scheduling. Every morning, two hours before the sunrise, VTS operators determine the daytime transit vessel schedule of that day.

They first decide on the Class T6 and Class A vessels that will pass that day in both directions based on the list of vessels that have submitted their SP 2 but have not entered the Strait. Then, they schedule the rest of the vessels that will enter between consecutive Class A vessels based on the schedules depicted in Figures 2.6 and 2.7. On the other hand, since two-way traffic is suspended during the passage of Class T6 vessels, no other vessel is scheduled until a Class T6 vessel the Strait.

STEP 1: SCHEDULING CLASS T6 AND CLASS A VESSELS

No other vessel is scheduled after the last Class A vessel in the initial direction. The next scheduled vessel should be a Class T6 or Class A vessel in the opposite direction.

The number of Class T6 and Class A vessels that will pass that day is determined considering the following VTS policies:

- Daytime starts at dawn and ends at sunset.
- Vessels with longer waiting times are schedule to enter the Strait first.
- Class T6 vessels have priority over Class A vessels.
- Indirect-passing vessels have priority over direct-passing vessels.
- Southbound indirect-passing stopover vessels have priority over northbound indirect-passing vessels.

Therefore, Class T6 and Class A vessels are first sorted in decreasing order of adjusted waiting times (W^a) within their respective classes. The two vessel groups are then combined in a tentative list, in which Class T6 vessels precede Class A vessels. This list includes all vessels ready to enter the Strait from both directions.

Adjusted Waiting Times

The *adjusted waiting time* of vessel *j* is defined by

$$W_j^a = c \times W_j \tag{2.1}$$

where $c = \begin{cases} 1.5 & \text{Vessel } j \text{ is a southbound indirect-passing vessel} \\ 1.25 & \text{Vessel } j \text{ is a northbound indirect-passing vessel} \\ 1 & \text{Otherwise} \end{cases}$.

The constant *c* introduced above is a priority factor used to update the waiting time of a vessel to capture the VTS policies mentioned above, which state that a southbound indirect-passing vessel has priority over a northbound indirect-passing vessel, which has priority over any direct-passing vessel. Values of *c* were decided upon jointly with the Istanbul Strait VTS.

A Tentative Vessel List

Next, the number of Class T6 and Class A vessels in the *tentative list* that will be able to enter the Strait that day is determined considering the *start time*, *ST*, and the *maximum operational duration* of the daytime schedule, *SD*. *ST* and *SD* values in different seasons are given in Table 2.6.

Table 2.6 Start time and maximum operational duration

SEASON	ST	SD (min.)
Winter	7:00 a.m.	615
Spring	6:30 a.m.	735
Summer	6:00 a.m.	855
Fall	6:30 a.m.	735

In addition, the allowed time gaps between consecutive Class T6 and Class A vessels as mentioned in section **Error! Reference source not found.** are given in Table 2.7. The time differential is due to the direction of the surface current (north to south) and the fact that the time it takes to navigate from the south entrance to Fil Burnu is longer than the one from the north entrance to the Boğaziçi Bridge.

Table 2.7 Time gap between consecutive Class T6 and Class A vessels

	SOUTHBOUND	NORTHBOUND
Class A	75 min.	90 min.
Class T6	105 min.	120 min.

The time gaps shown in Table 2.7 correspond to the time it takes for a northbound or a southbound Class A vessel to reach Fil Burnu or the Boğaziçi Bridge, respectively. According to the VTS, it takes an extra 30 minutes for a Class A vessel to leave the Strait. Therefore, the time gap between the last northbound or southbound Class A vessel and the following vessel from the opposite direction should be 120 or 105 minutes, respectively.

Starting from the top of the *tentative list*, the vessels are added to a *secondary list* one by one and the *cumulative passage time*, *CPT*, is calculated using the information given in Tables 2.6 and 2.7 until $CPT > SD$. Then, the last vessel for which $CPT > SD$ is returned to the *tentative list* and *CPT* is assigned to its previous value. The new list forms the *initial schedule* of Class T6 and Class A vessels that will enter the Strait that day from both directions.

Let $m = m^{(S)} + m^{(N)}$

where

m : Total number of Class T6 and Class A vessels in the *initial schedule*

$m^{(S)}$: Number of southbound Class T6 and Class A vessels in the *initial schedule*

$m^{(N)}$: Number of northbound Class T6 and Class A vessels in the *initial schedule*.

Through our discussions with the VTS operators, we concluded that there was a tendency to schedule more Class T6 and Class A vessels from the entrance, which had more set $\mathcal{L}$ vessels (Class P, E, and D) waiting. Scheduling more Class T6 and Class A vessels in a direction means allowing more time for the traffic flow, and therefore decreasing the vessel congestion in that direction. Another factor that influenced the operators' decisions was whether there were enough of set $\mathcal{L}$ vessels to schedule between consecutive Class A vessels. Therefore, in order to mimic the scheduling policies used by the operators we have decided to consider the following factors in addition to the factors listed above:

- Average waiting time of the Class T6 and Class A vessels
- Average waiting time of set $\mathcal{L}$ vessels
- Sufficient number of set $\mathcal{L}$ vessels to be scheduled between Class A vessels
- Average waiting time of Class C vessels
- Sufficient number of Class C vessels to be scheduled between Class A vessels
- Average waiting time of set $\mathcal{L}'$ vessels
- Sufficient number of set $\mathcal{L}'$ vessels to be scheduled between Class A vessels

where

$\mathcal{L}$: Set of Class P, E, and D vessels.

$\mathcal{L}'$: Set of Class P, C, E , and D vessels not requesting pilot.

Final Number of Class T6 and A Vessels

In order to determine the final number of Class T6 and Class A vessels in the schedule, we consider three different scenarios. *Scenario 1* is the base scenario, which represents the *initial schedule* with $m^{(S)}$ southbound and $m^{(N)}$ northbound Class T6 and/or Class A vessels. This scenario includes the Class T6 and Class A vessels with the longest waiting times, but it is also desired that there are enough Class C, set $\mathcal{L}$, and set $\mathcal{L}'$ vessels to fill the time gaps between consecutive Class A vessels in each direction.

In *Scenario 2*, the number of northbound Class T6 and/or Class A vessels is increased by 1 (i.e., $m^{(N)}+1$) and the number of southbound vessels is decreased by 1 (i.e., $m^{(S)}-1$) without changing the total number of vessels in the schedule (*m*). The purpose is to check to see if scheduling more northbound vessels during daytime will result in a better schedule at the end. To do so, the last southbound vessel in the *initial schedule* is taken out and instead the first northbound vessel in the *tentative list* is added.

On the other hand, *Scenario 3* includes $m^{(S)}+1$ southbound and $m^{(N)}-1$ northbound Class T6 and/or Class A vessels. In this scenario, more southbound vessels are scheduled while the total number of vessels in the schedule, *m*, remains the same. Similar to the procedure explained above, the last northbound vessel in the *initial schedule* is taken out and instead the first southbound vessel in the *tentative list* is added.

Let $m_i^{(l)}$ be the number of Class T6 and Class A vessels scheduled in direction *l* in scenario *i*. Therefore,

- $m_1^{(S)} = m^{(S)}$ and $m_1^{(N)} = m^{(N)}$
- $m_2^{(S)} = m^{(S)} - 1$ and $m_2^{(N)} = m^{(N)} + 1$
- $m_3^{(S)} = m^{(S)} + 1$ and $m_3^{(N)} = m^{(N)} - 1$

Note: If $m^{(S)} \in \{0,1\}$, then we only consider scenarios 1 and 3.

If $m^{(N)} \in \{0,1\}$, then we only consider scenarios 1 and 2.

The main goal of the scheduling algorithm is to schedule the vessels with longer adjusted waiting times first while filling the time windows between Class A vessels as much as possible. Therefore, in order to compare the scenarios, and determine which one gives the best schedule, the following objective function is evaluated for each:

$$Z_i = k_1 \times \bar{W}^{a}_{\{T6,A\},i} + k_2 \times \left(GW_i^{(N)} + GW_i^{(S)} \right) \tag{2.2}$$

where

Z_i: Weighted average of vessel waiting times in scenario *i*

$\bar{W}^{a}_{\{T6,A\},i}$: Average adjusted waiting time of Class T6 and Class A vessels in scenario *i* in both directions

$GW_i^{(l)}$: Generalized waiting time of vessels other than Class T6 and A vessels in direction *l* in scenario *i* $\left(l \in \{N, S\} \right)$

k_1: Weight of Class T6 and A vessel waiting times ($k_1 = 1$)

k_2: Weight of the generalized waiting times of vessels other than Class T6 and A ($k_2 = 0.75$)

As mentioned before, it is desired to give priority to the Class T6 and Class A vessels with longer adjusted waiting times. The first portion of the objective function ($k_1 \times \bar{W}^{a}_{\{T6,A\},i}$) represents the average waiting time of Class T6 and Class A vessels in schedule according to a particular scenario. The higher this value is the higher the objective function, Z_i, is.

In addition, it is important to schedule first the other vessels with longer adjusted waiting times between consecutive Class A vessels while utilizing time windows as much as possible. This means leaving as few empty time slots between Class A vessels as possible. This is emphasized by $(k_2 \times (GW_i^{(N)} + GW_i^{(S)}))$ in the second part of the objective function.

Furthermore, Class T6 and Class A vessels have priority over other vessels in daytime schedule. Therefore, multiplicative constants k_1 and k_2 indicating the relative importance of Class T6 and Class A vessels, and other vessels, respectively, are used. Current values of k_1 and k_2 are assumed to be 1 and 0.75, respectively as decided upon jointly with the VTS.

<u>Generalized Waiting Time of Other Vessels</u>

The generalized waiting time of vessels other than Class T6 and Class A vessels in direction *l* in scenario *i*, $GW_i^{(l)}$, is defined by

$$GW_i^{(l)} = \overline{W}_{\{\mathcal{L}\},i}^{a(l)} \times q_{\{\mathcal{L}\},i}^{(l)} + \overline{W}_{\{C\},i}^{a(l)} \times q_{\{C\},i}^{(l)} + \overline{W}_{\{\mathcal{L}'\},i}^{a(l)} \times q_{\{\mathcal{L}'\},i}^{(l)} \qquad (2.3)$$

where

$\overline{W}_{\{j\},i}^{a(l)}$: Average adjusted waiting time of class *j* vessels in direction *l* in scenario *i*

$q_{\{j\},i}^{(l)}$: Sufficiency constant of class *j* vessels in direction *l* in scenario *i*

The sufficiency constants introduced above are calculated using (2.4). A *sufficiency constant* is the ratio of the existing number of vessels to the necessary number of vessels to fill the time slots between consecutive Class A vessels. It corresponds to the utilization of a specific time slots.

$$q_{\{j\},i}^{(l)} = \min\left(1, \frac{E_{\{j\}}^{(l)}}{N_{\{j\},i}^{(l)}}\right) \tag{2.4}$$

where

$E_{\{j\}}^{(l)}$: Existing number of class *j* vessels in direction *l*

$N_{\{j\},i}^{(l)}$: Necessary number of class *j* vessels in direction *l* between Class A vessels in scenario *i*

<u>Necessary Number of Vessels between Class A Vessels</u>

Class C Vessels

The necessary number of Class C vessels in direction *l* to sail between Class A vessels in scenario *i* is defined by

$$N_{\{C\},i}^{(l)} = \max\left[\left(m_i^{(l)} - m_{\{T6\},i}^{(l)} - 1\right) \times K_C^{(l)} ; 10^{-6}\right] \tag{2.5}$$

where

$m_{\{T6\},i}^{(l)}$: Number of Class T6 vessels scheduled in direction *l* in scenario *i*

$K_C^{(l)}$: Number of Class C vessels that may be scheduled between two consecutive Class A vessels in direction *l*.

In (2.5), $m_i^{(l)} - m_{\{T6\},i}^{(l)}$ gives the number of consecutive Class A pairs, while $m_i^{(l)} - m_{\{T6\},i}^{(l)} - 1$ gives the number of time intervals between them. Further, $\left(m_i^{(l)} - m_{\{T6\},i}^{(l)} - 1\right) \times K_C^{(l)}$ is the number of Class C vessels in direction *l* that may be scheduled according to the schedule in scenario *i*. As seen in figures 2.6 and 2.7, the number of Class C vessels that may be scheduled between two consecutive Class A vessels is: $K_C^{(l)} = \begin{cases} 1 & l = \text{S} \\ 2 & l = \text{N} \end{cases}$. Also, the "max" term in (2.5) ensures that $N_{\{C\},i}^{(l)}$ is greater than 0 in case there are no time intervals in scenario *i*.

Class P, D, and E Vessels

The necessary number of set $\mathcal{L}$ vessels in direction *l* to sail between Class A vessels in scenario *i* is defined by

$$N_{\{\mathcal{L}\},i}^{(l)} = \max\left[\left(m_i^{(l)} - m_{\{T6\},i}^{(l)} - 1\right) \times K_{\mathcal{L}}^{(l)} + \max\left(0, \left(N_{\{C\},i}^{(l)} - E_{\{C\}}^{(l)}\right)\right); 10^{-6}\right] \tag{2.6}$$

where

$K_{\mathcal{L}}^{(l)}$: Number of set $\mathcal{L}$ vessels that may be scheduled between two consecutive Class A vessels in direction *l*

Similarly, $(m_i^{(l)} - m_{\{T6\},i}^{(l)} - 1) \times K_{\mathcal{L}}^{(l)}$ in (2.6) provides the total number of set $\mathcal{L}$ vessels in direction *l* that may be scheduled according to scenario *i*. As seen in figures 2.6 and 2.7, the number of set $\mathcal{L}$ vessels that may be scheduled between two consecutive Class A vessels is: $K_{\mathcal{L}}^{(l)} = \begin{cases} 5 & l = \mathrm{S} \\ 6 & l = \mathrm{N} \end{cases}$.

In order to obtain the necessary number of set $\mathcal{L}$ vessels in direction *l*, $N_{\{\mathcal{L}\},i}^{(l)}$, the number of empty time slots for Class C vessels represented by $\max\left(0,\left(N_{\{C\},i}^{(l)} - E_{\{C\}}^{(l)}\right)\right)$ is also added. $N_{\{C\},i}^{(l)} - E_{\{C\}}^{(l)}$ represents the shortage of Class C vessels, which may be replaced by set $\mathcal{L}$ vessels, while the "max" term ensures that only a positive shortage of Class C vessels is accounted for.

Vessels not requesting pilots

The necessary number of set $\mathcal{L}'$ vessels in direction *l* not requesting pilot to be scheduled between Class A vessels in scenario *i* is calculated using:

$$N_{\{\mathcal{L}'\},i}^{(l)} = \max\left[\left(m_i^{(l)} - m_{\{T6\},i}^{(l)} - 1\right) \times K_{\mathcal{L}'}^{(l)} - \left(2P^{(l)} - m_i^{(l)}\right); 10^{-6}\right] \tag{2.7}$$

where

$K_{\mathcal{L}'}^{(l)}$: Number of set $\mathcal{L}'$ vessels that may be scheduled in between Class A vessels in direction *l*

$P^{(l)}$: Number of available pilots in direction *l*

Correspondingly, $\left(m_i^{(l)} - m_{\{T6\},i}^{(l)} - 1\right) \times K_{\mathcal{L}'}^{(l)}$ in (2.7) provides the total number of set $\mathcal{L}'$ vessels in direction *l* that may be scheduled according to the schedule in scenario *i*. As seen in figures 2.6 and 2.7, the number of set $\mathcal{L}'$ vessels that may be scheduled between two consecutive Class A vessels is: $K_{\mathcal{L}'}^{(l)} = \begin{cases} 6 & l = \text{S} \\ 8 & l = \text{N} \end{cases}$.

To obtain the necessary number of set $\mathcal{L}'$ vessels in direction *l*, $N_{\{\mathcal{L}'\},i}^{(l)}$, the number of available pilots in scenario *i* represented by $2P^{(l)} - m_i^{(l)}$ is subtracted. $2P^{(l)}$ represents the maximum total number of pilots that may be available for the course of a daytime schedule in direction *l*. The number of available pilots in direction *l*, $P^{(l)}$, is multiplied by 2 because according to the *ST* and *SD* values introduced earlier and the current practice of taxiing the pilots from one entrance to another, it is concluded that each available pilot may be utilized twice during a daytime schedule in each direction. Then, the number of Class T6 and Class A vessels scheduled in direction *l* in scenario *i*, $m_i^{(l)}$ is subtracted from $2P^{(l)}$ to ensure that each Class T6 and Class A vessel receives a pilot.

In addition, the existing number of set $\mathcal{L}'$ vessels in direction *l* is defined by

$$E_{\{\mathcal{L}'\}}{}^{(l)} = E_{\{D'\}}{}^{(l)} + E_{\{E'\}}{}^{(l)} + E_{\{P'\}}{}^{(l)} + \min\left(E_{\{C'\}}{}^{(l)}, N_{\{C\},i}{}^{(l)}\right) \tag{2.8}$$

where

$E_{\{j'\}}{}^{(l)}$: Existing number of class *j* vessels in direction *l* not requesting pilot

To obtain the necessary number of vessels not requesting pilots, the minimum of existing and necessary number of Class C vessels not requesting pilot, $\min\left(E_{\{C'\}}{}^{(l)}, N_{\{C\},i}{}^{(l)}\right)$, should also be taken into account in addition to the number of Class D, E, and P vessels not requesting pilots. If there are more than the necessary number, these should not count towards the $E_{\{\mathcal{L}'\}}^{(l)}$ since Class C vessels can be replaced by Class D, E, and P vessels in the schedule but not vice versa.

Scenario comparison

In order to determine the number of Class T6 and Class A vessels that will pass through the Strait in each direction, we evaluate Z_i for each alternative scenario *i*, $i = \{1,2,3\}$.

If $Z_1 \geq \max(Z_2, Z_3)$, then we choose Scenario 1 (the original tentative schedule) with $m_1^{(S)} = m^{(S)}$ and $m_1^{(N)} = m^{(N)}$.

If $Z_2 \geq \max(Z_1, Z_3)$, then we choose Scenario 2 with $m_2^{(S)} = m^{(S)} - 1$ southbound and $m_2^{(N)} = m^{(N)} + 1$ northbound Class T6 and Class A vessels that will pass during the daytime schedule.

Otherwise, if $Z_3 \geq \max(Z_1, Z_2)$, then Scenario 3 is the best scenario with $m_3^{(S)} = m^{(S)} + 1$ and $m_3^{(N)} = m^{(N)} - 1$.

The objective function introduced in (2.2) can be shown in further detail below:

$$Z_i = k_1 \times \bar{W}^{a}_{\{T6,A\}}(i) + k_2 \times \begin{pmatrix} \bar{W}^{a(N)}_{\{\mathcal{L}\},i} \times q^{(N)}_{\{\mathcal{L}\},i} + \bar{W}^{a(N)}_{\{C\},i} \times q^{(N)}_{\{C\},i} + \bar{W}^{a(N)}_{\{\mathcal{L}'\},i} \times q^{(N)}_{\{\mathcal{L}'\},i} \\ +\bar{W}^{a(S)}_{\{\mathcal{L}\},i} \times q^{(S)}_{\{\mathcal{L}\},i} + \bar{W}^{a(S)}_{\{C\},i} \times q^{(S)}_{\{C\},i} + \bar{W}^{a(S)}_{\{\mathcal{L}'\},i} \times q^{(S)}_{\{\mathcal{L}'\},i} \end{pmatrix} \tag{2.9}$$

As seen in (2.9), if there are sufficient number of vessels to schedule between Class A vessels in scenario i, meaning all the sufficiency constants are equal to 1, then the scenario including the vessels with the longer average adjusted waiting times is the best option. Furthermore, the first part of the equation ($k_1 \times \bar{W}^{a}_{\{T6,A\}}(i)$) has the highest value in *Scenario 1*. Thus, the value of this term decreases in *Scenario 2* and *Scenario 3* but on the other hand the second part of the equation incorporating the sufficiency constants might increase. Therefore, the idea in comparing the additional two scenarios to the base scenario is to see if the increase in the vessel sufficiency is greater than the decrease in the average adjusted waiting time of the Class T6 and Class A vessels.

Eventually, the goal is to continue scenario comparisons until there is no improvement in the objective function. For example, if *Scenario 2* gives the best objective function in the first iteration, then an additional scenario with $m^{(S)}-2$ southbound and $m^{(N)}+2$ northbound Class T6 and Class A vessels is compared to *Scenario 2*. The iterations are then repeated until a new scenario does not improve the objective function. In the current application we have implemented only one iteration as described above.

STEP 2: SCHEDULING CLASS P, C, E, AND D VESSELS

As mentioned before, after deciding on the Class T6 and Class A vessels that will pass that day in both directions, the rest of the vessels are scheduled between consecutive Class A vessels according to the example schedules depicted in Figures 2.6 and 2.7.

Set $\mathcal{L}$ vessels (Class P, E, and D) are scheduled at 10-minute intervals between consecutive Class A vessels in the same direction. According to the VTS, passenger vessels have priority over any other type of vessels and tankers have priority over dry cargo vessels. Therefore, set $\mathcal{L}$ vessels are scheduled based on the following order of priority: $P > E > D$. If there are no set $\mathcal{L}$ vessels available, that time slot is left empty.

In addition, Class C vessels are scheduled at 30-minute intervals between consecutive Class A vessels in the same direction. If there are no Class C vessels available, then a set $\mathcal{L}$ vessel may be scheduled instead. If there are no set $\mathcal{L}$ vessels available, then that time slot is left empty.

Class P, E, D, and C vessels are scheduled within their classes and directions according to the same ordering policy. First, the vessels are listed in a decreasing order of adjusted waiting times. Then, the vessels necessary to fill the corresponding time slots between consecutive Class A vessels are removed from the list. This removed group of vessels is then separated in two groups: vessels requesting pilot and others. These two groups are then sorted in decreasing order of speed. Finally, the two sorted groups are combined into one final list where the vessels requesting pilot are listed first. The vessels are scheduled using this final list

STEP 3: INITIAL DIRECTION OF DAYTIME SCHEDULE

After determining the daytime schedule in both directions, operators at the VTS select the direction of traffic. Through our discussions with the officials, we have determined that they consider the following factors when deciding on which direction to start the daytime schedule:

- Total number of vessels waiting at both entrances
- Total waiting time of all vessels scheduled according to the chosen scenario
- Number of Class T6 and Class A vessels scheduled according to the chosen scenario

In order to compare the vessel congestion in the southern and the northern entrances, a score value is assigned to each direction. The score value of direction *l*, $S^{(l)}$ is defined by

$$S^{(l)} = a\frac{E_{\text{All}}{}^{(l)}}{E_{\text{All}}{}^{(l)} + E_{\text{All}}{}^{(l')}} + b\frac{TW^{(l)}}{TW^{(l)} + TW^{(l')}} + c\frac{m^{(l)}}{m^{(l)} + m^{(l')}} \qquad (2.10)$$

where

l: The opposite direction

$E_{\text{All}}{}^{(l)}$: Total number of vessels waiting in the queue in direction *l*

$TW^{(l)}$: Total waiting time of all vessels in direction *l* scheduled to the pass

The objective is to start the daytime schedule in the direction with greater number of vessels waiting, the longer total waiting times, and the greater number of Class T6 and Class A vessels scheduled in the chosen scenario. Each component in (2.10) corresponds to the relative value of a factor for a direction compared to the total value for both directions. All three terms represent ratios instead of individual values and they can therefore be added together.

The multiplicative constants a, b and c indicate the relative importance of the three decision factors listed above. Current values of a, b and c are assumed to be 0.5, 0.3 and 0.2, respectively as dictated by the VTS.

Finally, the direction with higher score is selected as the initial direction of the daytime traffic.

The daytime schedule described above is the initial schedule determined two hours before daytime starts. Additionally, at the end of daytime traffic schedule in each direction, the schedule is updated if $CPT < SD$ and there is a new Class A vessel waiting in the queue.

The summary of the scheduling algorithm procedure is given below.

Schedule of Class T6 and Class A Vessels

STEP 1: Let $\mathcal{J}$ be the set of Class T6 vessels and $\mathcal{H}$ be the set of Class A vessels

Sort $\mathcal{J}$ and $\mathcal{H}$ in decreasing order of *adjusted waiting times*

W_j^a : adjusted waiting time of vessel *j*

$W_j^a = c \times W_j$

where $c = \begin{cases} 1.5 & \text{vessel } j \text{ is a southbound indirect-passing vessel} \\ 1.25 & \text{vessel } j \text{ is a northbound indirect-passing vessel} \\ 1 & \text{otherwise} \end{cases}$

Let $\mathcal{K} = \mathcal{J} \cup \mathcal{H}$ where $\mathcal{J}$ precedes $\mathcal{H}$

Let $r^{(l)}$ be the number of vessel in $\mathcal{K}$ sailing in direction l.

STEP 2: If $r^{(N)} + r^{(S)} = 0$, STOP! NO NEED FOR DAYTIME SCHEDULING!

Otherwise,

Set $n = 1$, $CPT = 0$ and $I = \varnothing$

Let T_j be the time vessel *j* needs to travel until a consecutive vessel may enter.

STEP 3: Let $\mathcal{V}_n$ be the *n*th vessel in $\mathcal{K}$.

Set $CPT = CPT + T_{\mathcal{V}_n}$.

STEP 4: If $CPT > SD$, GO TO *STEP 5*

Otherwise,

If $\mathcal{V}_n$ is the last vessel in $\mathcal{K}$, GO TO *STEP 6*

Otherwise, set $n = n + 1$, $I = I \cup \{\mathcal{V}_n\}$, and GO TO *STEP 3*.

STEP 5: Set $CPT = CPT - T_{\mathcal{V}_n}$.

STEP 6: Set $\mathcal{K} = \mathcal{K} - I$

Let $m^{(S)}$ and $m^{(N)}$ be the number of southbound and northbound vessels in I, respectively.

Let $\mathcal{P}_l$, $\mathcal{C}_l$, $\mathcal{E}_l$, and $\mathcal{D}_l$ be the set of Class P, C, E, and D vessels in direction l, respectively.

Let $\mathcal{P}_l'$, $\mathcal{C}_l'$, $\mathcal{E}_l'$, and $\mathcal{D}_l'$ be the set of Class P, C, E, and D vessels not requesting pilot in direction l, respectively.

Sort $\mathcal{P}_l$, $\mathcal{P}_l'$, $\mathcal{C}_l$, $\mathcal{C}_l'$, $\mathcal{E}_l$, $\mathcal{E}_l'$, $\mathcal{D}_l$, and $\mathcal{D}_l'$ in decreasing order of W^a for $l = N$ and $l = S$.

Set $\mathcal{L}_l = \mathcal{P}_l \cup \mathcal{E}_l \cup \mathcal{D}_l$ for $l = N$ and $l = S$.

Set $\mathcal{L}_l' = \mathcal{P}_l' \cup \mathcal{C}_l' \cup \mathcal{E}_l' \cup \mathcal{D}_l'$ for $l = N$ and $l = S$.

STEP 7: Set $i = 1$ and $I_i = I$.

Let $m_i^{(l)}$ be the number of vessels scheduled in direction l in I_i.

Set $m_i^{(N)} = m^{(N)}$ and $m_i^{(S)} = m^{(S)}$.

Set $l = N$.

Set $Z_i = 0$ for $i = \{1,2,3\}$.

STEP 8: If $m^{(l)} = 0$, GO TO *STEP 15*

Otherwise,

Let $E_{\{\mathcal{L}\}}^{(l)}$ be the existing number of vessels in $\mathcal{L}_l$.

Let $E_{\{C\}}^{(l)}$ be the existing number of vessels in $\mathcal{C}_l$.

STEP 9: Let $m_{\{T6\},i}^{(l)}$ be the number of Class T6 vessels in direction *l* in I_i.

Let $K_C^{(l)}$ be the number of Class C vessels that may be scheduled in between two consecutive Class A vessels in direction *l*.

Set $K_C^{(l)} = \begin{cases} 1 & l = \mathrm{S} \\ 2 & l = \mathrm{N} \end{cases}$ and $N_{\{C\},i}^{(l)} = \max\left(\left(m_i^{(l)} - m_{\{T6\},i}^{(l)} - 1\right) \times K_C^{(l)}; 10^{-6}\right)$.

STEP 10: Let $K_{\mathcal{L}}^{(l)}$ be the number of set $\mathcal{L}_l$ vessels that may be scheduled in between Class A vessels.

Set $K_{\mathcal{L}}^{(l)} = \begin{cases} 5 & l = \mathrm{S} \\ 6 & l = \mathrm{N} \end{cases}$.

Set $N_{\{\mathcal{L}\},i}^{(l)} = \max\left[\left(m_i^{(l)} - m_{\{T6\},i}^{(l)} - 1\right) \times K_{\mathcal{L}}^{(l)} + \max\left(0, \left(N_{\{C\},i}^{(l)} - E_{\{C\}}^{(l)}\right)\right); 10^{-6}\right]$.

STEP 11: Let $K_{\mathcal{L}'}^{(l)}$ be the number of set $\mathcal{L}_l$' vessels that may be scheduled in between Class A vessels.

Let $P^{(l)}$ be the number of available pilots in direction *l*.

Set $K_{\mathcal{L}'}^{(l)} = \begin{cases} 6 & l = \mathrm{S} \\ 8 & l = \mathrm{N} \end{cases}$.

Set $N_{\{\mathcal{L}'\},i}^{(l)} = \max\left(\left(m_i^{(l)} - m_{\{T6\},i}^{(l)} - 1\right) \times K_{\mathcal{L}'}^{(l)} - \left(2P^{(l)} - m_i^{(l)}\right); 10^{-6}\right)$.

STEP 12: Let $E_{\{j'\}}{}^{(l)}$ be the existing number of class *j* vessels in direction *l* not requesting pilot.

Set $E_{\{\mathcal{L}'\}}{}^{(l)} = E_{\{D'\}}{}^{(l)} + E_{\{E'\}}{}^{(l)} + E_{\{P'\}}{}^{(l)} + \min\left(E_{\{C'\}}{}^{(l)}, N_{\{C\},i}{}^{(l)}\right)$.

STEP 13: Set $q_{\{\mathcal{L}\},i}^{(l)} = \min\left(1; \dfrac{E_{\{\mathcal{L}\}}^{(l)}}{N_{\{\mathcal{L}\},i}^{(l)}}\right)$, $q_{\{C\},i}^{(l)} = \min\left(1; \dfrac{E_{\{C\}}^{(l)}}{N_{\{C\},i}^{(l)}}\right)$, and $q_{\{\mathcal{L}'\},i}^{(l)} = \min\left(1; \dfrac{E_{\{\mathcal{L}'\}}^{(l)}}{N_{\{\mathcal{L}'\},i}^{(l)}}\right)$.

STEP 14: Let $\overline{W}^{a(l)}_{\{\mathcal{L}\},i}$ be the average adjusted waiting time of the first $\min\left(E^{(l)}_{\{\mathcal{L}\}}, N^{(l)}_{\{\mathcal{L}\},i}\right)$ vessels in $\mathcal{L}_l$.

Let $\overline{W}^{a(l)}_{\{\mathcal{C}\},i}$ be the average adjusted waiting time of the first $\min\left(E^{(l)}_{\{\mathcal{C}\}}, N^{(l)}_{\{\mathcal{C}\},i}\right)$ vessels in $\mathcal{C}_l$.

Let $\overline{W}^{a(l)}_{\{\mathcal{L}'\},i}$ be the average adjusted waiting time of the first $\min\left(E^{(l)}_{\{\mathcal{L}'\}}, N^{(l)}_{\{\mathcal{L}'\},i}\right)$ vessels in $\mathcal{L}_l{}'$.

Set $GW^{(l)}_i = \overline{W}^{a(l)}_{\{\mathcal{L}\},i} \times q^{(l)}_{\{\mathcal{L}\},i} + \overline{W}^{a(l)}_{\{\mathcal{C}\},i} \times q^{(l)}_{\{\mathcal{C}\},i} + \overline{W}^{a(l)}_{\{\mathcal{L}'\},i} \times q^{(l)}_{\{\mathcal{L}'\},i}$.

STEP 15: If $l = S$, GO TO *STEP 16*

Otherwise, set $l = S$ and GO TO *STEP 8*.

STEP 16: Let $\overline{W}^{a(l)}_{I,i}$ be the average adjusted waiting time of the vessels in I_i.

Set $k_1 = 1$, $k_2 = 0.75$, and $Z_i = k_1 \times \overline{W}^{a}_{\{I\},i} + k_2 \times \left(GW^{(N)}_i + G_iW^{(S)}\right)$.

STEP 17: If $i = 2$, GO TO *STEP 19*

If $i = 3$, GO TO *STEP 20*

Otherwise, GO TO *STEP 18*.

STEP 18: If $m^{(S)} = 0$ or $m^{(N)} = r^{(N)}$, GO TO *STEP 19*

Otherwise,

Set $i = 2$.

Let $\mathcal{W}^{(S)}$ be the last southbound vessel in I.

Set $I_i = I - \left\{\mathcal{W}^{(S)}\right\}$.

Let $\mathcal{V}^{(N)}$ be the first northbound vessel in $\mathcal{K}$.

Set $I_i = I_i \cup \{\mathcal{V}^{(N)}\}$.

Set $m_i^{(N)} = m^{(N)} + 1$, $m_i^{(S)} = m^{(S)} - 1$, $l = N$ and GO TO *STEP 8*.

STEP 19: If $m^{(N)} = 0$ or $m^{(S)} = r^{(S)}$, GO TO *STEP 20*

Otherwise,

Set $i = 3$.

Let $\mathcal{W}^{(N)}$ be the last northbound vessel in I.

Set $I_i = I - \{\mathcal{W}^{(N)}\}$.

Let $\mathcal{V}^{(S)}$ be the first southbound vessel in $\mathcal{K}$.

Set $I_i = I_i \cup \{\mathcal{V}^{(S)}\}$.

Set $m_i^{(N)} = m^{(N)} - 1$ and $m_i^{(S)} = m^{(S)} + 1$.

STEP 20: If $Z_1 \geq \max(Z_2, Z_3)$, set $I = I_1$ and $i = 1$.

If $Z_2 \geq \max(Z_1, Z_3)$, set $I = I_2$, $m^{(S)} = m_2^{(S)}$, $m^{(N)} = m_2^{(N)}$ and $i = 2$.

If $Z_3 \geq \max(Z_1, Z_2)$, set $I = I_3$, $m^{(S)} = m_3^{(S)}$, $m^{(N)} = m_3^{(N)}$ and $i = 3$.

Schedule northbound and southbound Class T6 vessels in I at 120 and 105-minute time intervals, respectively.

Schedule northbound and southbound Class A vessels in I at 90 and 75-minute time intervals, respectively.

<u>Schedule Class P, C, E, and D Vessels</u>

STEP 21: Set $\mathcal{C}_l*, \mathcal{L}_l* = \varnothing \ \ \forall l$

Let $j_l \in \{\mathcal{C}_l, \mathcal{L}_l\}$.

For $\forall j_l$ and $\forall l$,

- Remove first $\min\left(E_j^{(l)}, N_{j,i}^{(l)}\right)$ vessels from j_l and put them in $j_l *$.
- Divide $j_l *$ in two groups $j_l^1 *$ and $j_l^2 *$ such that all vessels in $j_l^1 *$ request pilot and all vessels in $j_l^2 *$ do not request pilot.
- Sort $j_l^1 *$ and $j_l^2 *$ in decreasing order of speed.
- Set $j_l * = j^1 * \cup j^2 *$ where $j_l *$ is the final list of class *j* vessels.

STEP 22: Schedule vessels in $\mathcal{L}_N *$ and $\mathcal{L}_S *$ at 10-minute and vessels in $\mathcal{C}_N *$ and $\mathcal{C}_S *$ at 30-minute time intervals.

<u>Initial Direction of Daytime Schedule</u>

STEP 24: Let $E_{\text{All}}^{(l)}$ be the total number of vessels waiting in direction *l*

Let $TW^{(l)}$ be the total waiting time of all vessels in direction *l* scheduled to pass

Set $a = 0.5$, $a = 0.3$ and $a = 0.2$.

Set $S^{(N)} = a\dfrac{E_{\text{All}}^{(N)}}{E_{\text{All}}^{(N)} + E_{\text{All}}^{(S)}} + b\dfrac{TW^{(N)}}{TW^{(N)} + TW^{(S)}} + c\dfrac{m^{(N)}}{m^{(N)} + m^{(S)}}$.

Set $S^{(S)} = a\dfrac{E_{\text{All}}^{(S)}}{E_{\text{All}}^{(S)} + E_{\text{All}}^{(N)}} + b\dfrac{TW^{(S)}}{TW^{(S)} + TW^{(N)}} + c\dfrac{m^{(S)}}{m^{(S)} + m^{(N)}}$.

STEP 25: If $S^{(N)} > S^{(S)}$, select North

Otherwise, select South.

NUMERICAL EXAMPLE

In this section, we demonstrate the proposed algorithm using the data representing the vessel traffic on May 13, 2005 in the Istanbul Strait where the day started at 6:30 am and the day time duration was 735 minutes. According to the 2005 data, on May 13, there are no Class T6 and Class P vessels waiting in the queue. The list of Class A vessels that have submitted their SP 2 by 4:30 a.m. is listed in Table 2.8.

Table 2.8 List of Class A vessels that have submitted their SP 2 on May 13, 2005

Vessel No	Direction	Stopover	Pilot Request	Waiting Time (min.)	Adjusted Waiting Time (min.)
108615	S	N	Y	2,587.52	2,587.52
108658	S	Y	Y	2,823.22	4,234.83
108696	S	N	Y	1,927.58	1,927.58
108803	S	Y	Y	1,809.33	2,714.00
108829	S	N	Y	895.12	895.12
108830	S	Y	Y	1,099.13	1,648.70
109018	N	N	Y	798.75	798.75
109109	N	N	Y	447.15	447.15
109117	N	Y	Y	200.33	250.42
109122	N	Y	Y	397.00	496.25

Below, we demonstrate the algorithm for the aforementioned date.

<u>Schedule of Class T6 and Class A Vessels</u>

STEP 1:

$$\mathcal{J} = \varnothing \;\&\; \mathcal{K} = \mathcal{H} = \begin{Bmatrix} 108658,\ 108803,\ 108615,\ 108696,\ 108830, \\ 108829,\ 109018,\ 109122,\ 109109,\ 109117 \end{Bmatrix}$$

$$r^{(N)} = 4 \;\&\; r^{(S)} = 6$$

STEP 2: $n = 1 \;\&\; CPT = 30 \;\&\; I = \varnothing$

STEP 3: $\mathcal{V}_n = 108658$ & $CPT = 105$

STEP 4: $105 < 735 \Rightarrow n = 2$, $I = \{108658\}$, GO TO *STEP 3*

…

STEP 3: $\mathcal{V}_n = 109122$ & $CPT = 600 + 90 = 690$

STEP 4: $690 < 735 \Rightarrow n = 9$

$I = \{108658, 108803, 108615, 108696, 108830, 108829, 109018, 109122\}$

GO TO *STEP 3*

STEP 3: $\mathcal{V}_n = 109109$ & $CPT = 780$

STEP 4: $780 > 735 \Rightarrow$ GO TO *STEP 5*

STEP 5: $CPT = 690$
$I = \{108658, 108803, 108615, 108696, 108830, 108829, 109018, 109122\}$

STEP 6: $\mathcal{K} = \{109109, 109117\}$, $m^{(S)} = 6$ and $m^{(N)} = 2$

STEP 7: $i = 1$ &

$I_1 = \{108658, 108803, 108615, 108696, 108830, 108829, 109018, 109122\}$

$m_1^{(N)} = 2$ & $m_1^{(S)} = 6$

$l = N$ & $Z_1 = 0, Z_2 = 0, Z_3 = 0$

STEP 8: $E_{\{\mathcal{L}\}}^{(N)} = 15$ & $E_{\{C\}}^{(N)} = 11$

STEP 9: $m_{\{T6\},1}^{(N)} = 0$ & $K_C^{(N)} = 2$ & $N_{\{C\},1}^{(N)} = \max\left((2-0-1)\times 2; 10^{-6}\right) = 2$

STEP 10: $K_{\mathcal{L}}^{(N)} = 6$ & $N_{\{\mathcal{L}\},1}^{(N)} = \max\left[(2-0-1)\times 6 + \max\left(0,(2-11)\right); 10^{-6}\right] = 6$.

STEP 11: $P^{(N)} = 16$ & $K_{\mathcal{L}'}^{(N)} = 8$ & $N_{\{\mathcal{L}'\},1}^{(N)} = \max\left((2-0-1)\times 8 - (32-2); 10^{-6}\right) = 10^{-6}$

STEP 12: $E_{\{\mathcal{L}'\}}{}^{(N)} = 7 + 0 + 0 + \min(11, 2) = 9$

STEP 13: $q_{\{\mathcal{L}\},1}^{(N)} = \min\left(1; \frac{15}{6}\right) = 1$ & $q_{\{C\},1}^{(N)} = \min\left(1; \frac{11}{2}\right) = 1$ & $q_{\{\mathcal{L}'\},1}^{(N)} = \min\left(1; \frac{9}{10^{-6}}\right) = 1$

STEP 14: $\bar{W}_{\{\mathcal{L}\},1}^{a(N)} = 1,345.69$ & $\bar{W}_{\{C\},1}^{a(N)} = 1,895.17$ & $\bar{W}_{\{\mathcal{L}'\},1}^{a(N)} = 0$

$GW_1^{(N)} = 1,345.69 \times 1 + 1,895.17 \times 1 + 0 \times 1 = 3,240.86$.

STEP 15: $l = S$

GO TO *STEP 8*

STEP 8: $E_{\{\mathcal{L}\}}^{(S)} = 20$ & $E_{\{C\}}^{(S)} = 30$

STEP 9: $m_{\{T6\},1}^{(S)} = 0$ & $K_C^{(S)} = 1$ & $N_{\{C\},1}^{(S)} = \max\left((6 - 0 - 1) \times 1; 10^{-6}\right) = 5$

STEP 10: $K_{\mathcal{L}}^{(S)} = 5$ & $N_{\{\mathcal{L}\},1}^{(S)} = \max\left[(6 - 0 - 1) \times 5 + \max\left(0, (5 - 30)\right); 10^{-6}\right] = 30$

STEP 11: $P^{(S)} = 16$ & $K_{\mathcal{L}'}^{(S)} = 6$ & $N_{\{\mathcal{L}'\},1}^{(S)} = \max\left((6 - 0 - 1) \times 6 - (32 - 6); 10^{-6}\right) = 4$.

STEP 12: $E_{\{\mathcal{L}'\}}{}^{(S)} = 11 + 3 + 0 + \min(20, 5) = 19$

STEP 13: $q_{\{\mathcal{L}\},1}^{(S)} = \min\left(1; \frac{20}{30}\right) = 0.67$ & $q_{\{C\},1}^{(S)} = \min\left(1; \frac{30}{5}\right) = 1$ & $q_{\{\mathcal{L}'\},1}^{(S)} = \min\left(1; \frac{19}{4}\right) = 1$

STEP 14: $\bar{W}_{\{\mathcal{L}\},1}^{a(S)} = 1,631.38$ & $\bar{W}_{\{C\},1}^{a(S)} = 2,518.58$ & $\bar{W}_{\{\mathcal{L}'\},1}^{a(S)} = 2,219.3$

$GW_1^{(S)} = 1,631.38 \times 0.67 + 2,518.58 \times 1 + 2,219.3 \times 1 = 5,830.91$

STEP 15: GO TO *STEP 16*

STEP 16: $\bar{W}_{\{I\},1}^{a} = 1,912.84$ & $k_1 = 1$ & $k_2 = 0.75$

$Z_1 = 1 \times 1,912.84 + 0.75 \times (3,240.86 + 5,830.91) = 8,716.67$.

STEP 17: GO TO *STEP 18*

STEP 18: $i = 2 \ \& \ \mathcal{W}^{(S)} = 108829$

$I_2 = \{108658, 108803, 108615, 108696, 108830, 109018, 109122\}$.

$\mathcal{W}^{(N)} = 109109$

$I_2 = \{108658, 108803, 108615, 108696, 108830, 109018, 109122, 109109\}$

$m_2^{(N)} = 3 \ \& \ m_2^{(S)} = 5 \ \& \ l = N$

GO TO *STEP 8*

STEP 8: $E_{\{\mathcal{L}\}}^{(N)} = 15 \ \& \ E_{\{C\}}^{(N)} = 11$

STEP 9: $.\, m_{\{T6\},2}^{(N)} = 0 \ \& \ K_C^{(N)} = 2 \ \& \ N_{\{C\},2}^{(N)} = \max\left((3-0-1)\times 2; 10^{-6}\right) = 4$

STEP 10: $K_{\mathcal{L}}^{(N)} = 6 \ \& \ N_{\{\mathcal{L}\},2}^{(N)} = \max\left[(3-0-1)\times 6 + \max\left(0,(4-11)\right); 10^{-6}\right] = 12$

STEP 11: $P^{(N)} = 16 \ \& \ K_{\mathcal{L}'}^{(N)} = 8 \ \& \ N_{\{\mathcal{L}'\},2}^{(N)} = \max\left((3-0-1)\times 8 - (32-3); 10^{-6}\right) = 10^{-6}$

STEP 12: $E_{\{\mathcal{L}'\}}{}^{(N)} = 7 + 3 + 0 + \min(11, 2) = 9$.

STEP 13: $q_{\{\mathcal{L}\},2}^{(N)} = \min\left(1; \frac{15}{12}\right) = 1 \ \& \ q_{\{C\},2}^{(N)} = \min\left(1; \frac{11}{4}\right) = 1 \ \& \ q_{\{\mathcal{L}'\},2}^{(N)} = \min\left(1; \frac{9}{10^{-6}}\right) = 1$

STEP 14: $\bar{W}_{\{\mathcal{L}\},2}^{a(N)} = 965.4 \ \& \ \bar{W}_{\{C\},2}^{a(N)} = 1,888.57 \ \& \ \bar{W}_{\{\mathcal{L}'\},2}^{a(N)} = 0$

$GW_2{}^{(N)} = 965.4 \times 1 + 1,888.57 \times 1 + 0 \times 1 = 2,853.97$

STEP 15: $l = S$

GO TO *STEP 8*

STEP 8: $E_{\{\mathcal{L}\}}^{(S)} = 20 \ \& \ E_{\{C\}}^{(S)} = 30$

STEP 9: $m_{\{T6\},1}^{(S)} = 0 \ \& \ K_C^{(S)} = 1 \ \& \ N_{\{C\},2}^{(S)} = \max\left((5-0-1)\times 1; 10^{-6}\right) = 4$.

STEP 10: $K_{\mathcal{L}}^{(S)} = 5 \ \& \ N_{\{\mathcal{L}\},2}^{(S)} = \max\left[(5-0-1)\times 5 + \max\left(0,(4-30)\right); 10^{-6}\right] = 20$

STEP 11: $P^{(S)} = 16 \;\&\; K^{(S)}_{\mathcal{L}'} = 6 \;\&\; N^{(S)}_{\{\mathcal{L}'\},1} = \max\left(\left(5-0-1\right)\times 6-\left(32-5\right);10^{-6}\right)=10^{-6}$

STEP 12: $E_{\{\mathcal{L}'\}}^{(S)} = 11+3+0+\min\left(20,5\right)=19$.

STEP 13: $q^{(S)}_{\{\mathcal{L}\},2} = \min\left(1;\dfrac{20}{20}\right)=1 \;\&\; q^{(S)}_{\{C\},2} = \min\left(1;\dfrac{30}{4}\right)=1 \;\&\; q^{(S)}_{\{\mathcal{L}'\},2} = \min\left(1;\dfrac{19}{10^{-6}}\right)=1$

STEP 14: $\overline{W}^{a(S)}_{\mathcal{L},2} = 1,631.38 \;\&\; \overline{W}^{a(S)}_{C,2} = 2,735.82 \;\&\; \overline{W}^{a(l)}_{\mathcal{L}',i} = 0$

$GW_2^{(S)} = 1,631.38\times 1+2,735.82\times 1+0\times 1=4,357.19$

STEP 15: GO TO *STEP 16*

STEP 16: $\overline{W}^{a}_{I,2} = 1,856.85 \;\&\; k_1 = 1 \;\&\; k_2 = 0.75$

$Z_2 = 1\times 1,856.85+0.75\times\left(2,853.97+4,357.19\right)=7,265.22$

STEP 17: GO TO *STEP 19*

STEP 19: $m^{(S)} = r^{(S)} = 6 \Rightarrow$ GO TO *STEP 20*

The northbound and southbound schedules for Class A vessels are shown in Figures 2.8 and 2.9 respectively.

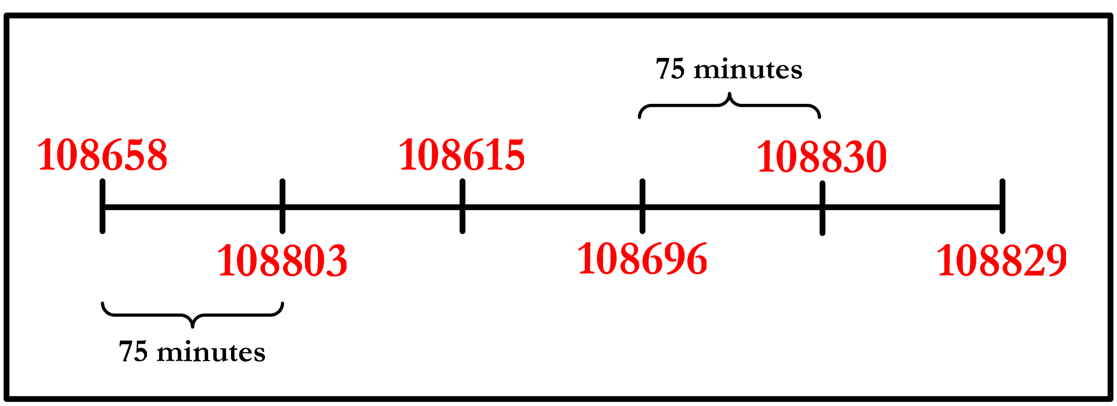

Figure 2.8 Schedule of the southbound Class A vessels in the example

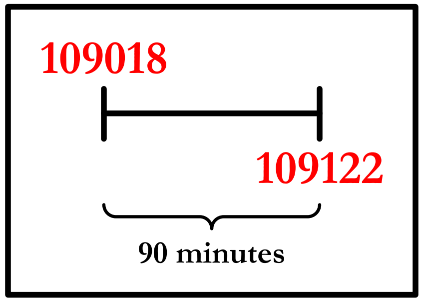

Figure 2.9 Schedule of the northbound Class A vessels in the example

Schedule Class P, C, E, and D Vessels

STEP 21: $\mathcal{P}^* = \varnothing$

$C_N^* = \{108902, 108879\}$ and

$C_S^* = \{108618, 108695, 108673, 108717, 108876\}$

$\mathcal{L}_N^* = \{109003, 108962, 108856, 108984, 108806, 108851\}$

$$\mathcal{L}_S^* = \begin{Bmatrix} 108793, 108915, 108719, 108812, 108811, 108884, 108781, \\ 108837, 108667, 108859, 108780, 108817, 108858, 109043, \\ 108646, 108802, 108881, 108930, 108764, 108774 \end{Bmatrix}$$

STEP 22: The final daytime schedule is given in Figure 2.10.

Initial Direction of Daytime Schedule

STEP 23:

$$S^{(N)} = 0.5\frac{76}{76+98} + 0.3\frac{59,838.65}{59,838.65+172,273.2} + 0.2\frac{2}{2+6} = 0.3457$$

$$S^{(S)} = 0.5\frac{98}{76+98} + 0.3\frac{172,273.2}{59,838.65+172,273.2} + 0.2\frac{6}{2+6} = 0.6543.$$

STEP 25: $S^{(N)} = 0.3457 < S^{(S)} = 0.6543$

Thus, south is selected as the initial direction of the daytime traffic.

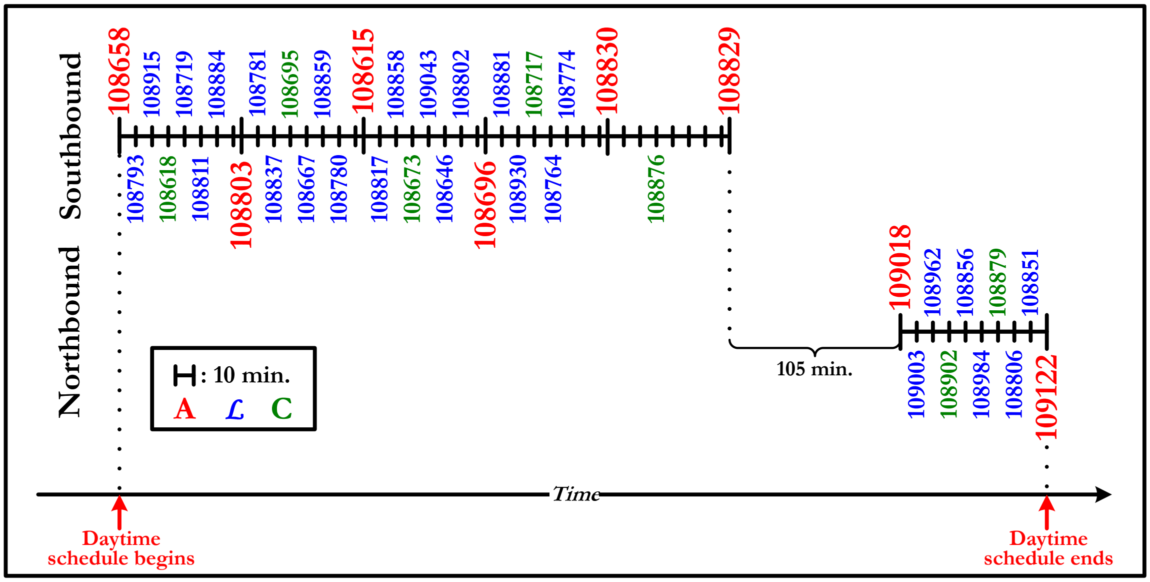

Figure 2.10 Final daytime schedule for May 13, 2005

VALIDATION

Table 2.9 shows the numerical results obtained by the daytime scheduling algorithm compared to the VTS schedules for 10 different dates in 2005 data. In 6 out of the 10 dates, the schedules generated by the algorithm match those of the VTS. Even though it appears that the rest of the results do not match the actual schedules, further analysis reveals that the differences come from individual operator decisions at the VTS. Although the operators adhere to the same regulations, we observe that in some cases they have used their judgment to make exceptions to the established rules.

For example, on December 1st, the VTS scheduled one more northbound Class A vessel than the scheduling algorithm. In order to do that, te operators allowed some of the northbound Class A vessels to enter the Strait at 75-minute intervals instead of the minimum requirement of 90 minutes. We observe the same difference on July 22.

In addition, on January 15 and May 27 the algorithm scheduled more Class A vessels than the actual VTS schedule. The difference is the result of traffic suspension due to unknown reasons.

The only example in which the schedule from the algorithm differs from the actual VTS schedule is on December 25. Still, although the number of scheduled Class A vessels is different, the initial direction of the daytime traffic is identical in both the algorithm and the VTS schedule.

Therefore, we conclude that the scheduling algorithm is successful 90% of the time at mimicking the current scheduling practice at the VTS.

Table 2.9 Numerical results compared to the VTS schedules

		Algorithm	**VTS**
1/15/2005	m_s	5	5
	m_n	2	1
	Initial Direction	Southbound	Northbound
2/28/2005	m_s	2	2
	m_n	4	4
	Initial Direction	Northbound	Northbound
4/10/2005	m_s	4	4
	m_n	4	4
	Initial Direction	Northbound	Northbound
5/13/2005	m_s	6	6
	m_n	2	2
	Initial Direction	Southbound	Southbound
5/27/2005	m_s	4	2
	m_n	5	5
	Initial Direction	Southbound	Southbound
7/22/2005	m_s	4	4
	m_n	4	5
	Initial Direction	Northbound	Southbound
8/5/2005	m_s	2	2
	m_n	3	3
	Initial Direction	Northbound	Northbound
9/10/2005	m_s	5	5
	m_n	2	2
	Initial Direction	Southbound	Southbound
12/1/2005	m_s	2	2
	m_n	4	5
	Initial Direction	Northbound	Northbound
12/25/2005	m_s	4	2
	m_n	3	5
	Initial Direction	Southbound	Southbound

NIGHTTIME SCHEDULE

In contrast to the daytime traffic, there is a two-way traffic flow during nighttime. Among all the vessels that can pass through the Strait at nights, Class B vessels are the most critical vessels due to their size and cargo. These vessels may enter the Strait at 60-minute intervals. Again, Class C vessels may enter at 30-minute intervals, while Class D, E and P vessels may enter at 10-minute intervals. A typical order of vessels entering the Strait during nighttime is given in Figure 2.11:

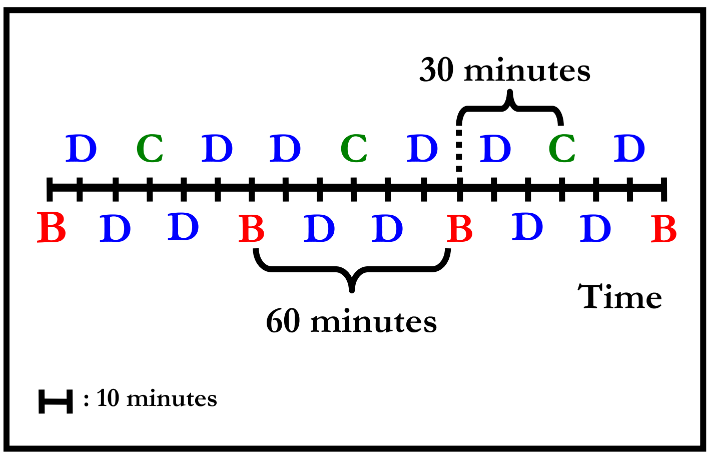

Figure 2.11 A typical schedule of vessels entering the Strait during nighttime

The 1998 regulations state that while a large vessel carrying dangerous cargo (oil tanker, chemical tanker, LNG, LPG, etc.) passes through the Istanbul Strait, another vessel carrying dangerous cargo cannot enter the Strait from the opposite direction regardless of its length. Therefore, while a Class B or C vessel navigates the Strait at night, no Class B, C, or E vessel is allowed to enter in the opposite direction. Each night, depending on the vessel congestion at the entrances, the VTS allows the passage of the aforementioned classes, first in one direction and then in the other. This procedure is carried out once in a given night. Thus, in order to schedule the nighttime traffic, we use the daytime vessel scheduling algorithm explained in section 2.4.3.1 by replacing Class A vessels with Class B vessels.

2.4.4 LANE STRUCTURE

The transit maritime traffic in the Strait is regulated within officially established traffic lanes. In the simulation model, the predetermined vessel routes are arranged to coincide with the center lines of the official lanes. The Strait is divided at certain locations, where stations are placed. Each separation, defined as a slice, is 8 cables long, and consequently there are 21 slices in total. Vessels start their passage at an entrance station, and navigate going through the aforementioned stations in the Strait.

Eventhough overtaking is forbidden in the regulations; the VTS allows overtaking under safe conditions except at the narrowest part between Kanlica and Vaniköy points. A vessel (*X*) arriving at a station overtakes the vessel in front of it (*Y*) if it can reach the next station first. During this time, if *Y* is being overtaken by another vessel (*Z*), and if X can pass *Z*, then *X* slows down and follows *Y*. Note that regulations do not allow passing an overtaking vessel. If *X* can not pass *Z*, then X simply follows *Z* and overtakes *Y*.

Also, we assume that vessels do not stop for loading and unloading within the Strait and the local traffic does not interfere with the transit vessel traffic.

2.4.5 LOCAL TRAFFIC

The local traffic flow model presented in [Mırık and Karayakalı, 2008] is incorporated into the simulation as a sub-model. The schedules, time patterns, routes, and speeds of local vessels are entered into the model, which in turn reports the local traffic densities in the Strait. The local traffic in this model consists of:

- Ferries
- Motorboats, tourist boats and fishing boats
- Fishing motors

2.4.6 DATA COLLECTION

Data collection was completed in collaboration with Boğaziçi University.

2.4.6.1 ARRIVAL DATA

Vessel arrival data is gathered using the following:

- 2005 and 2006 data including inter-arrival time, speed, pilot request percentage, tugboat request percentage, anchorage percentage, anchorage duration, stopover percentage, age and flag of different classes of vessels obtained from the Turkish Straits Vessel Traffic Services (VTS). The data are divided into separate groups based on cargo type and vessel length. A separate distribution is fit to inter-arrival time, speed, and anchorage duration for each group.
- The local traffic schedules for the ferries, motorboats, and tourist boats obtained from the websites of various private companies
- The schedules for the fishing boats and motors obtained through the research conducted by [Mırık and Karayakalı, 2008]

2.4.6.2 VISIBILITY DATA

Visibility data is obtained from various sources lited below:

- 1988-2005 visibility data obtained from the Kandilli Observatory and Earthquake Research Institute (KOERI)
- 1991-2005 visibility data obtained from the International Weather Information Website www.weatherunderground.com (WU)
- 2004-2005 traffic suspension data including the interruption due to poor visibility obtained from the Coastal Safety and Salvage Administration

2.4.6.3 CURRENT DATA

Current data consists of

- 2005 surface current data obtained from the VTS
- Surface current data obtained from the Department of Navigation, and Oceanography of the Turkish Navy

2.4.6.4 STORM DATA

Storm information is obtained from the 2005 traffic suspension data due to inclement weather provided by the VTS.

2.4.6.5 VALIDATION DATA

2005 and 2006 data including waiting and transit times of different classes of vessels obtained from the VTS are used for validation purposes.

2.4.7 INTERRUPTIONS

The types of interruptions that affect the transit vessel traffic flow include poor visibility, strong surface currents, and storms in the Black Sea. Each interruption type is incorporated into the vessel traffic model using a separate sub-model in Arena.

2.4.7.1 VISIBILITY

The visibility model of [Almaz, 2006] is used. This model utilizes the data sources stated in Section 2.4.6.2 for different purposes. The KOERI data are used to capture the seasonal effects and to generate fog in fall/spring and summer seasons. On the other hand, the Weather Underground data are used to generate fog in winter and to model the fog duration through all seasons. Further, traffic suspension data obtained from the Coastal Safety are used to mimic the decisions made by the Authorities to suspend the traffic due to poor visibility.

2.4.7.2 SURFACE CURRENTS

The surface current model presented in [Almaz, 2006] is used. This model considers only the surface currents. The surface currents are crucial for the vessel traffic model, mainly because of the regulations shown in Table 2.3. Also, surface currents affect the ground speed of vessels and ultimately their transit times.

2.4.7.3 STORMS

The storm data in 2005 obtained from the VTS is replicated in the model. According to the regulations, northbound vessels less than 150 meters in length are not allowed to enter the Strait when there is a storm in the Black Sea. As a result of our discussions with the VTS, we found out that the southbound vessels less than 150 meters in length are also affected by a storm in the Black Sea. The data show a decrease in the arrivals of these vessels the day before the storm, and a greater decrease during the storm. Then, a substantial increase is observed two days after the storm is over. This phenomenon is replicated in the model using average arrival increase and decrease rates obtained through analyzing the 2005 data.

2.4.8 ANIMATION

The simulation model of the transit vessel traffic in the Istanbul Strait also includes an animation component. It shows the transit and local vessel movements in the Strait and the anchoring area as well as the waiting queues and some waiting time and transit time statistics. The local traffic flow in the Strait is also animated in the model.

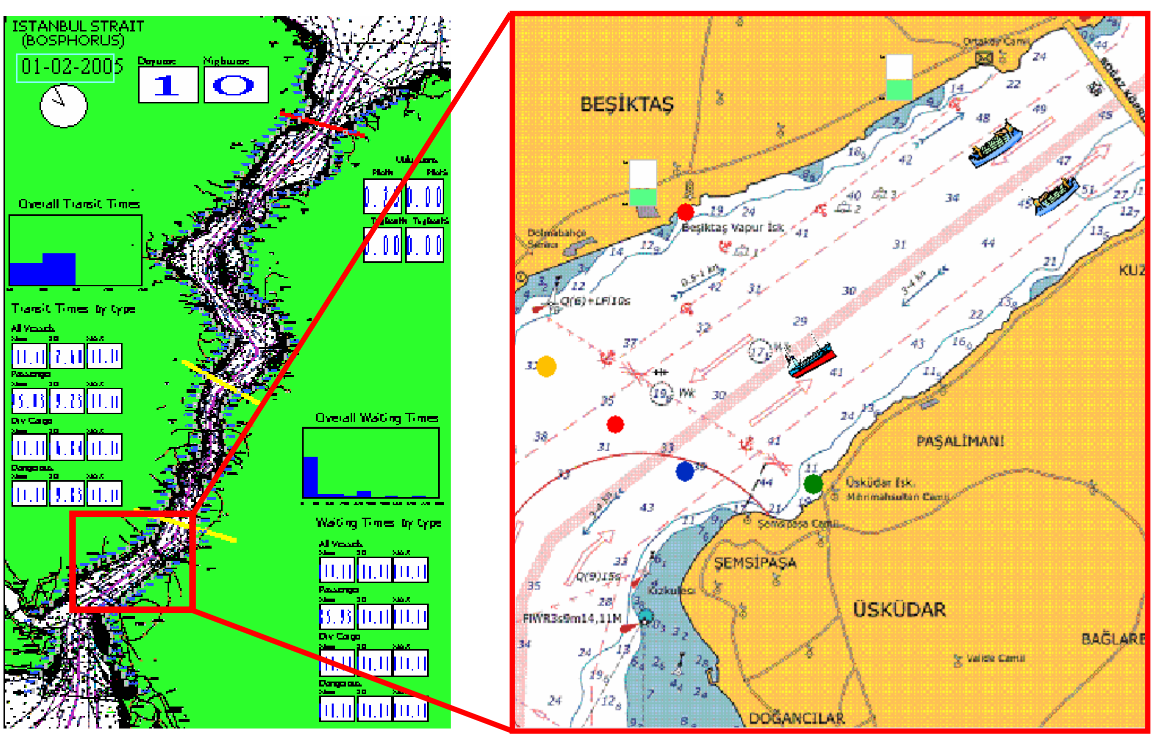

Figure 2.12 A snapshot of the Simulation Model

2.4.9 MODELING ASSUMPTIONS

As mentioned earlier, one of the objectives of developing a simulation model of the transit vessel traffic is to investigate the effect of various system attributes on the system performance. Therefore, some assumptions and simplifications are made to facilitate the development and the utilization of the simulation model. Our goal is not to represent the overall system, but to take into account some key components affecting its operation and to understand the impact of some key attributes on the system performance through a number of scenarios. We assume the following:

- At dawn, all the pilots and tugboats are gathered at the entrance that will constitute the initial direction for the daytime traffic schedule, e.g. southern entrance if the initial direction for the daytime traffic is northbound.
- The closures due to the Marmaray (subway construction) project are not considered.
- The scheduling decisions made by the operators are standardized and incorporated into an algorithm. Therefore, the instantaneous and subjective decisions by the operators are not modeled.

2.4.10 PERFORMANCE MEASURES

One of the objectives of the simulation model is to estimate the performance of the system through some predetermined performance measures and to investigate the effects of different factors on its operation. The following performance measures are collected from the model:

- Transit times
- Waiting times
- Pilot utilization
- Tugboat utilization
- Vessel density in the Strait

2.4.11 VALIDATION

Next, we make sure that the simulation model built for the vessel traffic represents the real system behavior closely enough to be used to test the effects of several system attributes on the various performance measures.

In order to validate the model, we have compared its output statistics with the data from 2005 provided by the Turkish Straits Vessel Traffic Services. The following simulation results are obtained from 10 5-year long replications. The actual number of vessels that passed through the Strait in 2005 and the average number of vessels that passed per year in the simulation are given in Table 2.10.

Table 2.10 Total Number of Vessels per year

NUMBER OF PASSING VESSELS PER YEAR						
Direction	**Simulation**				**2005 Data**	**Relative Error (%)**
	Average	**Half Width (95% CI)**	**Min**	**Max**	**Total**	
Northbound	26,940.32	1,007.94	26,660.60	27,083.80	27,402.00	1.68%
Southbound	27,772.04	75.824	27,449.20	27,977.80	27,388.00	1.40%
Total	54,712.36	123.256	54,109.80	54,971.80	54,790.00	0.14%

The average transit times of vessels obtained from both the simulation and the 2005 data are shown in Table 2.11. The results seem quite accurate given variation in the 2005 data.

Table 2.11 Average Transit Times of different types of vessels

TRANSIT TIME						
Vessel Type	**Simulation**		**2005 Data**			**Relative Error (%)**
	Average	**Half Width (95% CI)**	**Average**	**Min**	**Max**	
All Vessels	97.3952	0.02	99.1544	51.0167	9,271.37	1.77%
General Cargo	98.6468	0.01	98.9569	51.1667	2,268.82	0.31%
General Cargo NB	98.8776	0.03	101.1077	52.75	1,887.18	2.21%
General Cargo SB	98.4231	0.02	96.8061	51.1667	2,268.82	1.67%
Dangerous Cargo	86.8614	0.15	87.3001	59.8667	701.8833	0.50%
Dang. Cargo NB	83.9690	0.19	89.546	59.8667	701.8833	6.23%
Dang. Cargo NB	89.5104	0.19	85.0542	61.25	149.0833	5.24%
LNG-LPG	88.2230	0.14	93.4553	63.9667	176.8833	5.60%
LNG-LPG NB	87.4381	0.16	94.2355	63.9667	176.8833	7.21%
LNG-LPG SB	96.4023	0.7	88.949	64.75	114.75	8.38%
Tanker	92.8396	0.06	96.1582	51.0167	9,271.37	3.45%
Tanker NB	93.0770	0.12	99.2164	51.2833	1,528.40	6.19%
Tanker SB	92.6324	0.07	93.0999	51.0167	9,271.37	0.50%
Passenger	96.7084	0.26	100.1648	54.05	1,731.65	3.45%
Passenger NB	96.5936	0.47	100.439	54.65	812.1167	3.83%
Passenger SB	96.8238	0.32	99.8892	54.05	1,731.65	3.07%

The average waiting times of different types of vessels obtained from the simulation runs and the 2005 data provide varying results. The average waiting times of dangerous cargo vessels and LNG-LPG carriers obtained from the simulation are very close to the actual data. However, the average waiting times of all vessels and tankers are significantly shorter than the 2005 data. On the other hand, the values for the passenger vessels obtained from the simulation are considerably higher than its counterpart.

One possible reason of the shorter waiting times in the model is the Marmaray project. As mentioned before, the traffic interruptions due to the construction are not included in the simulation model. Therefore, the waiting times in the 2005 data are longer than what the model produces.

Another reason is clearly the lack of a standard scheduling algorithm used by the operators, which also explains longer waiting times for passenger vessels in the simulation. As stated earlier, a vessel scheduling algorithm has been developed and incorporated into the simulation model. Therefore, the model does not take into account the instantaneous decisions of the operator in charge. Also, shorter waiting times obtained from the model are promising in terms of the effectiveness of the scheduling algorithm that we have developed.

Based on the comparison of the results obtained from the model and the actual data collected in 2005, the total number of vessels passing through the Strait, the average transit times, and the average waiting times appear to be quite reasonable. Therefore, under the assumptions mentioned in section 2.4.9, the simulation model is considered to be adequately representing the general behavior of the vessel traffic in the Istanbul Strait.

2.4.12 ANALYSIS OF SYSTEM BEHAVIOR

In this section, we investigate the effects of some of the system attributes of concern on the system performance through several scenarios using the performance measures presented in Section 2.4.10.

The system attributes of concern in the analysis of the transit vessel traffic simulation of the Istanbul Strait are:

- Arrival rates
- Number of available pilots
- Number of available tugboats
- Required time duration between two consecutive Class D, E and P vessels

The available number of pilots and tugboats are treated as a group. The system attributes and their values applied to 5 distinct scenarios are displayed in Table 2.12. The shaded values correspond to the Base Scenario, which represents the current conditions in the Strait. All the subsequent scenarios obtained by changing the attribute values according to Table 2.12 are compared to the Base Scenario in the following section. Each scenario is run for 10 years. The results for two of these scenarios are given next. The outcomes for the rest of the scenarios are consistent with the results described below.

Table 2.12 Values of system attributes used in scenario analysis

Attributes	**Values**			
Arrival Rate Increase	0%	5%	10%	15%
# of Pilot - Tugboat	12 - 4	16 - 6	20 – 10	
Time duration btw Class D, E and P vessels	5 min.	10 min.		

SCENARIO 1

Arrival Rate Increase = 0%

# of Pilot - Tugboat = 20 -10

Time duration btw Class D, E and P vessels = 10 min.

According to the simulation results, the number of available pilots and tugboats has an impact on the vessel delays at the entrances. As seen in Table 2.13, the average waiting times decrease when the number of available pilots and tugboats increases from 16 and 6 to 20 and 10, respectively. The increase in the available number of resources affects mostly the average waiting time of the northbound LNG-LPG carriers. It affects the average waiting time of the southbound passenger vessels the least, which is consistent with the system policies since passenger vessels may obtain extra pilots and tugboats from the ports in case the VTS does not have any available.

Table 2.13 Waiting Times in Scenario 1 compared to the Base Scenario

	BASE SCENARIO		SCENARIO 1		% Increase in Average
Vessel Type	**Average**	**Half Width (95% CI)**	**Average**	**Half Width (95% CI)**	
All Vessels	342.64	107.98	318.54	39.77	-7.03%
General Cargo	242.91	40.76	236.34	31.66	-2.70%
General Cargo NB	214.78	40.24	206.72	37.42	-3.75%
General Cargo SB	270.18	41.83	265.04	27.88	-1.90%
Dangerous Cargo	694.52	257.11	631.46	80.3	-9.08%
Dang. Cargo NB	646.40	232.56	579.25	92.09	-10.39%
Dang. Cargo SB	738.57	279.99	679.45	77.76	-8.00%
LNG-LPG	1,243.29	797.35	1,067.88	162.88	-14.11%
LNG-LPG NB	1,299.94	850.09	1,103.22	164.96	-15.13%
LNG-LPG SB	655.41	233.45	673.98	167.86	2.83%
Tanker	802.13	399.32	702.16	81.72	-12.46%
Tanker NB	777.19	405.07	671.74	78.36	-13.57%
Tanker SB	823.92	394.56	728.90	85.04	-11.53%
Passenger	77.9315	10.07	75.6351	4.45	-2.95%
Passenger NB	73.8581	11.61	70.6946	4.97	-4.28%
Passenger SB	81.9032	9.26	80.6488	5.49	-1.53%

On the other hand, the results show that the number of available pilots and tugboats does not have any effect on the average number of vessels that pass per year as expected. This result assures us that the system stabilizes in the long run.

Finally, the pilot and tugboat utilizations are given in Table 2.14. According to these figures, the pilot utilization and the tugboat utilization are around 30% and 2%, respectively for the Base Scenario. Although, there is no similar data to compare, these values seem reasonable, taking into consideration the pilot and tugboat request percentages and the expected number of vessels in the Strait.

On the other hand, 25% and 67% increase in the number of pilots and tugboats, respectively, for Scenario 1, which corresponds to a 25% and a 40% decrease in the pilot and tugboat utilizations, respectively.

We observe that the resource utilizations decrease dramatically as the total number of available pilots and tugboats increase by 25% and 67%, respectively, while the average vessel waiting time decreases. Although the resources are not fully utilized because pilotage and towage are voluntary, they still do have a key impact on the waiting times.

Table 2.14 Resource utilizations in Scenario 1 compared to the Base Scenario

	BASE SCENARIO		**SCENARIO 1**		**% Increase in Average**
Resource	**Average**	**Half Width (95% CI)**	**Average**	**Half Width (95% CI)**	
Pilot Northbound	0.3077	0.0042	0.2307	0.0035	-25.01%
Pilot Southbound	0.2838	0.0033	0.2156	0.0023	-24.02%
Tugboat Northbound	0.0120	0.0004	0.0069	0.0002	-42.81%
Tugboat Southbound	0.0312	0.0007	0.0186	0.0005	-40.28%

SCENARIO 2

Arrival Rate Increase = 10%

# of Pilot - Tugboat = 16 – 6

Time duration btw Class D, E and P vessels = 10 min.

According to the results, the arrival rates do not have any impact on the transit times of the vessels. This is consistent with the system structure since the time a vessel spends in the Strait is not dependent on the vessel inter-arrival; it is affected by its speed, the traffic density and the current and visibility conditions in the Strait.

However, as seen in 2.15, a 10% increase in the arrival rates leads to an almost 270% increase in the average waiting times of vessels in general. Specifically, an increase in the number of vessel arrivals affects the average waiting time of the dangerous cargo vessels the most. It affects the average waiting time of the passenger vessels the least, which is consistent with the system policies since passenger vessels have higher priority than any other class of vessel.

Table 2.15 Waiting Times in Scenario 2 compared to the Base Scenario

	BASE SCENARIO		SCENARIO 2		% Increase in Average
Vessel Type	**Average**	**Half Width (95% CI)**	**Average**	**Half Width (95% CI)**	
All Vessels	342.64	107.98	1,258.23	1,006.17	267.22%
General Cargo	242.91	40.76	873.67	658.14	259.67%
General Cargo NB	214.78	40.24	791.11	631.57	268.34%
General Cargo SB	270.18	41.83	953.93	684.87	253.07%
Dangerous Cargo	694.52	257.11	3,364.60	2,945.53	384.45%
Dang. Cargo NB	646.40	232.56	3,430.84	3,060.95	430.76%
Dang. Cargo SB	738.57	279.99	3,300.18	2,830.15	346.83%
LNG-LPG	1,243.29	797.35	2,641.21	1,919.45	112.44%
LNG-LPG NB	1,299.94	850.09	2,789.22	2,055.30	114.57%
LNG-LPG SB	655.41	233.45	1,001.50	468.29	52.81%
Tanker	802.13	399.32	3,122.03	2,681.13	289.22%
Tanker NB	777.19	405.07	2,953.30	2,533.63	280.00%
Tanker SB	823.92	394.56	3,271.03	2,814.10	297.01%
Passenger	77.9315	10.07	87.0963	7.23	11.76%
Passenger NB	73.8581	11.61	82.0913	5.41	11.15%
Passenger SB	81.9032	9.26	92.1096	9.23	12.46%

Also, Table 2.16 shows that the average number of transit vessels per year increases as the arrival rate increases, as expected. A 10% increase in the number of vessel arrivals is reflected as an 11% increase in the number of vessels that pass through the Strait.

Table 2.16 Average number of vessels in Scenario 2 compared to the Base Scenario

Direction	**BASE SCENARIO**	**SCENARIO 2**	**% Increase**
Northbound	26,963	30,047	11.44%
Southbound	27,822	30,864	10.93%
Total	54,785	60,911	11.18%

Finally, the pilot and tugboat utilizations are given in Table 2.17. According to these figures, the pilot utilization increases almost 15% as the number of vessel arrivals increase 10%. The increase is around 12% and 15% for the southbound and northbound tugboat utilizations, respectively. The increase in the northbound tugboat utilization is greater than the southbound tugboat utilization due to the higher percentage of tugboats requested by the northbound vessels.

Table 2.17 Resource utilizations in Scenario 2 compared to the Base Scenario

	BASE SCENARIO		**SCENARIO 2**		**% Increase in Average**
Resource	**Average**	**Half Width (95% CI)**	**Average**	**Half Width (95% CI)**	
Pilot Northbound	0.3049	0.00	0.3409	0.00	11.81%
Pilot Southbound	0.3009	0.00	0.3456	0.00	14.86%
Tugboat Northbound	0.0112	0.00	0.0125	0.00	11.61%
Tugboat Southbound	0.0152	0.00	0.0174	0.00	14.47%

SCENARIO 3

Arrival Rate Increase = 0%

# of Pilot - Tugboat = 16 – 6

Time duration btw Class D, E and P vessels = 5 min.

According to the results, the required time gap between between consecutive Class D, E and P vessels does not have any impact on the transit times of the vessels. Even though we are scheduling more vessels, their passage through the Strait is not affected.

However, as seen in Table 2.18, a 50% increase in the number of scheduled Class D, E and P vessels leads to an almost 20% decrease in the average waiting times of all vessels. Specifically, the increase affects the average waiting time of the general cargo vessels the most since Class D represent the general cargo vessels that are less than 150 m. in length as shown in Table 2.5. It affects the average waiting time of the dangerous cargo vessels the least, since the number of Class T6, A and C vessels, which constitute the majority of dangerous cargo vessels, is not changed.

Table 2.18 Waiting Times in Scenario 3 compared to the Base Scenario

	BASE SCENARIO		**SCENARIO 3**		**% Increase in Average**
Vessel Type	**Average**	**Half Width (95% CI)**	**Average**	**Half Width (95% CI)**	
All Vessels	342.64	107.98	279.05	69.82	-18.56%
General Cargo	242.91	40.76	176.16	29.56	-27.48%
General Cargo NB	214.78	40.24	161.12	23.85	-24.98%
General Cargo SB	270.18	41.83	190.74	35.63	-29.40%
Dangerous Cargo	694.52	257.11	695.23	216.81	0.10%
Dang. Cargo NB	646.40	232.56	642.72	178.82	-0.57%
Dang. Cargo SB	738.57	279.99	744.11	254.33	0.75%
LNG-LPG	1,243.29	797.35	1,103.34	457.61	-11.26%
LNG-LPG NB	1,299.94	850.09	1,150.20	489.74	-11.52%
LNG-LPG SB	655.41	233.45	600.01	109.02	-8.45%
Tanker	802.13	399.32	745.84	246.29	-7.02%
Tanker NB	777.19	405.07	711.41	232.87	-8.46%
Tanker SB	823.92	394.56	775.98	259.46	-5.82%
Passenger	77.9315	10.07	68.528	6.37	-12.07%
Passenger NB	73.8581	11.61	66.2714	4.96	-10.27%
Passenger SB	81.9032	9.26	70.8369	9.53	-13.51%

On the other hand, the results show that the required time gap between between consecutive Class D, E and P vessels does not have any effect on the average number of vessels that pass per year as expected.

Finally, according to Table 2.19, the pilot utilization increases 4% as the number of scheduled vessels increases 50%. However, tugboat utilization is not affected much.

Table 2.19 Resource utilizations in Scenario 3 compared to the Base Scenario

	BASE SCENARIO		SCENARIO 3		% Increase in Average
Resource	**Average**	**Half Width (95% CI)**	**Average**	**Half Width (95% CI)**	
Pilot Northbound	0.3049	0.00	0.3175	0.00	4.13%
Pilot Southbound	0.3009	0.00	0.3133	0.00	4.12%
Tugboat Northbound	0.0112	0.00	0.0113	0.00	0.89%
Tugboat Southbound	0.0152	0.00	0.0153	0.00	0.66%

3 RISK ANALYSIS OF THE TRANSIT VESSEL TRAFFIC IN THE ISTANBUL STRAIT

3.1 INTRODUCTION

The concepts of risk analysis, assessment and management are becoming more important as the future becomes less predictable in today's chaotic society. Numerous papers and books have been written on the subject in the last 15 years (see [Ansell and Wharton, 1992], [Steward *et al*., 1997], [Koller, 1999, 2000], [Wang and Rousch, 2000], Bedford and Cooke, 2001], [Aven, 2003], [Ayyub, 2003], and [Modarres, 2006].

[Rausand and Høyland, 2004] defines *risk* as an expectation of an unwanted consequence, which combines both the severity and the likelihood of the consequence. [Kaplan and Garrick, 1981] and [Kaplan, 1997] provide a quantitative definition of risk. The authors argue that in order to define risk one must answer three questions:

i. What can go wrong?
ii. How likely is that to happen?
iii. If it does happen, what are the consequences?

To answer these questions, a list of scenarios is constructed as shown in Table **3.3**. Let s_i be the ith scenario, and p_i and x_i be its probability and consequence, respectively.

Table 3.1 List of scenarios

Scenario	Probability	Consequence
s_1	p_1	x_1
s_2	p_2	x_2
$\vdots$	$\vdots$	$\vdots$
s_N	p_N	x_N

Thus, the triplet $\langle s_i, p_i, x_i \rangle$ represents an answer to the above questions. Consequently, risk is defined as the complete set of triplets including all possible scenarios.

$$R = \{\langle s_i, p_i, x_i \rangle\}, \qquad i = 1, \ldots, N$$

The scenarios are sorted in an increasing order of severity of consequence such that $x_1 \le x_2 \le \cdots \le x_N$. Table 3.2 is obtained by adding a column representing the cumulative probabilities calculated starting with the most severe scenario s_N.

Table 3.2 List of scenarios with Cumulative Probability

Scenario	Probability	Consequence	Cumulative Probability
s_1	p_1	x_1	$P_1 = P_2 + p_1$
s_2	p_2	x_2	$P_2 = P_3 + p_2$
$\vdots$	$\vdots$	$\vdots$	$\vdots$
s_i	p_i	x_i	$P_i = P_{i+1} + p_i$
$\vdots$	$\vdots$	$\vdots$	$\vdots$
s_{N-1}	p_{N-1}	x_{N-1}	$P_{N-1} = P_N + p_{N-1}$
s_N	p_N	x_N	$P_N = p_N$

By plotting the consequence versus cumulative probability, a *risk curve* can be obtained as depicted in Figure 3.1.

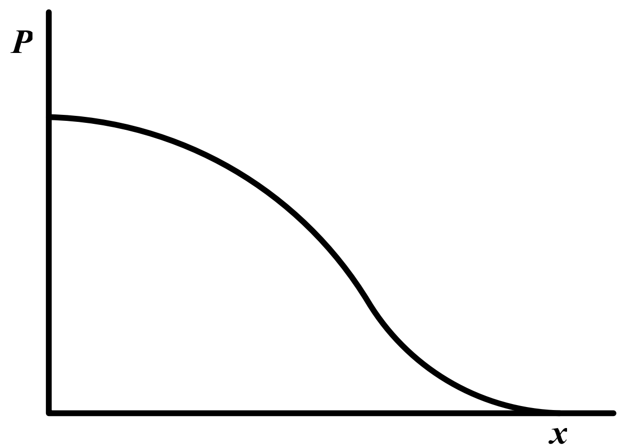

Figure 3.1 Risk Curve

The Society for Risk Analysis, on the other hand, defines risk as “the potential for realization of unwanted, adverse consequences to human life, health, property, or the environment” [SRA, 2007], whereas [Ayyub, 2003] provides a quantitative engineering definition of risk as follows:

$$R = \text{Probability}(E) \times \text{Consequence Impact}(E)$$

where E is an unwanted event.

Risk analysis can be defined as “a detailed examination … performed to understand the nature of unwanted negative consequences to human life, health, property, or the environment" [SRA, 2007]. However, *risk management* builds on the risk analysis process by seeking answers to a set of three questions [Haimes, 1991]:

i. What can be done and what options are available to mitigate risks?
ii. What are the associated tradeoffs in terms of all costs, benefits, and risks?
iii. What are the impacts of current management decisions on future options?

The steps of risk analysis and management are presented in Figure 3.2.

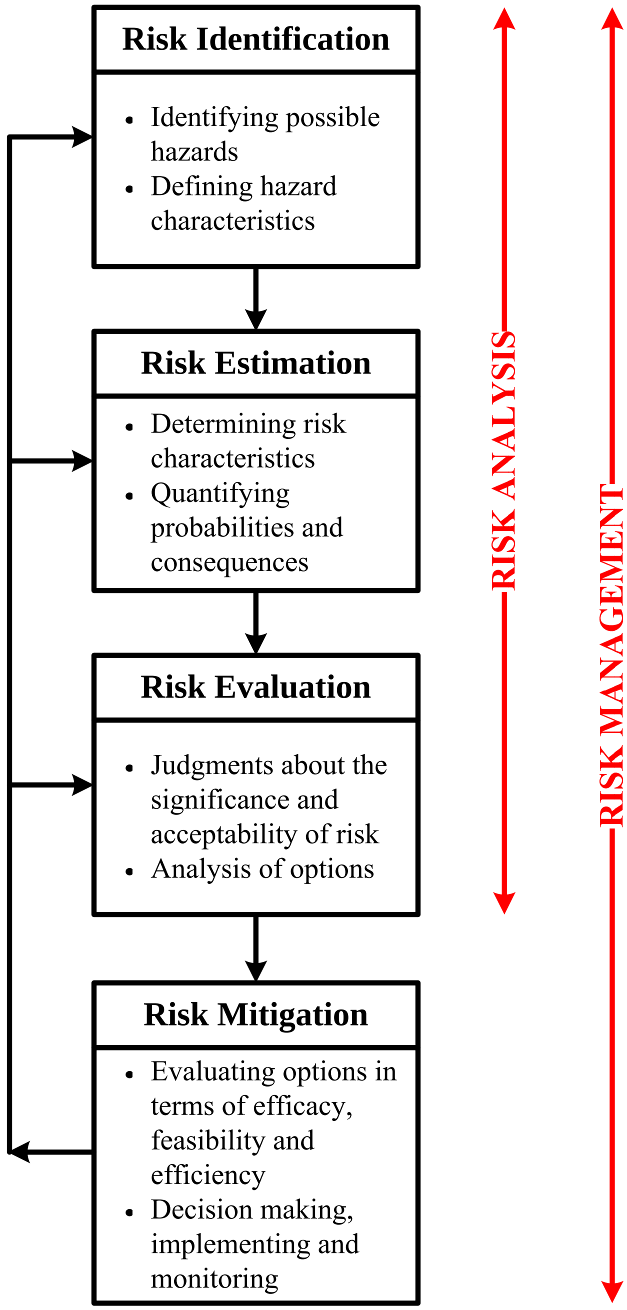

Figure 3.2 Risk analysis and management

Furthermore, *probabilistic risk analysis (PRA)* is a risk analysis method, which uses experimental and actual data to quantify risks in a system. It is also referred to as *quantitative risk analysis (QRA)* or *probabilistic safety analysis (PSA)* depending on the field.

Even though the concepts of risk analysis and management are relatively new, the thinking on the topic of risk was initiated by the notion of insurance, a risk management tool that reduces risk for a person or a party by sharing potential financial burdens with others. Insurance has roots that reach back to 1800 B.C. when it was used to help finance sea expeditions. An early form of life insurance was provided by trade and craft guilds in Greece and Rome. As trade expanded in the Middle Ages, new forms of insurance were used to protect farmers and traders from droughts, floods, and other disasters.

Risk has also been an integral part of money markets and financial services. Options, a financial instrument that allows individuals to buy and sell goods from one another at pre-arranged prices, were traded in the U.S. in the 1790s in what would later become the New York Stock Exchange. Futures, in use in Europe since medieval times, were another type of financial instrument that helped reduce risk for farmers and commodity buyers. Futures on products such as grain and copper have been sold on the Chicago Board of Trade starting in 1865. Between the 1970s and the 1990s, derivatives, financial contracts that derive their value from one or more assets, became popular among individuals and organizations [Vesper, 2006].

Since the Industrial Revolution, the nature of risk has changed. Hazardous agents have increased significantly in size such as bridges, airplanes, oil tankers and skyscrapers. They have also gotten smaller, e.g. pesticides and biological weapons.

In recent years, risk analysis has been utilized in numerous industries, leading to the improvement of existing methodologies as well as the development of new ones. Probabilistic risk analysis originated in the aerospace industry. One of the earliest studies was launched after the fire in the Apollo flight AS-204 in 1967, in which three astronauts were killed. In 1969, the Space Shuttle Task Group was created. [Colglazier and Weatherwas, 1986] conducted a probabilistic risk analysis of shuttle flights. Since the Challenger accident in 1986, NASA has instituted various programs of quantitative risk analysis to assure safety during the design and operations phases of manned space travel [Bedford and Cooke, 2001]. Examples of such risk analyses include the SAIC Shuttle Risk Assessment [Fragola, 1995] and the risk assessment of tiles of the space shuttle orbiter [Paté-Cornell and Fischbeck, 1993].

In the nuclear industry, the focus has always been on reactor safety. The first risk analysis study was the Reactor Safety Study [NRC, 1975] published by the US Nuclear Regulatory Commission (NRC). This study was criticized by a series of reviews: American Physical Society [APS, 1975], Environmental Protection Agency [EPA, 1976], [Union of Concerned Scientists, 1977], and [Lewis *et al*., 1979]. However, two independent analyses of the Three Mile Island accident, [Kemeny *et al*., 1979] and [Rogovin and Frampton, 1980], re-emphasized the need for conducting probabilistic risk analysis. The US NRC released *The Fault Tree Handbook* [Vesely *et al.*, 1981] in 1981 and the *PRA Procedures Guide* [NRC, 1983] in 1983, which standardized the risk assessment methodology.

Probabilistic risk analysis has been applied to study a variety of natural disasters. These studies include predicting earthquakes [Chang *et al.*, 2000], floods [Voortman *et al.*, 2002], [Mai and Zimmermann, 2003], [Kaczmarek, 2003], and environmental pollution [Slob, Pieters 1998], [Moore *et al.*, 1999]. A large number of studies focus on waste disposal and environmental health [Sadiq *et al.*, 2003], [Cohen, 2003], and [Garrick and Kaplan, 1999].

In the 1990s, the U.S. Food and Drug Administration (FDA) began requiring manufacturers of certain types of foods to use a risk management method called hazard analysis and critical control points (HACCP) to identify, control, and monitor risks. The U.S. Department of Agriculture also requires that meat and poultry processing plants use HACCP as a risk management process [Vesper, 2006].

In health care, probabilistic risk analysis has focused on analyzing the causes of unwanted events such as medical errors or failure mode and effect analysis of near catastrophic events [Bonnabry *et al.*, 2005]. PRA is also utilized in the pharmaceutical industry to make decisions on new product development [Keefer, 2001]. Further, the FDA is expanding use of risk analysis and risk management within the industry.

Risk analysis and management has also become important in maritime transportation industry. The National Research Council identified it as an important problem domain [NRC, 1986, 1991, 1994, 2000]. The grounding of the *Exxon Valdez*, the capsize of the *Herald of Free Enterprise* and the *Estonia* passenger ferries are some of the most widely known accidents in maritime transportation. [Merrick *et al*., 2006] states that the consequences of these accidents ranged from severe environmental and property damage to high casualties. These and other similar accidents have led researches to focus on maritime risk analysis. Early work concentrated on risk assessment of structural designs using reliability engineering tools. The studied structures included nuclear powered vessels [Pravda and Lightner, 1966], vessels transporting liquefied natural gas [Stiehl, 1977] and offshore oil and gas platforms [Paté-Cornell, 1990]. Recently, researchers have applied Probabilistic Risk Analysis to maritime transportation. A detailed literature review on this topic is provided in Section 3.3.

The application of risk analysis to terrorism is new. In terrorism, risk is defined as “the result of a *threat* with negative effects to a *vulnerable* system” [Haimes, 2004, 2006]. Here, the threat refers to “the intent and capability to cause harm or damage to the system by negatively changing its states”. [Taylor *et al*., 2002] has applied probabilistic risk analysis in cyber terrorism risk assessment. Other works have suggested the use of these techniques in assessment of terrorism [Apostolakis and Lemon, 2005], [Haimes and Longstaff, 2002].

In this chapter, we will focus our attention to the risk analysis of the maritime transit traffic in the Istanbul Strait.

3.2 BACKGROUND INFORMATION

The Istanbul Strait is among the world's busiest waterways. The heavy traffic through the Istanbul Strait presents substantial risks to the local environment. Various reasons including the increase in maritime traffic and the number of vessels carrying dangerous and hazardous cargo, the unpredictable weather conditions, the unusual characteristics of the Istanbul Strait and the failure to request pilotage have led to over 500 accidents in the last decade alone.

The first major accident occurred in 1960 when the Greek-flagged M/T World Harmony collided with the Yugoslavian-flagged M/T Peter Zoranic. 20 crew members, including both shipmasters, died; the resulting oil pollution and fire lasted several weeks, suspending the traffic in the Strait.

Although numerous catastrophic accidents have occurred in the Strait, some incidents should especially be mentioned because of their magnitude, both in terms of damage they caused, and their impact on the Turkish psyche:

- In 1960, Yugoslavian flagged tanker Petar Zoranić collided with the Greek tanker World Harmony at Kanlıca. 50 members of the crew died. 18,000 tons of oil spilled into the sea, causing severe pollution. Fire lasted for some weeks, suspending transit traffic in the Strait. Petar Zoranić's wreck led to more accidents. In 1964, Norwegian flagged vessel Norborn crashed into the wreck, causing fire and pollution.

- In March 1966, two Soviet flagged vessels M/T Lutsk and M/T Cransky Oktiabr collided at Kızkulesi. 1,850 tons of oil spilled into the fire. The resulting fire burned down the Karaköy ferry terminal and a ferry.

- In July 1966, the ferry Yeni Galatasaray collided with the Turkish coaster Aksaray. 13 people died in the fire.

- In November 1966, the ferry Bereket hit the Romanian flagged Ploesti. 8 people drowned.

- In 1979, Greek freighter M/V Evriyalı collided with Romanian-flagged Independenta near Haydarpasa, at the southern entrance. The Romanian tanker sank and 43 members of the crew died. 64,000 tons of oil spilled into the sea, while 30,000 tons of oil burned into the atmosphere. An area of 5.5 kilometers in diameter was covered with thick tar, and the mortality rate of the marine life was estimated at 96 percent according to [Oguzülgen, 1995]. The incident was ranked as the 10th worst tanker accident in the world.

- In 1988, Panama-flagged M/T Blue Star carrying ammonium chloride collided with Turkish tanker M/T Gaziantep. 1,000 tons of the corrosive chemical spilled into the sea, causing severe pollution.

- In March 1990, Iraqi tanker M/T Jambur and Chinese bulk carrier M/V Da Tong Shan collided in the Strait. About 2,600 tons of oil spilled into the sea as Jambur ran aground after the collision. The cleaning efforts lasted several weeks.

- In 1991, the Turks witnessed yet another incident involving improper navigation, when Phillippine-flagged bulk carrier M/V Madonna Lily and Lebanese live stock carrier Rabunion 18 collided in November. Three members of the Rabunion 18 crew died as the ship sank with its cargo of 21,000 sheep.

- In yet another catastrophe in March 1994, the Greek Cypriot vessels M/T Nassia and M/V Shipbroker collided in the Strait, just north of Istanbul. 29 people died; over 20,000 tons of crude oil burned for five days, suspending the traffic in the Strait for a week.

- The Russian tanker Volganeft-248 ran aground and split in two at the southern entrance of the Istanbul Strait in December 1999. 1,500 tons of oil spilled into the sea, polluting both the water and the shores. Clean-up efforts lasted for several months.

- In October 2002, Maltese-flagged M/V Gotia ran into the Emirgan pier in the Strait, damaging its fuel tank. 18 tons of oil spilled into the sea.

- Georgian-flagged cargo carrier M/V Svyatov Panteleymon ran aground and broke apart while navigating the Istanbul Strait in November 2003. Its fuel spilled into the sea, polluting a strip of about 600 meters of the shore.

- In February 2004, severe weather caused Cambodian-flagged M/V Hera to sink in the Black Sea, just a few miles off the northern entrance of the Strait. None of the 19 members of the crew survived.

- Just a few days after the M/V Hera incident, North-Korean flagged Lujin-1 carrying scrap iron ran aground while entering the Strait, damaging its hull. It took several days to rescue the ship's 15 crewmembers and months to salvage the ship.

As indicated in the above examples, the heavy traffic through the Strait undoubtedly presents substantial risks. The impact of heavy tanker traffic is already evident in the ecology of the marine life. Though a potential major spill could bring immediate environmental catastrophe, a key problem caused by the presence of large tankers is the day to day release of contaminated water as the ships ballast their holds and discharge their bilge water.

The Istanbul Strait possesses features that make heavy volumes of traffic dangerous. Over the last few decades as the magnitude of traffic has increased, accidents in the Strait have become common. With the increase in oil production projected as a result of the exploitation of Central Asian oil fields, the traffic through the Strait is expected to increase significantly, putting both the local environment and the inhabitants of Istanbul at risk of a major catastrophe. In addition to claiming lives, destroying the historical heritage and polluting the environment, a major accident in the Strait could cause significant economic problems for the Black Sea littoral states in the event of a prolonged suspension of traffic.

3.3 LITERATURE REVIEW ON MARITIME RISK ANALYSIS

The existing risk assessment studies in maritime systems may be categorized in two main groups: risk assessment of the structural design using the tools of reliability engineering, and the probabilistic risk analysis of the system as a whole.

[Guedes Soares and Teixeira, 2001] provides a review of the studies that have been published on the structural design risk assessment in maritime systems. It concentrates on the global assessment of risk levels and its differentiation in ship types and main types of ship losses.

In our research, we consider the vessel traffic system as a whole instead of concentrating only on the vessel failures. In our risk analysis methodology, we utilize probabilistic risk analysis tools and simulation modeling. Therefore, we concentrate on the work that has been done in the second category.

[Atallah and Athens, 1984] provides general guidelines for the application of risk assessment methodology to existing or proposed marine terminal operations. The proposed methodology includes four consecutive stages: identification of potential hazards, quantification of risks, evaluation of risk acceptability; and reduction of unacceptable risks. Specifically, the authors focus on the accidental releases of hazardous flammable and/or toxic cargoes in or near harbors and inland waterways.

[Haya and Nakamura, 1995] proposes a quantitative risk evaluation procedure that systematically combines various simulation techniques. Also, the degree of collision risk of a ship felt by the ship handler is incorporated in the risk evaluation procedure using a method introducing Subjective Judgment values as indexes expressing the subjective degree of danger felt by the ship handler.

[Amrozowicz, 1996] and [Amrozowicz *et al*., 1997] focus on the first level of a proposed three-level risk model to determine the probability of oil tanker grounding. The approach utilizes fault trees and event trees and incorporates the Human Error Rate Prediction data to quantify individual errors. The high-leverage factors are identified in order to determine the most effective and efficient use of resources to reduce the probability of grounding. The authors present results showing that the development of the Electronic Chart Display and Information System incorporated with the International Safety Management Code can significantly reduce the probability of grounding.

[Dougligeris *et al*., 1997] provides a methodology of analyzing, quantifying and assigning risk cost estimates in maritime transportation of petroleum products. The objective of the risk analysis, as stated in the paper, is to identify shipping routes that minimize a function of transportation and risk cost while maintaining an equitable distribution of risk. In addition, the proposed methodology is implemented in a case study involving the oil transportation in the Gulf of Mexico during the 1990-1994 time periods.

Similarly, [Iakovou, 2001] considers the maritime transportation of crude oil and petroleum products. The paper presents the development of a strategic multi-objective network flow model, allowing for risk analysis and routing, with multiple commodities, modalities and origin-destination pairs. The authors demonstrate the development of an interactive solution methodology and its implementation via a Internet-based software package. The objective is to facilitate the government agencies to determine how regulations should be set to derive desirable routing schemes.

[Slob, 1998] presents a study for the purpose of optimizing the combating and disposing of spills on the Dutch inland waterways. A system is developed for the determination of risks on inland waters and to classify the inland waterways into four risk-classes. The study also determines per location whether the amount of preparation of combating acute spills measures the risks of these locations. Finally, standard contingency plans are developed for combating spills for the different relevant locations in the Netherlands.

[Harrald *et al*., 1998] describes the modeling of human error related accident event sequences in a risk assessment of maritime oil transportation in Prince William Sound, Alaska. A two stage human error framework and the conditional probabilities implied by this framework are obtained from system experts such as tanker masters, mates, engineers, and state pilots. A dynamic simulation to produce the risk analysis results of the base case is also discussed.

[Merrick *et al*., 2000] and [Merrick *et al*., 2002] present the detailed model of the Prince William Sound oil transportation system, using system simulation, data analysis, and expert judgment. The authors also propose a systems approach to risk assessment and management by a detailed analysis of the sub-systems and their interactions and dependencies.

[Merrick *et al*., 2001] explains the Washington State Ferries Risk Assessment. A modeling approach that combines system simulation, expert judgment and available data is used to estimate the contribution of risk factors to accident risk. A simulation model is utilized to capture the dynamic environment of changing risk factors, such as traffic interactions, visibility or wind conditions.

[Van Dorp *et al*., 2001] describes a study that has been carried out to assess the sufficiency of passenger and crew safety in the Washington state ferry system, estimate the level of risk present, and develop recommendations for prioritized risk reduction measures. As a supplement to [Merrick *et al*., 2001], the potential consequences of collisions are modeled to determine the requirements for onboard and external emergency response procedures and equipment. In addition, potential risk reduction measures are evaluated and various risk management recommendations are resulted.

[Merrick and Van Dorp, 2006] combines a Bayesian simulation of the occurrence of situations with accident potential and a Bayesian multivariate regression analysis of the relationship between factors describing these situations and expert judgments of accident risk for two case studies. The first is an assessment of the effects of proposed ferry service expansions in San Francisco Bay. The second is an assessment of risk of the Washington State Ferries, the largest ferry system in the United States.

[Kuroda *et al*., 1982] proposes a mathematical model for estimating the probability of the collision of ships passing through a uniform channel. The model takes into account traffic characteristics such as traffic volume, ship size distribution, and sailing velocity distribution, as well as channel conditions such as width, length and centerline. The proposed model is examined on the basis of collision statistics for some channels and straits in Japan and it is concluded that the model gives a good estimation of the collision risk of a channel.

[Kaneko, 2002] considers probabilistic risk assessment methods applied to ships. The author presents a holistic methodology for risk evaluation and a method used in the process of estimating the probability of collision. In addition, he examines a method to reduce the number of fire escalation scenarios and demonstrates a trial risk evaluation of cabin fire.

Whereas the literature referred to above utilizes probabilistic risk assessment techniques and simulation modeling, there are many other studies on risk assessment, which are based on statistical analysis of the data. These are performed through modeling accident probabilities and casualties using statistical estimation methods and time-series analysis utilizing the past data. The following include some of these studies:

[Fortson *et al.*, 1973] proposes a methodological approach and task plan for assessing alternative methods of reducing the potential risk caused by the spill of hazardous cargo as the result of vessel collisions and groundings.

[Van der Tak and Spaans, 1976] explains the research conducted by Navigation Research Centre of the Netherlands Maritime Institute to develop a “maritime risk criterium number” for a certain sea area. The main purpose is to calculate the criterium number for different traffic alternatives in a certain area to find the best regulatory solution for the overall traffic situation.

[Maio *et al*., 1991] develops a regression model as part of a study by the U.S. Department of Transportation for the U.S. Coast Guard's Office of Navigation Safety and Waterway to estimate the waterway casualty rate depending on the type of waterway, average current velocity, visibility, wind velocity, and channel width. In [Kornhauser and Clark, 1995] this regression model is used to estimate the vessel casualties resulting from additional oil tanker traffic through the Istanbul Strait.

[Roeleven *et al*., 1995] describes the fitting procedures in order to obtain the model that forecasts the probability of accidents as function of waterway attributes and circumstances. The authors use Generalized Linear Models (GLM), which do not require the assumption that the accident probability is normally distributed. Therefore, the binomial approach is used instead. The authors conclude that the circumstances such as visibility and wind speed are more explanatory with respect to the probability of accidents than the waterway characteristics.

While [Talley, 1995a] analyzes the cause factors of accident severity to evaluate the policies for reducing the vessel damage and the subsequent oil spillage of tanker accidents, [Talley, 1995b] investigates the causes of accident passenger-vessel damage cost.

In addition, [Anderson and Talley, 1995] uses a similar approach to study the causal factors of the oil cargo spill, and tanker barge vessel accidents, and [Talley, 1996] investigates the main factors of the risk and the severity of cargo of containership accidents by using vessel accident data.

Similarly, [Psaraftis *et al*., 1998] presents an analysis on the factors that are important determinants of maritime transportation risk. The purpose of the analysis is to identify technologies and other measures to improve maritime safety.

[Le Blanc and Rucks, 1996] describes the cluster analysis performed on a sample of over 900 vessel accidents that occurred on the lower Mississippi River. The objective is to generate four groups that are relatively unique in their respective attribute values such as type of accident, river stage, traffic level, and system utilization. The four groups resulting from the cluster analysis are characterized as Danger Zone, Bad Conditions for Good Navigators, Probably Preventable, and Accidents That Should Not Have Happened.

[Kite-Powell *et al*., 1998] explains the Ship Transit Risk project. The developed physical risk model is based on the assumption that the probability of an accident depends on a set of risk factors, which include operator skill, vessel characteristics, traffic characteristics, topographic and environmental difficulty of the transit, and quality of operator's information about the transit. The objective is to investigate the relationship between these factors.

In [Le Blanc *et al*., 2001], the authors use a neural network model to build logical groups of accidents instead of the cluster analysis. The groups generated in [Le Blanc and

Rucks, 1996] and in this paper are compared and found to be radically different in terms of the relative number of records in each group and the descriptive statistics describing each comparable set of groups.

[Degre *et al*., 2003] describes the general principles of risk assessment models, the nature of input data required and the methods used to collect certain category of these data. It then describes more deeply the SAMSON model developed in the Netherlands. Finally, the authors show how the concepts used in these models may be generalized in order to assign a dynamic risk index to certain types of ships.

[Yudhbir and Iakovou, 2005] presents the development of an oil spill risk assessment model. The goal of this model is to first determine and assign risk costs to the links of a maritime transportation network, and then to provide insights on the factors contributing to the spills.

[Moller *et al*., 2005] reviews the current status of the government-industry partnerships for dealing with oil spills as the result of maritime transportation. The main factors of oil spill risk are identified, analyzed, and discussed in relation to the oil transportation pattern of each region. These are compared to the data on major oil pollution incidents. The authors also consider priorities and activities in different regions, and the implications for oil spill response before estimating the capabilities for increasing effective spill response measures in different regions at the end.

Specifically, our research involves the risk analysis of the Istanbul Strait. Even though, there have been major contributions on the maritime risk analysis literature, the previous work done on the risk modeling of the Istanbul Strait is limited.

A physics based mathematical model is developed in [Otay and Özkan, 2003] to simulate the random transit maritime traffic through the Istanbul Strait. The developed model estimates the probability distribution of vessel casualties using the geographical characteristics of the Strait. Risk maps showing the expected number of accidents in different sections of the Strait are also presented for different vessel sizes and casualty types including collision, ramming and grounding.

[Tan and Otay, 1998] and later [Tan and Otay, 1999] present a physics-based stochastic model to investigate casualties resulting from tanker accidents in the narrow waterway. The authors demonstrate a state-space model developed to represent the waterway and the location of vessels at a given time. By incorporating the drift probabilities and random arrival of vessels into a Markov chain model they obtain the probability of casualty at a given location and also the expected number of casualties for a given number of vessels arriving per unit time.

[Or and Kahraman, 2002] investigates possible factors contributing to accidents in the Istanbul Strait using Bayesian analysis and simulation modeling. The Bayesian analysis is used to obtain estimates for conditional maritime accident probabilities in the Strait. The resulting probabilities are then combined with the Strait's characteristics and traffic regulations in the simulation model. Simulation results indicate the significant impact of transit traffic arrivals, local traffic density, and the meteorological conditions on the number of accidents in the Istanbul Strait.

[Örs and Yılmaz, 2003] and [Örs, 2005] study the oil spill development in the Istanbul Strait. The developed model is based on a flow field computed by finite element analysis of the shallow water equations. A stochastic Lagrangian particles cluster tracking approach is adopted for the simulation of the oil movement. The results of the study show that the timescale of a major spill is as little as a few hours.

3.4 MODELING RISK

3.4.1 FRAMEWORK

In this chapter, our objective is to determine operational policies that will mitigate the risk of having an accident that will endanger the environment, the residents of Istanbul and impact the economy, while maintaining an acceptable level of vessel throughput.

We will start by defining the events that may trigger an accident as *instigators*. Various instigators include human error, rudder failure, propulsion failure, communication and/or navigation equipment failure, and mechanical and/or electrical failure. The *1st tier accident* types occurring as a result of instigators include collision, grounding, ramming, and fire and/or explosion. The 2^{nd} *tier accident* types that may occur following 1^{st} tier accidents include grounding, ramming, fire and/or explosion, and sinking. The potential consequences of such accidents include human casualty, property and/or infrastructure damage, environmental damage and traffic effectiveness. These represent consequences of both 1^{st} and 2^{nd} tier accidents. Note that in some instances, there may not be a 2^{nd} tier accident following a 1^{st} tier one.

The first step of a risk analysis process is the identification of the series of events leading to an accident and its consequences. An accident is not a single event, but the result of a series of events.

Figure 3.3 shows the classification of different risk elements in the transit vessel traffic system in the Istanbul Strait.

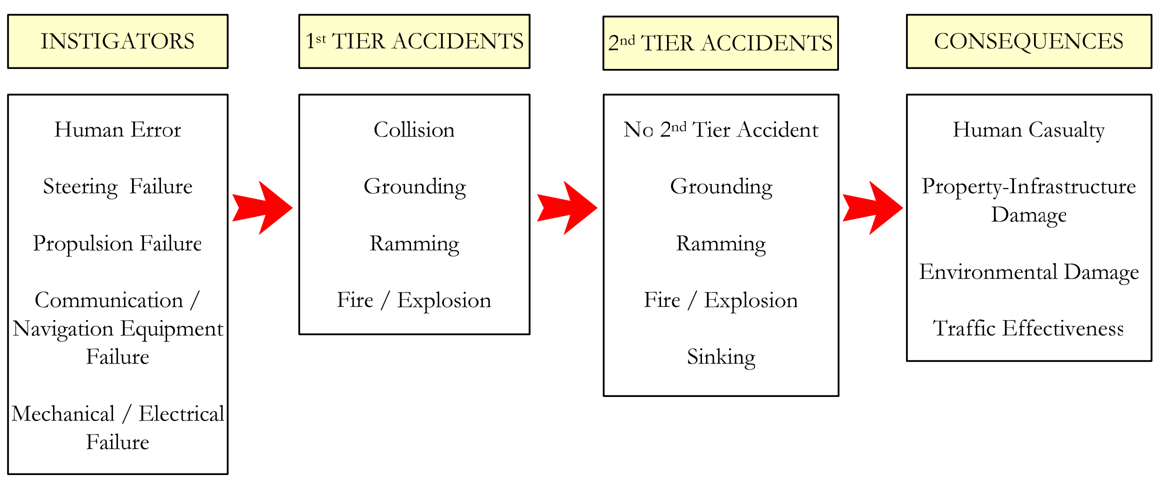

Figure 3.3 The framework of the risk model

In addition to identifying different types of instigators, accidents, and consequences, risk analysis includes the estimation of the probabilities of these events and the evaluation of the consequences of different degrees of severity. This assessment establishes the basis of our mathematical risk model.

3.4.2 A MATHEMATICAL RISK MODEL

The accidents that occurred in the Istanbul Strait in the last 58 years have varied in frequency and severity. Some of them were high probability and low consequence accidents whereas others were low probability and high consequence ones. Specifically, the existence of the latter leads to difficulties in the risk analysis process. Due to the rare occurrence of such accidents, there is a lack of available data to determine the contribution of various situational attributes to accident risks. Therefore, we constructed a risk model, which incorporates vessel traffic simulation and available data as well as subject matter expert judgments in order to quantify accident risks through the estimation of the contribution of situational attributes to accident risk.

While a transit vessel navigates in the Istanbul Strait, there is a possibility that something could go wrong. For example, there can be a mechanical failure in the vessel or the pilot can make an error. We have called these events that may trigger an accident as *instigators*. The occurrence of an instigator depends on the *situation*, which is the vector of situational attributes. Obviously, some system states are more "risky" than others. For instance, a vessel navigating on a clear day is at lower "risk" than a vessel navigating in a poor visibility situation.

An instigator may lead to an accident. For example, a short-circuit problem in a vessel may cause a fire. Here, the probability of a fire occurring after a short-circuit depends on the situational attributes. For example, short-circuit occurrence on an LNG carrier is more "risky" than on a container vessel.

Similarly, the consequence of an accident and its impact depends not only on the accident itself but also on the vessels themselves as well as a number of attributes of the Strait. For instance, a fire on an oil tanker would have a bigger impact on the human life and the environment than a fire on a dry cargo vessel.

Since the system state influences the risk of an accident at every step starting from the occurrence of an instigator up to the consequences of the accident, we utilize Probabilistic Risk Assessment (PRA) to emphasize the effect of the dynamic nature of the vessel traffic system on the risk.

To clarify the effect of different situational attributes on the various steps of the risk model shown in Figure 3.3, we divide the situational attributes into two categories: attributes influencing accident occurrence and attributes influencing consequences and their impact. These two categories are listed in Figure 3.4 and Figure 3.5.

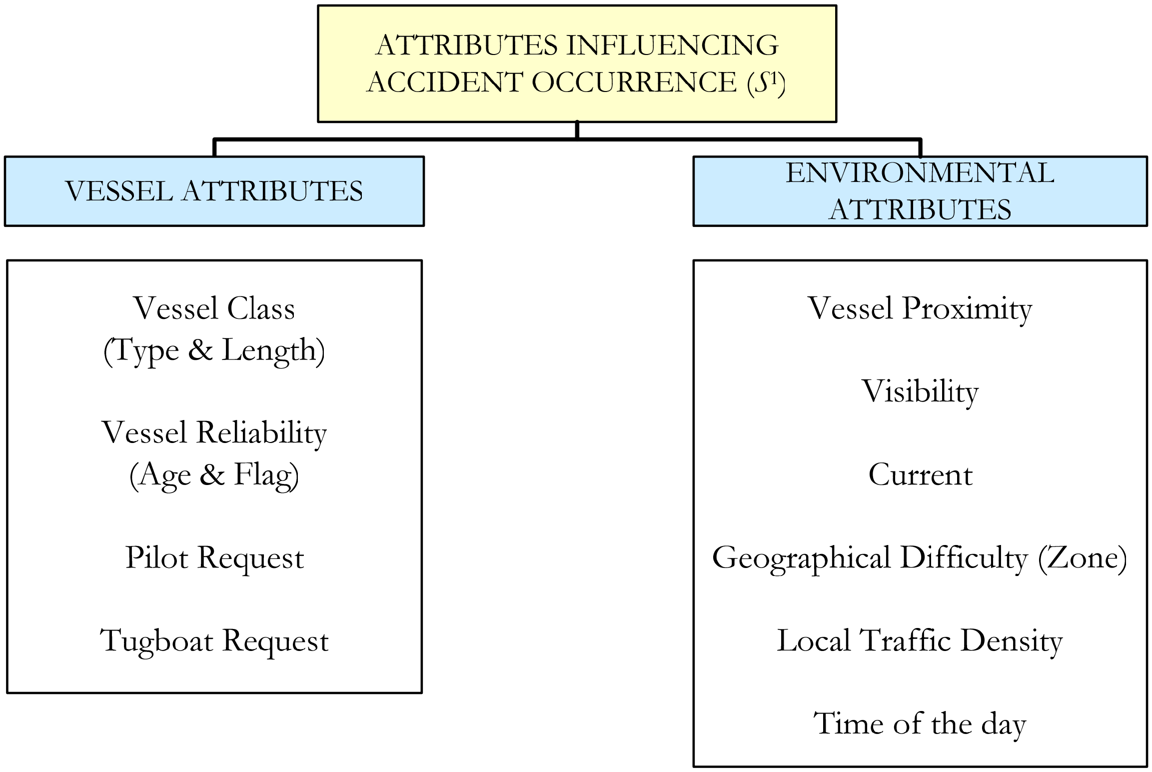

Figure 3.4 Situational attributes influencing accident occurrence

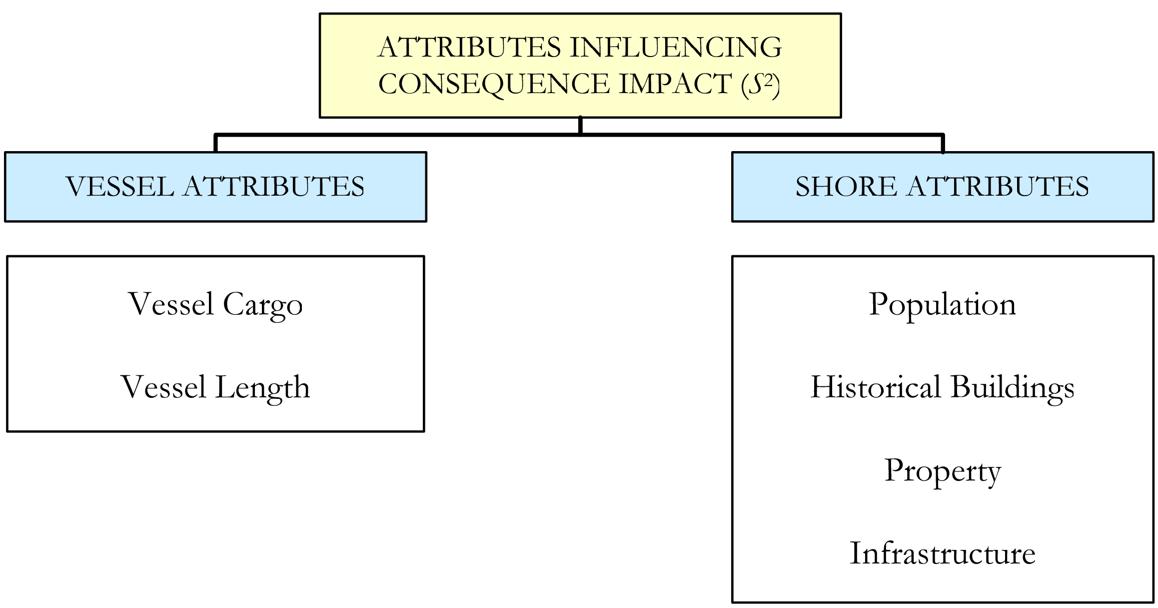

Figure 3.5 Situational attributes influencing the consequences and their impact

In order to quantify the risk, we need to answer the following questions:

- How often do the various situations occur?
- For a particular situation, how often do instigators occur?
- If an instigator occurs, how likely is an accident?
- If an accident occurs, what would the damage to human life, property, environment and infrastructure be?

In the simulation model, the Istanbul Strait is divided into 21 slices for risk analysis purposes as depicted in Figure 3.6. Each slice is 8 cables long.

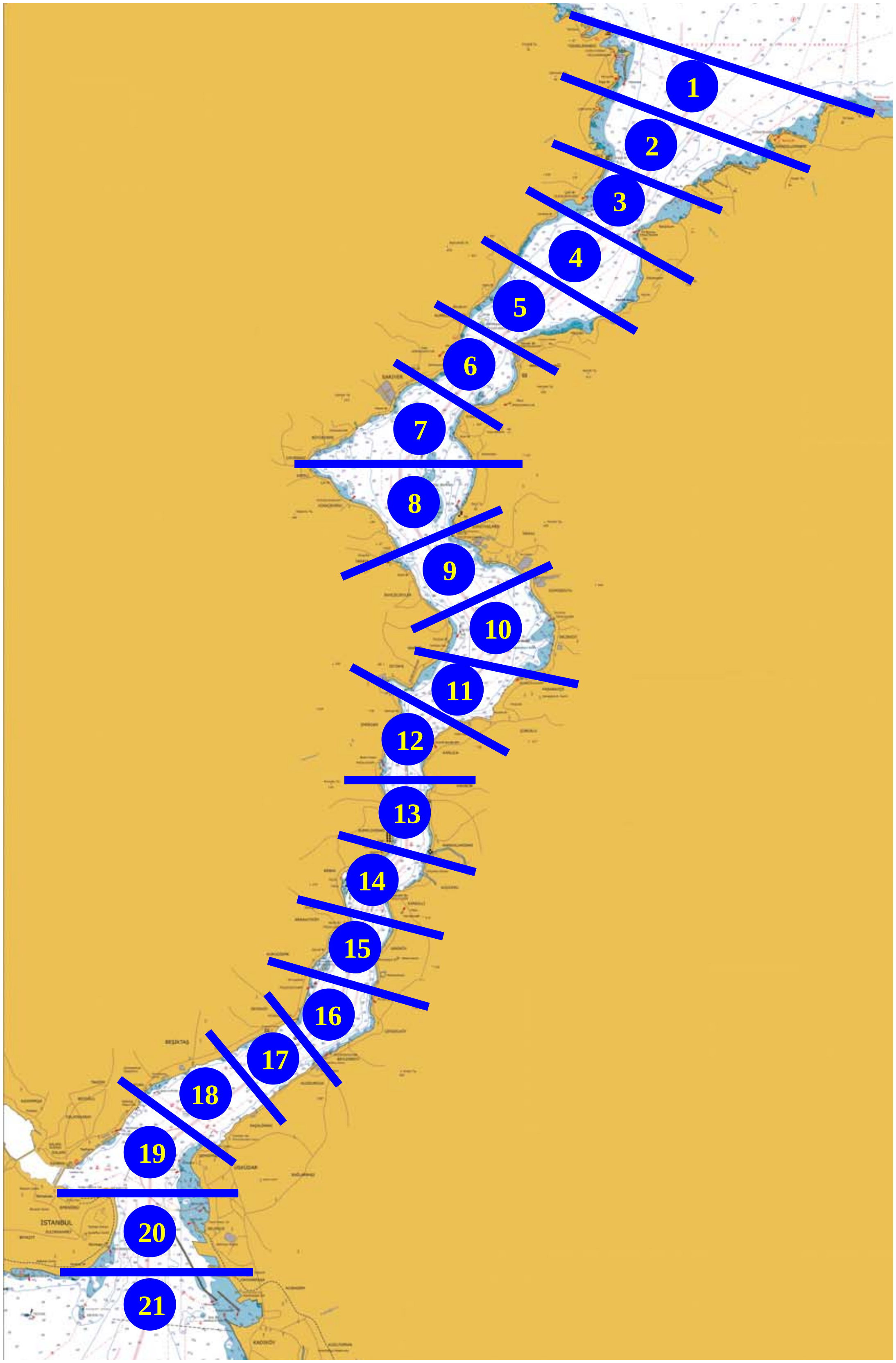

Figure 3.6 Risk Slices

The risk at slice s, R_s, is defined by

$$R_s = \sum_{r \in \mathcal{V}_s} \sum_{m \in \mathcal{A}^1} \sum_{i \in \mathcal{A}_m^2} \left(\sum_{j \in \mathcal{C}_i} E\left[C_{jirs} \middle| A_{irs}^2 \right] \times \Pr\left(A_{irs}^2 \right) + \sum_{j \in \mathcal{C}_m} E\left[C_{jmrs} \middle| A_{mrs}^1 \right] \times \Pr\left(A_{mrs}^1 \right) \right) \quad (3.1)$$

where

A_{mrs}^1 : 1st tier accident type m at slice s involving vessel r

A_{irs}^2 : 2nd tier accident type i at slice s involving vessel r

$\mathcal{A}^1$: Set of 1st tier accident types

$\mathcal{A}_m^2$: Set of 2nd tier accident types that may be caused by 1st tier accident type m as indicated in Table 3.3.

C_{jirs} : Consequence type j of 2nd tier accident type i at slice s involving vessel r

C_{jmrs} : Consequence type j of 1st tier accident type m at slice s involving vessel r

$\mathcal{C}_i$: Set of consequence types of accident type i as indicated in Table 3.4

$\mathcal{V}_s$: Set of vessels navigating at slice s as seen by an observing vessel entering the slice

Note: In the case where there are no 2nd tier accidents, the first term in (3.1) equals zero.

Table 3.3 Causal relationship between 1st and 2nd tier accident types

1st Tier Accident Type		No 2nd Tier Accident	2nd Tier Accident Type			
			Grounding	Ramming	Fire / Explosion	Sinking
	Collision	X	X	X	X	X
	Grounding	X			X	X
	Ramming	X	X		X	X
	Fire / Explosion	X	X	X		X

(Information presented in this table can be interpreted as: collision may either not cause a 2nd tier accident or it may cause grounding, ramming, fire/explosion, or sinking as a 2nd tier accident)

Table 3.4 Set of consequence types of accident types

Accidents Types		Consequences			
		Property / Infrastructure Damage	Human Causalty	Environmental Damage	Traffic Effectiveness
	Collision		X	X	X
	Grounding			X	X
	Ramming	X	X	X	X
	Fire/Explosion	X	X	X	X
	Sinking	X	X	X	X

The probability of 1st tier accident type m at slice s involving vessel r is defined by

$$\Pr\left(A^1_{mrs}\right) = \sum_{k \in \mathcal{J}_m} \sum_{l \in \boldsymbol{S}^1} \Pr\left(A^1_{mrs} \middle| I_{ks}, S^1_{ls}\right) \times \Pr\left(I_{ks} \middle| S^1_{ls}\right) \times \Pr\left(S^1_{ls}\right) \tag{3.2}$$

where

I_{ks} : Instigator type k at slice s

$\mathcal{J}_m$: Set of instigator types that may cause accident type m as indicated in **Error! Reference source not found.**

S^1_{ls} : Situation l influencing 1st tier accident occurrence at slice s

$\boldsymbol{S}^1$: Set of situations influencing accident occurrence.

Table 3.5 Set of instigators that may cause an accident

		1st Tier Accidents			
		Collision	Grounding	Ramming	Fire / Explosion
Instigators	Human Error	X	X	X	X
	Steering Failure	X	X	X	
	Propulsion Failure	X	X	X	
	Communication/Navigation Equipment Failure	X	X	X	
	Mechanical/Electrical Failure				X

The probability of 2nd tier accident type *i* at slice *s* involving vessel *r* is calculated by

$$\Pr\left(A_{irs}^{2}\right) = \sum_{m \in \mathcal{A}_{i}^{1}} \Pr\left(A_{irs}^{2} \middle| A_{mrs}^{1}\right) \times \Pr\left(A_{mrs}^{1}\right) \tag{3.3}$$

The expected value of consequence *j* at slice *s* given n^{th} tier accident type *i* is defined by

$$E\left[C_{jirs} \middle| A_{irs}^{n}\right] = \sum_{h \in \mathcal{L}_{ij}} \sum_{l \in \mathcal{S}^{2}} C_{jirs}\left(h\right) \times \Pr\left(C_{jirs}\left(h\right) \middle| A_{irs}^{n}, S_{ls}^{2}\right) \times \Pr\left(S_{ls}^{2}\right) \tag{3.4}$$

where

$\mathcal{L}_{ij}$: Set of impact levels of consequence *j* of accident type *i*

S_{ls}^{2} : Situation *l* influencing consequence at slice *s*

$\mathcal{S}^{2}$: Set of situations influencing consequence impact

C_{jirs} : Consequence type *j* of nth tier accident type *i* at slice *s* contributed by vessel *r*.

The methodology used to calculate each component of the risk expression, R_s, is explained in the following section.

3.4.3 METHODOLOGY

In the simulation model, the risk at slice *s*, R_s, is calculated every time a vessel enters that slice. The observing vessel entering the slice first calculates its own contribution to the slice risk. Then, it calculates the contribution of each vessel navigating in the slice. Since the collision risk involves the interaction of two vessels, the simulation logic ensures that there is no double counting when calculating the collision risk of each vessel.

In this section, we demonstrate how to calculate various conditional probabilities that are used in risk calculations. We present an example for each type of conditional probability. The same approach may also be applied to other conditions.

3.4.3.1 1ST TIER ACCIDENT PROBABILITY

3.4.3.1.1 PROBABILITY OF A 1ST TIER ACCIDENT GIVEN AN INSTIGATOR

Once an instigator has occurred, the probability of a 1^{st} tier accident is affected by the situation, which represents the system condition. Due to lack of data to determine the contribution of various situational attributes to accident risks, the estimation of the probability of an accident given an instigator requires elicitation of expert judgments.

There are a number of elicitation methods available as noted in [Cooke, 1991], and we are using a paired comparisons elicitation method in this research. Our decision to use this method is based on the observation that experts are more comfortable making paired comparisons rather than directly assessing a probability value for a given situation. The specific paired comparison elicitation method used in this research was also used in [Merrick *et al*., 2001], [Merrick and Van Dorp, 2006] and [Szwed *et al*., 2006].

Similar to the Analytical Hierarchy Process (AHP) the paired comparison approach focuses on the functional relationship between situational attributes $\underline{S}^{1T} = (X_1, X_2, \ldots, X_p)$ and an accident probability rather than a value function. The probability of a 1st tier accident given an instigator can be defined as

$$\Pr\left(A^1 \middle| I, \underline{S}^1\right) = P_0 \exp\left(\underline{\beta}^T \underline{S}^1\right) \tag{3.5}$$

where $\underline{S}^1$ represents a column vector of situational attributes describing a situation during which an instigator has occurred, $\underline{\beta}$ is a vector of parameters and P_0 is a calibration constant. The accident probability model (3.5) was proposed in [Roeleven *et al*., 1995], [Merrick *et al*., 2000] and [Van Dorp *et al*., 2001]. It is based on the proportional hazards model originally proposed by [Cox, 1972], which assumes that accident probability behaves exponentially with changes in covariate values.

The probability of an accident, defined by (3.5) where $\underline{S}^1 \in [0,1]^p$, $\underline{\beta} \in R^p$ and $P_0 \in [0,1]$, is assumed to depend on the situational attributes listed in

Table 3.6. The situational attributes X_i, $i = 1, \ldots, p$ are normalized so that $X_i = 1$ describes the "worst" case scenario while $X_i = 0$ describes the "best" case scenario. For example, for the 11[th] attribute, that is time of the day, $X_{11} = 1$ represents the nighttime, while $X_{11} = 0$ represents the daytime.

Unfortunately, sorting the possible values of situational attributes from worst to best as it relates to an accident probability is not an easy task. Also, the accident probability behaves much like a value function. That is, not only the order amongst different values of a situational attribute is important, but also their relative differences. Therefore, a scale is needed to rank especially the lesser evident situational attributes. The possible values of situational attributes and their scales were obtained through discussions with the VTS. The possible values of the situational attributes influencing accident occurrence ($\underline{S}^1$) are listed in Table 3.6 while their normalized scale values are given in Appendix A.

Among the situational attributes, the reliability of a vessel is difficult to measure. Thus, we define it in terms of vessel age and flag type. The age of a vessel is categorized as new, middle age or old. Additionally, the flag of a vessel may be used as an indicator of the education and experience of the captain and crew as well as the technology and maintenance level of the equipment. The flag of a vessel may be defined as low, medium or high risk depending on the flag state. Consequently, the reliability of a vessel is defined as the combination of age and flag and is represented through nine possible values.

The grouping of vessel age into the three categories (i.e. new, middle age or old) within each vessel type is determined through an age survey collected from experts. In addition, each flag is assigned to one of the three flag categories (i.e. low, medium or high risk) based on the 2006 Shipping Industry Flag State Performance Table [MISS, 2006]. The performance table includes measures such as the annual reports of Port State Control Organizations (i.e. Paris MOU, Tokyo MOU and US Cost Guard), convention ratifications, age information, STCW and ILO (International Labor Organization) reports, and IMO meeting attendance. An importance factor for each measure is determined through the interviews with the experts. These factors and the information in the Flag State Performance Table are then used to calculate a mathematical performance measure for each flag state. Finally, the mathematical value is transformed to one of the three flag categories mentioned earlier using a scale.

Table 3.6 Possible values of situational attributes influencing accident occurrence S^1

	Attribute Name	# of Possible Values	Description
X_1	1st Interacting Vessel Class	9	1-3, 6-11 (see Table 3.2)
X_2	2nd Interacting Vessel Class	11	1-11 (see Table 3.2)
X_3	1st Vessel Tugboat Request	2	Yes, No
X_4	1st Vessel Pilot Request	2	Yes, No
X_5	Nearest Transit Vessel Proximity	9	same direction 0-4 cables, same direction 4-8 cables; same direction >8 cables, 1 knot/hr speed difference overtaking lane, 2 knots/hr speed difference overtaking lane, 3 knots/hr speed difference overtaking lane, 4 knots/hr speed difference overtaking lane, opposite direction normal lane, opposite direction overtaking lane
X_6	Visibility	3	<0.5 mile, 0.5-1 mile , >1 mile
X_7	Current	8	0-2 knots/hr same direction with 1st vessel, 2-4 knots/hr same direction with 1st vessel, 4-6 knots/hr same direction with 1st vessel, > 6 knots/hr same direction with 1st vessel, 0-2 knots/hr opposite to 1st vessel, 2-4 knots/hr opposite to 1st vessel, 4-6 knots/hr opposite to 1st vessel, > 6 knots/hr opposite to 1st vessel
X_8	Local Traffic Density	3	1-2, 3-5, >5
X_9	Zone	12	Anadolu Feneri-Sarıyer SB, Anadolu Feneri-Sarıyer NB, Sarıyer-Beykoz SB, Sarıyer-Beykoz NB, Beykoz-Kanlıca SB, Beykoz-Kanlıca NB, Kanlıca-Vaniköy SB, Kanlıca-Vaniköy NB, Vaniköy-Üsküdar SB, Vaniköy-Üsküdar NB, Üsküdar-Kadıköy SB, Üsküdar-Kadıköy NB
X_{10}	Vessel Reliability	9	Age (New, Middle Age, Old) x Flag Category (Low Risk, Medium Risk, High Risk)
X_{11}	Time of the Day	2	Daytime, Nighttime

Table 3.7 Possible values for 1st and 2nd Interacting Vessel Class (X_1, X_2)

<table>
<tr><th></th><th colspan="6">Vessel Type</th></tr>
<tr><th>Length(m)</th><th>Tanker</th><th>LNG-LPG</th><th>Dry Cargo</th><th>Passenger</th><th>Local ferry</th><th>Local others</th></tr>
<tr><td>0 - 100</td><td colspan="3">1</td><td rowspan="2">3</td><td>4</td><td>5</td></tr>
<tr><td>100 - 150</td><td colspan="3">2</td><td colspan="2" rowspan="5"></td></tr>
<tr><td>150 - 200</td><td colspan="3">6</td><td rowspan="3">9</td></tr>
<tr><td>200 - 250</td><td colspan="3">7</td></tr>
<tr><td>250 -300</td><td colspan="3">8</td></tr>
<tr><td>300-350</td><td colspan="3">11</td><td>10</td></tr>
</table>

For the situational attribute X_9, Istanbul Strait is divided into 12 different zones as depicted in Figure 3.7 and listed in Table 3.8. Each zone is unique in terms of population, historical buildings, property, and infrastructure located on its shores, as well as its geographical difficulty, and local traffic density. These zones are determined through our discussions with the VTS.

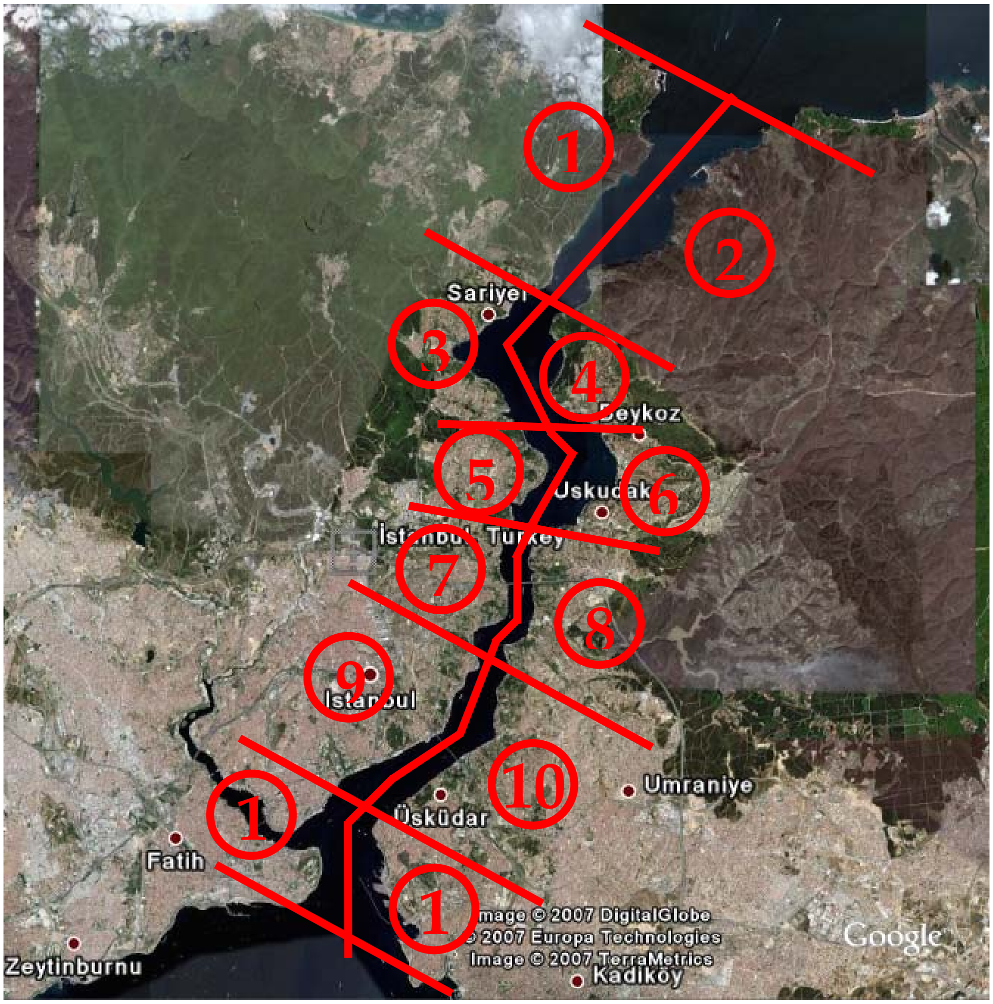

Figure 3.7 Risk Zones

Table 3.8 List of zones

Zone Number	Zone Name
1	Anadolu Feneri - Sarıyer Southbound
2	Anadolu Feneri - Sarıyer Northbound
3	Sarıyer - Beykoz Southbound
4	Sarıyer - Beykoz Northbound
5	Beykoz - Kanlıca Southbound
6	Beykoz - Kanlıca Northbound
7	Kanlıca -Vaniköy Southbound
8	Kanlıca -Vaniköy Northbound
9	Vaniköy -Üsküdar Southbound
10	Vaniköy -Üsküdar Northbound
11	Üsküdar - Kadıköy Southbound
12	Üsküdar – Kadıköy Northbound

In addition to the individual situational attributes listed in Table 3.6, attributes describing interaction effects are included in the model. For example, $X_{12} = X_1 \cdot X_9$ represents the interaction between the 1st interacting vessel class and the zone. The objective is to model the combined impact of certain key attributes on the accident probability. There are 12 interaction attributes as seen in Table 3.9. Again, these interaction attributes are determined through interviews with authorities at the VTS.

Table 3.9 Interaction Attributes

	Interaction	**Description**
X_{12}	$X_1 \cdot X_9$	1st Interacting Vessel Class x Zone
X_{13}	$X_4 \cdot X_7$	1st Vessel Pilot Request x Current
X_{14}	$X_4 \cdot X_9$	1st Vessel Pilot Request x Zone
X_{15}	$X_3 \cdot X_9$	1st Vessel Tugboat Request x Zone
X_{16}	$X_3 \cdot X_7$	1st Vessel Tugboat Request x Current
X_{17}	$X_5 \cdot X_6$	Nearest Transit Vessel Proximity x Visibility
X_{18}	$X_5 \cdot X_7$	Nearest Transit Vessel Proximity x Current
X_{19}	$X_7 \cdot X_9$	Current x Zone
X_{20}	$X_6 \cdot X_8$	Visibility x Local Traffic Density
X_{21}	$X_6 \cdot X_9$	Visibility x Zone
X_{22}	$X_9 \cdot X_8$	Zone x Local Traffic Density
X_{23}	$X_{10} \cdot X_4$	Time of the Day x 1st Vessel Pilot Request

To assess the accident probability given an instigator, subject matter experts were asked to compare two situations $\underline{S}_1^1$ and $\underline{S}_2^1$. Figure 3.8 provides a sample question appearing in one of the accident probability questionnaires used in the risk analysis of the transit vessel traffic in the Istanbul Strait. The questionnaires were answered by numerous experts with different backgrounds (e.g. pilots, captains, VTS authorities, academia, etc.)

In each question, compared situations differ only in one situational attribute. If the expert thinks that the likelihood of an accident is the same in situations 1 and 2, then he/she circles “1”. If the expert thinks that it is more likely to have an accident in one situation than other, then he/she circles a value towards that situation. For example, if “5” is circled towards Situation 2, then the expert thinks that it is 5 times more likely to have an accident in Situation 2 than Situation 1. The experts don’t have to select one of the values on the given scale. They can also enter other values as they see fit.

QUESTION 1

Situation 1	Situational Attribute	Situation 2
1	1st Interacting Vessel Class	11
1	2nd Interacting Vessel Class	-
Yes	1st Vessel Tugboat Request	-
Yes	1st Vessel Pilot Request	-
Same direction >8 cables	Nearest Transit Vessel Proximity	-
>1 mile	Visibility	-
0-2 knot/hr opposite to 1st vessel	Current	-
1-2	Local Traffic Density	-
Anadolu Feneri - Sarıyer Northbound	Zone	-
Daytime	Time of the Day	-

HUMAN ERROR		
Other: ____	**9 8 7 6 5 4 3 2 1 2 3 4 5 6 7 8 9**	**Other:** ____
STEERING FAILURE		
Other: ____	**9 8 7 6 5 4 3 2 1 2 3 4 5 6 7 8 9**	**Other:** ____
PROPULSION FAILURE		
Other: ____	**9 8 7 6 5 4 3 2 1 2 3 4 5 6 7 8 9**	**Other:** ____
COMMUNICATION/NAVIGATION EQUIPMENT FAILURE		
Other: ____	**9 8 7 6 5 4 3 2 1 2 3 4 5 6 7 8 9**	**Other:** ____
COLLISION is more likely in Situation 1	⟷	**COLLISION is more likely in Situation 2**

Figure 3.8 A Sample Accident Probability Question

A separate questionnaire is prepared for each 1st tier accident. The experts are asked to compare situations for each instigator type in a given question as seen in Figure 3.8. Note that the instigators specified in the questionnaires are assumed to take place in the 1st interacting vessels. We ask 4 questions per situational attribute, one question representing the worst case scenario, one representing the best case, and two others corresponding to ordinary cases. Since not all accident types are influenced by every situational attribute, the total number of questions differs from one questionnaire to another.

Consider two situations defined by the situational attribute vectors $\underline{S}_1^1$ and $\underline{S}_2^1$. The relative probability is the ratio of the accident probabilities as defined by

$$\frac{\Pr\left(A^1 \middle| I, \underline{S}_1^1\right)}{\Pr\left(A^1 \middle| I, \underline{S}_2^1\right)} = \frac{P_0 \exp\left(\underline{\beta}^T \underline{S}_1^1\right)}{P_0 \exp\left(\underline{\beta}^T \underline{S}_2^1\right)} = \exp\left(\underline{\beta}^T \left(\underline{S}_1^1 - \underline{S}_2^1\right)\right) \tag{3.6}$$

where $(\underline{S}_1^1 - \underline{S}_2^1)$ denotes the difference vector of the two situations. Therefore, the relative probability of an accident given an instigator in two situations depends only on the difference vector $(\underline{S}_1^1 - \underline{S}_2^1)$ and the parameter vector $\underline{\beta}$. Since the experts are asked to assess the above ratio in (3.6), the parameter vector $\underline{\beta}$ can be estimated without determining the accident probability itself.

Let $z_{l,j}$ the response of an expert l ($l = 1,\ldots,m$) to a question j ($j = 1,\ldots,n$). To aggregate the expert responses, their geometric mean is taken as follows:

$$\bar{z}_j = \left(\prod_{l=1}^{m} z_{l,j} \right)^{\frac{1}{m}}. \tag{3.7}$$

The geometric mean is thought to be appropriate since the responses represent ratios of probabilities. Using (3.6) and (3.7), we have

$$\bar{z}_j = \frac{\Pr\left(A^1 \middle| I, \underline{S}_{1j}^1\right)}{\Pr\left(A^1 \middle| I, \underline{S}_{2j}^1\right)} = \exp\left(\underline{\beta}^T \left(\underline{S}_{1j}^1 - \underline{S}_{2j}^1\right)\right) \tag{3.8}$$

which makes the basis for a regression equation used to determine the relative effect of the situational attributes on the accident probability. This equation is

$$y_j = \underline{\beta}^T \left(\underline{S}_{1j}^1 - \underline{S}_{2j}^1\right) + \varepsilon_j \tag{3.9}$$

where $y_j = \ln(\bar{z}_j)$ and ε_j is the residual error term. Since in each question, compared situations differ only in one situational attribute, the difference vector has all “0” except a “1” term.

Under the assumption that ε is normally distributed ($\varepsilon_j \sim i.i.d\ N(0,\sigma^2)$), this equation can be explained as a standard multiple linear regression equation. The aggregate expert response is the dependent variable, $(\underline{S}^1_{1j} - \underline{S}^1_{2j})$ is the vector of independent variables and $\underline{\beta}$ is a vector of regression parameters. Subsequently, the $\underline{\hat{\beta}}$ vector is estimated using a standard linear regression analysis. The results of the regression analysis for each accident probability questionnaire are given in Appendix B.

3.4.3.1.2 PROBABILITY OF HUMAN ERROR

We have relied on the expert judgment to estimate the probability of human error due to the lack of data. We have assumed that the human error probability depends on situational attributes. We estimate this probability using the paired comparison approach described in section 3.4.3.1.1. Thus the probability of human error is defined as

$$\Pr\left(\text{Human Error}\,\middle|\,\underline{S}^1\right) = P_0^1 \exp\left(\underline{\beta}^{1T}\,\underline{S}^1\right) \tag{3.10}$$

where P_0^1 is the calibration constant and $\underline{\beta}^1$ is the parameter vector for the human error probability. To assess the human error probability, experts were asked to make many two-situation $\underline{S}^1_1$ and $\underline{S}^1_2$ comparisons. Figure 3.9 provides a sample question appearing in the human error questionnaire, which consists of 40 questions.

QUESTION 34

Situation 1	**Situational Attribute**	**Situation 2**
10	1st Interacting Vessel Class	-
2	2nd Interacting Vessel Class	-
Yes	1st Vessel Pilot Request	-
2 knots/hr speed difference overtaking lane	Nearest Transit Vessel Proximity	-
0.5 - 1 mile	Visibility	-
4-6 knots/hr opposite to 1st vessel	Current	-
3-5	Local Traffic Density	-
Sariyer - Beykoz Northbound	Zone	-
New & High Risk	Vessel Reliability	Medium Age x Low Risk
Daytime	Time of the Day	-
Other: ____	**9 8 7 6 5 4 3 2 1 2 3 4 5 6 7 8 9**	**Other:** ____
HUMAN ERROR is more likely in Situation 1	⟵⟶	**HUMAN ERROR is more likely in Situation 2**

Figure 3.9 A Sample Human Error Question

The regression equation used to determine the relative effect of situational attributes on the human error probability is

$$y_j = \underline{\beta}^{1T}\left(\underline{S}^1_{1j} - \underline{S}^1_{2j}\right) + \varepsilon_j \tag{3.11}$$

where ε is the residual error term. Under the assumption that ε is normally distributed, this equation is a standard multiple linear regression. Therefore, the estimate parameter vector $\hat{\underline{\beta}}$ is obtained using a linear regression analysis. The results of the regression analysis for the human error questionnaire are given in Appendix C.

Since the expert responses are used to estimate relative comparisons, these relative results are then calibrated into probability values using the calibration constant P_0. The calibration constants are obtained using accident data. As an example, consider the probability of collision, which is evaluated by

$$\begin{aligned}\Pr(\text{Collision}) = &\sum_{l\in S^1} \Pr\left(\text{Collision}\middle|\text{Human Error}, S_{ls}^1\right)\times\Pr\left(\text{Human Error}\middle|S_{ls}^1\right)\times\Pr\left(S_{ls}^1\right)\\ &+\sum_{l\in S^1} \Pr\left(\text{Collision}\middle|\text{Steering Fail}, S_{ls}^1\right)\times\Pr\left(\text{Steering Fail}\middle|S_{ls}^1\right)\times\Pr\left(S_{ls}^1\right)\\ &+\sum_{l\in S^1} \Pr\left(\text{Collision}\middle|\text{Propulsion Fail}, S_{ls}^1\right)\times\Pr\left(\text{Propulsion Fail}\middle|S_{ls}^1\right)\times\Pr\left(S_{ls}^1\right)\\ &+\sum_{l\in S^1} \Pr\left(\text{Collision}\middle|\text{Comm/Nav Fail}, S_{ls}^1\right)\times\Pr\left(\text{Comm/Nav Fail}\middle|S_{ls}^1\right)\times\Pr\left(S_{ls}^1\right)\end{aligned} \tag{3.12}$$

where each term of the summation represents the joint probability of collision and an instigator such as

$$\Pr(\text{Collision,Human Error}) = \sum_{l\in S^1} \Pr\left(\text{Collision}\middle|\text{Human Error}, S_{ls}^1\right)\times\Pr\left(\text{Human Error}\middle|S_{ls}^1\right)\times\Pr\left(S_{ls}^1\right). \tag{3.13}$$

Using (3.5) and (3.10), we obtain

$$\begin{aligned}\Pr(\text{Collision}) = &\sum_{l\in S^1} P_0^2 \exp\left(\sum_{i=1}^{p}\beta_i^2 x_i + \beta_0^2\right)\times P_0^1 \exp\left(\sum_{i=1}^{p}\beta_i^1 x_i + \beta_0^1\right)\times\Pr\left(S_{ls}^1\right)\\ &+\sum_{l\in S^1} P_0^3 \exp\left(\sum_{i=1}^{p}\beta_i^3 x_i + \beta_0^3\right)\times\Pr\left(\text{Steering Fail}\middle|S_{ls}^1\right)\times\Pr\left(S_{ls}^1\right)\\ &+\sum_{l\in S^1} P_0^4 \exp\left(\sum_{i=1}^{p}\beta_i^4 x_i + \beta_0^4\right)\times\Pr\left(\text{Propulsion Fail}\middle|S_{ls}^1\right)\times\Pr\left(S_{ls}^1\right)\\ &+\sum_{l\in S^1} P_0^5 \exp\left(\sum_{i=1}^{p}\beta_i^5 x_i + \beta_0^5\right)\times\Pr\left(\text{Comm/Nav Fail}\middle|S_{ls}^1\right)\times\Pr\left(S_{ls}^1\right)\end{aligned}. \tag{3.14}$$

In simulation, the collision probability at time t is evaluated using the following expression:

$$\begin{aligned}\Pr\left(\text{Collision}\right) = & \sum_{l\in S^1} P_0^2 \exp\left(\sum_{i=1}^{p}\beta_i^2 x_i + \beta_0^2\right)\times P_0^1 \exp\left(\sum_{i=1}^{p}\beta_i^1 x_i + \beta_0^1\right)\times \mathbf{I}_{S_{ls}^1} \\ & + \sum_{l\in S^1} P_0^3 \exp\left(\sum_{i=1}^{p}\beta_i^3 x_i + \beta_0^3\right)\times \Pr\left(\text{Steering Fail}\middle|S_{ls}^1\right)\times \mathbf{I}_{S_{ls}^1} \\ & + \sum_{l\in S^1} P_0^4 \exp\left(\sum_{i=1}^{p}\beta_i^4 x_i + \beta_0^4\right)\times \Pr\left(\text{Propulsion Fail}\middle|S_{ls}^1\right)\times \mathbf{I}_{S_{ls}^1} \\ & + \sum_{l\in S^1} P_0^5 \exp\left(\sum_{i=1}^{p}\beta_i^5 x_i + \beta_0^5\right)\times \Pr\left(\text{Comm/Nav Fail}\middle|S_{ls}^1\right)\times \mathbf{I}_{S_{ls}^1}\end{aligned}. \qquad (3.15)$$

where $\mathbf{I}_{S_{ls}^1}$ is the indicator function and $\mathbf{I}_{S_{ls}^1} = \begin{cases} 1 & S_{ls}^1 \text{ represents the current situation} \\ 0 & \text{Otherwise} \end{cases}$ and $\sum_{l\in S^1} \mathbf{I}_{S_{ls}^1} = 1$.

In order to calibrate the joint probabilities, we first assign $P_0^1 = P_0^2 = \text{L} = P_0^5 = 1$ and $\Pr\left(\text{Steering Fail}\middle|S_{ls}^1\right) = \Pr\left(\text{Propulsion Fail}\middle|S_{ls}^1\right) = \Pr\left(\text{Comm/Nav Fail}\middle|S_{ls}^1\right) = 1$. We then take the long run average of each component of the summation in (3.15) considering all the possible situations in the simulation. We then compare these values with their counterparts (e.g. $\Pr\left(\text{Collision,Human Error}\right)$, etc.) obtained from the historical accident data.

According to the Bayes' Theorem,

$$\Pr\left(\text{Human Error}\,\middle|\,\text{Collision}\right) = \frac{\Pr\left(\text{Collision,Human Error}\right)}{\Pr\left(\text{Collision}\right)} \tag{3.16}$$

which gives

$$\Pr\left(\text{Collision,Human Error}\right) = \Pr\left(\text{Human Error}\,\middle|\,\text{Collision}\right) \times \Pr\left(\text{Collision}\right). \tag{3.17}$$

From the accident database, we can estimate $\Pr\left(\text{Human Error}\,\middle|\,\text{Collision}\right)$ and $\Pr\left(\text{Collision}\right)$ using

$$\Pr\left(\text{Human Error}\,\middle|\,\text{Collision}\right) = \frac{\text{\# of collisions due to human error}}{\text{Total \# of collisions}} \tag{3.18}$$

and

$$\Pr\left(\text{Collision}\right) = \frac{\text{Total \# of collisions}}{\text{Total \# of vessels}}. \tag{3.19}$$

Thus, using (3.17) we can estimate $\Pr\left(\text{Collision,Human Error}\right)$. The joint probability values obtained from the historical data are given in Table 3.10.

Table 3.10 Pr(1st tier Accident,Instigator) obtained from accident data

		Instigator				
		Human Error	Steering Failure	Propulsion Failure	Comm/Nav Eq. Failure	Mech/Elec Failure
1st tier Accident	Collision	0.000293584	0.000008720	0	0	
	Ramming	0.000152593	0.000026227	0.000023843	0	
	Grounding	0.000167023	0.000038396	0.000019198	0	
	Fire/Explo	0.000063801				0.000079751

Let G_1 be the long run average of $\sum_{l\in S^1} P_0^2 \exp\left(\sum_{i=1}^{p}\beta_i^2 x_i + \beta_0^2\right)\times P_0^1 \exp\left(\sum_{i=1}^{p}\beta_i^1 x_i + \beta_0^1\right)\times \mathbf{I}_{S_{ls}^1}$ in (3.15), which can also be expresses as $P_0^1 P_0^2 C_1$ where $C_1 \in R$. Thus, the comparison of G_1 with its counterpart (e.g. $\Pr(\text{Collision,Human Error})$) obtained from the historical data shown in Table 3.10, will provide an estimate for the product of calibration constants $P_0^1 P_0^2$ using

$$P_0^1 P_0^2 = \frac{\Pr(\text{Collision,Human Error})}{C_1}. \tag{3.20}$$

Similarly,

$$P_0^3 \times \Pr\left(\text{Steering Fail}\middle|S_{ls}^1\right) = \frac{\Pr(\text{Collision,Steering Fail})}{C_2}, \tag{3.21}$$

$$P_0^4 \times \Pr\left(\text{Propulsion Fail}\middle|S_{ls}^1\right) = \frac{\Pr(\text{Collision,Propulsion Fail})}{C_3} \tag{3.22}$$

and

$$P_0^5 \times \Pr\left(\text{Comm/Nav Fail}\,\middle|\,S_{ls}^1\right) = \frac{\Pr\left(\text{Collision,Comm/Nav Fail}\right)}{C_4}. \tag{3.23}$$

Therefore, we do not need to estimate the individual probability of human error or any other instigator probability in order to calibrate the probabilities obtained through expert judgment elicitation and simulation. The particular values of the aforementioned expressions obtained from the simulation are shown in Table 3.11.

Table 3.11 Calibration expressions for joint accident probabilities

Expression	Value
$P_0^1 P_0^2$	4.58692E-08
$P_0^3 \times \Pr(\text{Steering Fail})$	1.52547E-09
$P_0^4 \times \Pr(\text{Propulsion Fail})$	0
$P_0^5 \times \Pr(\text{Comm/Nav Fail})$	0
$P_0^1 P_0^6$	1.01135E-07
$P_0^7 \times \Pr(\text{Steering Fail})$	4.05626E-08
$P_0^8 \times \Pr(\text{Propulsion Fail})$	1.29715E-08
$P_0^9 \times \Pr(\text{Comm/Nav Fail})$	0
$P_0^1 P_0^{10}$	5.28376E-08
$P_0^{11} \times \Pr(\text{Steering Fail})$	6.03708E-08
$P_0^{12} \times \Pr(\text{Propulsion Fail})$	5.20445E-08
$P_0^{13} \times \Pr(\text{Comm/Nav Fail})$	0
$P_0^1 P_0^{14}$	6.11866E-06
$P_0^{15} \times \Pr(\text{Mech/Elec Fail})$	2.73693E-05

Although we guarantee that the long-run average accident probabilities are legitimate through calibration, we can not ensure that the instantaneously calculated accident probabilities will have values between 0 and 1 in a given simulation run. Thus, these terms resemble likelihood functions rather than actual probabilities.

3.4.3.2 2ND TIER ACCIDENT PROBABILITY

The conditional probability of a 2nd tier accident given a 1st tier accident in (3.3) is estimated using the historical accident data utilizing

$$\Pr\left(A_i^2 \middle| A_m^1\right) = \frac{\text{\# of type } m \text{ 1}^{\text{st}} \text{ tier accidents that lead to a type } i \text{ 2}^{\text{nd}} \text{ tier accident}}{\text{Total \# of type } m \text{ 1}^{\text{st}} \text{ tier accidents}}. \quad (3.24)$$

The values of these conditional probabilities are given in Table 3.12.

Table 3.12 Values for Pr(2nd tier Accident|1st tier Accident)

		2nd tier Accident				
		No 2nd Tier Accident	Grounding	Ramming	Fire / Explosion	Sinking
1st tier Accident	Collision	0.8737	0.0289	0.0000	0.0158	0.0816
	Grounding	0.9794			0.0041	0.0165
	Ramming	0.8325	0.1218		0.0102	0.0355
	Fire / Explosion	0.9355	0.0081	0.0000		0.0565

3.4.3.3 EXPECTED CONSEQUENCE

3.4.3.3.1 PROBABILITY OF A CONSEQUENCE GIVEN AN ACCIDENT

Due to the lack of any sort of consequence data, we rely on the expert judgment to estimate the probability of a consequence. We assume that the probability of consequence depends on the accident type and the situational attributes. The list of the situational attributes influencing consequence impact (including interaction attributes) and their possible values are given in Table 3.13.

Table 3.13 Possible values of situational attributes influencing consequence impact S^2

	Attribute Name	# of Possible Values	Description
W_1	1st Interacting Vessel Type	6	LNG-LPG, Tanker, Empty LNG-LPG, Empty Tanker; Passenger, other vessel
		2	Passenger vessel, other vessel
		3	Loaded LNG-LPG and Tanker, Passenger, other vessel
W_2	2nd Interacting Vessel Type	6	LNG-LPG, Tanker, Empty LNG-LPG, Empty Tanker; Passenger, other vessel
		2	Passenger vessel, other vessel
		3	Loaded LNG-LPG and Tanker, Passenger, other vessel
W_3	1st Interacting Vessel Length	2	0-150m., 150-300m.
W_4	2nd Interacting Vessel Length	2	0-150m., 150-300m.
W_5	Zone	6	Anadolu Feneri-Sarıyer, Sarıyer-Beykoz, Beykoz-Kanlıca, Kanlıca-Vaniköy, Vaniköy-Üsküdar, Üsküdar-Kadıköy
W_6	$W_1 \cdot W_2$		1st Interacting Vessel Type x 2nd Interacting Vessel Type
W_7	$W_3 \cdot W_4$		1st Interacting Vessel Length x 2nd Interacting Vessel Length
W_8	$W_1 \cdot W_5$		1st Interacting Vessel Type x Zone
W_9	$W_3 \cdot W_5$		1st Interacting Vessel Length x Zone

As seen in Table 3.13, 1st interacting vessel type has three different sets for different consequence-accident type pairs. For example, for environmental damage-collision, 1st Interacting Vessel Type is categorized in five possible values in terms of cargo type and amount. However, for human casualty-collision pair, it is categorized in three values based on the number of people in the vessel.

We estimate this probability using the paired comparison approach described in section 3.4.3.1.1. Thus the probability of a consequence given an accident and situation is defined by

$$\Pr\left(C_j\left(h\right)\middle| A^n, \underline{S}^2\right) = P_0 \exp\left(\underline{\beta}^T \underline{S}^2\right) \tag{3.25}$$

where P_0 is the calibration constant and $\underline{\beta}$ is the parameter vector. To assess the probability of a consequence given an accident, experts were asked to compare two situations $\underline{S}_1^2$ and $\underline{S}_2^2$. Figure 3.10 provides a sample question appearing in the consequence questionnaire given a fire/explosion. A separate questionnaire is prepared for each consequence-accident type pair. The experts are asked to compare situations for each consequence impact level in a given question as seen in Figure 3.10. We ask 4 questions per situational attribute, one question representing the worst case scenario, one representing the best case, and two others corresponding to ordinary cases. Since not all consequence-accident type pairs are influenced by every situational attribute, the total number of questions differs from one questionnaire to another.

QUESTION 5 - FIRE/EXPLOSION

Situation 1	Situational Attribute	Situation 2
General Cargo Vessel	1st Interacting Vessel Class	-
≤150m.	Length of the 1st Interacting Vessel	>150m.
Anadolu Feneri - Sarıyer	Zone	-
Other: ___	9 8 7 6 5 4 3 2 1 2 3 4 5 6 7 8 9	Other: ___
LOW SEVERITY HUMAN CASUALTY is more likely in Situation 1	⟷	LOW SEVERITY HUMAN CASUALTY is more likely in Situation 2
Other: ___	9 8 7 6 5 4 3 2 1 2 3 4 5 6 7 8 9	Other: ___
MEDIUM SEVERITY HUMAN CASUALTY is more likely in Situation 1	⟷	MEDIUM SEVERITY HUMAN CASUALTY is more likely in Situation 2
Other: ___	9 8 7 6 5 4 3 2 1 2 3 4 5 6 7 8 9	Other: ___
HIGH SEVERITY HUMAN CASUALTY is more likely in Situation 1	⟷	HIGH SEVERITY HUMAN CASUALTY is more likely in Situation 2

Figure 3.10 A Sample Consequence Question

The regression equation used to determine the relative effect of situational attributes on the probability of a consequence given an accident is

$$y_j = \underline{\beta}^T \left(\underline{S}_{1j}^2 - \underline{S}_{2j}^2 \right) + \varepsilon_j \qquad (3.26)$$

where ε_j is the residual error term. The results of the regression analysis for the consequence questionnaires are given in Appendix D.

Since the expert responses are used to estimate relative comparisons, these relative results are then calibrated into probability values using the calibration constant P_0. The calibration constants are obtained using accident data. As an example, consider the probability of low casualty given collision, which is evaluated by

$$\begin{aligned}\Pr\left(\text{Casualty}\left(\text{Low}\right)\middle|\text{Collision}\right) &= \sum_{l\in S^2} \Pr\left(\text{Casualty}\left(\text{Low}\right)\middle|\text{Collision}, S_{ls}^2\right)\times\Pr\left(S_{ls}^2\right) \\ &= \sum_{l\in S^2} P_0^{20}\exp\left(\sum_{i=1}^{q}\beta_i^{20}x_i+\beta_0^{20}\right)\times\Pr\left(S_{ls}^2\right)\end{aligned}. \quad (3.27)$$

In simulation, the low casualty probability given collision at time *t* is evaluated using the following expression:

$$\Pr\left(\text{Casualty}\left(\text{Low}\right)\middle|\text{Collision}\right) = \sum_{l\in S^2} P_0^{20}\exp\left(\sum_{i=1}^{q}\beta_i^{20}x_i+\beta_0^{20}\right)\times\mathbf{I}_{S_{ls}^2}\ . \quad (3.28)$$

where $\mathbf{I}_{S_{ls}^2}$ is the indicator function and $\mathbf{I}_{S_{ls}^2} = \begin{cases}1 & S_{ls}^2 \text{ represents the current situation} \\ 0 & \text{Otherwise}\end{cases}$ and $\sum_{l\in S^2}\mathbf{I}_{S_{ls}^2} = 1$.

In order to calibrate the joint probabilities, we first assign $P_0^{20} = 1$. We then take the long run average of the conditional probability expression in (3.28) considering all the possible situations in the simulation. We then compare these values with their counterparts (e.g. $\Pr\left(\text{Casualty}\left(\text{Low}\right)\middle|\text{Collision}\right)$, etc.) obtained from the accident data using

$$\Pr\left(\text{Casualty}\left(\text{Low}\right)\middle|\text{Collision}\right) = \frac{\text{\# of collisions with low casualty}}{\text{Total \# of collisions}}. \tag{3.29}$$

The conditional probability values obtained from the historical accident data for each consequence-accident pair are given in Table 3.14, 3.15, 3.16, and 3.17.

Table 3.14 Pr(Human Casualty|Accident) obtained from accident data

	Human Casualty		
	Low	Medium	High
Collision	0.9579	0.0421	
Ramming	0.9695	0.0305	
Grounding			
Fire/Explo	0.9248	0.0376	0.0376
Sinking	0.8241	0.1759	

Table 3.15 Pr(Property/Infrastructure Damage|Accident) obtained from accident data

	Property/Infrastructure Damage		
	Low	Medium	High
Collision			
Ramming	0.6497	0.3503	
Grounding			
Fire/Explo	0.8195	0.1579	0.0226
Sinking	0.2222	0.7778	

Table 3.16 Pr(Environmental Damage|Accident) obtained from accident data

	Environmental Damage		
	Low	Medium	High
Collision	0.9763	0.0237	
Ramming	0.9797	0.0203	
Grounding	0.9928	0.0072	
Fire/Explo	0.9474	0.0226	0.0301
Sinking	0.9537	0.0463	

Table 3.17 Pr(Traffic Effectiveness|Accident) obtained from accident data

	Traffic Effectiveness		
	Low	Medium	High
Collision	0.9737	0.0263	
Ramming	0.9695	0.0305	
Grounding	0.9857	0.0143	
Fire/Explo	0.9398	0.0226	0.0376
Sinking	0.9815	0.0185	

Let G_{20} be the long run average of $\sum_{l \in S^2} P_0^{20} \exp\left(\sum_{i=1}^{q} \beta_i^{20} x_i + \beta_0^{20}\right) \times \mathbf{I}_{S_{ls}^2}$ in (3.28), which can be represented by $P_0^{20} C_{20}$ where $C_{20} \in R$. Thus, the comparison of G_{20} with its counterpart (e.g. $\Pr\left(\text{Casualty}\left(\text{Low}\right)\middle|\text{Collision}\right)$) obtained from the historical data shown in Table 3.14, will provide an estimate for the calibration constant P_0^{20} using

$$P_0^{20} = \frac{\Pr\left(\text{Casualty}\left(\text{Low}\right)\middle|\text{Collision}\right)}{C_{20}}. \tag{3.30}$$

The calibration constants for all consequence impact-accident pairs are calculated similarly. The values of these calibration constants are shown in Table 3.18

Table 3.18.

Table 3.18 Calibration constants of conditional consequence probabilities

Calibration Constant	Value
P020	0.080896
P021	0.003151
P022	0.228763
P023	0.006421
P024	0.088635
P025	0.003153
P026	0.001873
P027	0.129700
P028	0.022069
P029	0.106948
P030	0.001634
P031	0.273184
P032	0.001239
P033	0.204376
P034	0.003266
P035	0.170421
P036	0.003201
P037	0.000164
P038	0.152176
P039	0.004361
P040	0.008278
P041	0.000121
P042	0.042430
P043	0.000236
P044	0.025447
P045	0.000324
P046	0.014419
P047	0.000101
P048	0.000078
P049	0.060872
P050	0.000121
P051	0.162954
P052	0.041665
P053	0.037044
P054	0.004607
P055	0.000389
P056	0.188596
P057	0.098551
P058	0.080896
P059	0.003151
P060	0.106948
P061	0.001634
P062	0.008278
P063	0.000121

Similar to section 3.4.3.1, the calibration constants do not ensure that the instantaneously calculated conditional probabilities of consequences given accidents are legitimate probabilities. Thus, we normalize these conditional probabilities so that $\sum_{h \in \mathcal{L}_{ij}} \Pr\left(C_{ji}(h) \middle| A_i^n\right) = 1$.

3.4.3.3.2 CONSEQUENCE

The consequence impact of a consequence type *j* of an accident type *i* at slice *s* contributed by vessel *r,* C_{jirs}, is assumed to follow a uniform distribution. We have assumed the parameters for different levels of consequence impact given in Table 3.19. These values do not represent the actual consequence of an accident in a specific unit (e.g. dollars or number of casualties). Instead, we utilize index values that represent the user's perception of a low, medium and high consequence. Therefore, the calculated risk values are meaningful when compared to each other in a given context. For example, comparing risk at different slices helps to determine high and low risk zones.

Table 3.19 Consequence Impact Levels

Impact Level	Value
Low	Uniform(0-1,000)
Medium	Uniform(4,000-6,000)
High	Uniform(8,000-10,000)

3.4.3.4 QUESTIONNAIRE DESIGN

The linear regression function in (3.9) with p coefficients (situational attributes), the intercept β_0, and n data points (number of questions) with $n \geq (p+1)$ allows us to construct the following:

$$\mathbf{Y} = \mathbf{X} \cdot \underline{\beta} + \underline{\varepsilon} \tag{3.31}$$

which can be written in the following vector-matrix equation format.

$$\begin{bmatrix} y_1 \\ y_2 \\ \vdots \\ y_n \end{bmatrix}_{n\times 1} = \begin{bmatrix} 1 & \left(x_{1,1}^1 - x_{1,1}^2\right) & \left(x_{2,1}^1 - x_{2,1}^2\right) & \cdots & \left(x_{p,1}^1 - x_{p,1}^2\right) \\ 1 & \left(x_{1,2}^1 - x_{1,2}^2\right) & \left(x_{2,2}^1 - x_{2,2}^2\right) & \cdots & \left(x_{p,2}^1 - x_{p,2}^2\right) \\ \vdots & \vdots & \vdots & & \vdots \\ 1 & \left(x_{1,n}^1 - x_{1,n}^2\right) & \left(x_{2,n}^1 - x_{2,n}^2\right) & \cdots & \left(x_{p,n}^1 - x_{p,n}^2\right) \end{bmatrix}_{n\times(p+1)} \begin{bmatrix} \beta_0 \\ \beta_1 \\ \vdots \\ \beta_p \end{bmatrix}_{(p+1)\times 1} + \begin{bmatrix} \varepsilon_1 \\ \varepsilon_2 \\ \vdots \\ \varepsilon_n \end{bmatrix}_{n\times 1} \tag{3.32}$$

where $x_{i,j}^1$ is the scale value of situational attribute i in Situation 1 of question j and $x_{i,j}^1 - x_{i,j}^2$ is the difference of the scale values.

Therefore, the estimated values of the parameters can be obtained using

$$\hat{\underline{\beta}} = \left(\mathbf{X}^T \mathbf{X}\right)^{-1} \mathbf{X}^T \mathbf{Y} \tag{3.33}$$

where $\mathbf{X}^T$ is the questionnaire matrix and $\mathbf{X}^T\mathbf{X}$, which is a $(p+1)\times(p+1)$ matrix, is called the design matrix $\mathbf{D}$ of the questionnaire. Note that the questionnaire needs to be designed in a manner such that the resulting matrix $\mathbf{D}$ is invertible in order to be able to obtain the estimated values of the parameters, $\underline{\hat{\beta}}$.

3.4.4 NUMERICAL RESULTS

We have incorporated the risk analysis model described in this chapter into the simulation model developed to mimic the transit vessel traffic in the Istanbul Strait, briefly described in Chapter 2. We then performed a scenario analysis to evaluate the characteristics of accident risk in the Strait. This analysis has provided us with the ability to investigate how changes in various policies and practices impact risk. These include vessel arrival rates, scheduling policies, pilotage, overtaking, and local traffic density.

In the scenario analysis, the base scenario represents the present system with all the current regulations and policies in place. The simulation results of each scenario are compared to the results of the base scenario. The findings are presented below.

3.4.4.1 IMPACT OF ARRIVAL RATES

We start our analysis by focusing on the impact of arrival rates of some of the vessels. In Scenario 1, we increase the arrival rates of dangerous cargo vessels (Class A, B, C, and E) 5%. As a result, the average risk in most of the slices increases as seen in Table 3.20

Table 3.20. In those slices where the average risk decreases, the observed change in percentage is very small.

On the other hand, when we decrease the arrival rates of dangerous cargo vessels 20% in Scenario 2, the average risk decreases in most of the slices.

Thus, the average slice risk is directly proportional to the vessel arrival rates. However, vessel arrivals have a small impact on the accident risk since the scheduling policy to take vessels into the Strait and subsequently the required time gap between vessels do not change. In order to obtain a significant impact on the accident risks, the change in the arrival rates must be substantial.

Table 3.20 Average Slice Risk in scenarios 1 and 2 compared to the Base Scenario

	BASE SCENARIO		**SCENARIO 1**			**SCENARIO 2**		
Slice	**Average**	**Half Width (95% CI)**	**Average**	**Half Width (95% CI)**	**% Increase in Average**	**Average**	**Half Width (95% CI)**	**% Increase in Average**
1	1.3748	0.34	1.3932	0.32	1.34%	1.2815	0.26	-6.79%
2	1.6021	0.63	1.6279	0.61	1.61%	1.461	0.45	-8.81%
3	1.5105	0.35	1.5078	0.26	-0.18%	1.3895	0.23	-8.01%
4	1.4257	0.30	1.4255	0.24	-0.01%	1.3309	0.23	-6.65%
5	1.4322	0.19	1.4315	0.22	-0.05%	1.3626	0.28	-4.86%
6	1.4484	0.26	1.4386	0.17	-0.68%	1.402	0.32	-3.20%
7	1.1723	0.08	1.1863	0.06	1.19%	1.1276	0.10	-3.81%
8	1.1943	0.08	1.2193	0.10	2.09%	1.1408	0.08	-4.48%
9	1.2002	0.09	1.2313	0.12	2.59%	1.1486	0.10	-4.30%
10	1.1972	0.10	1.2175	0.11	1.70%	1.1489	0.12	-4.03%
11	1.185	0.09	1.2003	0.07	1.29%	1.139	0.09	-3.88%
12	1.3361	0.07	1.343	0.06	0.52%	1.2767	0.06	-4.45%
13	1.2676	0.06	1.2822	0.06	1.15%	1.2228	0.07	-3.53%
14	1.36	0.06	1.3788	0.06	1.38%	1.313	0.06	-3.46%
15	1.3427	0.05	1.3581	0.07	1.15%	1.2955	0.08	-3.52%
16	1.3462	0.06	1.367	0.08	1.55%	1.3021	0.08	-3.28%
17	1.3794	0.07	1.3956	0.10	1.17%	1.3316	0.08	-3.47%
18	7.0459	0.15	6.9457	0.06	-1.42%	7.1591	0.13	1.61%
19	25.441	0.60	24.8969	0.41	-2.14%	26.4149	0.30	3.83%
20	6.9067	0.09	6.8969	0.18	-0.14%	7.2625	0.07	5.15%
21	4.4412	0.10	4.5107	0.10	1.56%	4.5574	0.07	2.62%

The maximum risks observed at different slices are displayed in Figure 3.11. The overall maximum risk value in Scenario 1 and Scenario 2 decreases 11% and 4%, respectively compared to the maximum value observed in the Base Scenario. However, note that the maximum risk values do not necessarily reflect the impact of a given factor on the overall risk. They are contingent upon the occurrence of a random situation at an instance.

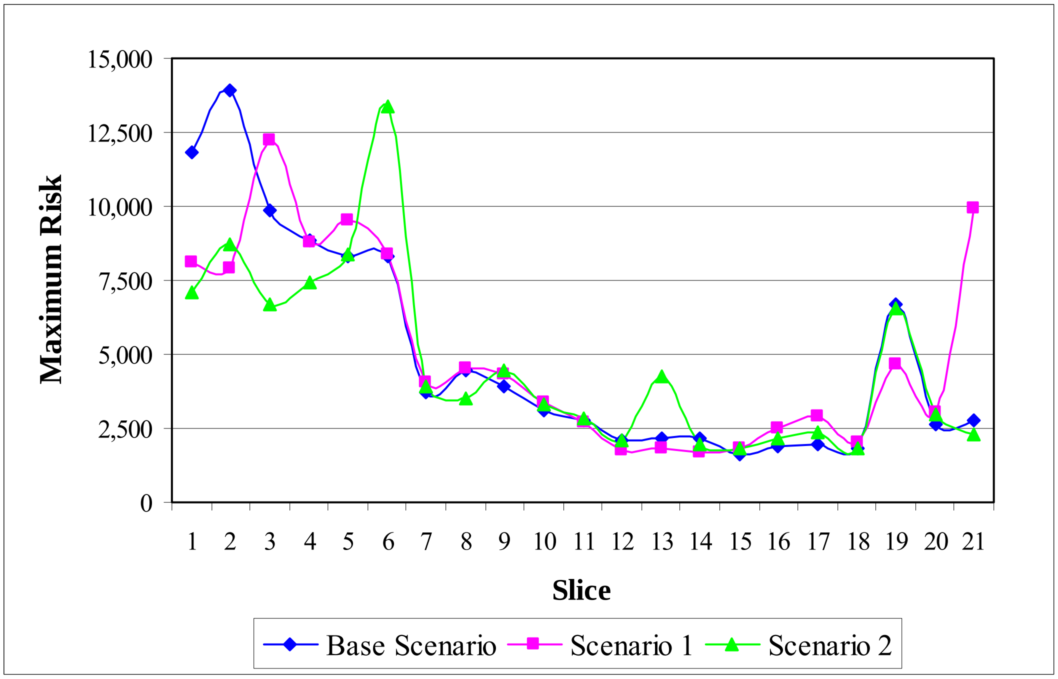

Figure 3.11 Maximum Slice Risk in scenarios 1 and 2 compared to the Base Scenario

In the simulation model, the maximum slice risk observed by a vessel throughout its passage is recorded. The distributions of maximum risk as observed by vessels in each scenario are displayed in Figure 3.12. The patterns are very similar in all scenarios and the majority of the observations result in low maximum risk values. Note that Scenario 2 provides a lower number of observations with high maximum risk values compared to the other scenarios.

Additionally, the distributions for the maximum risk values that are greater than 50 are shown in Figure 3.13. The distributions for all scenarios are very similar at the higher values of risk as well.

Further, while recording the maximum slice risk as observed by a vessel, we also record the slice at which the vessel observes this value. The resulting histograms representing the distribution of slices at which the maximum risk is observed are given in Figure 3.14. In all scenarios, the slice distributions are identical. Also, the majority of the vessels observe the maximum risk at slice 19. Slice 19 is the area between Beşiktaş and Üsküdar, which has a very heavy local traffic.

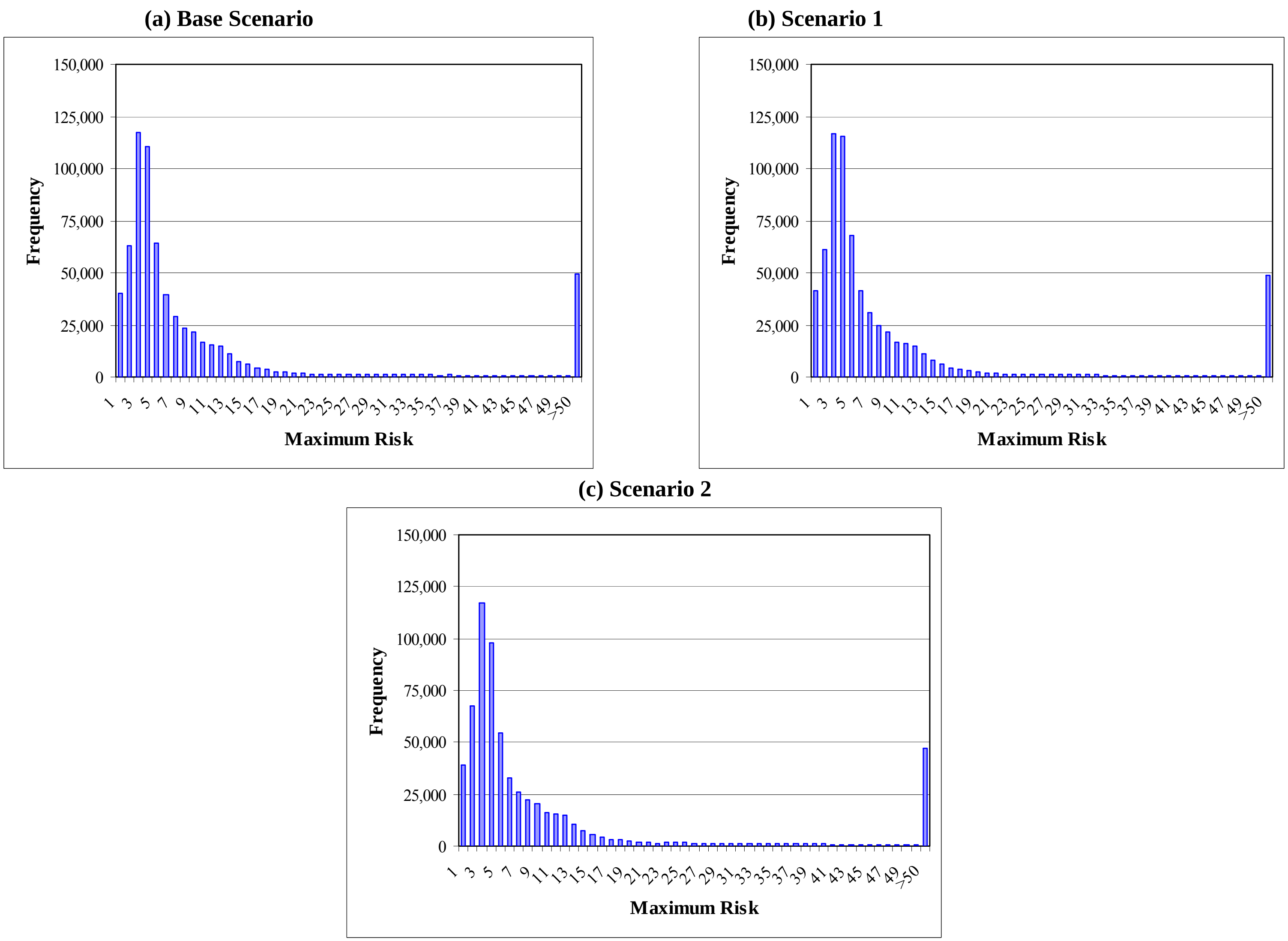

Figure 3.12 Maximum risk distribution as observed by vessels in scenarios 1 and 2 compared to the Base Scenario

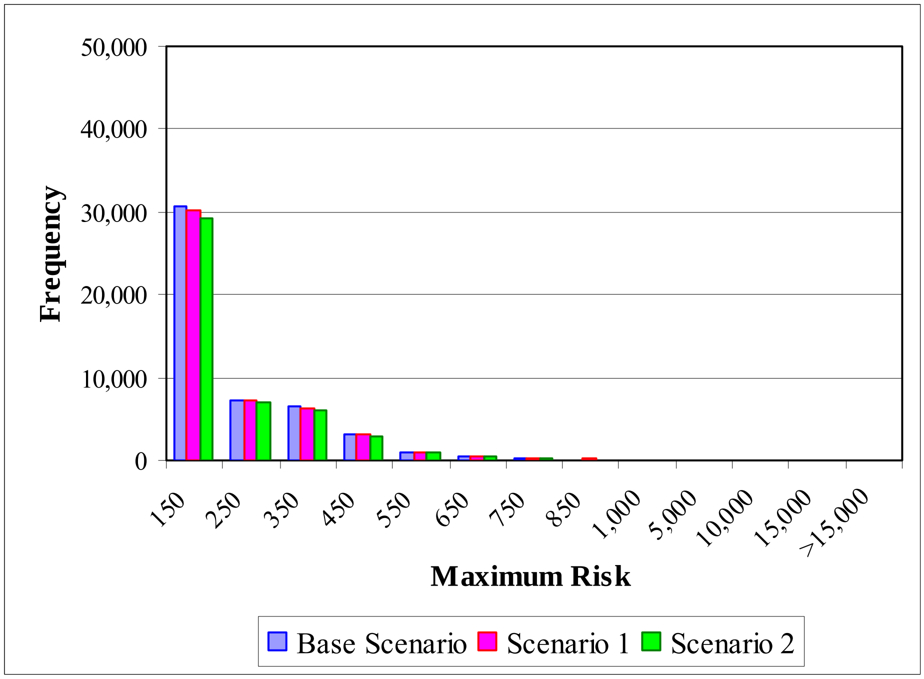

Figure 3.13 Maximum risk distribution as observed by vessels in scenarios 1 and 2 compared to the Base Scenario for values >50

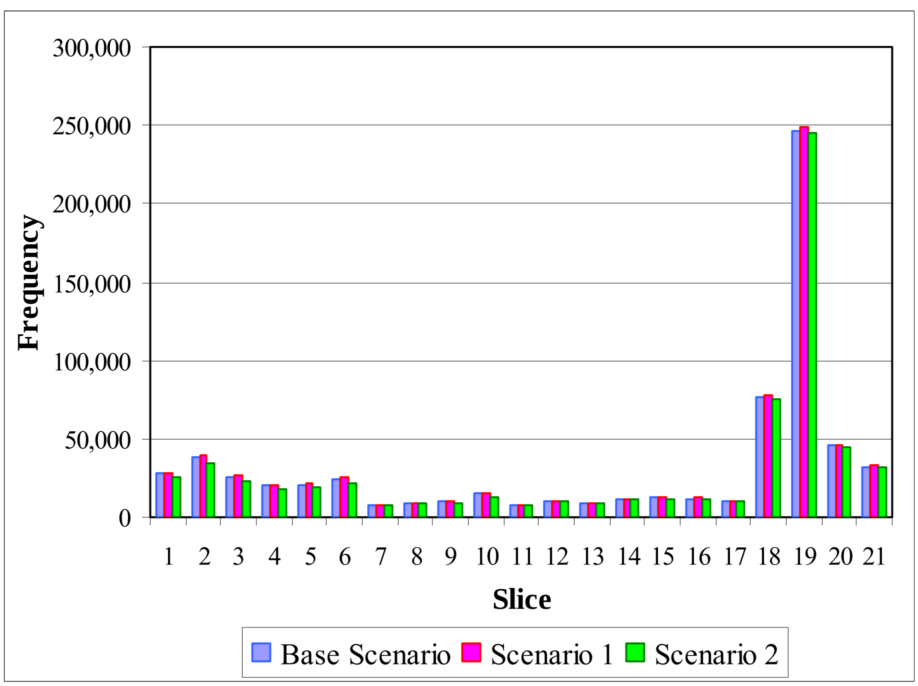

Figure 3.14 Distribution of slices at which maximum risk is observed in scenarios 1 and 2 compared to the Base Scenario

As seen in Table 3.21, the vessel waiting times increase (decrease) in general as we increase (decrease) the arrival rates. Only class B vessels behave differently due to their special circumstances in scheduling.

Table 3.21 Waiting Times in scenarios 1 and 2 compared to the Base Scenario

	BASE SCENARIO		SCENARIO 1			SCENARIO 2		
Class (Direction)	**Average**	**Half Width (95% CI)**	**Average**	**Half Width (95% CI)**	**% Increase in Average**	**Average**	**Half Width (95% CI)**	**% Increase in Average**
A	1,987.15	1,564.30	2,488.50	1,469.88	25.23%	1,157.18	169.59	-41.77%
A(N)	2,127.69	1,642.60	2,696.50	1,664.47	26.73%	1,211.58	181.23	-43.06%
A(S)	1,847.74	1,479.95	2,281.79	1,276.72	23.49%	1,098.75	159.52	-40.54%
B	492.48	19.55	474.40	21.53	-3.67%	562.46	28.61	14.21%
B(N)	500.55	20.51	485.08	21.97	-3.09%	568.33	19.65	13.54%
B(S)	459.77	44.04	427.13	23.89	-7.10%	532.30	23.39	15.78%
C	684.42	112.21	1,067.01	154.54	55.90%	430.23	39.92	-37.14%
C(N)	609.80	110.12	947.54	130.45	55.39%	371.22	30.46	-39.12%
C(S)	754.87	115.01	1,179.56	177.15	56.26%	486.08	40.34	-35.61%
D	172.48	29.67	190.26	29.14	10.31%	144.52	22.25	-16.21%
D(N)	151.75	29.14	163.02	29.45	7.43%	121.53	23.29	-19.91%
D(S)	192.53	30.89	216.61	30.07	12.51%	166.69	22.53	-13.42%
E	180.19	19.37	197.55	17.41	9.63%	142.09	12.96	-21.14%
E(N)	194.60	23.56	216.12	22.66	11.06%	148.96	12.27	-23.45%
E(S)	165.93	15.56	179.36	12.45	8.09%	135.34	13.86	-18.44%
P	77.93	10.07	82.82	4.22	6.27%	67.13	6.15	-13.86%
P(N)	73.86	11.61	78.47	1.81	6.25%	62.25	6.03	-15.72%
P(S)	81.90	9.26	87.23	8.16	6.51%	72.00	6.38	-12.09%

Policy Indication 1: In the wake of an increase in arrival rates, the scheduling regime should be kept as is to maintain the risks at the current levels. A 10% increase in the dangerous cargo vessel arrival rates results in rather acceptable waiting times at the entrance. However, further increases in vessel traffic may result in discouraging ships away from the Strait due to excessive waiting times.

3.4.4.2 IMPACT OF SCHEDULING POLICIES

3.4.4.2.1 SCHEDULING MORE VESSELS

In scenarios 3, 4, 5, and 6, we decrease the required time gap between vessels, thereby scheduling more vessels within a given time frame. Specifically, in Scenario 3, we schedule Class C and Class D vessels every 15 and 5 minutes, respectively, without changing the required time gap between Class A and Class B vessels as seen in Figure 3.15. This allows us, for instance, to schedule 5 Class C and 12 Class D vessels between consecutive northbound Class A vessels as opposed to 2 Class C and 6 Class D vessels in the Base Scenario.

On the other hand, we schedule Class C and Class D vessels every 25 and 6.25 minutes, respectively, in Scenario 4 as depicted in Figure 3.16. This time, we increase the required time gap between consecutive northbound Class A vessels to 100 minutes, thereby scheduling 3 Class C and 12 Class D vessels.

In Scenario 5, we change the time gap between Class C and Class D vessels from 30 and 10 to 20 and 10 minutes, respectively, as shown in Figure 3.17. We also schedule northbound and southbound Class A vessels every 100 and 80 minutes, respectively, instead of 90 and 75 minutes. Finally, in Scenario 6, we combine the scheduling policy in Scenario 3 with the 5% arrival rate increase in Scenario 1.

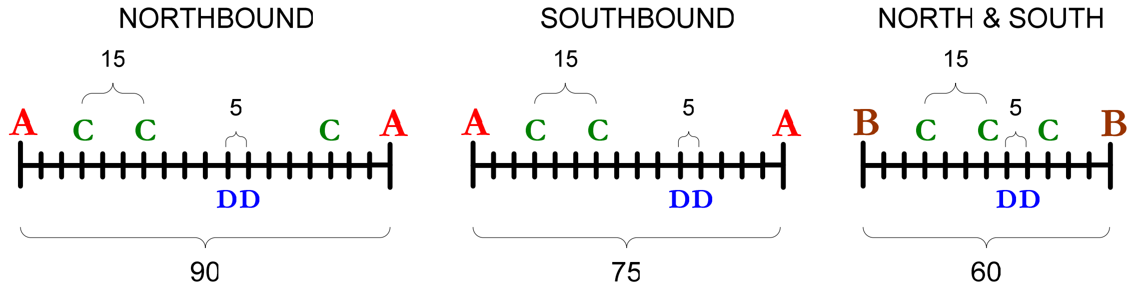

Figure 3.15 Scheduling Policy in Scenario 3

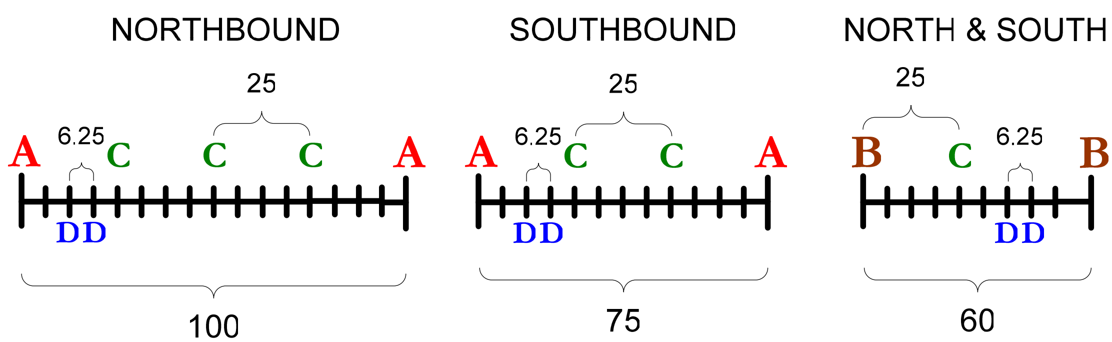

Figure 3.16 Scheduling Policy in Scenario 4

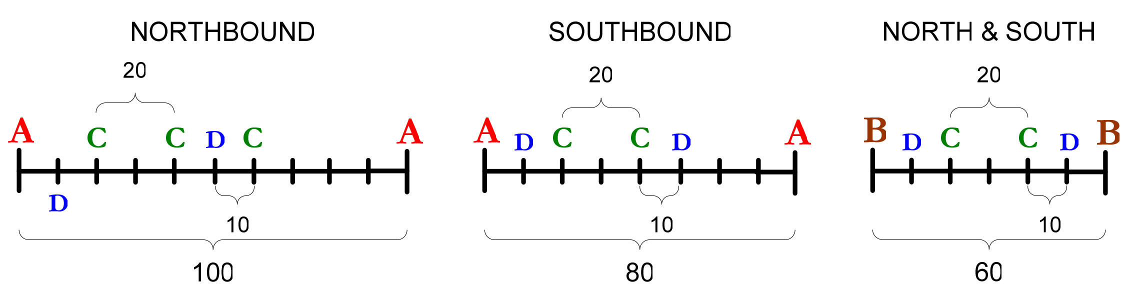

Figure 3.17 Scheduling Policy in Scenario 5

The average risk at each slice for all scenarios is listed in Table 3.22. We observe that the average slice risk increases as the required time gap between consecutive vessels decreases. The greatest increase in average risk is detected in Scenario 6, where both the vessel arrival rates and the number of scheduled vessels are increased. The combined effect of these factors results in a greater increase in average risk.

Table 3.22 Slice Risk in scenarios 3, 4, 5, and 6 compared to the Base Scenario

	BASE SCENARIO		SCENARIO 3			SCENARIO 4			SCENARIO 5			SCENARIO 6		
Slice	**Average**	**Half Width (95% CI)**	**Average**	**Half Width (95% CI)**	**% Increase in Average**	**Average**	**Half Width (95% CI)**	**% Increase in Average**	**Average**	**Half Width (95% CI)**	**% Increase in Average**	**Average**	**Half Width (95% CI)**	**% Increase in Average**
1	1.3748	0.34	1.3826	0.27	0.57%	1.388	0.34	0.96%	1.4055	0.34	2.23%	1.4524	0.34	5.64%
2	1.6021	0.63	1.6453	0.58	2.70%	1.6558	0.61	3.35%	1.6056	0.53	0.22%	1.6809	0.54	4.92%
3	1.5105	0.35	1.6257	0.41	7.63%	1.6293	0.35	7.86%	1.5200	0.28	0.63%	1.6198	0.25	7.24%
4	1.4257	0.30	1.4788	0.37	3.72%	1.4793	0.30	3.76%	1.4227	0.22	-0.21%	1.4793	0.24	3.76%
5	1.4322	0.19	1.4664	0.31	2.39%	1.5075	0.34	5.26%	1.4495	0.25	1.21%	1.4724	0.21	2.81%
6	1.4484	0.26	1.4588	0.24	0.72%	1.5278	0.33	5.48%	1.4651	0.23	1.15%	1.4989	0.23	3.49%
7	1.1723	0.08	1.1928	0.09	1.75%	1.2355	0.12	5.39%	1.2046	0.11	2.76%	1.2362	0.11	5.45%
8	1.1943	0.08	1.2216	0.11	2.29%	1.2592	0.13	5.43%	1.2180	0.09	1.98%	1.2587	0.11	5.39%
9	1.2002	0.09	1.2128	0.10	1.05%	1.2527	0.12	4.37%	1.2330	0.13	2.73%	1.2419	0.08	3.47%
10	1.1972	0.10	1.1961	0.09	-0.09%	1.2442	0.13	3.93%	1.2192	0.11	1.84%	1.2282	0.07	2.59%
11	1.185	0.09	1.2033	0.09	1.54%	1.2410	0.11	4.73%	1.2173	0.12	2.73%	1.2306	0.07	3.85%
12	1.3361	0.07	1.3971	0.07	4.57%	1.4059	0.08	5.22%	1.3524	0.07	1.22%	1.4173	0.04	6.08%
13	1.2676	0.06	1.2968	0.06	2.30%	1.3320	0.07	5.08%	1.2881	0.06	1.62%	1.3303	0.06	4.95%
14	1.36	0.06	1.4086	0.07	3.57%	1.4423	0.08	6.05%	1.3817	0.06	1.60%	1.4463	0.05	6.35%
15	1.3427	0.05	1.3898	0.08	3.51%	1.4247	0.09	6.11%	1.3666	0.07	1.78%	1.4168	0.06	5.52%
16	1.3462	0.06	1.3893	0.08	3.20%	1.4354	0.09	6.63%	1.3700	0.08	1.77%	1.4322	0.07	6.39%
17	1.3794	0.07	1.4172	0.08	2.74%	1.4630	0.09	6.06%	1.3973	0.09	1.30%	1.4533	0.06	5.36%
18	7.0459	0.15	8.8172	0.15	25.14%	8.4584	0.23	20.05%	7.0167	0.17	-0.41%	8.9337	0.17	26.79%
19	25.441	0.60	34.0901	0.52	34.00%	31.9745	0.58	25.68%	25.3566	0.47	-0.33%	34.6849	0.92	36.33%
20	6.9067	0.09	9.2728	0.32	34.26%	8.8498	0.14	28.13%	7.0728	0.32	2.40%	9.496	0.21	37.49%
21	4.4412	0.10	5.9615	0.13	34.23%	5.7542	0.22	29.56%	4.5270	0.12	1.93%	6.1129	0.25	37.64%

Based on the results in Figure 3.18, the maximum risks observed at the middle slices are similar across all four scenarios. Yet they vary at the first six and the last three slices. Note that the last three slices constitute the southern entrance of the Strait where the local traffic is very heavy.

The maximum slice risk observed in all four scenarios is lower than the one observed in the Base Scenario. Scenario 5 provides the lowest maximum risk value. The highest variance in the maximum risk is observed in slices 2 and 20. Finally, Scenario 3 deviates the most from the Base Scenario.

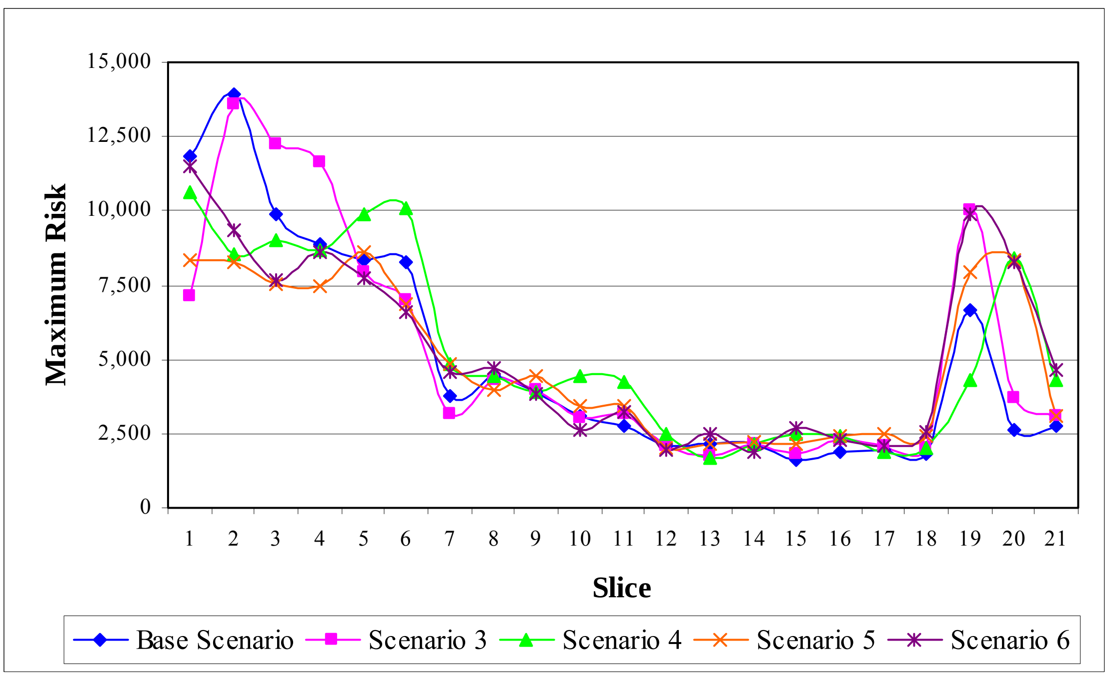

Figure 3.18 Maximum Slice Risk in scenarios 3, 4, 5, and 6 compared to the Base Scenario

The distributions of maximum risk as observed by vessels in the Base Scenario and scenarios 3, 4, 5, and 6 are displayed in Figure 3.19. The results observed in Scenario 5 are very similar to the Base Scenario. However, scenarios 3, 4, and 6 differ from the Base Scenario in that they result in a greater number of observations with high maximum risk values.

Moreover, the distributions for the maximum risk values that are greater than 50 are shown in Figure 3.20. The distributions for all four scenarios are very similar at the higher values of risk as well. The only exception is that Scenario 5 provides a greater number of high maximum risk values.

The histograms representing the distribution of slices at which vessels observe the maximum risk are given in Figure 3.21. In all scenarios, the distributions of slices are very similar. Once again, the majority of the vessels observe the maximum risk at slice 19.

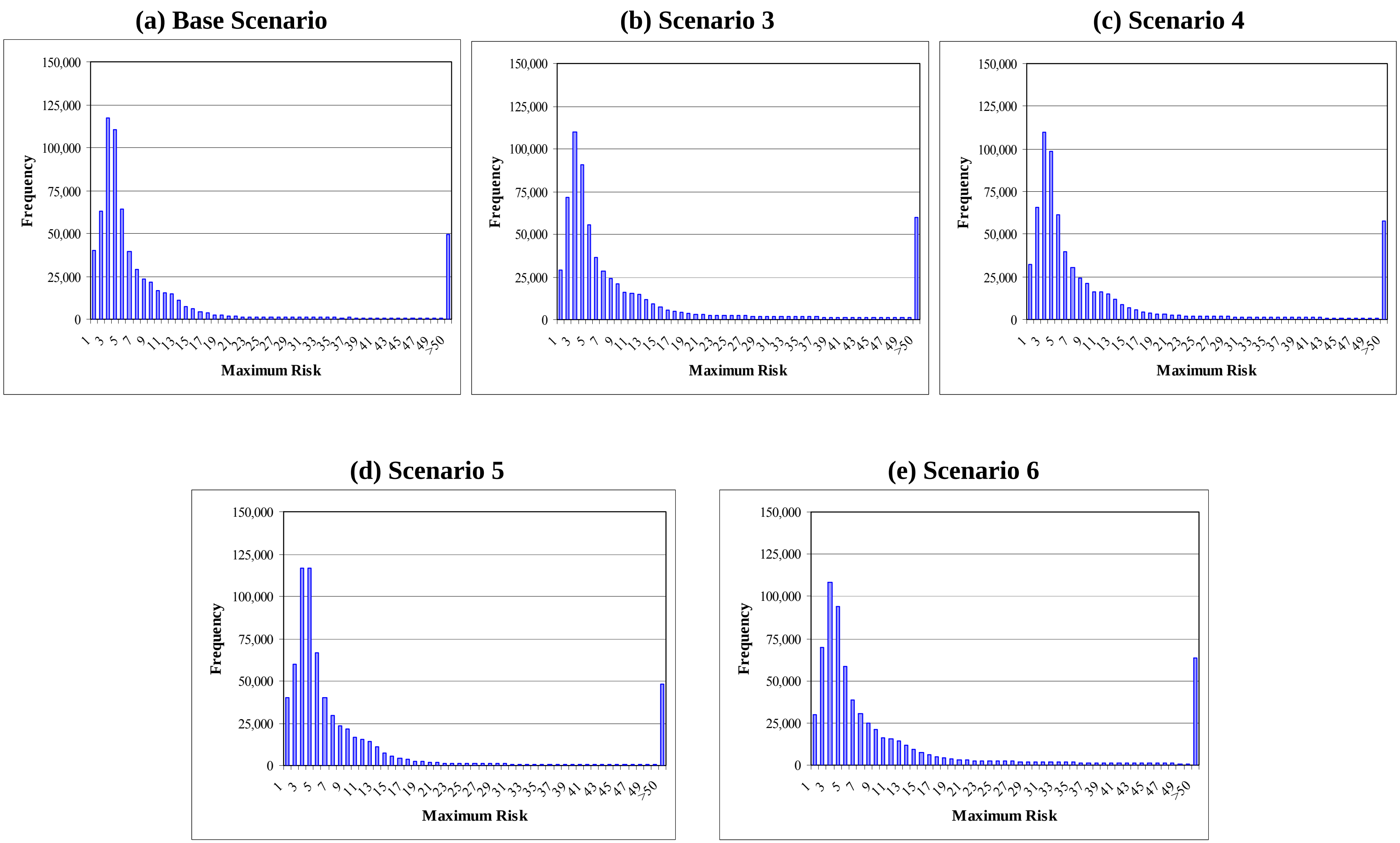

Figure 3.19 Maximum risk distribution as observed by vessels in scenarios 3, 4, 5, and 6 compared to the Base Scenario

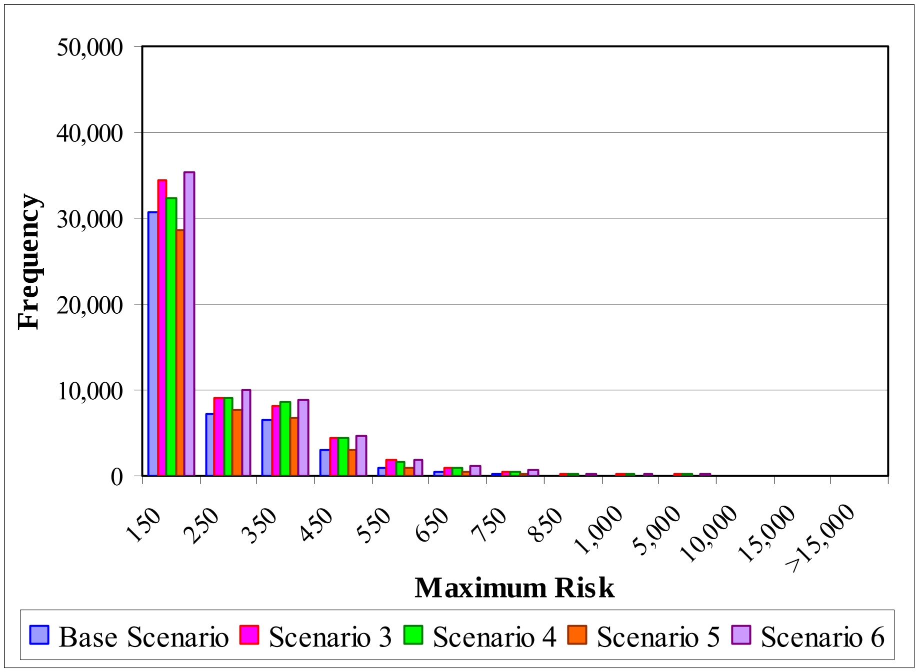

Figure 3.20 Maximum risk distribution as observed by vessels in scenarios 3, 4, 5, and 6 compared to the Base Scenario for values >50

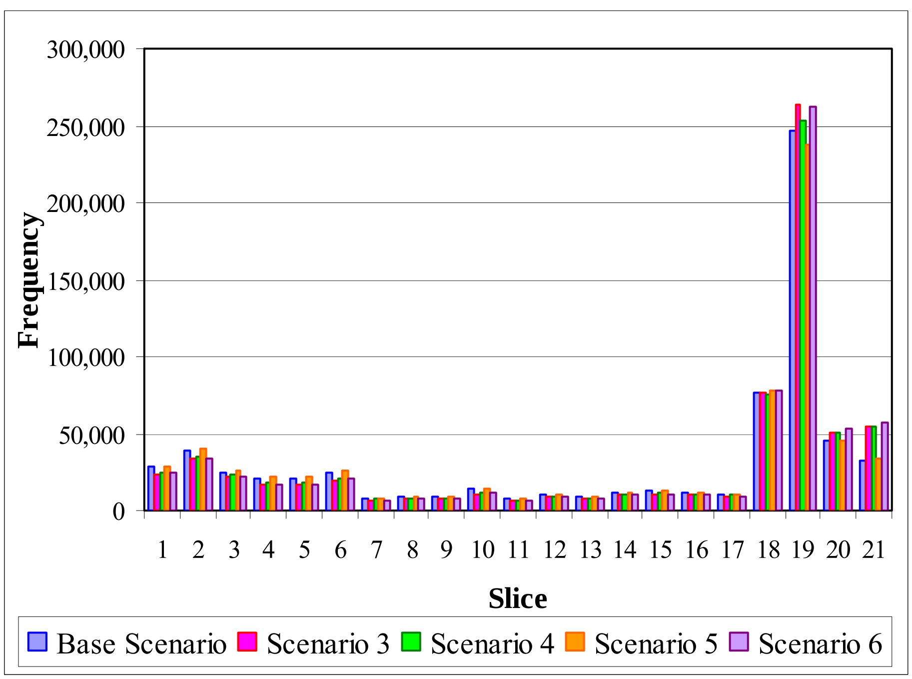

Figure 3.21 Distribution of maximum risk observations per slice in scenarios 3, 4, 5, and 6 compared to the Base Scenario

In all four scenarios, Class C, D, E, and P vessels are scheduled more frequently compared to the Base Scenario. Thus, the average waiting times of these vessel classes decrease in all of them as seen in Table 3.23.

We also observe a high increase in the average waiting time of Class A vessels in scenarios 4 and 5 since we increase the required time gap between consecutive Class A vessels.

Policy Indication 2: Scheduling changes that are made to reduce vessel waiting times increase risks in the Strait. Thus, scheduling decisions to balance out delays vs. risks should be made based on extensive experimentation with the model developed in this study.

Table 3.23 Waiting Times in scenarios 3, 4, 5, and 6 compared to the Base Scenario

	BASE SCENARIO		SCENARIO 3			SCENARIO 4			SCENARIO 5			SCENARIO 6		
Class (Direction)	**Average**	**Half Width (95% CI)**	**Average**	**Half Width (95% CI)**	**% Increase in Average**	**Average**	**Half Width (95% CI)**	**% Increase in Average**	**Average**	**Half Width (95% CI)**	**% Increase in Average**	**Average**	**Half Width (95% CI)**	**% Increase in Average**
A	1,987.15	1,564.30	2,160.80	915.57	8.74%	3,911.61	1,619.54	96.85%	7,843.32	2,794.68	294.70%	3,265.44	1,726.58	64.33%
A(N)	2,127.69	1,642.60	2,251.54	914.17	5.82%	4,124.65	1,693.80	93.86%	8,200.43	2,900.44	285.41%	3,384.67	1,750.81	59.08%
A(S)	1,847.74	1,479.95	2,071.68	917.17	12.12%	3,702.12	1,539.97	100.36%	7,488.01	2,680.75	305.25%	3,149.85	1,700.74	70.47%
B	492.48	19.55	699.37	30.18	42.01%	621.12	78.32	26.12%	680.05	46.51	38.09%	699.59	24.35	42.05%
B(N)	500.55	20.51	710.53	35.94	41.95%	627.37	19.39	25.34%	690.11	43.47	37.87%	706.08	16.72	41.06%
B(S)	459.77	44.04	644.56	67.69	40.19%	592.37	20.27	28.84%	636.55	62.2	38.45%	669.80	64.36	45.68%
C	684.42	112.21	273.29	21.1	-60.07%	391.18	29.06	-42.85%	323.79	25.53	-52.69%	281.13	21.93	-58.92%
C(N)	609.80	110.12	217.80	15.16	-64.28%	315.69	27.95	-48.23%	252.79	25.99	-58.55%	227.39	13.40	-62.71%
C(S)	754.87	115.01	326.06	28.53	-56.81%	463.25	28.60	-38.63%	389.82	26.92	-48.36%	331.89	35.58	-56.03%
D	172.48	29.67	94.53	9.20	-45.19%	114.53	32.30	-33.60%	201.56	24.44	16.86%	100.28	7.12	-41.86%
D(N)	151.75	29.14	88.99	12.01	-41.36%	101.72	10.67	-32.97%	171.99	22.63	13.34%	94.43	9.09	-37.77%
D(S)	192.53	30.89	99.90	7.76	-48.11%	126.90	11.85	-34.09%	230.27	27.01	19.60%	105.94	7.76	-44.97%
E	180.19	19.37	103.25	8.85	-42.70%	130.26	14.26	-27.71%	169.02	16.59	-6.20%	109.69	10.44	-39.13%
E(N)	194.60	23.56	101.78	11.91	-47.70%	128.99	16.07	-33.72%	167.85	17.99	-13.75%	109.87	13.68	-43.54%
E(S)	165.93	15.56	104.65	6.88	-36.93%	131.49	13.38	-20.76%	170.14	15.34	2.54%	109.52	8.30	-34.00%
P	77.93	10.07	72.54	7.04	-6.91%	80.74	5.50	3.61%	88.07	6.81	13.01%	77.88	4.36	-0.07%
P(N)	73.86	11.61	68.77	7.44	-6.89%	72.56	5.10	-1.76%	82.63	7.21	11.88%	73.75	4.62	-0.14%
P(S)	81.90	9.26	76.35	7.50	-6.78%	89.10	7.09	8.79%	93.78	8.09	14.50%	81.98	6.63	0.09%

3.4.4.2.2 SCHEDULING FEWER VESSELS

In scenarios 7, 8, and 9, we increase the required time gap between vessels, thereby scheduling fewer vessels within a given time frame. Specifically, in Scenario 7, we schedule Class C and Class D vessels every 35 and 10 minutes, respectively, while changing the required time gap between Class A and Class B vessels to 105 and 70 minutes, respectively, as seen in Figure 3.22.

On the other hand, in Scenario 8 we schedule northbound Class A, southbound Class A and Class B vessels every 105, 75 and 70 minutes, respectively as shown in Figure 3.23. We keep the required time gaps between Class C and Class D vessels at 35 and 10 minutes, respectively.

Finally, in Scenario 9, we combine the scheduling policy in Scenario 8 with the 20% arrival rate decrease in Scenario 2.

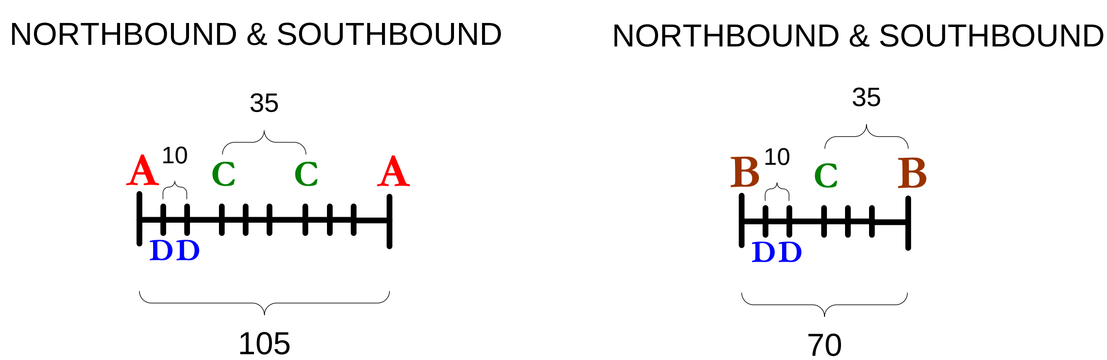

Figure 3.22 Scheduling Policy in Scenario 7

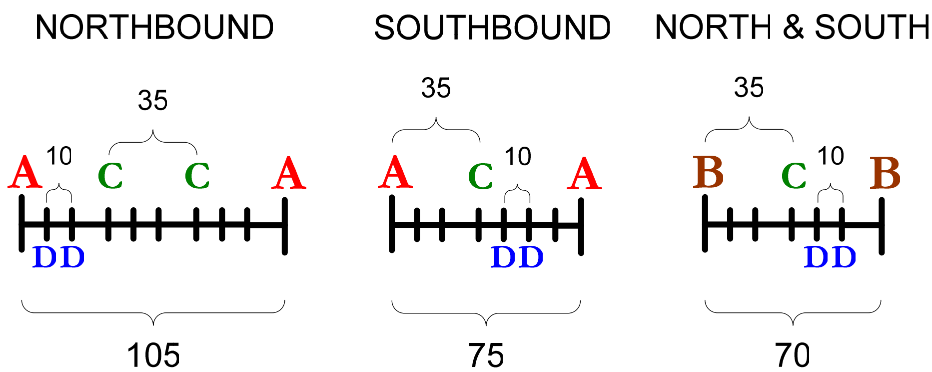

Figure 3.23 Scheduling Policy in Scenario 8

The average risk at each slice for all scenarios is listed in Table 3.24
Table 3.24. We observe that the average slice risk decreases in general as the required time gap between consecutive vessels increases. The greatest decrease in average risk is detected in Scenario 9, where both the vessel arrival rates and the number of scheduled vessels are decreased. The combination of these factors results in a greater decrease in average risk.

Table 3.24 Slice Risk in scenarios 7, 8, and 9 compared to the Base Scenario

	BASE SCENARIO		SCENARIO 7			SCENARIO 8			SCENARIO 9		
Slice	**Average**	**Half Width (95% CI)**	**Average**	**Half Width (95% CI)**	**% Increase in Average**	**Average**	**Half Width (95% CI)**	**% Increase in Average**	**Average**	**Half Width (95% CI)**	**% Increase in Average**
1	1.3748	0.34	1.4522	0.26	5.63%	1.3683	0.22	-0.47%	1.2889	0.21	-6.25%
2	1.6021	0.63	1.6536	0.45	3.21%	1.6018	0.54	-0.02%	1.4420	0.33	-9.99%
3	1.5105	0.35	1.5664	0.26	3.70%	1.5057	0.29	-0.32%	1.3557	0.10	-10.25%
4	1.4257	0.30	1.4765	0.20	3.56%	1.4264	0.25	0.05%	1.3005	0.11	-8.78%
5	1.4322	0.19	1.4846	0.21	3.66%	1.4336	0.26	0.10%	1.3201	0.14	-7.83%
6	1.4484	0.26	1.4874	0.17	2.69%	1.4552	0.27	0.47%	1.3531	0.18	-6.58%
7	1.1723	0.08	1.2158	0.06	3.71%	1.1776	0.10	0.45%	1.1165	0.07	-4.76%
8	1.1943	0.08	1.2231	0.04	2.41%	1.1917	0.08	-0.22%	1.1404	0.09	-4.51%
9	1.2002	0.09	1.2362	0.06	3.00%	1.1965	0.09	-0.31%	1.1433	0.09	-4.74%
10	1.1972	0.10	1.2306	0.07	2.79%	1.1934	0.10	-0.32%	1.1442	0.10	-4.43%
11	1.1850	0.09	1.2270	0.08	3.54%	1.1855	0.09	0.04%	1.1338	0.09	-4.32%
12	1.3361	0.07	1.3746	0.05	2.88%	1.3295	0.06	-0.49%	1.2743	0.06	-4.63%
13	1.2676	0.06	1.3015	0.05	2.67%	1.2634	0.05	-0.33%	1.2153	0.05	-4.13%
14	1.3600	0.06	1.3927	0.05	2.40%	1.3500	0.05	-0.74%	1.3064	0.06	-3.94%
15	1.3427	0.05	1.3743	0.05	2.35%	1.3384	0.05	-0.32%	1.2878	0.05	-4.09%
16	1.3462	0.06	1.3823	0.07	2.68%	1.3388	0.06	-0.55%	1.2916	0.06	-4.06%
17	1.3794	0.07	1.4069	0.06	1.99%	1.3685	0.08	-0.79%	1.3243	0.07	-3.99%
18	7.0459	0.15	6.4746	0.05	-8.11%	6.6342	0.12	-5.84%	6.8381	0.14	-2.95%
19	25.4410	0.60	22.1711	0.21	-12.85%	23.3101	0.50	-8.38%	24.6535	0.41	-3.10%
20	6.9067	0.09	6.3464	0.07	-8.11%	6.5582	0.11	-5.05%	6.8424	0.14	-0.93%
21	4.4412	0.10	4.0757	0.07	-8.23%	4.2196	0.10	-4.99%	4.3661	0.18	-1.69%

Based on the results in Figure 3.24, maximum risk observed at each slice varies across the scenarios. The maximum slice risks observed in Scenario 8 and Scenario 9 are lower than the one observed in the Base Scenario, with Scenario 8 providing the lowest maximum risk.

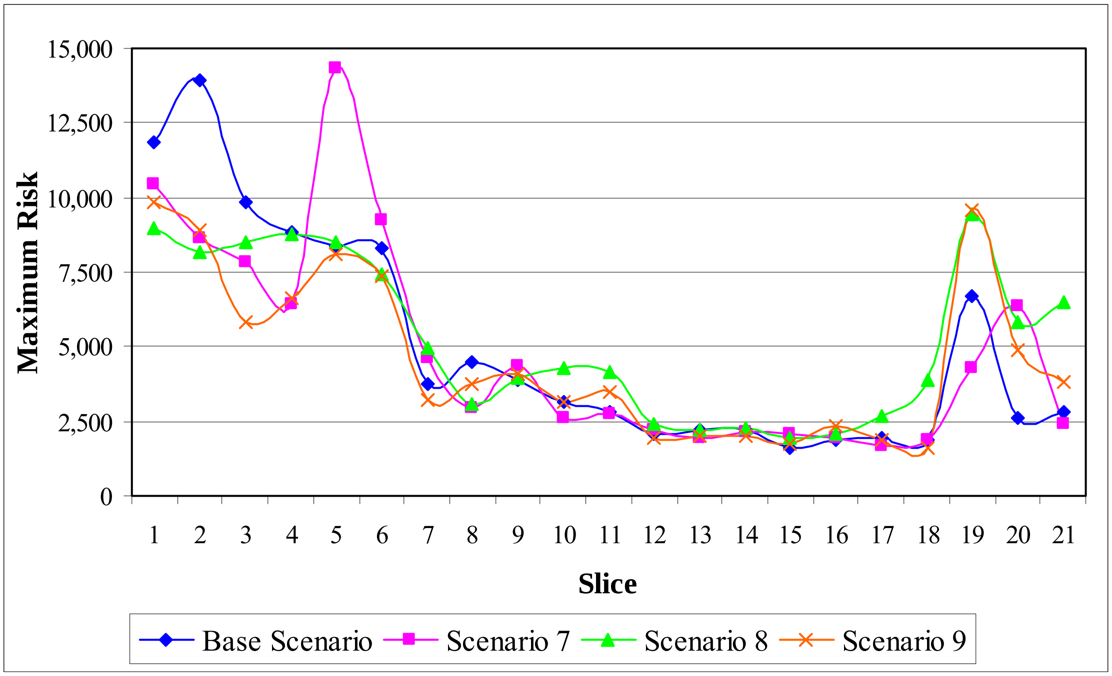

Figure 3.24 Maximum Slice Risk in scenarios 7, 8, and 9 compared to the Base Scenario

The distributions of maximum risk as observed by vessels in the Base Scenario and scenarios 7, 8, and 9 are displayed in Figure 3.25. The results observed in all three scenarios are similar to the Base Scenario. The only exception is that scenarios 8 and 9 provide fewer observations with high maximum risk values.

The distributions for the maximum risk values for all three scenarios are very similar for higher values of risk as seen in Figure 3.26.

As seen in Figure 3.27, in all three scenarios the distributions of slices at which the maximum risk is observed are very similar to the Base Scenario, with slice 19 having the greatest number of observations.

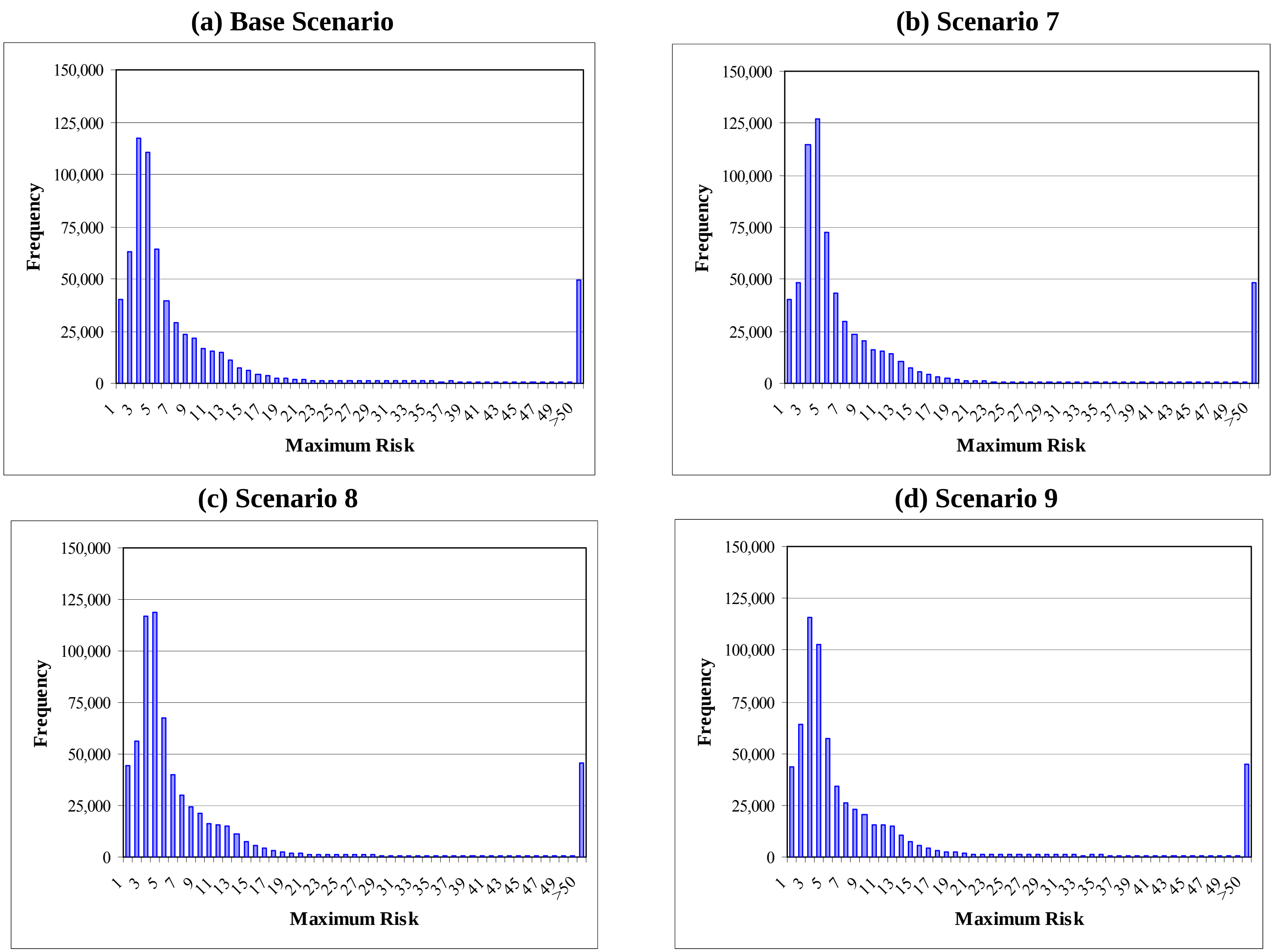

Figure 3.25 Maximum risk distribution as observed by vessels in scenarios 7, 8, and 9 compared to the Base Scenario

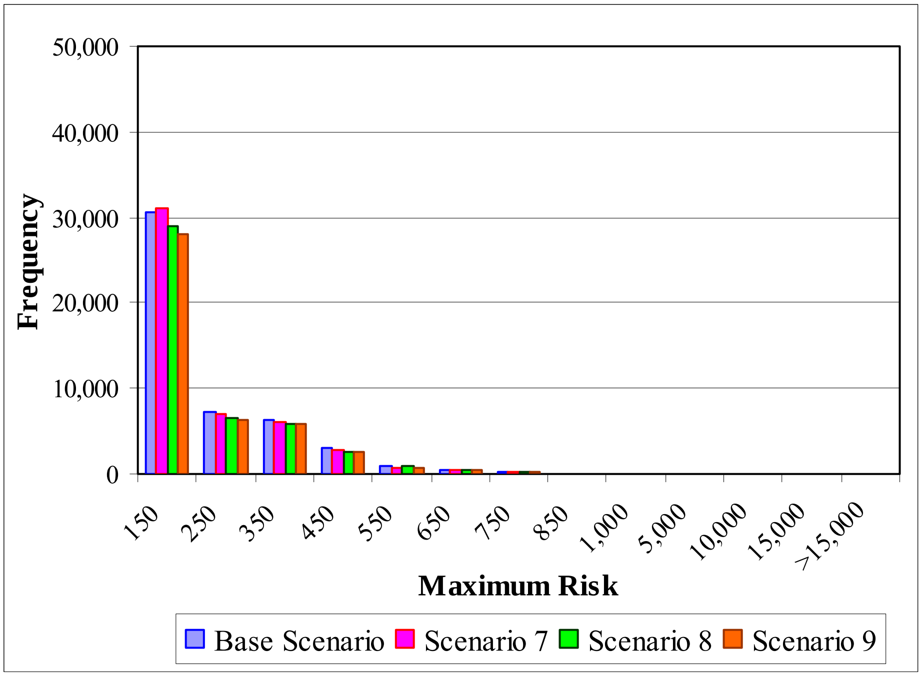

Figure 3.26 Maximum risk distribution as observed by vessels in scenarios 7, 8, and 9 compared to the Base Scenario for values >50

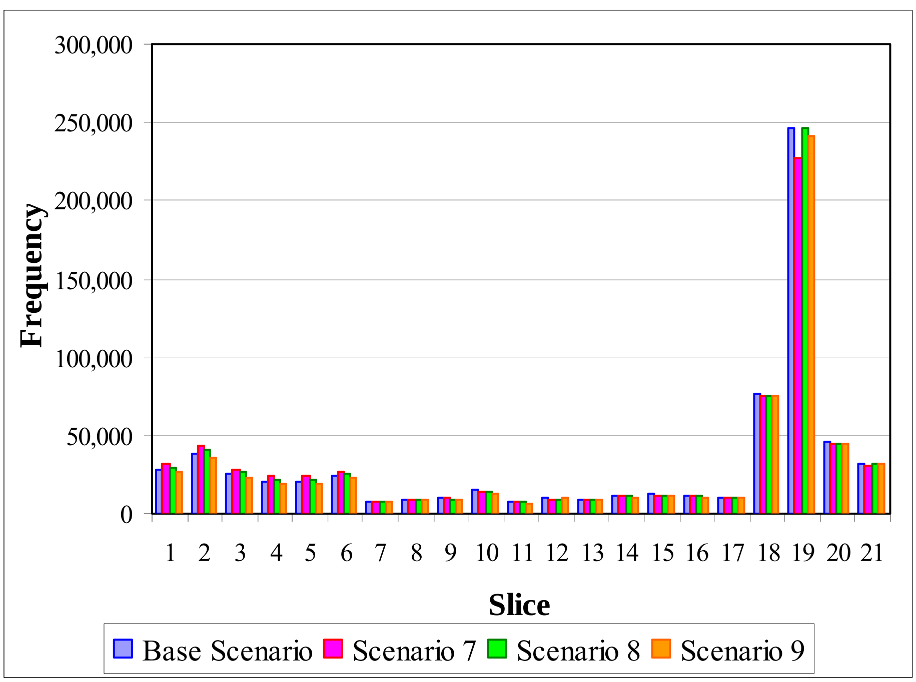

Figure 3.27 Distribution of maximum risk observations per slice in scenarios 7, 8, and 9 compared to the Base Scenario

Table **3.25** shows that the average waiting times of all vessel classes increase substantially in all three scenarios compared to the Base Scenario, since the vessels are scheduled less frequently. The resulting increases observed in Scenario 7 and Scenario 8 are unacceptable. Therefore, these scenarios are rendered infeasible even though they result in lower average slice risks. On the other hand, Scenario 9, in which vessel arrivals are decreased 20%, provides acceptable waiting times coupled with lower average and maximum slice risks, clearly at the expense of 20% lesser traffic.

Policy Indication 3: In the current situation, scheduling policy changes that are made to reduce risks cause major increases in average vessel waiting times. The benefits obtained in risks do not justify the resultant waiting times. In case of future major decreases in dangerous cargo traffic may occur due to alternative transport modes such as pipelines and other routes. In this case, scheduling changes can be made to take lesser number of vessels into the Strait and can still be justified due to the resultant insignificant increases in delays.

Table 3.25 Waiting Times in scenarios 7, 8, and 9 compared to the Base Scenario

	BASE SCENARIO		SCENARIO 7			SCENARIO 8			SCENARIO 9		
Class (Direction)	**Average**	**Half Width (95% CI)**	**Average**	**Half Width (95% CI)**	**% Increase in Average**	**Average**	**Half Width (95% CI)**	**% Increase in Average**	**Average**	**Half Width (95% CI)**	**% Increase in Average**
A	1,987.15	1,564.30	16,696.04	16,696.04	740.20%	4,610.02	2,187.49	131.99%	1,841.05	271.95	-7.35%
A(N)	2,127.69	1,642.60	17,193.56	18,192.67	708.09%	4,988.77	2,271.92	134.47%	1,997.02	275.45	-6.14%
A(S)	1,847.74	1,479.95	16,208.59	17,636.09	777.21%	4,236.06	2,108.72	129.26%	1,678.78	273.99	-9.14%
B	492.48	19.55	486.00	457.65	-1.32%	477.36	477.36	-3.07%	509.69	23.13	3.49%
B(N)	500.55	20.51	483.13	458.08	-3.48%	485.25	485.25	-3.06%	518.28	20.19	3.54%
B(S)	459.77	44.04	499.34	455.74	8.61%	445.26	445.26	-3.16%	475.31	41.72	3.38%
C	684.42	112.21	62,129.49	38,085.47	8977.68%	35,522.74	13,222.85	5090.20%	621.01	103.53	-9.26%
C(N)	609.80	110.12	63,268.26	38,199.69	10275.25%	35,758.80	13,523.03	5764.02%	559.02	113.13	-8.33%
C(S)	754.87	115.01	61,056.72	23,179.62	7988.38%	35,297.09	12,940.10	4575.92%	679.82	97.68	-9.94%
D	172.48	29.67	321.67	47.10	86.50%	279.17	44.24	61.86%	204.72	27.77	18.69%
D(N)	151.75	29.14	298.35	49.92	96.61%	202.20	38.01	33.25%	162.91	36.3	7.35%
D(S)	192.53	30.89	344.26	48.98	78.81%	353.80	53.82	83.76%	245.39	22.77	27.46%
E	180.19	19.37	266.54	22.87	47.92%	252.51	21.07	40.14%	188.71	17.11	4.73%
E(N)	194.60	23.56	288.83	30.43	48.42%	267.09	24.43	37.25%	198.61	20.2	2.06%
E(S)	165.93	15.56	244.76	16.89	47.51%	238.20	17.81	43.55%	179.06	14.73	7.91%
P	77.93	10.07	104.39	7.09	33.95%	92.05	8.39	18.12%	79.47	4.99	1.98%
P(N)	73.86	11.61	106.73	6.17	44.51%	82.91	9.33	12.26%	70.65	8.32	-4.34%
P(S)	81.90	9.26	102.03	12.42	24.57%	101.29	7.95	23.67%	88.51	5.04	8.07%

3.4.4.3 IMPACT OF OTHER FACTORS

In Scenario 10, we turn the pilotage option off. That is, none of the vessels request pilots for their passage through the Strait. Scenario 11 represents the case where overtaking is not allowed within the Strait. Finally, local traffic density in the Strait is decreased 50% in Scenario 12. Table 3.26 reveals that the average risk increases at each slice when pilotage is not available. The resulting average increase is 50% across all slices.

Surprisingly, the average risk also increases in Scenario 11 when overtaking is not allowed. This is a result of expert opinions stating that two vessels following each other in a normal traffic lane creates a riskier situation than a vessel overtaking another.

Finally, the average slice risk decreases in Scenario 12. The 50% decrease in local traffic density results in a 50% average decrease in slice risk.

Table 3.26 Slice Risk in scenarios 10, 11, and 12 compared to the Base Scenario

	BASE SCENARIO		SCENARIO 10			SCENARIO 11			SCENARIO 12		
Slice	Average	Half Width (95% CI)	Average	Half Width (95% CI)	% Increase in Average	Average	Half Width (95% CI)	% Increase in Average	Average	Half Width (95% CI)	% Increase in Average
1	1.3748	0.34	1.7581	0.27	27.88%	1.5762	0.64	14.65%	1.3416	0.34	-2.41%
2	1.6021	0.63	1.7584	0.25	9.76%	1.8805	1.05	17.38%	1.5689	0.63	-2.07%
3	1.5105	0.35	1.7985	0.28	19.07%	1.817	0.81	20.29%	1.4746	0.35	-2.38%
4	1.4257	0.30	1.8366	0.32	28.82%	1.6895	0.68	18.50%	1.3885	0.30	-2.61%
5	1.4322	0.19	1.8711	0.30	30.65%	1.665	0.60	16.25%	1.3835	0.29	-3.40%
6	1.4484	0.26	1.9207	0.29	32.61%	1.6843	0.59	16.29%	1.3826	0.26	-4.54%
7	1.1723	0.08	1.5367	0.12	31.08%	1.2864	0.18	9.73%	1.0880	0.08	-7.19%
8	1.1943	0.08	1.5792	0.12	32.23%	1.3052	0.19	9.29%	1.1039	0.08	-7.57%
9	1.2002	0.09	1.5951	0.17	32.90%	1.3182	0.23	9.83%	1.1156	0.09	-7.05%
10	1.1972	0.10	1.5883	0.15	32.67%	1.2846	0.16	7.30%	1.1106	0.10	-7.23%
11	1.1850	0.09	1.5688	0.14	32.39%	1.2913	0.17	8.97%	1.0850	0.09	-8.44%
12	1.3361	0.07	1.8574	0.11	39.02%	1.4573	0.16	9.07%	1.1069	0.07	-17.15%
13	1.2676	0.06	1.7249	0.13	36.08%	1.4035	0.17	10.72%	1.1114	0.06	-12.32%
14	1.3600	0.06	1.8699	0.14	37.49%	1.5082	0.15	10.90%	1.1204	0.05	-17.62%
15	1.3427	0.05	1.8483	0.13	37.66%	1.477	0.14	10.00%	1.1186	0.06	-16.69%
16	1.3462	0.06	1.8236	0.14	35.46%	1.4944	0.17	11.01%	1.1222	0.06	-16.64%
17	1.3794	0.07	1.8642	0.14	35.15%	1.4995	0.15	8.71%	1.1303	0.08	-18.06%
18	7.0459	0.15	11.6996	0.20	66.05%	8.0102	0.17	13.69%	1.6180	0.06	-77.04%
19	25.4410	0.60	45.3467	0.69	78.24%	30.3149	0.15	19.16%	5.0426	0.08	-80.18%
20	6.9067	0.09	11.9161	0.30	72.53%	8.3434	0.23	20.80%	1.3933	0.05	-79.83%
21	4.4412	0.10	7.2117	0.22	62.38%	5.3849	0.18	21.25%	1.3170	0.06	-70.35%

Based on Figure 3.28, Scenario 12 provides maximum risk values similar to the Base Scenario at each slice except slices 19, 20 and 21. These slices are affected by local traffic density the most. In addition, the highest maximum risk observed in Scenario 12 is identical to the Base Scenario.

On the other hand, the highest maximum risk values observed in scenarios 10 and 11 are lower than the Base Scenario. However, as stated before, the maximum risk values do not necessarily reflect the impact of a given factor on the overall risk. They are contingent upon the occurrence of a random situation at an instance. Thus, we need to consider the maximum risk distribution.

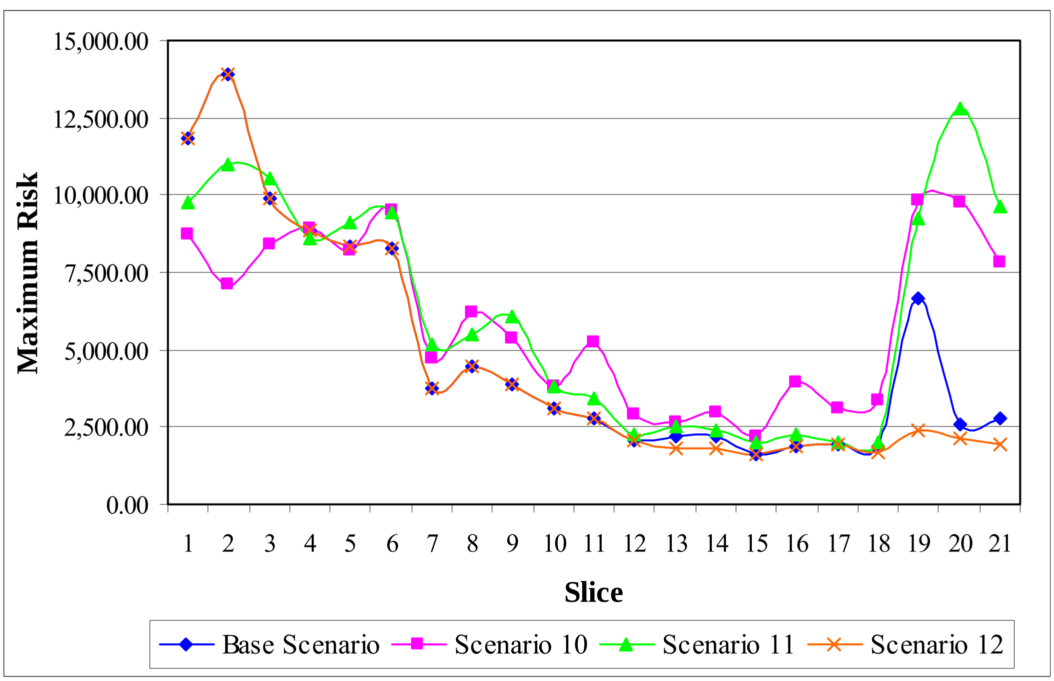

Figure 3.28 Maximum Slice Risk in scenarios 10, 11, and 12 compared to the Base Scenario

As seen in Figure 3.29, the maximum risk distributions observed in Scenario 11 are very similar to the Base Scenario. On the other hand, Scenario 10 results in a substantially greater number of observations with high maximum risk values while Scenario 12 provides a significantly greater number of low maximum risk values. These phenomena are also observed in Figure 3.30.

The histograms representing the distribution of slices at which the maximum risk is observed are given in Figure 3.31. In scenarios 10 and 11, the distributions of slices are very similar to the Base Scenario. However, in Scenario 12 the observations are more evenly distributed across all slices. This is due to the fact that the discrepancies in observations in the Base Scenario are caused by heavier local traffic density in the last four slices. Thus, decreasing the local traffic density 50% in Scenario 12 dampens this effect.

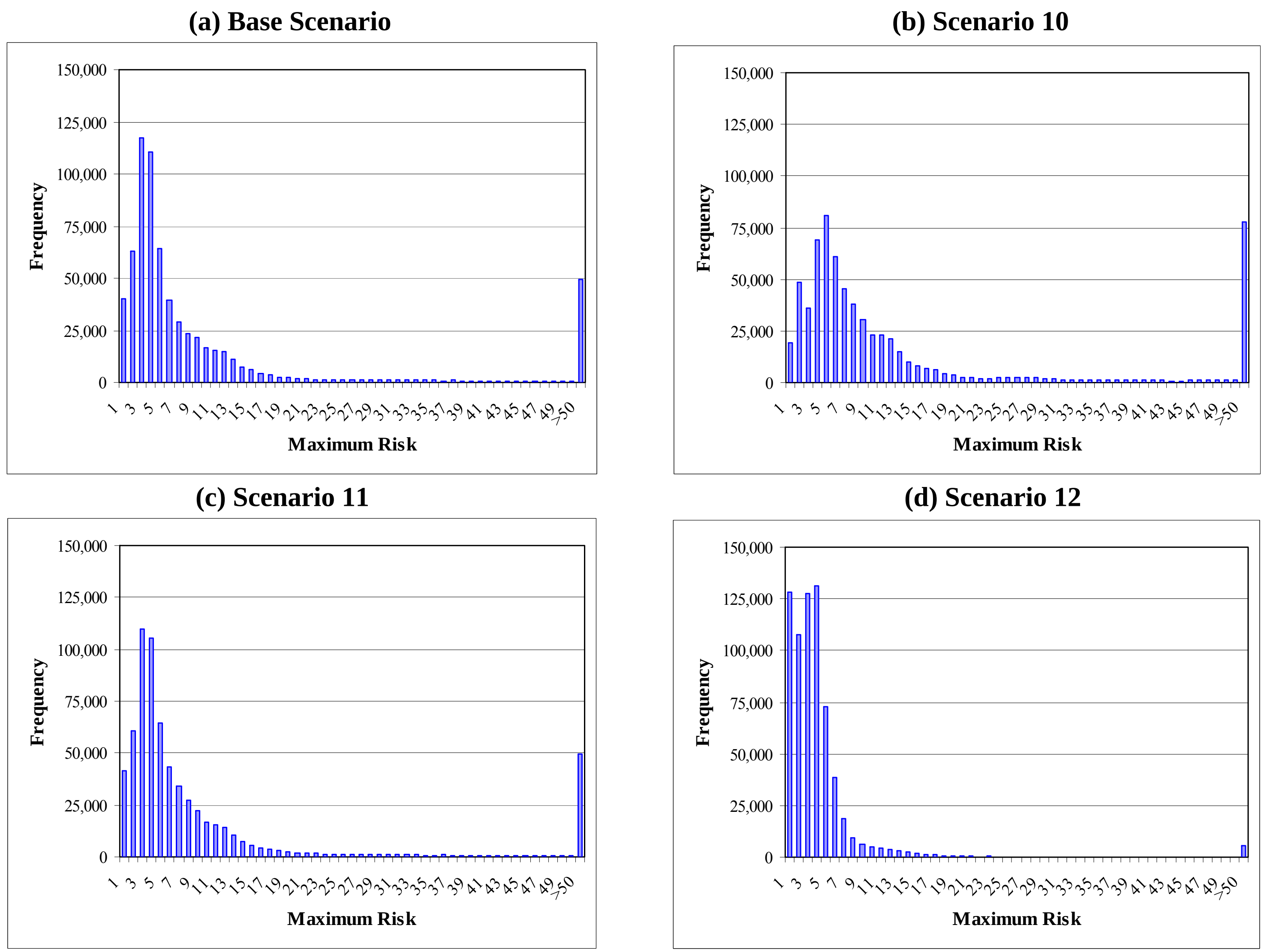

Figure 3.29 Maximum risk distribution as observed by vessels in scenarios 10, 11, and 12 compared to the Base Scenario

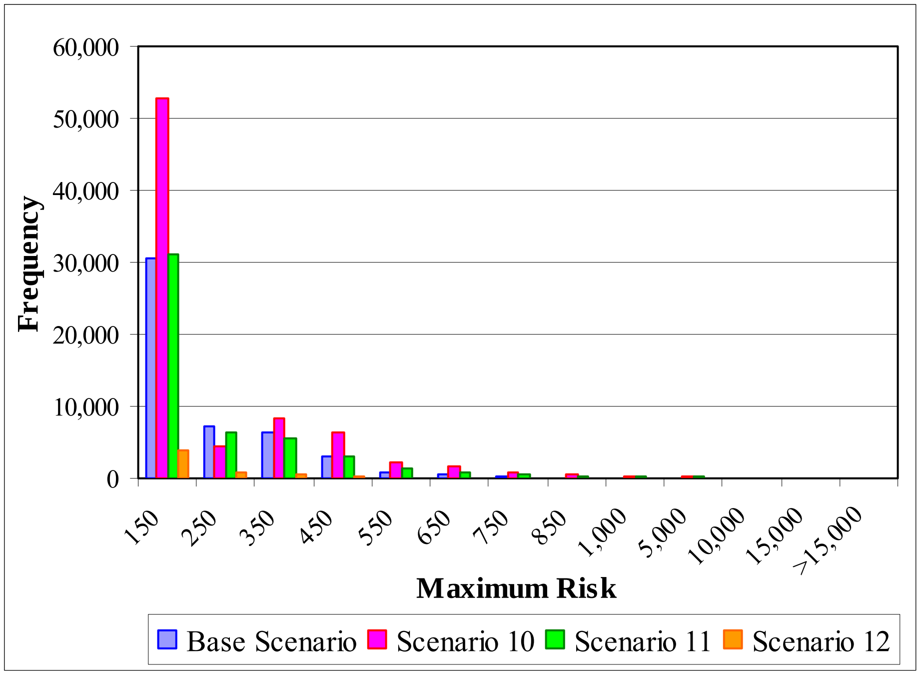

Figure 3.30 Maximum risk distribution as observed by vessels in scenarios 10, 11, and 12 compared to the Base Scenario for values >50

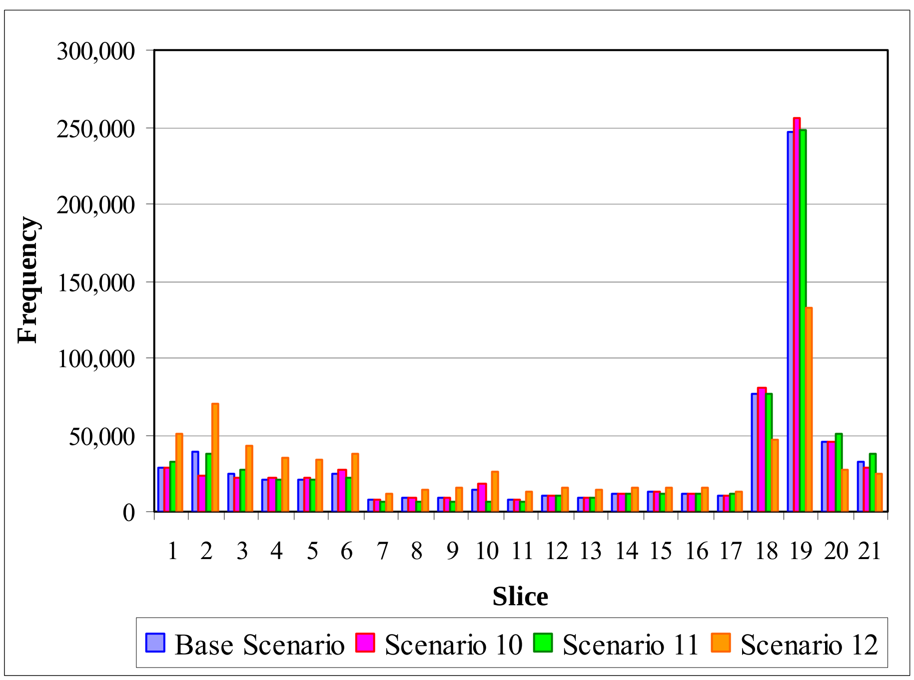

Figure 3.31 Distribution of maximum risk observations per slice in scenarios 10, 11, and 12 compared to the Base Scenario

The average vessel waiting times in scenarios 10, 11 and 12 are displayed in Table 3.27. When we turn the pilotage option off in Scenario 10, the average waiting times decrease in general as the vessels do not have to wait for the next available pilot.

We observe that the average vessel waiting times decrease slightly when overtaking is not allowed. Although overtaking does not have a direct effect on scheduling, the observed decrease in waiting times is a result of changing event sequences in the simulation due to variability.

On the other hand, the average waiting times in Scenario 12 are identical to the ones in the Base Scenario since local traffic density has no effect on scheduling.

Policy Indication 4: The model indicates that pilots are of utmost importance for safe passage, and lack of pilotage significantly increases the risks in the Strait. In the current practice, vessels greater than 300 m. in length are mandated to take a pilot, and it is voluntary for the rest. Thus, we recommend mandatory pilotage for vessels greater than 150 m. in length.

Policy Indication 5: Even though current regulations do not allow overtaking anywhere in the Strait, the risk model indicates that overtaking a vessel is less risky as opposed to slowing down behind it. Therefore, in the areas where the width of the Strait tolerates it (except between Kanlıca and Vaniköy), overtaking proves to be a safe practice as confirmed by the expert opinion.

Policy Indication 6: The most significant contributor to the risk appears to be the juxtaposition of the transit and local traffic. To reduce risk significantly, the scheduling procedure should be revised to move more of the dangerous cargo vessels to nighttime traffic. This requires further research on what kind of modifications can be done to the nighttime scheduling practice to control vessel delays.

Table 3.27 Waiting Times in scenarios 10, 11, and 12 compared to the Base Scenario

	BASE SCENARIO		SCENARIO 10			SCENARIO 11			SCENARIO 12		
Class (Direction)	**Average**	**Half Width (95% CI)**	**Average**	**Half Width (95% CI)**	**% Increase in Average**	**Average**	**Half Width (95% CI)**	**% Increase in Average**	**Average**	**Half Width (95% CI)**	**% Increase in Average**
A	1,987.15	1,564.30	1,845.96	827.24	-7.11%	1,820.49	699.20	-8.39%	1,987.15	1,564.30	0.00%
A(N)	2,127.69	1,642.60	1,967.03	878.73	-7.55%	1,944.66	759.58	-8.60%	2,127.69	1,642.60	0.00%
A(S)	1,847.74	1,479.95	1,727.09	774.69	-6.53%	1,698.94	640.07	-8.05%	1,847.74	1,479.95	0.00%
B	492.48	19.55	493.16	13.15	0.14%	493.47	16.38	0.20%	492.48	19.55	0.00%
B(N)	500.55	20.51	502.31	11.85	0.35%	501.75	13.96	0.24%	500.55	20.51	0.00%
B(S)	459.77	44.04	452.30	32.83	-1.62%	456.70	33.55	-0.67%	459.77	44.04	0.00%
C	684.42	112.21	664.54	143.31	-2.90%	688.43	105.91	0.59%	684.42	112.21	0.00%
C(N)	609.80	110.12	577.92	118.51	-5.23%	606.51	89.57	-0.54%	609.80	110.12	0.00%
C(S)	754.87	115.01	746.70	169.56	-1.08%	766.30	122.94	1.51%	754.87	115.01	0.00%
D	172.48	29.67	169.55	26.72	-1.70%	170.37	24.91	-1.22%	172.48	29.67	0.00%
D(N)	151.75	29.14	147.96	27.36	-2.50%	150.69	29.93	-0.70%	151.75	29.14	0.00%
D(S)	192.53	30.89	190.42	28.40	-1.10%	189.46	20.66	-1.59%	192.53	30.89	0.00%
E	180.19	19.37	176.26	18.37	-2.18%	176.93	16.40	-1.81%	180.19	19.37	0.00%
E(N)	194.60	23.56	191.42	23.53	-1.63%	191.22	20.62	-1.74%	194.60	23.56	0.00%
E(S)	165.93	15.56	161.27	13.79	-2.81%	162.94	12.41	-1.80%	165.93	15.56	0.00%
P	77.93	10.07	74.86	7.94	-3.95%	76.90	8.88	-1.33%	77.93	10.07	0.00%
P(N)	73.86	11.61	69.96	6.76	-5.28%	71.94	11.84	-2.59%	73.86	11.61	0.00%
P(S)	81.90	9.26	79.73	9.78	-2.65%	81.99	6.43	0.11%	81.90	9.26	0.00%

4 SINGLE-CLASS QUEUES WITH MULTIPLE TYPES OF INTERRUPTIONS

Maritime Transportation is an important part of the world trade since it is economical and most of the time the only means of transportation. More than 90% of international cargo moves through maritime transportation. This includes containerized goods, petroleum products, minerals, grains, chemicals, and others. Chokepoints such as the Istanbul Strait in Turkey, the Malacca Strait in Malaysia/Singapore, the Strait of Hormuz in Persian Gulf, and others cause significant delays and therefore increase costs in maritime transportation. Estimation of these delays is a significant issue in maintaining regularity in maritime transportation.

Vessel traffic at waterway entrances gives rise to challenging queueing problems. Policies to manage traffic coupled with natural conditions make the estimation of vessel delays quite difficult. A case in point is the Istanbul Strait. Transit vessels arrive randomly at the northern and southern entrances of the Strait, and wait in queues until they are allowed to start their passage. Vessels enter the Strait one at a time at either the southern or the northern entrance. Traffic may be interrupted due to poor visibility, high currents, storms, and other factors such as lane closures caused by vessel accidents or sporting events. Once a vessel enters the Strait, it continues its passage even if conditions which may interrupt the traffic develop. However, the next vessel waiting in the queue cannot enter the Strait until conditions return to normal. Vessels generally do not stop in the Strait since they may create a high risk situation for other vessels and the environment. These arguments are also valid for narrow waterways at large including canals, rivers, and straits.

In this chapter, we propose a queueing analysis to estimate the average vessel waiting times at the entrance points of waterways. These problems can be studied as queues with multiple types of service interruptions, as discussed in detail in section 4.2.

4.1 LITERATURE REVIEW

The literature on the queueing models subject to multiple types of interruptions is scarce. Some of the related work is presented below. The first set of papers discusses the machine interference problem with multiple types of failures. The second set considers a general queueing model where the server is subject to several types of independent breakdowns. The last paper treats the aforementioned queueing model as an application in computer science, and is relevant to our research the most.

[Jaiswal and Thiruvengadam, 1963] deals with the machine interference problem when each machine is subject to two types of failures with generally distributed repair times. Unlike the problem considered in our research, the authors focus on a priority structure applied to the failure types. One type of failure is assumed to have a “non-preemptive” priority over the other. The steady-state probabilities of the number of machines running are obtained using the supplementary variable technique.

[Elsayed, 1981] also considers a machine interference problem when machines are subject to two types of failures with two repair policies. In policy I, priority is placed on one type of failure, while two failure types have equal probability of repair in policy II. They have obtained the optimal number of machines needed to be assigned to the repair crew for these two policies. The repair crew efficiency and machine availability are calculated.

The machine interference problem with multiple types of failures is extended to k types of failures in [Palesano and Chandra, 1986]. Specifically, a numerical method to obtain performance measures for a single group of N identical machines, each subject to k types of failures is presented. Times to breakdown are exponentially distributed while the repair times are arbitrarily distributed. The failure/repair policy follows a non-preemptive fixed-priority rule with different priorities assigned to different types of failures. They have obtained the average time spent by a machine waiting for service, average number of idle machines and machine/operator utilization via an imbedded Markov chain analysis.

[Hsieh and Andersland, 1995] studies a queueing model where the server is subject to several types of breakdowns and each type has two possible stages of repair. In this model, the repair rates depend on the type and severity of the breakdown. The authors derive expressions for availability, steady-state queue length distribution, mean queue length, and server utilization using a Markovian approach.

[Gray *et al*., 2003] considers a queueing model with one type of operation-dependent breakdowns that require a phase-type repair process with K phases. The repair process starts at stage 1 and continues in a sequential order until it reaches the stage i (any) where the repair is completed with probability q_i. They have obtained steady-state characteristics of the system under the assumption of exponentiality for inter-arrival times, service times and time to breakdowns.

Similarly, [Gray *et al*., 2004] considers a queueing model with server breakdowns which require a sequence of stages of testing and/or repair before service is restored. The authors assume that the server consists of M modules, numbered $1,\ldots,M$, where module v consists of K_v components. The availability of the server depends on all modules being functional. The components of each module are subject to random breakdowns, and the malfunction of one component within a module may cause a breakdown of other components. The order in which the components within a module are to be tested, and if necessary, repaired is predetermined. In this model, all service, breakdown and repair times are exponentially distributed. The authors demonstrate a necessary and sufficient condition for the stationary queue length distribution to exist and use a matrix geometric approach for analysis.

[Nikola, 1986] considers a single-server M/G/1 queue subject to multiple types of simultaneous Poisson interruptions. Nikola obtains closed-form expressions for the average waiting time and queue length distribution for the case where simultaneous presence of interruptions is not allowed. He derives the Laplace transform of the density function of the service completion time and obtains the average number of customers in the system.

4.2 A QUEUEING MODEL

The incoming vessels form the customer arrival stream, which can be identified by the time between consecutive arrivals. We assume that customers arrive from a Poisson process with rate λ per unit time and that there is only one class of customers receiving service in the system. This argument is attained by combining various vessel streams into a single stream. Poisson arrivals assumption is consistent with the Istanbul Strait arrival data due to superposition of several independent vessel arrival streams.

After a vessel enters the Strait, a second vessel starts its passage as soon as the first one traverses the minimum required distance between two consecutive vessels. Therefore, the time it takes for a vessel to traverse the required distance before the next vessel may enter the Strait is considered the *service time* of a customer in the queueing model, since a second vessel can enter the Strait at the end of this time period. This is typically a short period of time since the distance to be maintained between consecutive vessels is about 0.5-1 nautical miles. The practice in Istanbul results in about 2.5 minutes. In this study, we assume that the service time S has an arbitrary distribution, and that the customers are served based on the “first come, first served” policy. In reality, the service discipline is decided upon by the resident Vessel Traffic Services system and it may change from one location to another.

Service may be interrupted and the waterway may be closed due to poor visibility, storms, high currents and other random stoppages. We assume that the server is subject to k different types of operation-independent interruptions. Typically, the vessel that is given the go-ahead and proceeding to the entrance does not get interrupted even if a condition erupts that would normally stop the traffic. That is, the current customer is not affected by an interruption even though that interruption starts during its service. However, that interruption would stop the following vessels from entering the Strait. We assume that times to interruptions, Z, follow an exponential distribution with rate δ, while their downtimes, Y, have an arbitrary distribution. A point of observation is that due to the nature of closures in waterways, the downtimes are much longer than the service times.

Thus, the vessel traffic at the entrance points of waterways may very well be considered a single-class queueing model with a single-server, and an infinite queue, which is subject to multiple types of interruptions. Clearly, our main point of interest is the average vessel waiting time due to its impact on the congestion in maritime traffic. In this chapter, we consider two different interruption policies; *non-simultaneous interruptions* and *possibly simultaneous interruptions*.

In the case of non-simultaneous interruptions, when an interruption occurs, other interruptions cannot occur during its downtime. In this case, the system may be down due to **one and only one interruption at a time**.

In the possibly simultaneous interruptions case, the server experiences different types of interruptions which may possibly occur simultaneously. That is, an interruption can occur during a downtime caused by another interruption. For example, high current speeds may be experienced while the Strait is already closed due to poor visibility.

In this chapter, we propose an approximation method to obtain the expected waiting time of a customer in the queue using the "completion-time approach". The *service completion time*, C, is defined as the time interval between the service start time of a customer, which corresponds to a vessel entry, and the time the next customer may start its service, representing the instance the next vessel is allowed to enter. It is equal to the service time if no interruptions occur. In case of interruptions, the service completion time is longer than the service time due to downtimes since the service is available to the next customer in line only after the system becomes operational.

Taking into account the three facts that the aforementioned service times are much shorter than downtimes, the vessel in service continues its passage during the interruption, and the remaining service times are over by the time the down cycle ends, the queueing model is equivalent to one with scrapping where the customer is assumed to be scrapped upon an interruption. This is only a modeling convenience to keep track of the time until the first interruption occurs, which we refer to as the *actual service time* in the model.

So far, we have introduced the queueing problem in the Istanbul Strait and briefly discussed the underlying queueing system. In the following sections, we focus our attention to the queueing system and refer to vessels as customers.

4.3 WAITING TIME IN QUEUES SUBJECT TO NON-SIMULTANEOUS INTERRUPTIONS

We consider a single-server queueing system with single class of customers arriving according to a Poisson distribution with rate λ per unit time. Service time, S, of a customer follows an arbitrary distribution. The server is subject to k operation-independent, non-identical, non-simultaneous interruptions. The time to interruption of type i, Z_i, follows an exponential distribution with rate δ_i, while its downtime, Y_i, has an arbitrary distribution.

Let W and N be the waiting time of a customer until its service starts, and the number of customers waiting in the queue at any time, respectively. The arriving customer begins its service immediately if the server is idle upon arrival. If the server is busy upon arrival, the arriving customer waits until the service of the current customer is completed. If the customer arrives when the server is down, it waits until it is up again. The arriving customer also has to wait until all the customers that arrived earlier are served, and the downtimes of the possible interruptions that may occur during their services are completed. Thus, the waiting time of an arriving customer can be expressed as follows:

$$W = \left(N \times C\right) + \begin{cases} 0 & \text{w.p. } P\left(\text{Server idle upon arrival}\right) \\ C_r & \text{w.p. } P\left(\text{Server busy upon arrival}\right) \\ Y_{r_1} & \text{w.p. } P\left(\text{Server down due to interruption } 1\right) \\ \vdots & \vdots \\ Y_{r_k} & \text{w.p. } P\left(\text{Server down due to interruption } k\right) \end{cases} \tag{4.1}$$

where C, C_r, and Y_{r_i} represent the service completion time of a customer, the remaining service completion time of the customer found in the server upon arrival, and the remaining downtime of the server when it is down upon arrival due to interruption type *i* $(i = 1,...,k)$, respectively. Note that no other interruption can occur during Y_{r_i} due to our assumption of non-simultaneous failures.

Let ρ_a be the actual server utilization. It is also the probability that the server is busy at the time of an arrival due to the PASTA property of Poisson arrivals. Additionally, let $P_{d,i}$ be the long-run probability of the server being down due to interruption *i*. This is equivalent to the probability that an arriving customer finds the server down due to interruption type i $(i = 1,...,k)$. Using these definitions, we can write the following probability functions.

$$\mathrm{P}\left(\text{Server busy upon arrival}\right) = \rho_a = \lambda E\left[S_a\right] \tag{4.2}$$

$$P\left(\text{System down upon arrival due to failure } i\right) = P_{d,i} \tag{4.3}$$

where S_a represents the actual service time of a customer. This is equivalent to the time a customer spends in service until it either finishes its service or is scrapped upon a possible interruption.

Since we have operation-independent non-simultaneous interruptions, the steady-state probability that the server is down, $P_{d,i}$, can be calculated using the following expression:

$$P_{d,i} = \frac{E[Y_i]}{E[Y_i] + \frac{1}{\delta_i}} \left[\prod_{\substack{l=1 \\ l \neq i}}^{k} \left(1 - P_{d,l}\right) \right]. \tag{4.4}$$

Thus, using the waiting time expression in (4.1) and the system state probabilities in (4.2) and (4.3), the expected waiting time of a customer in the queue can be expressed as

$$E[W] = E[N]E[C] + \rho_a \, E[C_r] + \sum_{i=1}^{k} P_{d,i} Y_{r_i} \, . \tag{4.5}$$

Then, using the Little's formula $\left(E\left[N\right] = \lambda \, E\left[W\right]\right)$, (4.5) reduces to

$$E[W] = \frac{\rho_a \, E[C_r] + \sum_{i=1}^{k} Pd_i Y_{r_i}}{\left(1 - \lambda \, E[C]\right)} \tag{4.6}$$

where $E[C]$ can be viewed as the expected service time in an imaginary server that experiences downtimes only when it is idle as mentioned in [Altıok, 1997]. Recall that the service dynamics such as scrapings are hidden in this service time (the completion time process). The $\lambda E[C]$ expression in (4.6) represents the utilization of the imaginary server, denoted by $P(B)$, which is the percentage of the time the imaginary server is busy. The server is stable if and only if $P(B) = \lambda E[C] < 1$.

$E[C]$ and $E[C_r]$ in (4.6) will be discussed in detail in the following sections.

4.3.1 SERVICE COMPLETION TIME (C)

As mentioned earlier, the time a customer spends in service, *C*, is also known as the *service completion time*. *C* consists of two parts; the actual service time of a customer, S_a, and the downtime experienced by a customer during its service as shown in Figure 4.1. The actual customer is scrapped upon interruption but the downtime continues and the imaginary customer remains in service.

$$C = S_a + \begin{cases} Y_1 & \text{w.p. } P(\text{Server fails due to failure 1}) \\ Y_2 & \text{w.p. } P(\text{Server fails due to failure 2}) \\ \vdots & \vdots \\ Y_k & \text{w.p. } P(\text{Server fails due to failure } k) \end{cases} \tag{4.7}$$

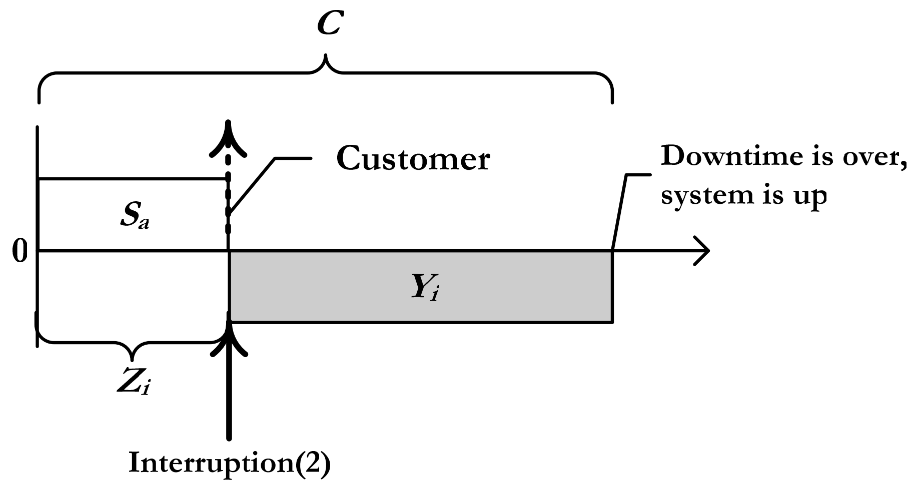

Figure 4.1 The service completion time *C* if an interruption occurs during a service

Therefore, the expected service completion time can be written as follows:

$$E\left[C\right]=E\left[S_a\right]+\sum_{i=1}^{k}P(Z_i<\min(S,Z_1,Z_2,...,Z_{i\text{-}1},Z_{i+1},...,Z_k))\cdot E[Y_i]. \tag{4.8}$$

The actual service time, S_a, is equal to the service time *S* if the server does not fail during a service. Otherwise, S_a is equal to the time to interruption. The actual service time can be expressed as follows:

$$S_a=\begin{cases} S & \text{w.p. } \Pr\left(\text{Server does not fail during service}\right) \\ Z_1 & \text{w.p. } \Pr\left(\text{Server fails due to interruption type } 1\right) \\ Z_2 & \text{w.p. } \Pr\left(\text{Server fails due to interruption type } 2\right) \\ \vdots & \vdots \\ Z_k & \text{w.p. } \Pr\left(\text{Server fails due to interruption type } k\right) \end{cases} \tag{4.9}$$

where the probability that the server does not fail during the service time of the customer is equal to the probability that the service time S is less than or equal to the time to interruption, Z_i, of all of the interruption types $(i = 1,...,k)$. Also, the probability that the server fails during a service time due to interruption type i $(i = 1,...,k)$ is equal to the probability that the interruption type i occurs before all the other types of interruptions and before the server finishes its service. Thus, it is equivalent to the probability that the time to interruption of type i is less than or equal to the service time S and the time to interruption of all the other types. Therefore, we can write

$$P(\text{Server does not fail during service}) = P\left(S \le \min\left(Z_1,...,Z_k\right)\right), \tag{4.10}$$

$$P(\text{Server fails due to interruption type } i) = P\left(Z_i \le \min\left(S, Z_1, \ldots, Z_{i-1}, Z_{i+1}, \ldots, Z_k\right)\right). \tag{4.11}$$

Using (4.9) and the probabilities defined in (4.10), and (4.11), we can write the following LST of the density function of the actual service time, S_a:

$$\begin{aligned} F^*_{S_a}(s) &= E\left[e^{-sS} \middle| S \le \min\left(Z_1,...,Z_k\right)\right] P\left(S \le \min\left(Z_1,...,Z_k\right)\right) \\ &\quad + \sum_{i=1}^{k} E\left[e^{-sZ_i} \middle| Z_i \le \min\left(S, Z_1,...,Z_{i-1}, Z_{i+1},...,Z_k\right)\right] P\left(Z_i \le \min\left(S, Z_1,...,Z_{i-1}, Z_{i+1},...,Z_k\right)\right) \end{aligned} \tag{4.12}$$

which can be expressed in terms of the density functions:

$$F_{S_a}^*(s) = \left(\int_0^\infty e^{-sx} f_{S|S \le \min(Z_1,...,Z_k)}(x)\,dx \right) P\left(S \le \min\left(Z_1,...,Z_k\right)\right)$$
$$+ \sum_{i=1}^{k} \left(\int_0^\infty e^{-sz} f_{Z_i|Z_i \le \min(S, Z_1,...,Z_{i-1},Z_{i+1},...,Z_k)}(z)\,dz \right) P\left(Z_i \le \min\left(S, Z_1,...,Z_{i-1},Z_{i+1},...,Z_k\right)\right). \tag{4.13}$$

For simplicity, let us assume **deterministic** service times, that is $S = x$. Then, the LST of S_a is given by

$$F_{S_a}^*(s) = e^{-x\left(s+\sum_{m=1}^{k}\delta_m\right)} + \sum_{i=1}^{k}\left(\frac{\delta_i}{\left(s+\sum_{m=1}^{k}\delta_m\right)}\left(1-e^{-x\left(s+\sum_{m=1}^{k}\delta_m\right)}\right)\right) \tag{4.14}$$

The detailed derivation of the above expression is given in Appendix E.

The first two moments of the actual service time depend on the distribution of the service time *S*. The first two moments of the actual service time are given by

$$m_1 = x\,e^{-\sum_{i=1}^{k}\delta_i x} + \sum_{j=1}^{k}\left(\frac{\delta_j}{\sum_{i=1}^{k}\delta_i}\left(1-e^{-\sum_{i=1}^{k}\delta_i x}\right)\left(\frac{1}{\sum_{i=1}^{k}\delta_i} - \frac{x\,e^{-\sum_{i=1}^{k}\delta_i x}}{\left(1-e^{-\sum_{i=1}^{k}\delta_i x}\right)}\right)\right) \tag{4.15}$$

$$m_2 = x^2 e^{-\sum_{i=1}^{k}\delta_i x} + \sum_{j=1}^{k}\left(\frac{\delta_j}{\sum_{i=1}^{k}\delta_i}\left(1-e^{-\sum_{i=1}^{k}\delta_i x}\right)\left(x^2 - \frac{x}{\left(1-e^{-\sum_{i=1}^{k}\delta_i x}\right)}\left(x + \frac{2e^{-\sum_{i=1}^{k}\delta_i x}}{\sum_{i=1}^{k}\delta_i}\right) + \frac{2}{\left(\sum_{i=1}^{k}\delta_i\right)^2}\right)\right). \quad (4.16)$$

The first two moments of S_a when the service time follows a **4-phase Erlang** distribution with rate α is given in Appendix F.

Using (4.7), we can write the LST of the density function of the service completion time, *C*, as follows

$$F_C^*(s) = F_{S_a}^*(s) + \sum_{i=1}^{k} F_{Y_i}^*(s)\, P\left(Z_i \le \min\left(S, Z_1, ..., Z_{i-1}, Z_{i+1}, ..., Z_k\right)\right) \quad (4.17)$$

where $F_{S_a}^*(s)$ is given by (4.13).

Hence, under the deterministic service time assumption $\left(S = x\right)$, we have

$$F_C^*(s) = e^{-x\left(s+\sum_{m=1}^{k}\delta_m\right)} + \sum_{i=1}^{k}\left(\frac{\delta_i}{\left(s+\sum_{m=1}^{k}\delta_m\right)}\left(1-e^{-x\left(s+\sum_{m=1}^{k}\delta_m\right)}\right)\right) + \sum_{i=1}^{k} F_{Y_i}^*(s)\left(\frac{\delta_i}{\sum_{m=1}^{k}\delta_m}\left(1-e^{-\left(\sum_{m=1}^{k}\delta_m\right)x}\right)\right). \quad (4.18)$$

4.3.2 REMAINING SERVICE COMPLETION TIME (CR)

The remaining service completion time of a customer in service as seen by an arriving customer, C_r, is the time until the next customer (if any) may start its service. It consists of the remaining actual service time of the customer, S_{r_a}, and the downtime experienced by the customer during its remaining service completion time. We can write

$$E\left[C_r\right] = E\left[S_{r_a}\right] + \sum_{i=1}^{k} P(Z_i < \min(S_r, Z_1, Z_2, ..., Z_{i\text{-}1}, Z_{i+1}, ..., Z_k)) \cdot E\left[Y_i\right] \qquad (4.19)$$

where S_r and S_{r_a} represent the remaining service time and the remaining actual service time, respectively. Both of these expressions are derived using the residual life idea discussed in [Ross, 1980] as follows:

$$E\left[S_r\right] = \frac{E\left[S^2\right]}{2E\left[S\right]} \qquad (4.20)$$

and

$$E\left[S_{r_a}\right] = \frac{E\left[S_a{}^2\right]}{2E\left[S_a\right]}. \qquad (4.21)$$

4.3.3 EXPECTED WAITING TIME (E[W])

The expressions presented in (4.6), (4.8), and (4.19) can be used in arriving at the expression for expected waiting time $\left(E\left[W\right]\right)$:

$$E[W] = \frac{\rho_a \left(E\left[Sr_a\right] + \sum_{i=1}^{k} P(Z_i < \min(Sr, Z_1, Z_2, ..., Z_{i\text{-}1}, Z_{i+1}, ..., Z_k)) \cdot E\left[Y_i\right] \right) + \sum_{i=1}^{k} P_{d,i} E\left[Yr_i\right]}{1 - \lambda \left(E\left[S_a\right] + \sum_{i=1}^{k} P(Z_i < \min(S, Z_1, Z_2, ..., Z_{i\text{-}1}, Z_{i+1}, ..., Z_k)) \cdot E[Y_i] \right)} \tag{4.22}$$

4.3.4 NUMERICAL RESULTS

In this section, we present the impact of a change in different system parameters such as service time variability, downtime variability, system utilization, downtime probability, and number of interruptions on the expected service completion time, $E[C]$, and the expected waiting time of customers in the queue, $E[W]$, in different scenarios.

We use the following common assumptions for all scenarios:

- Poisson customer arrivals
- Exponential times to interruption

Different values of parameters used in the runs are presented in Table 4.1. The shaded values are the base values, indicating that when one of the parameters is changed in a run, all the other parameters are kept at their base values.

Table 4.1 Parameters used in the scenario analysis of the non-simultaneous interruptions case

Parameter	Values				
Cv^2(Service Time)	0	0.25	3		
Cv^2(Downtime)	0.25	1	3		
System Utilization ($P(B)$)	60%	70%	80%	90%	
Downtime Probability (P_d)	5%	10%	15%	20%	25%
Number of Interruptions (k)	4	5	6		

4.3.4.1 IMPACT OF SERVICE TIME VARIABILITY

As the squared coefficient of variation of the service time, Cv_S^2, increases, the average waiting time of a customer also increases due to high variability of the service time as seen in Figure 4.2. On the other hand, $E[W]$ decreases in general when the number of interruptions, k, increases. This is due to the fact that we kept the same down time probability as we have increased the number of interruptions resulting in smaller downtimes per interruption which in turn reduced customer waiting times.

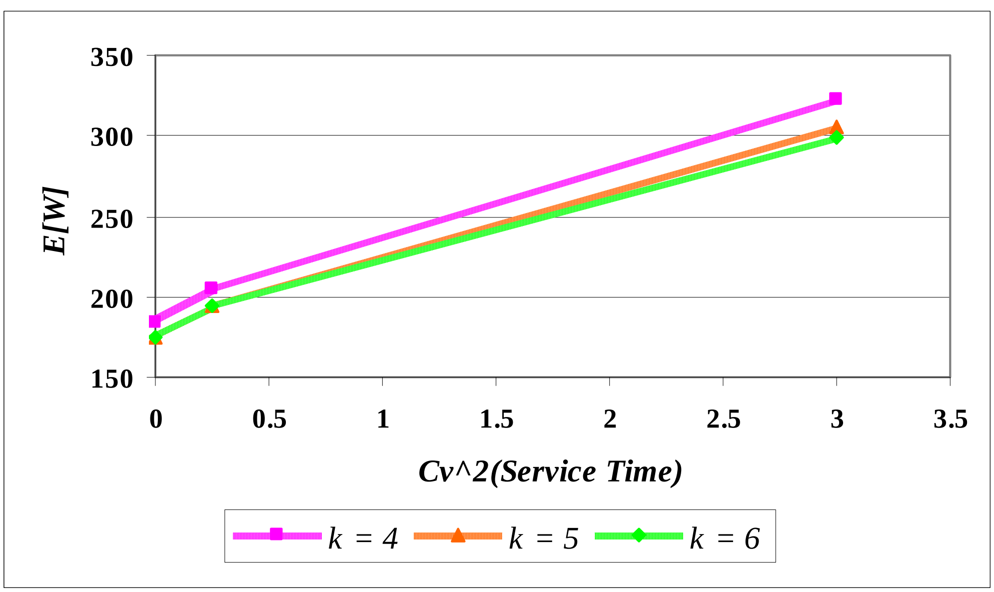

Figure 4.2 Impact of Cv_S^2 on $E[W]$ in the case of non-simultaneous interruptions

Results obtained by changing $Cv_S{}^2$ and the number of interruptions, *k*, are shown in Table **4.2**.

Table 4.2 $E[C]$ **and** $E[W]$ in the non-simultaneous interruptions case when changing $Cv_S{}^2$

k	$Cv^2(S)$	*E[C]*	*E[W]*
4	0 (Det.)	27.001	183.7874
	0.25 (4-Erlang)	26.3857	204.2849
	3 (2-HyperEx)	22.055	322.8874
5	0 (Det.)	26.9988	174.7455
	0.25 (4-Erlang)	26.3239	194.8195
	3 (2-HyperEx)	21.7417	305.2326
6	0 (Det.)	26.9995	174.9285
	0.25 (4-Erlang)	26.2784	194.6797
	3 (2-HyperEx)	21.5141	298.9094

4.3.4.2 IMPACT OF DOWNTIME VARIABILITY

The average waiting time of a customer, $E[W]$, increases as the squared coefficient of variation of all of the downtimes, $Cv_{Y_i}{}^2$ for $i = (1, \ldots, k)$, increases in Figure 4.3. Downtimes are modeled using PH distributions. On the other hand, $E[W]$ decreases in general when the number of interruptions, *k*, increases.

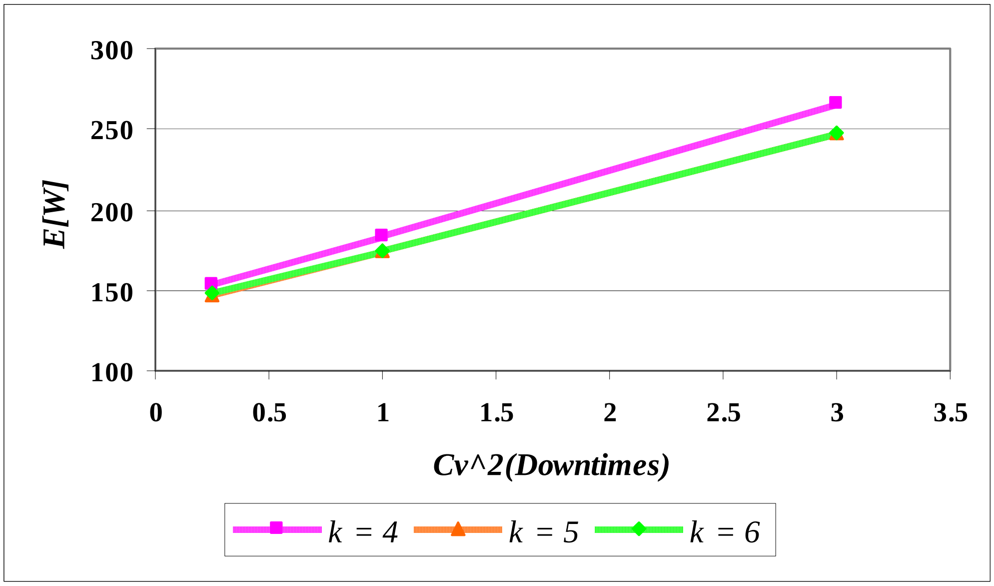

Figure 4.3 Impact of $Cv_Y^{\ 2}$ on $E[W]$ in the case of non-simultaneous interruptions

Results obtained by changing $Cv_{Y_i}^{\ 2}$ for $i = (1, \ldots, k)$ and the number of interruptions, k, are shown in Table 4.3. The service completion time, $E[C]$, is not affected by the change in downtime variability.

Table 4.3 $E[C]$ **and** $E[W]$ in the non-simultaneous interruptions case when changing $Cv_Y^{\ 2}$

k	$Cv^2(Y)$	E[C]	E[W]
4	0.25 (4-Erlang)	27.0001	152.9428
	1 (Expo)	27.0001	183.7874
	3 (2-HyperEx)	27.0007	265.9714
5	0.25 (4-Erlang)	26.9988	147.489
	1 (Expo)	26.9988	174.7455
	3 (2-HyperEx)	26.9993	247.5245
6	0.25 (4-Erlang)	26.9995	147.8009
	1 (Expo)	26.9995	174.9285
	3 (2-HyperEx)	27.0002	247.3949

4.3.4.3 IMPACT OF SYSTEM UTILIZATION

According to the simulation results, the average waiting time of a customer, $E[W]$, increases as the system utilization increases. There is also a slight decrease in $E[W]$ when the number of interruptions, k, increases from 4 to 5 and then to 6. On the other hand, system utilization does not have any impact on the service completion time, $E[C]$.

4.3.4.4 IMPACT OF DOWNTIME PROBABILITY

An increasing trend is observed in the average waiting time of a customer, $E[W]$, when the downtime probability increases. At the same time, $E[W]$ decreases when the number of interruptions increases from 4 to 5 and then to 6. Also, the service completion time, $E[C]$, increases as the downtime probability, P_d, increases.

4.4 WAITING TIME IN QUEUES SUBJECT TO POSSIBLY SIMULTANEOUS INTERRUPTIONS

In this case, the server is subject to *k* operation-independent, non-identical, possibly simultaneous interruptions. The interruptions are independent and the downtimes do not affect each other. That is, it is possible to have a number of downtimes progressing simultaneously. A *down cycle* starts when an interruption occurs during an uptime and ends when the system turns up again. Since the interruptions are operation-independent, the server can also be down when it is idle as mentioned in (Altıok 1997).

Thus, the waiting time of an arriving customer in the case of possibly simultaneous interruptions can be expressed as follows:

$$W = \left(N \times C\right) + \begin{cases} 0 & \text{w.p. } P\left(\text{Server idle upon arrival}\right) \\ C_r & \text{w.p. } P\left(\text{Server busy upon arrival}\right) \\ T_{RD} & \text{w.p. } P\left(\text{Server down upon arrival}\right) \end{cases} \tag{4.23}$$

where T_{RD} represents the total remaining downtime of the system when it is down upon arrival. The probability that the server is busy upon arrival is obtained using (3.2). Thus, the average waiting time of a customer in the queue is given by

$$E[W] = E[N]\,E[C] + \rho_a\, E[C_r] + E[T_{RD}]\,. \tag{4.24}$$

Then, using the Little's formula $\left(E\left[N\right] = \lambda\, E\left[W\right]\right)$, (4.24) is reduced to

$$E[W] = \frac{\rho_a\, E[C_r] + E[T_{RD}]}{\left(1 - \lambda\, E[C]\right)} \tag{4.25}$$

where $E[C]$ can be viewed as the expected service time of an imaginary server that experiences downtimes when it is idle only, as mentioned in [Altıok, 1997]. The $\lambda E[C]$ expression in (4.25) represents the utilization of this imaginary server, denoted by $P(B)$. The server is said to be stable if and only if $P(B) = \lambda\, E[C] < 1$.

4.4.1 SERVICE COMPLETION TIME (C)

In this section, we present the characteristics of the service completion time, *C*, considering different cases of possibly simultaneous interruptions. First, recall that *C* consists of two parts; the actual service time of a customer, S_a, and the downtime experienced by a customer during its service, T_{DS}. We have

$$E[C] = E[S_a] + E[T_{DS}] \tag{4.26}$$

The expression for the actual service time, S_a, used in the case of non-simultaneous interruptions (section 4.3.1) can also be applied in this case, and the LST of S_a is given by (4.12) and (4.13).

On the other hand, the downtime experienced by a customer during its service, T_{DS}, can be expressed as the time consisting of the downtimes of all the possible consecutive interruptions occurring in a down cycle. Due to the operation-independent nature of the interruptions, there may be infinitely many interruptions occurring in a down cycle. However, for practical purposes, we assume that each interruption type may occur **at most once** during the service of a customer, inducing approximation into our analysis. This is especially true in waterways due to short service times and much longer down times. In a short service time, it is very unlikely to have fog develop, clear up and develop back again.

Contrary to the previous work on the queueing models with multiple types of simultaneous interruptions, the downtime experienced by a customer is not simply the sum of the downtimes of all possible interruptions during its service. Interruption types are operation-independent and they may occur at anytime, and their downtime processes start immediately after their occurrences. Therefore, T_{DS} involves a rather complicated expression than a simple summation.

Consider the case where there are two different types of interruptions. Total downtime experienced by a customer during its service, T_{DS}, is zero if no interruption occurs. If only one interruption occurs, T_{DS} is equal to the downtime of that interruption. On the other hand, in the event that both interruption types occur during a service, let Interr(1) and Interr(2) be the first and second occurring interruption, respectively. In this case, T_{DS} is equal to the time to interruption of Interr(2) plus the maximum of the remaining downtime of Interr(1) and the downtime of Interr(2). The two possible outcomes for the maximum term are shown in Figures 4.4 and 4.5. Note that either one of the interruption types may occur first.

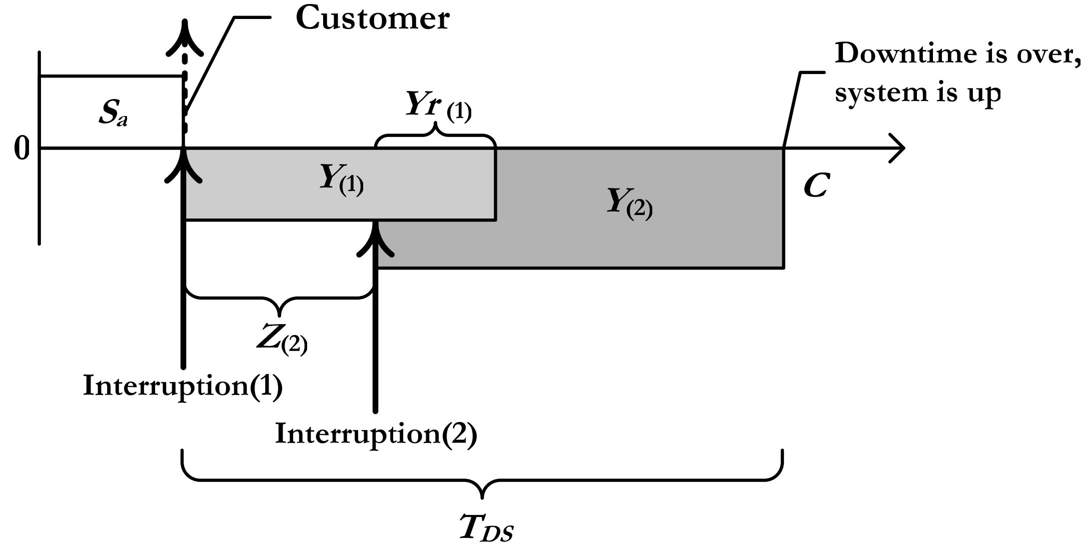

Figure 4.4 T_{DS} if both interruptions occur and if $Y_{r_{(1)}} \leq Y_{(2)}$

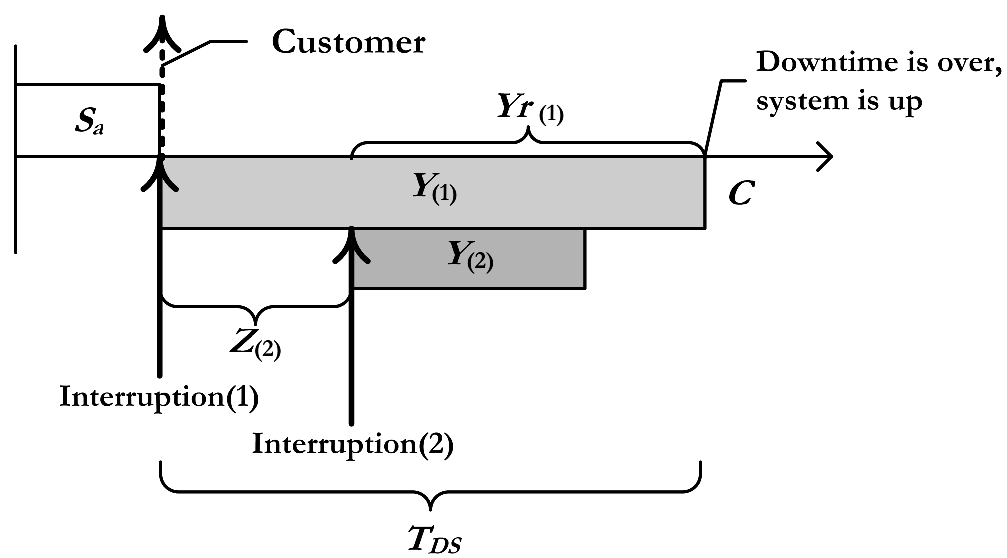

Figure 4.5 T_{DS} if both interruptions occur and if $Y_{r_{(1)}} > Y_{(2)}$

Thus, for the 2-interruption case, the expected downtime experienced by a customer during its service, $E[T_{DS}]$, is given by

$$E\left[T_{DS}\right]=\begin{pmatrix} P\left(Z_1 \le \min(S,Z_2)\right)P\left(Y_1 \le Z_2\right)E[Y_1 \mid Y_1 \le Z_2] \\ +P\left(Z_1 \le \min(S,Z_2)\right)P\left(Z_2 \le Y_1\right)\begin{pmatrix} P\left(Yr_1 > Y_2\right)E[Yr_1 \mid Yr_1 > Y_2] \\ +P\left(Y_2 > Yr_1\right)E[Y_2 \mid Y_2 > Yr_1] \end{pmatrix} \end{pmatrix} \\ +\begin{pmatrix} P\left(Z_2 \le \min(S,Z_1)\right)P\left(Y_2 \le Z_1\right)E[Y_2 \mid Y_2 \le Z_1] \\ +P\left(Z_2 \le \min(S,Z_1)\right)P\left(Z_1 \le Y_2\right)\begin{pmatrix} P\left(Yr_2 > Y_1\right)E[Yr_2 \mid Yr_2 > Y_1] \\ +P\left(Y_1 > Yr_2\right)E[Y_1 \mid Y_1 > Yr_2] \end{pmatrix} \end{pmatrix} \tag{4.27}$$

When we try to generalize the above expression to a k-interruption case, we observe the need to include the possibility of all k interruptions occurring successively during a down cycle. As a result, the above expression expands significantly as k increases. In view of this, we propose an approximation that limits the number of interruptions that can occur during a service time. The approximation is based on the assumption that there may be **at most three** interruptions occurring consecutively during a down cycle. This approximation is supported by the fact that the service time of a customer is relatively small compared to times to interruption. Recall that the service time in waterways is the time interval between two vessel entrances, which can be measured in minutes as opposed to downtimes of possibly many hours and days in the event of traffic closures. Furthermore, the probability of having a large number of interruptions in the same down cycle may be negligible. The selection of number "three" is largely due to the increased effort in modeling the case with "four" possible interruptions during a down cycle.

Based on the assumption described above, the downtime experienced by a customer during a service completion time, T_{DS}, can be expressed as follows:

$$T_{DS} = \begin{cases} Y_{\text{Interr}(1)} & \text{w.p. } P(\text{One interruption occurs}) \\ Z_{\text{Interr}(2)} + \max\left(Y_{r_{\text{Interr}(1)}}, Y_{\text{Interr}(2)}\right) & \text{w.p. } P(\text{Two interruptions occur}) \\ Z_{\text{Interr}(2)} + Z_{\text{Interr}(3)} + \max\left(Y_{r_{\text{Interr}(1)}}, Y_{r_{\text{Interr}(2)}}, Y_{\text{Interr}(3)}\right) & \text{w.p. } P(\text{Three interruptions occur}) \end{cases} \quad (4.28)$$

where Interr(m) is the mth occurring interruption.

Thus, we obtain the expression for the expected downtime experienced by a customer during its service, $E[T_{DS}]$, given in (4.29).

$$E\left[T_{DS}\right]=\sum_{i=1}^{k}\left(P\left(Z_i\le\min\left(S,\mathcal{Z}\text{-}\{i\}\right)\right)\left[\begin{array}{l}P\left(Y_i\le\min\left(\mathcal{Z}\text{-}\{i\}\right)\right)E\left[Y_i\mid Y_i\le\min\left(\mathcal{Z}\text{-}\{i\}\right)\right]\\+\sum\limits_{\substack{h=1\\h\ne i}}^{k}P\left(Z_h\le\min\left(Y_i,\mathcal{Z}\text{-}\{i,h\}\right)\right)\left[\begin{array}{l}E\left[Z_h\mid Z_h\le\min\left(Y_i,\mathcal{Z}\text{-}\{i,h\}\right)\right]\\+\left[\begin{array}{l}P\left(\max(Y_{r_i},Y_h)\le\min\left(\mathcal{Z}\text{-}\{i,h\}\right)\right)\\\times E\left[\max(Y_{r_i},Y_h)\mid\max(Y_{r_i},Y_h)\le\min\left(\mathcal{Z}\text{-}\{i,h\}\right)\right]\end{array}\right]\\+\sum\limits_{\substack{l=1\\l\ne h\ne i}}^{k}\left[\begin{array}{l}P\left(Z_l\le\min\left(\max(Y_{r_i},Y_h),\mathcal{Z}\text{-}\{i,h,l\}\right)\right)\\\times\left[\begin{array}{l}+\left(\begin{array}{l}P\left(Y_{r_i}>\max(Y_{r_h},Y_l)\right)\\\times\left(\begin{array}{l}E\left[Z_l\mid Z_l\le\min\left(Y_{r_i},\mathcal{Z}\text{-}\{i,h,l\}\right)\right]\\+E[Y_{r_i}\mid Y_{r_i}>\max(Y_{r_h},Y_l)]\end{array}\right)\end{array}\right)\\+\left(\begin{array}{l}P\left(Y_{r_h}>\max(Y_{r_i},Y_l)\right)\\\times\left(\begin{array}{l}E\left[Z_l\mid Z_l\le\min\left(Y_h,\mathcal{Z}\text{-}\{i,h,l\}\right)\right]\\+E[Y_{r_h}\mid Y_{r_h}>\max(Y_{r_i},Y_l)]\end{array}\right)\end{array}\right)\\+\left(\begin{array}{l}P\left(Y_l>\max(Y_{r_h},Y_{r_i})\right)\\\times\left(\begin{array}{l}E\left[Z_l\mid Z_l\le\min\left(\max(Y_{r_i},Y_h),\mathcal{Z}\text{-}\{i,h,l\}\right)\right]\\+E[Y_l\mid Y_l>\max(Y_{r_h},Y_{r_i})]\end{array}\right)\end{array}\right)\end{array}\right]\end{array}\right]\end{array}\right]\end{array}\right]\right) \tag{4.29}$$

where $\mathcal{Z}\text{-}\{i,h,l\}=\left(Z_1,...,Z_{i-1},Z_{i+1},Z_{h-1},Z_{h+1},Z_{l-1},Z_{l+1},...,Z_k\right)$ is the set of time to interruptions, which excludes interruptions i, h, and l.

Also, using (4.28), we can write the LST of the density function of the downtime experienced by a customer during its service, T_{DS},

$$
\begin{aligned}
F^*_{T_{DS}}(s) &= \sum_{i=1}^{k}\left(F^*_{Y_i}(s)\, P\left(Z_i \le \min\left(S, \mathcal{Z}\text{-}\{i\}\right)\right) P\left(Y_i \le \min\left(\mathcal{Z}\text{-}\{i\}\right)\right)\right) \\
&+ \sum_{i=1}^{k}\left(\sum_{\substack{h=1\\ h\ne i}}^{k} \left(\begin{array}{l}
E\left[e^{-sZ_h} \middle| Z_h \le \min\left(Y_i, \mathcal{Z}\text{-}\{i,h\}\right)\right] \\
\times E\left[e^{-s\max(Y_{r_i},Y_h)} \mid \max(Y_{r_i},Y_h) \le \min\left(\mathcal{Z}\text{-}\{i,h\}\right)\right] \\
\times P\left(Z_i \le \min\left(S,\mathcal{Z}\text{-}\{i\}\right)\right) \times P\left(Z_h \le \min\left(Y_i,\mathcal{Z}\text{-}\{i,h\}\right)\right) \\
\times P\left(\max(Y_{r_i},Y_h) \le \min\left(\mathcal{Z}\text{-}\{i,h\}\right)\right)
\end{array}\right)\right) \\
&+ \sum_{i=1}^{k}\left(\sum_{\substack{h=1\\ h\ne i}}^{k} \left(\sum_{\substack{l=1\\ l\ne h\ne i}}^{k} \left(\begin{array}{l}
\left(\begin{array}{l}
E\left[e^{-sZ_h} \middle| Z_h \le \min\left(Y_i, \mathcal{Z}\text{-}\{i,h\}\right)\right] \\
\times E\left[e^{-sZ_l} \mid Z_l \le \min\left(Y_{r_i}, \mathcal{Z}\text{-}\{i,h,l\}\right)\right] \\
\times E\left[e^{-sYr_i} \mid Y_{r_i} > \max(Y_{r_h},Y_l)\right] \\
\times P\left(Z_i \le \min\left(S,\mathcal{Z}\text{-}\{i\}\right)\right) \times P\left(Z_h \le \min\left(Y_i,\mathcal{Z}\text{-}\{i,h\}\right)\right) \\
\times P\left(Z_l \le \min\left(\max(Yr_i,Y_h),\mathcal{Z}\text{-}\{i,h,l\}\right)\right) \times P\left(Y_{r_i} > \max(Y_{r_h},Y_l)\right)
\end{array}\right) \\
+ \left(\begin{array}{l}
E\left[e^{-sZ_h} \middle| Z_h \le \min\left(Y_i, \mathcal{Z}\text{-}\{i,h\}\right)\right] \\
\times E\left[e^{-sZ_l} \mid Z_l \le \min\left(Y_h, \mathcal{Z}\text{-}\{i,h,l\}\right)\right] \\
\times E\left[e^{-sYr_h} \mid Yr_h > \max(Y_{r_i},Y_l)\right] \\
\times P\left(Z_i \le \min\left(S,\mathcal{Z}\text{-}\{i\}\right)\right) \times P\left(Z_h \le \min\left(Y_i,\mathcal{Z}\text{-}\{i,h\}\right)\right) \\
\times P\left(Z_l \le \min\left(\max(Y_{r_i},Y_h),\mathcal{Z}\text{-}\{i,h,l\}\right)\right) \times P\left(Y_{r_h} > \max(Y_{r_i},Y_l)\right)
\end{array}\right) \\
+ \left(\begin{array}{l}
E\left[e^{-sZ_h} \middle| Z_h \le \min\left(Y_i, \mathcal{Z}\text{-}\{i,h\}\right)\right] \\
\times E\left[e^{-sZ_l} \mid Z_l \le \min\left(\max(Y_{r_i},Y_h), \mathcal{Z}\text{-}\{i,h,l\}\right)\right] \\
\times E\left[e^{-sY_l} \mid Y_l > \max(Y_{r_i},Y_{r_h})\right] \\
\times P\left(Z_i \le \min\left(S,\mathcal{Z}\text{-}\{i\}\right)\right) \times P\left(Z_h \le \min\left(Y_i,\mathcal{Z}\text{-}\{i,h\}\right)\right) \\
\times P\left(Z_l \le \min\left(\max(Y_{r_i},Y_h),\mathcal{Z}\text{-}\{i,h,l\}\right)\right) \times P\left(Y_l > \max(Y_{r_i},Y_{r_h})\right)
\end{array}\right)
\end{array}\right)\right)\right)
\end{aligned}
\tag{4.30}
$$

Replacing all the probabilities in (4.30) by their corresponding expressions leads to (4.31). The expected length of the down cycle is given in detail in AppendiG.

$$
\begin{aligned}
F^{*}_{T_{DS}}(s) = \sum_{i=1}^{k} & \left(F^{*}_{Y_i}(s) \left(\frac{\delta_i}{\sum\limits_{m=1}^{k}\delta_m} \left(1 - e^{-\left(\sum\limits_{m=1}^{k}\delta_m\right)x} \right) \right) \left(\frac{\gamma_i}{\gamma_i + \sum\limits_{\substack{m=1 \\ m\neq i}}^{k}\delta_m} \right) \right) \\
+ \sum_{i=1}^{k} \sum_{\substack{h=1 \\ h\neq i}}^{k} & \left(\begin{array}{l} E\left[e^{-sZ_h} \middle| Z_h \leq \min\left(Y_i, \mathcal{Z}\text{-}\{i,h\}\right) \right] \times E\left[e^{-s\max(Y_{r_i},Y_h)} \mid \max(Y_{r_i},Y_h) \leq \min\left(\mathcal{Z}\text{-}\{i,h\}\right) \right] \\
\dfrac{\delta_i}{\sum\limits_{m=1}^{k}\delta_m} \left(1 - e^{-\left(\sum\limits_{m=1}^{k}\delta_m\right)x} \right) \times \dfrac{\delta_h}{\gamma_i + \sum\limits_{\substack{m=1 \\ m\neq i}}^{k}\delta_m} \times \left(1 - \sum\limits_{\substack{m=1 \\ m\neq i\neq h}}^{k}\delta_m \left(\dfrac{1}{\gamma_i + \sum\limits_{\substack{m=1 \\ m\neq i\neq h}}^{k}\delta_m} + \dfrac{1}{\gamma_h + \sum\limits_{\substack{m=1 \\ m\neq i\neq h}}^{k}\delta_m} - \dfrac{1}{\gamma_i + \gamma_h + \sum\limits_{\substack{m=1 \\ m\neq i\neq h}}^{k}\delta_m} \right) \right) \end{array} \right) \\
+ \sum_{i=1}^{k} \sum_{\substack{h=1 \\ h\neq i}}^{k} \sum_{\substack{l=1 \\ l\neq h\neq i}}^{k} & \left(\left(\begin{array}{l} E\left[e^{-sZ_h} \middle| Z_h \leq \min\left(Y_i, \mathcal{Z}\text{-}\{i,h\}\right) \right] \times \dfrac{\delta_i}{\sum\limits_{m=1}^{k}\delta_m} \left(1 - e^{-\left(\sum\limits_{m=1}^{k}\delta_m\right)x} \right) \times \dfrac{\delta_h}{\delta_h + \gamma_i + \sum\limits_{\substack{m=1 \\ m\neq i\neq h}}^{k}\delta_m} \\
\times \left(1 - \dfrac{\gamma_i + \sum\limits_{\substack{m=1 \\ m\neq i\neq h\neq l}}^{k}\delta_m}{\delta_l + \gamma_i + \sum\limits_{\substack{m=1 \\ m\neq i\neq h\neq l}}^{k}\delta_m} - \dfrac{\gamma_h + \sum\limits_{\substack{m=1 \\ m\neq i\neq h\neq l}}^{k}\delta_m}{\delta_l + \gamma_h + \sum\limits_{\substack{m=1 \\ m\neq i\neq h\neq l}}^{k}\delta_m} + \dfrac{\gamma_i + \gamma_h + \sum\limits_{\substack{m=1 \\ m\neq i\neq h\neq l}}^{k}\delta_m}{\delta_l + \gamma_i + \gamma_h + \sum\limits_{\substack{m=1 \\ m\neq i\neq h\neq l}}^{k}\delta_m} \right) \\
\times \left(\begin{array}{l} \left(E\left[e^{-sZ_l} \mid Z_l \leq \min\left(Y_{r_i}, \mathcal{Z}\text{-}\{i,h,l\}\right) \right] \times E\left[e^{-sYr_i} \mid Y_{r_i} > \max(Y_{r_h}, Y_l) \right] \times \left(\dfrac{\gamma_h}{\gamma_i + \gamma_h} + \dfrac{\gamma_l}{\gamma_i + \gamma_l} - \dfrac{\gamma_h + \gamma_l}{\gamma_i + \gamma_h + \gamma_l} \right) \right) \\
+ \left(E\left[e^{-sZ_l} \mid Z_l \leq \min\left(Y_h, \mathcal{Z}\text{-}\{i,h,l\}\right) \right] \times E\left[e^{-sYr_h} \mid Y_{r_h} > \max(Y_{r_i}, Y_l) \right] \times \left(\dfrac{\gamma_i}{\gamma_h + \gamma_i} + \dfrac{\gamma_l}{\gamma_h + \gamma_l} - \dfrac{\gamma_i + \gamma_l}{\gamma_h + \gamma_i + \gamma_l} \right) \right) \\
+ \left(E\left[e^{-sZ_l} \mid Z_l \leq \min\left(\max(Y_{r_i}, Y_h), \mathcal{Z}\text{-}\{i,h,l\}\right) \right] \times E\left[e^{-sY_l} \mid Y_l > \max(Y_{r_i}, Y_{r_h}) \right] \times \left(\dfrac{\gamma_i}{\gamma_l + \gamma_i} + \dfrac{\gamma_h}{\gamma_l + \gamma_h} - \dfrac{\gamma_i + \gamma_h}{\gamma_l + \gamma_i + \gamma_h} \right) \right) \end{array} \right) \end{array} \right) \right)
\end{aligned}
\qquad (4.31)
$$

4.4.2 REMAINING SERVICE COMPLETION TIME (CR)

The remaining service completion time of a customer in service as seen by an arriving customer, C_r, is the time until the next customer (if any) may start its service. It consists of the remaining actual service time of the customer, S_{r_a}, and the downtime experienced by the customer during its remaining service completion time, T_{DRS}, as seen in Figure 4.6. We can write

$$E\left[C_r\right] = E\left[S_{r_a}\right] + E\left[T_{DRS}\right] \tag{4.32}$$

The remaining actual service time, S_{r_a}, can be evaluated using (4.21). Using arguments similar to $E[T_{DS}]$, we obtain the expression for the expected downtime experienced by a customer during its remaining service, $E[T_{DRS}]$, as shown in (4.33).

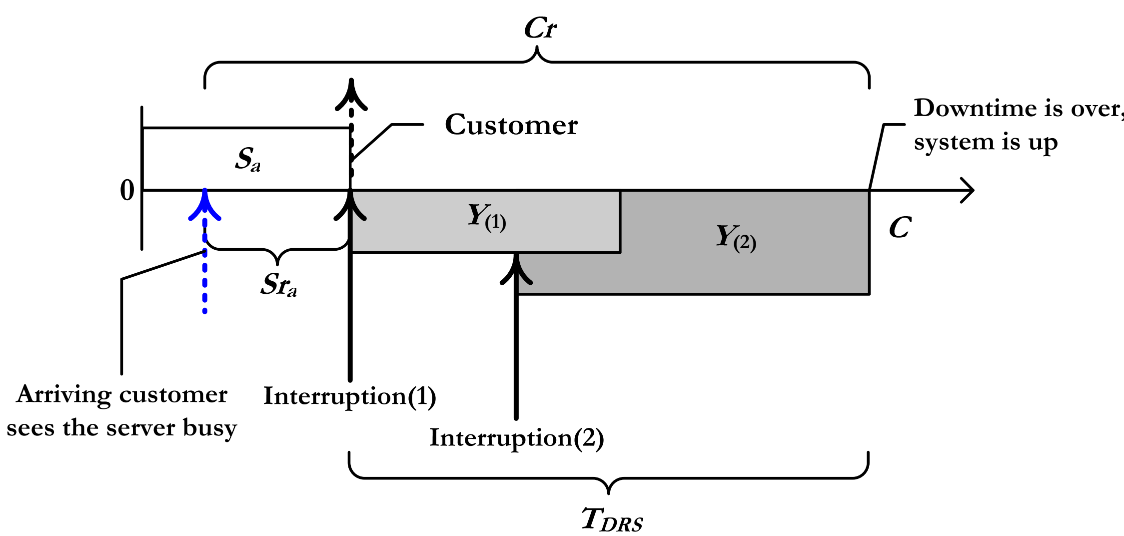

Figure 4.6 Remaining Service Completion Time, C_r.

$$
E\left[T_{DRS}\right]=\sum_{i=1}^{k}\left(P\left(Z_i\le\min\left(S_r,\mathcal{Z}\text{-}\{i\}\right)\right)\left[\begin{array}{l}
P\left(Y_i\le\min\left(\mathcal{Z}\text{-}\{i\}\right)\right)E\left[Y_i\mid Y_i\le\min\left(\mathcal{Z}\text{-}\{i\}\right)\right]\\
+\sum\limits_{\substack{h=1\\h\ne i}}^{k}P\left(Z_j\le\min\left(Y_i,\mathcal{Z}\text{-}\{i,h\}\right)\right)\left[\begin{array}{l}
E\left[Z_h\mid Z_h\le\min\min\left(Y_i,\mathcal{Z}\text{-}\{i,h\}\right)\right]\\
+\left[\begin{array}{l}P\left(\max(Y_{r_i},Y_h)\le\min\left(\mathcal{Z}\text{-}\{i,h\}\right)\right)\\
\times E\left[\max(Y_{r_i},Y_h)\mid\max(Y_{r_i},Y_h)\le\min\left(\mathcal{Z}\text{-}\{i,h\}\right)\right]\end{array}\right]\\
+\sum\limits_{\substack{l=1\\l\ne h\ne i}}^{k}\left[\begin{array}{l}
P\left(Z_l\le\min\left(\max(Y_{r_i},Y_h),\mathcal{Z}\text{-}\{i,h,l\}\right)\right)\\
\times\left[\begin{array}{l}
+\left(\begin{array}{l}P\left(Y_{r_i}>\max(Y_{r_h},Y_l)\right)\\
\times\left(\begin{array}{l}E\left[Z_l\mid Z_l\le\min\left(Y_{r_i},\mathcal{Z}\text{-}\{i,h,l\}\right)\right]\\
+E[Y_{r_i}\mid Y_{r_i}>\max(Y_{r_h},Y_l)]\end{array}\right)\end{array}\right)\\
+\left(\begin{array}{l}P\left(Y_{r_h}>\max(Y_{r_i},Y_l)\right)\\
\times\left(\begin{array}{l}E\left[Z_l\mid Z_l\le\min\left(Y_h,\mathcal{Z}\text{-}\{i,h,l\}\right)\right]\\
+E[Y_{r_h}\mid Y_{r_h}>\max(Y_{r_i},Y_l)]\end{array}\right)\end{array}\right)\\
+\left(\begin{array}{l}P\left(Y_l>\max(Y_{r_h},Y_{r_i})\right)\\
\times\left(\begin{array}{l}E\left[Z_l\mid Z_l\le\min\left(\max(Y_{r_i i},Y_h),\mathcal{Z}\text{-}\{i,h,l\}\right)\right]\\
+E[Y_l\mid Y_l>\max(Y_{r_h},Y_{r_i})]\end{array}\right)\end{array}\right)
\end{array}\right]
\end{array}\right]
\end{array}\right]
\end{array}\right]\right) \tag{4.33}
$$

where $\mathcal{Z}\text{-}\{i,h,l\}=\left(Z_1,\ldots,Z_{i-1},Z_{i+1},Z_{h-1},Z_{h+1},Z_{l-1},Z_{l+1},\ldots,Z_k\right)$.

4.4.3 REMAINING SYSTEM DOWNTIME (TRD)

In this section, we present the remaining system downtime as observed by an arriving customer. The remaining system downtime is the remaining length of a down cycle.

Since we limit the number of interruptions that can occur during a service time to three, the server may be down due to at most three different interruptions upon a customer arrival. If the system is down due to an interruption, one or two more interruptions may still occur during the down cycle. Conversely, if the system is experiencing two interruptions simultaneously, then a third one may still occur during the same down cycle.

Therefore, in case of possibly simultaneous interruptions, the remaining system downtime, if down upon a customer arrival, T_{RD}, can be expressed as follows:

$$T_{RD} = \begin{cases} T_{RD_1} & \text{w.p. } P(\text{One interruption observed upon arrival}) \\ T_{RD_2} & \text{w.p. } P(\text{Two interruptions observed upon arrival}) \\ T_{RD_3} & \text{w.p. } P(\text{Three interruptions observed upon arrival}) \end{cases} \tag{4.34}$$

where T_{RD_1}, T_{RD_2}, and T_{RD_3} are the remaining system downtimes when the server is down due to one, two, or three simultaneous interruptions, respectively. The expressions for these scenarios illustrated in Figures 4.7, 4.8, and 4.9, are demonstrated below:

$$T_{RD_1} = \begin{cases} Y_{r_i} & \text{w.p. } P\left(\text{No more interruptions}\right) \\ Z_{\text{Interr}(1)} + \max\left(Y_{r_i}, Y_{\text{Interr}(1)}\right) & \text{w.p. } P\left(\text{One more interruption occurs}\right) \\ Z_{\text{Interr}(1)} + Z_{\text{Interr}(2)} + \max\left(Y_{r_i}, Y_{r_{\text{Interr}(1)}}, Y_{\text{Interr}(2)}\right) & \text{w.p. } P\left(\text{Two more interruptions occur}\right) \end{cases} \quad (4.35)$$

and

$$T_{RD_2} = \begin{cases} \max\left(Y_{r_i}, Y_{r_j}\right) & \text{w.p. } P\left(\text{No more interruptions}\right) \\ Z_{\text{Interr}(1)} + \max\left(Y_{r_i}, Y_{r_j}, Y_{\text{Interr}(1)}\right) & \text{w.p. } P\left(\text{One more interruption occurs}\right) \end{cases} \quad (4.36)$$

and

$$T_{RD_3} = \max\left(Y_{r_i}, Y_{r_j}, Y_{r_l}\right) \quad (4.37)$$

where i, j, and l (each, $\{1, \ldots, k\}$) are the interruptions observed by an arriving customer, and Interr(m) is the mth occurring interruption following the arrival.

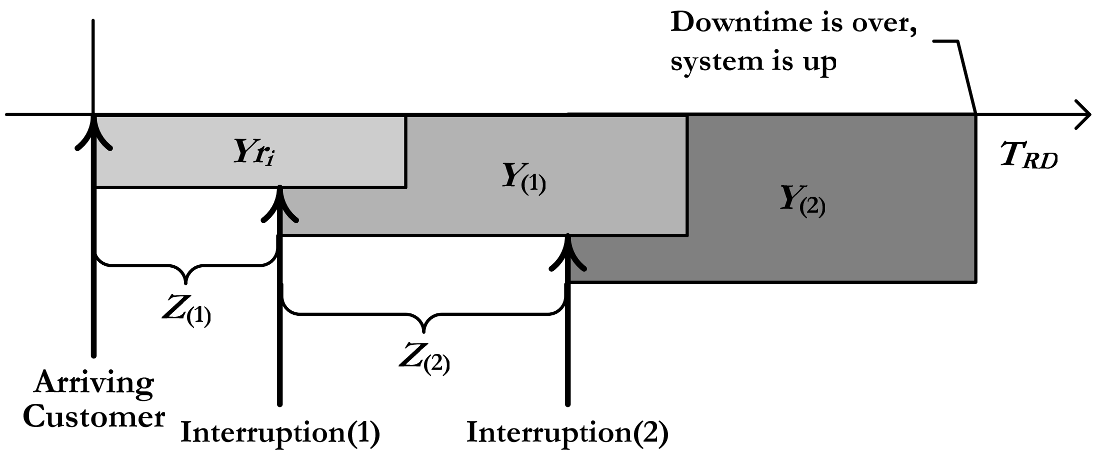

Figure 4.7 T_{RD} if an interruption is observed upon arrival and other interruptions follow

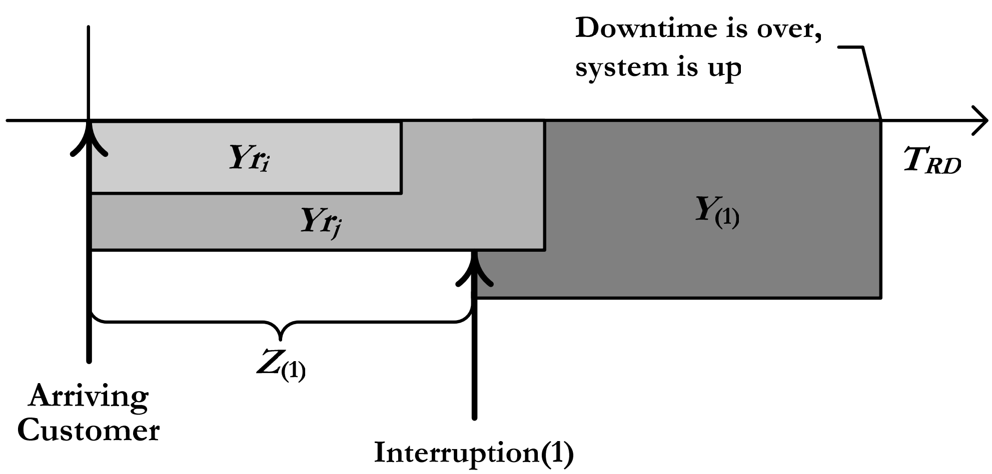

Figure 4.8 T_{RD} if the server is down due to two interruptions upon arrival and another follows

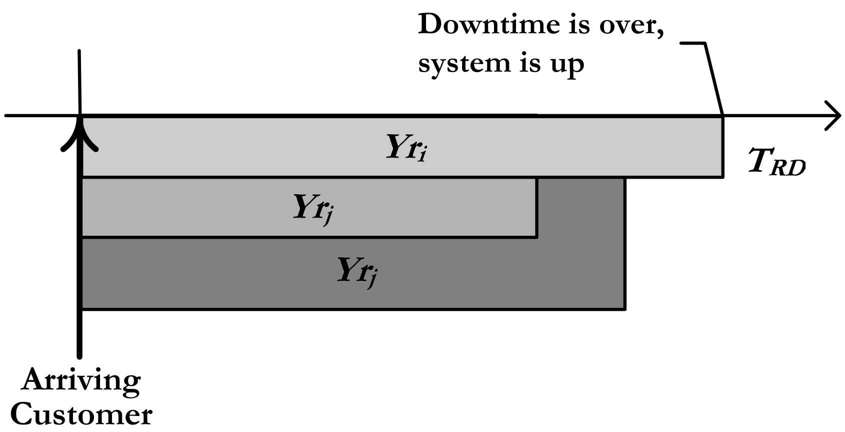

Figure 4.9 T_{RD} if the server is down due to three interruptions upon arrival

Furthermore, the probability that an arriving customer finds the server down due to interruption type i $\left(i = 1,\ldots,k\right)$, $P_{d,i}$ is defined by

$$P_{d,i} = \frac{E\left[Y_i\right]}{E\left[Y_i\right] + \frac{1}{\delta_i}}. \tag{4.38}$$

Thus, we obtain the expression for the expected remaining system downtime, $E[T_{RD}]$, shown in (4.39).

$$
\begin{aligned}
E\left[T_{RD}\right]=\sum_{i=1}^{k}&\begin{bmatrix} P_{d,i}\left(\prod_{\substack{m=1\\ m\neq i}}^{k}\left(1-P_{d,m}\right)\right)\begin{bmatrix} P\left(Y_{r_i}\le\min\left(\mathcal{Z}\text{-}\{i\}\right)\right)E\left[Y_{r_i}\mid Y_{r_i}\le\min\left(\mathcal{Z}\text{-}\{i\}\right)\right] \\ +\sum_{\substack{h=1\\ h\neq i}}^{k}P\left(Z_h\le\min\left(Y_{r_i},\mathcal{Z}\text{-}\{i\}\right)\right)\begin{bmatrix} E\left[Z_h\mid Z_h\le\min\left(Yr_i,\mathcal{Z}\text{-}\{i\}\right)\right] \\ +\left[P\left(\max(Y_{r_i},Y_h)\le\min\left(\mathcal{Z}\text{-}\{i,h\}\right)\right)\times E\left[\max(Y_{r_i},Y_h)\mid\max(Y_{r_i},Y_h)\le\min\left(\mathcal{Z}\text{-}\{i,h\}\right)\right]\right] \\ +\sum_{\substack{l=1\\ l\neq h\neq i}}^{k}\times\begin{bmatrix} P\left(Z_l\le\min\left(\max(Y_{r_i},Y_h),\mathcal{Z}\text{-}\{i,h,l\}\right)\right) \\ \begin{bmatrix} +\left(P\left(Y_{r_i}>\max(Y_{r_h},Y_l)\right)\times\begin{pmatrix} E\left[Z_l\mid Z_l\le\min\left(Y_{r_i},\mathcal{Z}\text{-}\{i,h,l\}\right)\right] \\ +E\left[Y_{r_i}\mid Y_{r_i}>\max(Y_{r_h},Y_l)\right]\end{pmatrix}\right) \\ +\left(P\left(Y_{r_h}>\max(Y_{r_i},Y_l)\right)\times\begin{pmatrix} E\left[Z_l\mid Z_l\le\min\left(Y_{r_h},\mathcal{Z}\text{-}\{i,h,l\}\right)\right] \\ +E\left[Y_{r_h}\mid Y_{r_h}>\max(Y_{r_i},Y_l)\right]\end{pmatrix}\right) \\ +\begin{pmatrix} P\left(Y_l>\max(Y_{r_i},Y_{r_h})\right) \\ \times\begin{pmatrix} E\left[Z_l\mid Z_l\le\min\left(\max(Y_{r_i},Y_h),\mathcal{Z}\text{-}\{i,h,l\}\right)\right] \\ +E\left[Y_l\mid Y_l>\max(Y_{r_i},Y_{r_h})\right]\end{pmatrix}\end{pmatrix}\end{bmatrix}\end{bmatrix}\end{bmatrix}\end{bmatrix}\end{bmatrix} \\
&+\sum_{i=1}^{k-1}\begin{bmatrix} P_{d,i}\sum_{h=i+1}^{k}\begin{bmatrix} P_{d,h}\left(\prod_{\substack{m=1\\ m\neq i\neq h}}^{k}\left(1-P_{d,m}\right)\right)\begin{bmatrix} P\left(\max(Y_{r_i},Y_{r_h})\le\min\left(\mathcal{Z}\text{-}\{i,h\}\right)\right)\times E\left[\max(Y_{r_i},Y_{r_h})\middle|\max(Y_{r_i},Y_{r_h})\le\min\left(Z-\{i,h\}\right)\right] \\ +\sum_{\substack{j=1\\ j\neq h\neq i}}^{k}\times\begin{bmatrix} P\left(Z_l\le\min\left(\max(Y_{r_i},Y_{r_h}),\mathcal{Z}\text{-}\{i,h,l\}\right)\right) \\ \begin{bmatrix} P\left(Y_{r_i}>\max(Y_{r_h},Y_l)\right)\left(E\left[Z_l\mid Z_l\le\min\left(Y_{r_i},Z-\{i,h\}\right)\right]+E\left[Y_{r_i}\mid Yr_i>\max(Y_{r_h},Y_l)\right]\right) \\ +P\left(Y_{r_h}>\max(Y_{r_i},Y_l)\right)\left(E\left[Z_l\mid Z_l\le\min\left(Y_{r_h},Z-\{i,h\}\right)\right]+E\left[Y_{r_h}\mid Y_{r_h}>\max(Y_{r_i},Y_l)\right]\right) \\ +P\left(Y_l>\max(Y_{r_i},Y_{r_h})\right)\begin{pmatrix} E\left[Z_l\mid Z_l\le\min\left(\max(Y_{r_i},Y_{r_h}),Z-\{i,h\}\right)\right] \\ +E\left[Y_l\mid Y_l>\max(Y_{r_i},Y_{r_h})\right]\end{pmatrix}\end{bmatrix}\end{bmatrix}\end{bmatrix}\end{bmatrix}\end{bmatrix} \\
&+\sum_{i=1}^{k-2}\left[P_{d,i}\sum_{h=i+1}^{k-1}\left[P_{d,h}\left(\sum_{l=h+1}^{k}\left[P_{d,l}\left(\prod_{\substack{m=1\\ m\neq i\neq h\neq l}}^{k}\left(1-P_{d,m}\right)\right)E\left[\max(Y_{r_i},Y_{r_h},Y_{r_l})\right]\right]\right)\right]\right]
\end{aligned}
\tag{4.39}
$$

4.4.4 NUMERICAL RESULTS

In this section, the accuracy of the approximation method for systems with possibly simultaneous interruptions is evaluated by comparing its results with the results of a simulation model representing the queueing system under discussion in a number of different scenarios. The simulation model is developed using the ARENA© simulation tool. The simulated results were obtained from 10 replications, each simulating 3.5 million customers.

The expected service completion time, $E[C]$, and the expected waiting time of customers in the queue, $E[W]$, are estimated.

In addition, we present the impact of a change in different system parameters such as service time variability, downtime variability, system utilization, downtime probability, and number of interruptions on $E[C]$ and $E[W]$ in different scenarios.

We use the following common assumptions for all scenarios:

- Poisson customer arrivals
- Exponential times to interruption

© ARENA is a trademark of Rockwell software.

We conduct four sets of experiments changing the following key variables:

i. Cv^2 of service time

ii. Cv^2 of downtime

iii. System utilization ($P(B)$)

iv. Downtime probability (P_d)

v. Number of interruptions (k)

In each experiment, we vary one parameter at a time while keeping all the others invariant at their base values as shown in Table 4.4, where the shaded areas indicate the base values.

Table 4.4 Parameters used in experiments in the simultaneous interruptions case

PARAMETER	VALUES				
Cv^2(Service Time)	0	0.25	3		
Cv^2(Downtime)	0.25	1	3		
System Utilization ($P(B)$)	60%	70%	80%	90%	
Downtime Probability (P_d)	5%	10%	15%	20%	25%
Number of Interruptions (k)	4	5	6		

4.4.4.1 IMPACT OF SERVICE TIME VARIABILITY

As seen in Figure 4.10, the average waiting time of a customer, $E[W]$, increases as the squared coefficient of variation of the service time, $Cv_S^{\,2}$, increases.

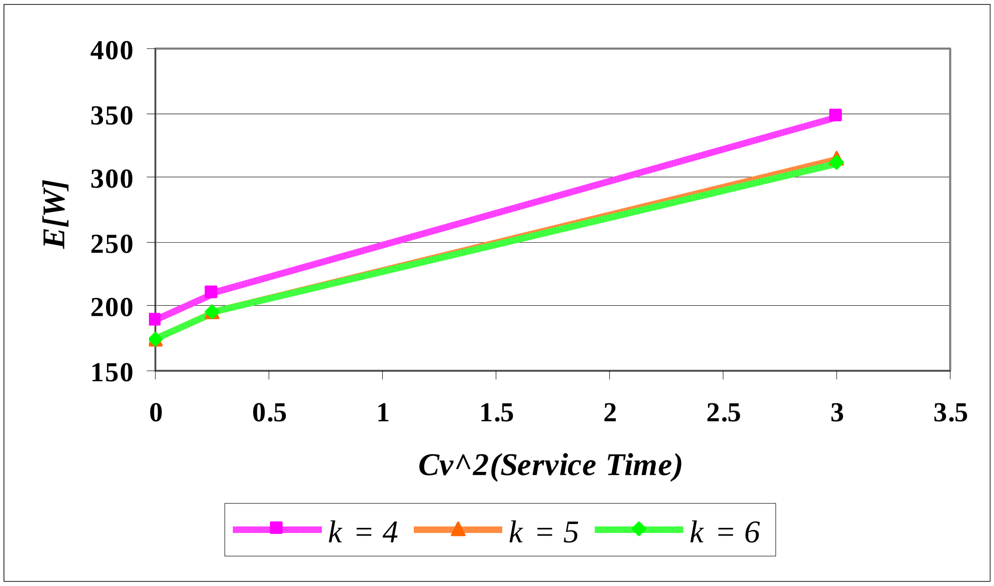

Figure 4.10 Impact of $Cv_S^{\ 2}$ on $E[W]$ in the simultaneous interruptions case

The detailed results obtained by changing $Cv_S^{\ 2}$ and the number of interruptions, *k*, are shown in Table 4.5, including relative error.

The average service completion time decreases as the service time variability increases. This is due to the decrease in the probability that the service of a customer is stopped by any of the interruptions, $P\left(Z_i \leq \min\left(S, \mathcal{Z}\text{-}\{i\}\right)\right)$ for $i = 1, \ldots, k$, as seen in Figure 4.11.

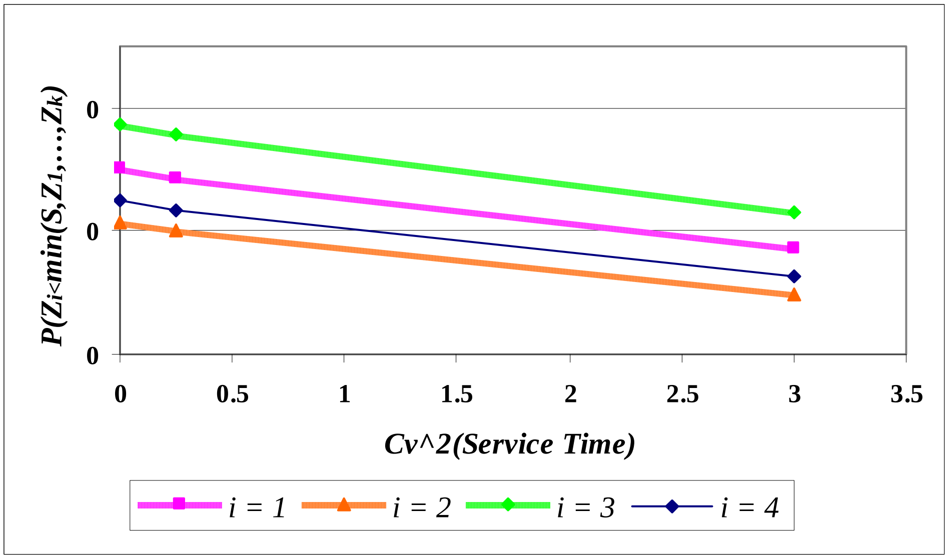

Figure 4.11 Impact of $Cv_S^{\ 2}$ on $P\left(Z_i \le \min\left(S, \mathcal{Z}\text{-}\{i\}\right)\right)$ for $i = 1, \ldots, k$

We observe that the error for the completion time remains below 0.1% as we increase the squared coefficient of variation of the service time, $Cv_S^{\ 2}$, from 0 to 3, and the number of interruptions, k, from 4 to 6. Furthermore, the error for the average waiting time of a customer is less than or equal to 2% for all the values of $Cv_S^{\ 2}$ and k.

Table 4.5 $E[C]$ and $E[W]$ in the simultaneous interruptions case when changing $Cv_S^{\,2}$

k	***Cv²(S)***	***E[C]***			***E[W]***		
		Analytical	**Simulation**	**Error**	**Analytical**	**Simulation**	**Error**
4	0 (Det.)	27.0009	27.0182	0.0640	189.3527	191.0200	0.8728
	0.25 (4-Erlang)	26.4861	26.4968	0.0404	210.6862	211.1300	0.2102
	3 (2-HyperEx)	22.6271	22.6542	0.1196	346.9512	344.4700	0.7203
	AVERAGE ERROR			0.0747	AVERAGE ERROR		0.6011
5	0 (Det.)	27.0944	27.1195	0.0926	175.1370	178.7900	2.0432
	0.25 (4-Erlang)	26.4853	26.5040	0.0706	196.1690	198.9100	1.3780
	3 (2-HyperEx)	22.1745	22.1908	0.0735	314.3800	311.4800	0.9310
	AVERAGE ERROR			0.0789	AVERAGE ERROR		1.4507
6	0 (Det.)	26.9235	26.9454	0.0813	175.1898	177.0200	1.0339
	0.25 (4-Erlang)	26.2852	26.2986	0.0510	195.8472	197.2500	0.7112
	3 (2-HyperEx)	21.8578	21.8722	0.0658	312.2176	307.5800	1.5078
	AVERAGE ERROR			0.0660	AVERAGE ERROR		1.0843

4.4.4.2 IMPACT OF DOWNTIME VARIABILITY

As the squared coefficient of variation of the downtime, $Cv_Y^{\,2}$**,** increases, so does the average waiting time of a customer due to higher variability of the downtimes as seen in Figure 4.12. On the other hand, $E[W]$ decreases in general when the number of interruptions, *k*, increases.

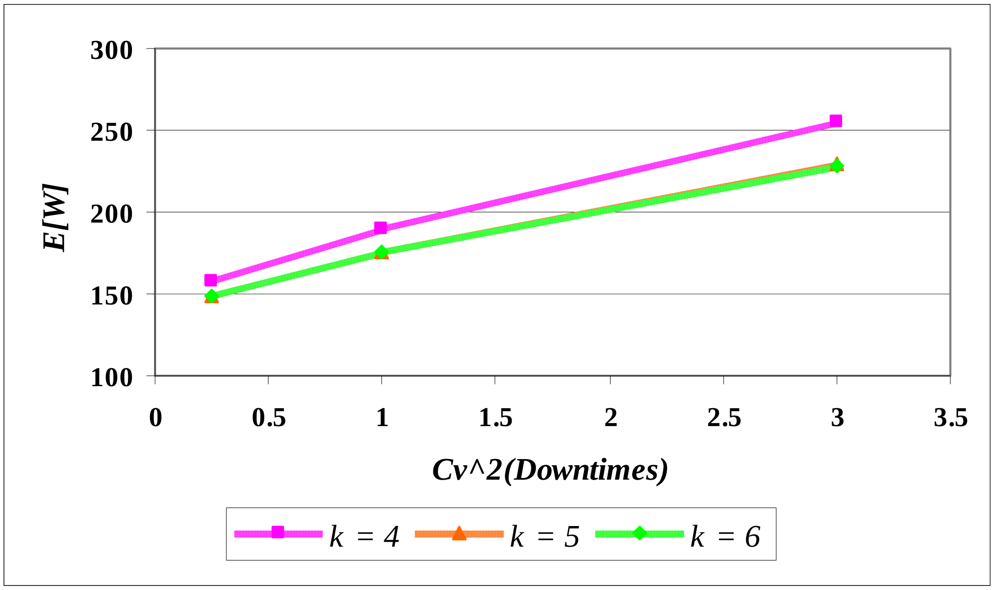

Figure 4.12 Impact of Cv_Y^2 on $E[W]$ in the simultaneous interruptions case

The detailed analytical and simulated results obtained by changing $Cv_{Y_i}^{\;2}$ for $i = (1, \ldots, k)$ and the number of interruptions, *k*, are shown in Table 4.6. The service completion time, $E[C]$, is not affected by the change in downtime variability.

In addition, we see that the error for $E[C]$ remains below 1% as we increase the squared coefficient of variation of the downtime, $Cv_{Y_i}^{\;2}$ for $i = (1, \ldots, k)$, from 0.25 to 3, and the number of interruptions, *k*, from 4 to 6. The error for $E[C]$ increases in general as the downtime variability increases.

Furthermore, the error for the average waiting time of a customer, $E[W]$, is less than 5% for all the values of $Cv_{Y_i}^{\;2}$ and *k*, and it increases in general as the downtime variability increases. Also, the average error for the $E[C]$ across different ${Cv_{Y_i}}^2$ increases as the number of interruptions increases. On the other hand, the average error for the $E[W]$ across different ${Cv_{Y_i}}^2$ decreases as the number of interruptions increases.

Table 4.6 $E[C]$ and $E[W]$ in the simultaneous interruptions case when changing ${Cv_Y}^2$

k	***Cv²(Y)***	***E[C]***			***E[W]***		
		Analytical	**Simulation**	**Error**	**Analytical**	**Simulation**	**Error**
4	0.25 (4-Erlang)	26.9969	27.0164	0.0722	157.916	159.13	0.7631
	1 (Expo)	27.0009	27.0182	0.0640	189.353	191.02	0.8728
	3 (2-HyperEx)	27.1325	27.0097	0.4547	254.666	266.02	4.2683
			AVERAGE ERROR	0.1970		AVERAGE ERROR	1.9681
5	0.25 (4-Erlang)	27.0885	27.1108	0.0823	149.312	151.28	1.3011
	1 (Expo)	27.0944	27.1195	0.0926	175.137	178.79	2.0432
	3 (2-HyperEx)	27.2379	27.1018	0.5022	229.292	233.99	2.0079
			AVERAGE ERROR	0.2257		AVERAGE ERROR	1.7841
6	0.25 (4-Erlang)	26.9167	26.9386	0.0813	149.196	150.36	0.7739
	1 (Expo)	26.9235	26.9454	0.0813	175.19	177.02	1.0339
	3 (2-HyperEx)	27.0817	26.9379	0.5338	228.249	235.31	3.0007
			AVERAGE ERROR	0.2321		AVERAGE ERROR	1.6028

4.4.4.3 IMPACT OF SYSTEM UTILIZATION

As seen in Figure 4.13, the average waiting time of a customer, $E[W]$**,** increases as the system utilization, $P(B)$, increases.

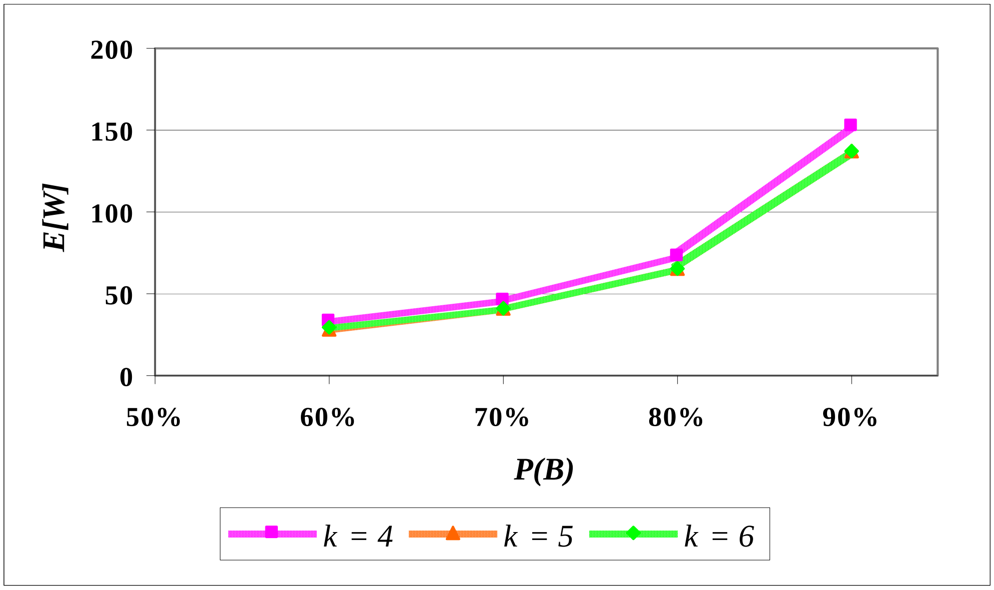

Figure 4.13 Impact of $P(B)$ on $E[W]$ in the simultaneous interruptions case

According to the detailed results shown in Table 4.7, the system utilization does not have any impact on the service completion time, $E[C]$.

Furthermore, the error for $E[C]$ remains below 0.1% as we increase the system utilization, $P(B)$, from 60% to 90%, and the number of interruptions, k, from 4 to 6. Also, the error for the average waiting time of a customer is less than 1% for all values of $P(B)$ and k.

Table 4.7 $E[C]$ and $E[W]$ in the simultaneous interruptions case when changing $P(B)$

k	***P(B)***	***E[C]***			***E[W]***		
		Analytical	**Simulation**	**Error**	**Analytical**	**Simulation**	**Error**
4	60%	17.753	17.7585	0.031	32.7687	32.9035	0.4097
	70%	17.753	17.7692	0.0912	46.1438	46.4959	0.7573
	80%	17.753	17.7603	0.0411	72.8926	73.2327	0.4644
	90%	17.753	17.7586	0.0315	153.1296	153.76	0.41
			AVERAGE ERROR	0.0546		AVERAGE ERROR	0.5439
5	60%	17.582	17.5933	0.0642	28.8392	29.0391	0.6884
	70%	17.582	17.5954	0.0762	40.8889	41.2482	0.8711
	80%	17.582	17.5931	0.0631	64.9872	65.5575	0.8699
	90%	17.582	17.591	0.0512	137.3342	138.53	0.8632
			AVERAGE ERROR	0.0635		AVERAGE ERROR	0.8681
6	60%	17.5117	17.5179	0.0354	28.9063	29.0257	0.4114
	70%	17.5117	17.5226	0.0622	40.9789	41.2734	0.7135
	80%	17.5117	17.5257	0.0799	65.1002	65.7865	1.0432
	90%	17.5117	17.5189	0.0411	137.4695	138.49	0.7369
			AVERAGE ERROR	0.0611		AVERAGE ERROR	0.8312

4.4.4.4 IMPACT OF DOWNTIME PROBABILITY

Figure 4.14 shows an increasing trend in the average waiting time of a customer, $E[W]$, as the downtime probability of the system increases. Also, $E[W]$ decreases as the number of interruptions, *k*, increases.

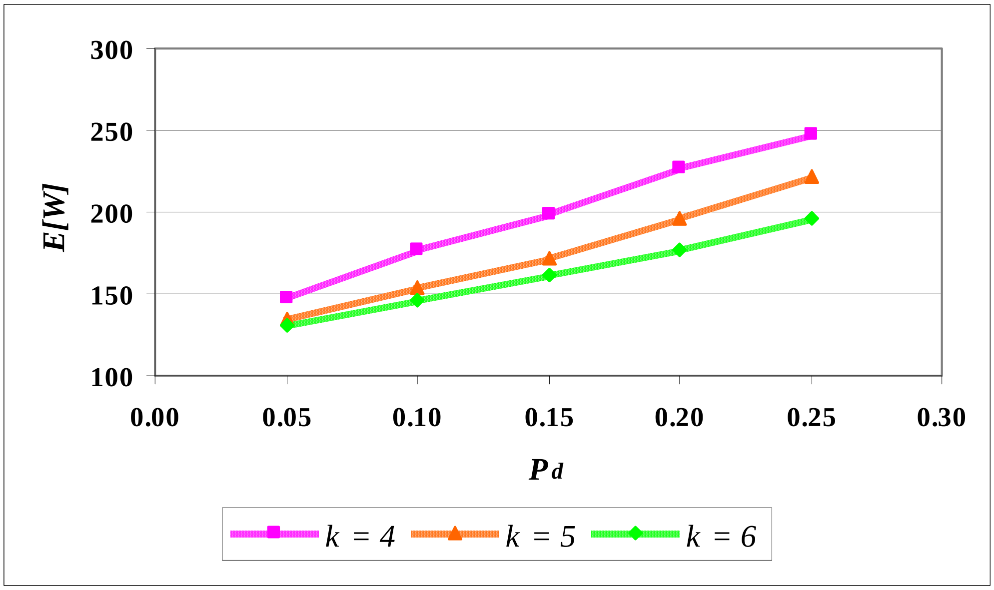

Figure 4.14 Impact of P_d on $E[W]$ in the simultaneous interruptions case

According to the detailed results shown in Table 4.8

Table 4.8, the service completion time, $E[C]$, increases as the downtime probability, P_d, increases.

Furthermore, the error for $E[C]$ remains below 0.5% as we increase the downtime probability, P_d, from 5% to 25%, and the number of interruptions, *k*, from 4 to 6. Also, the error for the average waiting time of a customer is less than 5% for these values of P_d and *k*.

Table 4.8 $E[C]$ and $E[W]$ in the simultaneous interruptions case when changing P_d

k	P_d	***E[C]***			***E[W]***		
		Analytical	**Simulation**	**Error**	**Analytical**	**Simulation**	**Error**
4	5%	26.9333	26.9358	0.0093	147.4216	147.39	0.0214
	10%	27.8625	27.8602	0.0083	177.5231	177.3	0.1258
	15%	28.7298	28.7308	0.0035	198.8244	199.46	0.3187
	20%	29.5912	29.6152	0.081	226.4288	229.83	1.4799
	25%	30.4375	30.4794	0.1375	247.4625	253.9	2.5354
	AVERAGE ERROR			0.074	AVERAGE ERROR		1.4447
5	5%	26.8159	26.8149	0.0037	134.73	134.31	0.3127
	10%	27.7337	27.7265	0.026	154.4704	154.15	0.2078
	15%	28.5801	28.5831	0.0105	171.6895	172.95	0.7288
	20%	29.7593	29.772	0.0427	195.7991	197.95	1.0866
	25%	31.02	31.0691	0.158	221.8111	228.38	2.8763
	AVERAGE ERROR			0.0704	AVERAGE ERROR		1.5639
6	5%	26.6692	26.6681	0.0041	131.1974	131.92	0.5478
	10%	27.3995	27.3985	0.0036	146.1686	146.83	0.4505
	15%	28.1682	28.1704	0.0078	161.3348	162.02	0.4229
	20%	28.9975	29.0149	0.06	177.0922	178.6	0.8442
	25%	30.1508	30.1948	0.1457	196.4725	202.84	3.1392
	AVERAGE ERROR			0.0712	AVERAGE ERROR		1.4688

4.4.5 CONCLUSION

In this chapter, we have considered a single-server, single-class queueing system subject to multiple types of independent interruptions motivated by the transit vessel entrances in the Istanbul Strait. Since the complexity of the system makes the exact analysis difficult, an analytical model is developed to approximate the expected service completion time and the expected waiting time in the aforementioned queueing model.

The numerical results show that the approximation works reasonably well for the $E[C]$ and $E[W]$ for a wide range of system parameters. In addition, we conclude that it is not the service time, arrival process, times-to-interruption, or the number of interruptions, but the variability of downtime processes that determines the accuracy of the approximation.

We also analyze the impact of various key parameters on the system behavior. We observe that an increase in any of the system parameters cause an increase in the expected waiting time of a customer in the queue. However, a similar increase in the service completion time is only seen when the downtime probability increases. On the other hand, $E[C]$ decreases as the service time variation increases due to the decrease in the probability that the service of a customer is stopped by an interruption, e.g. $P\left(Z_i \leq \min\left(S, \mathcal{Z}\text{-}\{i\}\right)\right)$ for $i = 1,\ldots,k$. In addition, $E[C]$ is not affected by any change in the downtime variability or system utilization.

The main contribution of our work is that contrary to the previous studies on queueing models with multiple interruptions, in our model the downtime experienced by a customer is not simply the sum of the downtimes of all possible interruptions during its service. Interruption types are operation-independent and they may occur at anytime, and their downtime processes start immediately after their occurrences. Therefore, the expected waiting time of a customer in the queue, $E[W]$, involves complicated scenarios of common downtimes rather than a simple summation. Thus, it requires an involved approach including approximations.

The main use of this model will be in predicting the impact of various system parameters on the congestion level in waterway entrances. In particular, the impact of various closure profiles (due to construction projects or traffic management strategies) and the impact of an increase in vessel traffic on vessel delays are crucial in long range capacity planning in waterways.

From a critical standpoint, even though we assume exponential time to interruptions, in reality some interruptions may have more regularity such as nighttime traffic closures.

4.5 CASE OF THE ISTANBUL STRAIT

In the case of Istanbul, transit vessels arrive randomly at north and south entrances of the Strait, and wait in queues until they are allowed to start their passage. We assume that vessels arrive from a Poisson process with rate λ per unit time and that there is only one class of arrivals in the system. Poisson arrivals assumption is consistent with the Istanbul Strait arrival data due to superposition of several independent vessel arrival streams.

Vessels enter the Strait one at a time at a given entrance. After a vessel enters the Strait, a second vessel starts its passage as soon as the first one traverses the minimum required distance between two consecutive vessels. Therefore, the time it takes for a vessel to traverse the required distance is considered as the service time. This is typically a short period of time due to the distance to be maintained between consecutive vessels, that is about 0.5-1 nautical miles. The practice in Istanbul is such that the service time is roughly 2-3 minutes.

Traffic may be interrupted due to poor visibility, high currents, storms, and other factors such as lane closures caused by vessel accidents. Once a vessel enters the Strait, it continues its passage even if conditions develop, which may interrupt the traffic. However, the next vessel waiting in the queue cannot enter the Strait until conditions return to normal. Vessels generally do not stop in the Strait since they may create a high risk situation for other vessels and the environment.

We have obtained the vessel arrival data and traffic stoppage data for 2006 from the Istanbul Strait Vessel Traffic Services (VTS). Data suggests that the inter-arrival times are Poisson distribution with rate $\lambda = 1/9.53$. There are four main interruption types in the 2006 data: poor visibility, Marmaray construction project, sporting events, and emergencies. The times to failure of these stoppages were fit into Exponential distributions. The downtimes, on the other hand, were fit into phase-type distributions using two moments. Table 4.9 shows the distributions for the times to interruptions and down times.

Table 4.9 Interruption times

	Interruption Times (min.)	
Interruption type	**Time to Interruptions (Z)**	**Down Times (Y)**
Poor Visibility	EXPO(14800)	H-2(0.0009,0.0033)
Marmaray	EXPO(636)	H-2(0.0001,0.0025)
Sporting Events	EXPO(33400)	H-2(0.0022,0.0079)
Emergency	EXPO(33000)	H-2(0.00445,0.0096)

We have tested two alternatives for the service time, *S*, that is uniform between 2 and 3 minutes and fixed 2.25 minutes. We have obtained the average waiting time, $E[W]$, using (5) and the above distributions. The result is compared to the average waiting time recorded in reality and the results are shown in Table 4.10.

Table 4.10 Accuracy of the approximation for estimating $E[W]$ in the Istanbul Strait

E[W] (min.)				
Real System	**S ~ UNIF(2,3)**		**S = 2.25**	
	Analytic	**% Rel. Error**	**Analytic**	**% Rel. Error**
1021	1024.64	0.3567	1024.97	0.3886

The results shown in Table 4.10 are approximate solutions since the number of interruptions, *k*, is greater than 3 $(k = 3 > 4)$. This comparison indicates that the proposed analytical model has a high degree of accuracy in approximating the average vessel waiting time in the Istanbul Strait.

5 MULTI-CLASS QUEUES WITH MULTIPLE TYPES OF CLASS-INDEPENDENT INTERRUPTIONS

In this chapter, we generalize the single-class queueing model subject to multiple types of operation-independent and possibly simultaneous interruptions to a multi-class queueing model with a non-preemptive priority structure.

In queueing systems where different types of customers are served, the question of which customer to select once the server is idle is crucial. Some customers may be more important than others, and therefore should be served first. This is especially true for vessel traffic at waterway entrances. A case in point is the Istanbul Strait. Different types of transit vessels arrive randomly at the northern and southern entrances of the Strait, and wait in queues until they are allowed to start their passage. Vessels are scheduled based on the priorities assigned to them. For example, passenger vessels always have the right of way so they experience the shortest waiting time among all the vessel classes. Such queueing systems where each type of customer has a relative priority for service are called **priority queues**; and the different types of customers are called **priority classes**.

In this chapter, we propose a queueing analysis to estimate the average waiting times of different types of vessels at the entrance points of waterways. These problems can be studied as queues with multiple classes of customers and multiple types of service interruptions, as discussed in detail in Section 5.1.

5.1 A QUEUEING MODEL

In waterway entrances, incoming vessels form customer arrival streams, which can be identified by the time intervals between consecutive arrivals. We assume that class *j* customers arrive from a Poisson process with rate λ_j per unit time and that there are *n* classes $(1,\ldots,n)$ of customers receiving service at the system.

After a vessel enters the Strait, a second vessel starts its passage as soon as the first one traverses the minimum required distance between two consecutive vessels. Therefore, the time it takes for a vessel to traverse the required distance before the next vessel may enter the Strait is considered the *service time* of a customer in the queueing model, since a second vessel can enter the Strait at the end of this time period. This is typically a short period of time due to the fact that the distance to be maintained between consecutive vessels is about 0.5-1 nautical miles. The practice in Istanbul results in about 2.5 minutes. In this study, we assume that the service time of a class *j* customer S_j has an arbitrary distribution, and the multiple classes of customers are served according to the **non-preemptive** priority discipline where Class *i* has the highest priority while the class *n* has the lowest. When the server becomes idle, a customer of the *i*th class is taken to service prior to the customer of a *j*th class for $i < j$ even if the class *j* customer arrives before a class *i* customer. Within each priority class, the "first come, first served" policy determines the order of service. The non-preemptive discipline ensures that the service integrity of a lower priority customer is maintained, while keeping higher priority customers that have arrived after the current service has started in the queue. In practice, the priority structure is decided upon by the resident Vessel Traffic Services system and it may change from one location to another.

Service may be interrupted and the waterway may be closed due to poor visibility, storms, high currents or other random stoppages. We assume that the server is subject to *k* different types of operation-independent, non-identical, possibly simultaneous interruptions. The interruptions are independent and the downtimes do not affect each other. That is, it is possible to have a number of downtimes progressing simultaneously. A *down cycle* starts when an interruption occurs during an uptime and ends when the system becomes operational again. Since the interruptions are operation-independent, the server can also be down when it is idle as mentioned in (Altıok 1997).

Also, we assume that the interruption processes are **class-independent**, which indicates that all priority classes are affected by all the interruption types that the server is subjected to. Typically, the vessel that is given the go-ahead and proceeding to the entrance does not get interrupted even if a condition that would normally stop the traffic erupts. That is, the current customer is not affected by an interruption that started during the current service. However, that interruption would stop the following vessels from entering the Strait. We assume that time to interruption of type *i*, Z_i, follows an exponential distribution with rate δ_i, while its downtime, Y_i, has an arbitrary distribution. A point of observation is that due to the nature of closures in waterways, the downtimes are much longer than the service times.

Thus, the vessel traffic at the entrance points of waterways may very well be considered as a multi-class priority queueing model with a single-server, and an infinite queue, which is subject to multiple types of possibly simultaneous interruptions.

In this dissertation, we propose an approximation method to obtain the expected waiting time of different classes of customers in the queue using the "completion-time approach". The *service completion time*, C_j, is defined as the time interval between the service start time of a class *j* customer, which corresponds to a vessel entry, and the time the next customer may start its service, representing the instance the next vessel is allowed to enter. It is equal to the service time if no interruptions occur. In case of interruptions, the service completion time is longer than the service time due to downtimes since the service is available to the next customer in line only after the system becomes operational.

Taking into account the three facts that the aforementioned service times are much shorter than downtimes, the vessels continue their passage during the interruption, and the remaining service times are over by the time the down cycle ends, the queueing model is equivalent to one with scrapping where the customer is assumed to be scrapped upon an interruption. This is only a modeling convenience to keep track of the time until the first interruption occurs, which is referred to as the *actual service time* of a customer *j*, S_{a_j}, in the model. In the following sections, we focus our attention to the queueing system and refer to vessels as customers.

5.2 WAITING TIME

Let us consider a single-server queueing system with *n* classes of customers. Let W_j be the waiting time of a class *j* customer until its service starts. A customer, regardless of its priority, observes N_j class *j* customers waiting in the queue at the time of its arrival.

If the server is busy upon arrival, an arriving class 1 customer waits until the service time of the current customer is completed. On the other hand, if the class 1 customer arrives when the server is down, it waits until it is up again. The arriving customer also has to wait until all the class 1 customers that arrived earlier are served, and the downtimes of the possible interruptions that may occur during their services are completed. Other priority classes do not interfere with this class, since it has the highest priority. Thus, the waiting time of an arriving class 1 customer can be expressed as follows:

$$E[W_1] = E\left[N_1\right]E\left[C_1\right] + E\left[C_r\right] + E\left[T_{RD}\right] \tag{5.1}$$

which, coupled with $E\left[N\right] = \lambda E\left[W\right]$ gives us

$$E[W_1] = \frac{E[C_r] + E[T_{RD}]}{\left(1 - \lambda_1 E[C_1]\right)}. \tag{5.2}$$

where C_1, C_r, and T_{RD} represent the service completion time of a class 1 customer, the remaining service completion time of the current customer found in the server upon arrival and the total remaining downtime of the system when it is down upon arrival, respectively.

A class 2 customer first waits until the current customer leaves the server if the server is busy upon arrival. Then, it waits until all the class 1 and class 2 customers that arrived earlier are served and the downtimes of the possible interruptions that may occur during their services are completed. It also waits for the class 1 customers arriving during its delay in the queue. The customer may also have to wait for the remaining system downtime if the server is down upon its arrival. Thus, using the expected length of the busy period as presented in [Altıok, 1997], we can write

$$E[W_2] = \frac{E\left[N_1\right]E\left[C_1\right] + E\left[N_2\right]E\left[C_2\right] + E\left[C_r\right] + E\left[T_{RD}\right]}{1-\rho_1} \tag{5.3}$$

with $\rho_1 = \lambda_1 E\left[C_1\right]$ resulting in

$$E\left[W_2\right] = \frac{\lambda_1 E[W_1]E\left[C_1\right] + E[C_r] + E\left[T_{RD}\right]}{1-\lambda_1\, E\left[C_1\right] - \lambda_2\, E\left[C_2\right]}\,. \tag{5.4}$$

In a similar manner, we obtain the expected waiting time of a class j customer $\left(j = 2,\ldots,n\right)$ $E[W_j]$,

$$E\left[W_j\right]=\frac{\sum_{m=1}^{j-1}\left(\lambda_m E[W_m]E\left[C_m\right]\right)+E[C_r]+E\left[T_{RD}\right]}{1-\sum_{m=1}^{j}\left(\lambda_m\, E\left[C_m\right]\right)}. \tag{5.5}$$

where $E[C_j]$ can be viewed as the service time of a class *j* customer in an imaginary server that does not experience interruptions during service time. Yet, notice that this is the same type of server mentioned in Chapter 4, which experiences downtime only when it is idle. However, in this case, the server serves multiple types of customers. Recall that the service dynamics such as scrapings are hidden in the service time (the completion time process). The $\sum_{j=1}^{n}\left(\lambda_j\, E[C_j]\right)$ expression in (5.5) represents the utilization of this imaginary server, denoted by $P(B)$, which is the percentage of the time the imaginary server is busy. Note that the server is stable if and only if $P(B)=\sum_{j=1}^{n}\left(\lambda_j\, E[C_j]\right)<1$.

5.2.1 SERVICE COMPLETION TIME (C_j)

In this section, we discuss the characteristics of the service completion time of a class *j* customer, C_j, in the case of *n* priority classes and *k* class-independent interruptions. Note that C_j is identical to C discussed in Section 4.4.1 and consists of two parts; the actual service time of a class *j* customer, S_{a_j}, and the downtime experienced by that customer during its service, T_{DS_j}. We have

$$E\left[C_j\right] = E\left[S_{a_j}\right] + E\left[T_{DS_j}\right]. \tag{5.6}$$

The actual service time of a class *j* customer, S_{a_j}, is equal to its service time S_j if the server does not fail during its service. Otherwise, S_{a_j} is equal to the time to interruption. The actual service time of a class *j* customer can be expressed as follows:

$$S_{a_j} = \begin{cases} S_j & \text{w.p. } P(\text{Server does not fail during service}) \\ Z_1 & \text{w.p. } P\left(\text{Server fails during service due to interruption type } 1\right) \\ Z_2 & \text{w.p. } P\left(\text{Server fails during service due to interruption type } 2\right) \\ \vdots & \vdots \\ Z_k & \text{w.p. } P\left(\text{Server fails during service due to interruption type } k\right) \end{cases} \tag{5.7}$$

with

$$P(\text{Server does not fail during service}) = P\left(S_j \le \min\left(Z_1,\ldots,Z_k\right)\right) \tag{5.8}$$

and

$$\begin{aligned} &P\left(\text{Server fails during service due to interruption type } i\right) \\ &\qquad = P\left(Z_i \le \min\left(S_j, Z_1,\ldots,Z_{i-1},Z_{i+1},\ldots,Z_k\right)\right). \end{aligned} \tag{5.9}$$

Using (5.7), (5.8), and (5.9), we can write the following LST of the density function of the actual service time of a class *j* customer, S_{a_j}:

$$F^*_{S_{a_j}}(s) = E\left[e^{-sS_j} \middle| S_j \le \min\left(Z_1,...,Z_k\right)\right] P\left(S_j \le \min\left(Z_1,...,Z_k\right)\right)$$
$$+\sum_{i=1}^{k} E\left[e^{-sZ_i} \middle| Z_i \le \min\left(S_j, Z_1,...,Z_{i-1}, Z_{i+1},...,Z_k\right)\right] P\left(Z_i \le \min\left(S_j, Z_1,...,Z_{i-1}, Z_{i+1},...,Z_k\right)\right) \quad (5.10)$$

This can be expressed in terms of density functions:

$$F^*_{S_{a_j}}(s) = \left(\int_0^\infty e^{-sx} f_{S_j|S_j \le \min\left(Z_1,...,Z_k\right)}(x)\,dx\right) P\left(S_j \le \min\left(Z_1,...,Z_k\right)\right)$$
$$+\sum_{i=1}^{k}\left[\left(\int_0^\infty e^{-sz} f_{Z_i|Z_i \le \min\left(S_j, Z_1,...,Z_{i-1}, Z_{i+1},...,Z_k\right)}(z)\,dz\right) P\left(Z_i \le \min\left(x, Z_1,...,Z_{i-1}, Z_{i+1},...,Z_k\right)\right)\right]. \quad (5.11)$$

Under a **deterministic** service time assumption $(S = x)$, the first two moments of the actual service time are presented in (4.15) and (4.16). Also, the first two moments of S_{a_j} when the service time follows a **4-phase erlang** distribution with rate is given in Appendix F.

The expected downtime experienced by a class *j* customer during its service, $E[T_{DS_j}]$, is similar to $E[T_{DS}]$ explained in Section 4.4.1 and is presented in (5.12).

$$E\left[T_{DS_j}\right]=\sum_{i=1}^{k}\left(P\left(Z_i\le\min\left(S_j,\mathcal{Z}\text{-}\{i\}\right)\right)\left[\begin{array}{l}P\left(Y_i\le\min\left(\mathcal{Z}\text{-}\{i\}\right)\right)E\left[Y_i\mid Y_i\le\min\left(\mathcal{Z}\text{-}\{i\}\right)\right]\\
+\displaystyle\sum_{\substack{h=1\\h\ne i}}^{k}P\left(Z_h\le\min\left(Y_i,\mathcal{Z}\text{-}\{i,h\}\right)\right)\left[\begin{array}{l}E\left[Z_h\mid Z_h\le\min\left(Y_i,\mathcal{Z}\text{-}\{i,h\}\right)\right]\\
+\left[\begin{array}{l}P\left(\max(Y_{r_i},Y_h)\le\min\left(\mathcal{Z}\text{-}\{i,h\}\right)\right)\\
\times E\left[\max(Y_{r_i},Y_h)\mid\max(Y_{r_i},Y_h)\le\min\left(\mathcal{Z}\text{-}\{i,h\}\right)\right]\end{array}\right]\\
+\displaystyle\sum_{\substack{l=1\\l\ne h\ne i}}^{k}\left[\begin{array}{l}P\left(Z_l\le\min\left(\max(Y_{r_i},Y_h),\min\left(\mathcal{Z}\text{-}\{i,h,l\}\right)\right)\right)\\
\times\left[\begin{array}{l}+\left(\begin{array}{l}P\left(Y_{r_i}>\max(Y_{r_h},Y_l)\right)\\
\times\left(\begin{array}{l}E\left[Z_l\mid Z_l\le\min\left(Y_{r_i},\min\left(\mathcal{Z}\text{-}\{i,h,l\}\right)\right)\right]\\
+E[Y_{r_i}\mid Y_{r_i}>\max(Y_{r_h},Y_l)]\end{array}\right)\end{array}\right)\\
+\left(\begin{array}{l}P\left(Y_{r_h}>\max(Y_{r_i},Y_l)\right)\\
\times\left(\begin{array}{l}E\left[Z_l\mid Z_l\le\min\left(Y_h,\min\left(\mathcal{Z}\text{-}\{i,h,l\}\right)\right)\right]\\
+E[Y_{r_h}\mid Y_{r_h}>\max(Y_{r_i},Y_l)]\end{array}\right)\end{array}\right)\\
+\left(\begin{array}{l}P\left(Y_l>\max(Y_{r_h},Y_{r_i})\right)\\
\times\left(\begin{array}{l}E\left[Z_l\mid Z_l\le\min\left(\max(Y_{r_i},Y_h),\min\left(\mathcal{Z}\text{-}\{i,h,l\}\right)\right)\right]\\
+E[Y_l\mid Y_l>\max(Y_{r_h},Y_{r_i})]\end{array}\right)\end{array}\right)\end{array}\right]\end{array}\right]\end{array}\right]\end{array}\right]\right)\tag{5.12}$$

where $\mathcal{Z}\text{-}\{i,h,l\}=\left(Z_1,...,Z_{i-1},Z_{i+1},Z_{h-1},Z_{h+1},Z_{l-1},Z_{l+1},...,Z_k\right)$.

5.2.2 REMAINING SERVICE COMPLETION TIME (C_r)

The remaining service completion time of the current customer in service as observed by an arrival, C_r, is the time until the next customer (if any) may start its service. It consists of the remaining actual service time of the customer, $S_{r_{a_j}}$, and the downtime experienced by the customer during its remaining service completion time, T_{DRS_j}. In the case of *n* priority classes and *k* class-independent interruptions, an arriving customer can find a customer of any of the *n* priority classes in service. Therefore, expected remaining service completion time can be expressed as follows:

$$E[C_r] = \sum_{j=1}^{n} \rho_j \left(E[S_{r_{a_j}}] + E[T_{DRS_j}] \right) \tag{5.13}$$

where ρ_j is the probability that the arriving customer finds a class *j* customer in service at the time of its arrival.

The remaining actual service time of a class *j* customer, $S_{r_{a_j}}$, can be evaluated using (4.21).

Using arguments similar to $E[T_{DS_j}]$ in Section 4.4.2, we obtain the expression for the expected downtime experienced by a class *j* customer during its remaining service, $E[T_{DRS_j}]$, as shown in (5.14).

$$
\begin{aligned}
E[T_{DRS_j}] = \sum_{i=1}^{k} \Bigg(& P\left(Z_i \le \min\left(S_{r_j}, \mathcal{Z}\text{-}\{i\}\right)\right) \Bigg[P\left(Y_i \le \min\left(\mathcal{Z}\text{-}\{i\}\right)\right) E\left[Y_i \mid Y_i \le \min\left(\mathcal{Z}\text{-}\{i\}\right)\right] \\
& + \sum_{\substack{h=1 \\ h \ne i}}^{k} P\left(Z_j \le \min\left(Y_i, \mathcal{Z}\text{-}\{i,h\}\right)\right) \Bigg[E\left[Z_h \mid Z_h \le \min\min\left(Y_i, \mathcal{Z}\text{-}\{i,h\}\right)\right] \\
& \quad + \left[\begin{array}{l} P\left(\max(Y_{r_i}, Y_h) \le \min\left(\mathcal{Z}\text{-}\{i,h\}\right)\right) \\ \times E\left[\max(Y_{r_i}, Y_h) \mid \max(Y_{r_i}, Y_h) \le \min\left(\mathcal{Z}\text{-}\{i,h\}\right)\right] \end{array} \right] \\
& \quad + \sum_{\substack{l=1 \\ l \ne h \ne i}}^{k} \Bigg[P\left(Z_l \le \min\left(\max(Y_{r_i}, Y_h), \min\left(\mathcal{Z}\text{-}\{i,h,l\}\right)\right)\right) \\
& \qquad \times \Bigg[\left(\begin{array}{l} P\left(Y_{r_i} > \max(Y_{r_h}, Y_l)\right) \\ \times \left(\begin{array}{l} E\left[Z_l \mid Z_l \le \min\left(Y_{r_i}, \min\left(\mathcal{Z}\text{-}\{i,h,l\}\right)\right)\right] \\ + E[Y_{r_i} \mid Y_{r_i} > \max(Y_{r_h}, Y_l)] \end{array} \right) \end{array} \right) \\
& \qquad + \left(\begin{array}{l} P\left(Y_{r_h} > \max(Y_{r_i}, Y_l)\right) \\ \times \left(\begin{array}{l} E\left[Z_l \mid Z_l \le \min\left(Y_h, \min\left(\mathcal{Z}\text{-}\{i,h,l\}\right)\right)\right] \\ + E[Y_{r_h} \mid Y_{r_h} > \max(Y_{r_i}, Y_l)] \end{array} \right) \end{array} \right) \\
& \qquad + \left(\begin{array}{l} P\left(Y_l > \max(Y_{r_h}, Y_{r_i})\right) \\ \times \left(\begin{array}{l} E\left[Z_l \mid Z_l \le \min\left(\max(Y_{r_i}, Y_h), \min\left(\mathcal{Z}\text{-}\{i,h,l\}\right)\right)\right] \\ + E[Y_l \mid Y_l > \max(Y_{r_h}, Y_{r_i})] \end{array} \right) \end{array} \right) \Bigg] \Bigg] \Bigg] \Bigg] \Bigg)
\end{aligned}
\tag{5.14}
$$

where $\mathcal{Z}\text{-}\{i,h,l\} = \left(Z_1, ..., Z_{i-1}, Z_{i+1}, Z_{h-1}, Z_{h+1}, Z_{l-1}, Z_{l+1}, ..., Z_k\right)$.

5.2.3 REMAINING SYSTEM DOWNTIME (T_{RD})

In this section, we present the remaining system downtime as observed by an arriving customer. The remaining system downtime is the remaining length of a down cycle.

Since we limit the number of interruptions that can occur during a service time to three, the server may be down due to at most three different interruptions upon a customer arrival. If the system is down due to one type of interruption, one or two more types of interruptions may still occur during the down cycle. Conversely, if the system is experiencing two interruptions simultaneously, then the third may still occur during the same down cycle.

In the case of n priority classes and k class-independent interruptions, the remaining system downtime when it is down upon arrival, T_{RD}, is identical to the remaining system downtime expression presented in Section 4.4.3. Its expected value can be obtained using (4.39).

5.3 NUMERICAL RESULTS

In this section, the accuracy of the approximation method for multi-class systems with possibly simultaneous interruptions is evaluated by comparing its results to the results of a simulation model representing the queueing system under discussion in a number of different scenarios. The simulation model is developed using the ARENA© simulation tool. The simulated results were obtained from 10 replications, each simulating 3.5

million customers. The average waiting time of a class j ($j = 1, \ldots, n$) customer, $E[W_j]$, is estimated.

In addition, we present the impact of a change in different system parameters such as service time variability, downtime variability, system utilization, downtime probability, and number of interruptions on $E[C]$ and $E[W]$ in different scenarios.

We use the following assumptions common to all scenarios:

- Poisson customer arrivals
- Exponential times to interruption

We conduct six sets of experiments changing the following key variables:

i. Cv^2 of service time

ii. Cv^2 of downtime

iii. System utilization ($P(B)$)

iv. Downtime probability (P_d)

v. Number of priority classes (n)

vi. Number of interruptions (k)

In each experiment, we vary one parameter at a time while keeping all the others invariant at their base values as shown in Table 5.1. The shaded areas indicate the base values.

Table 5.1 Parameters used in experiments in the case of multiple priority classes

Parameter	**Values**				
Cv^2(Service Time)	0	0.25	3		
Cv^2(Downtime)	0.25	0.5	1	1.5	3
System Utilization ($P(B)$)	60%	70%	80%	90%	
Downtime Probability (P_d)	5%	10%	15%	20%	25%
Number of Classes (n)	3	4	5		
Number of Interruptions (k)	4	5	6		

5.3.1 IMPACT OF SERVICE TIME VARIABILITY

Figures 5.1 and 5.2 illustrate the impact of the squared coefficient of variation of the service times, Cv_S^2, on the average waiting time of a highest priority customer, $E[W_1]$, and a lowest priority customer, $E[W_5]$, respectively, where $n = 5$. Higher Cv_S^2 values result in higher expected waiting time values for both of the classes.

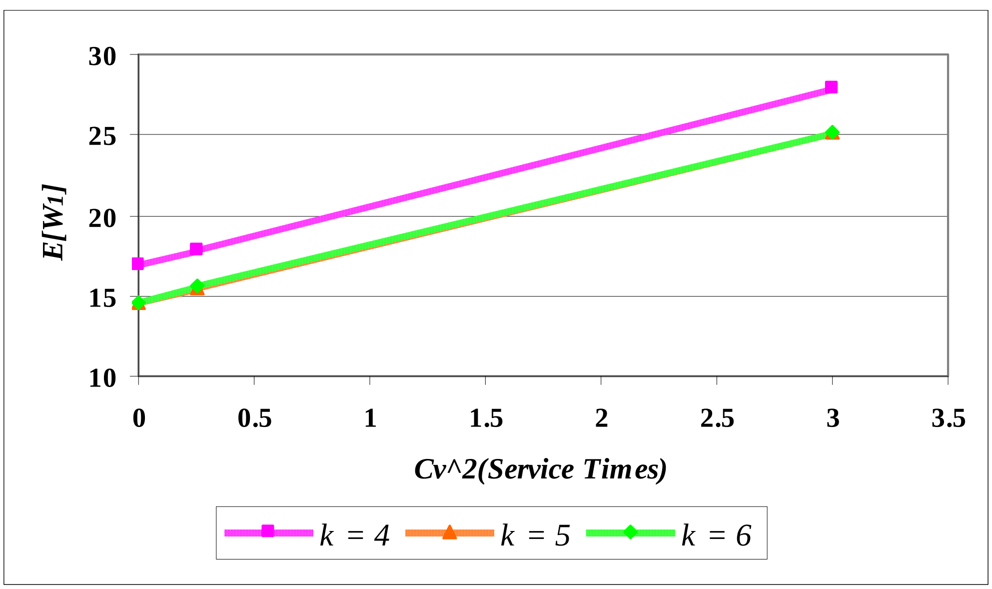

Figure 5.1 Impact of Cv_S^2 on $E[W_1]$ in the case of 5 priority classes

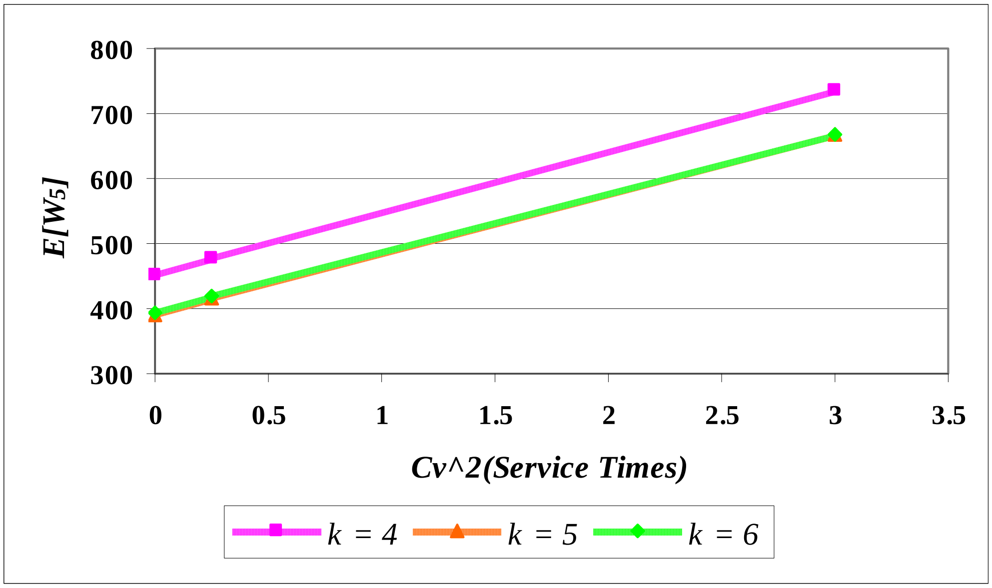

Figure 5.2 Impact of $Cv_S^{\ 2}$ on $E[W_5]$ in the case of 5 priority classes

The detailed results obtained by changing $Cv_S^{\ 2}$, the number of priority classes, *n*, and the number of interruptions, *k*, are shown in Table 5.2. The results also include the relative errors comparing the analytical and simulation results for the expected waiting time of the highest priority class, $E[W_1]$, and the lowest priority class, $E[W_n]$.

We observe that the error levels associated with $E[W_1]$ and $E[W_n]$ remain below 1% and 5%, respectively, as we increase the squared coefficient of variation of the service time, $Cv_S^{\ 2}$, from 0 to 3, the number of priority classes, *n*, from 3 to 4, and the number of interruptions, *k*, from 4 to 6.

Furthermore, the error levels do not show a distinct pattern as we increase the values of $Cv_S^{\ 2}$, *n* and *k*.

Table 5.2 $E[W_j]$ in the case of multiple priority classes when changing $Cv_S^{\ 2}$

n	k	$Cv^2(S)$	E[W1] Analytical	E[W1] Simulation	E[W1] Error	E[Wn] Analytical	E[Wn] Simulation	E[Wn] Error
3	4	0 (Det.)	22.7283	22.8157	0.3831	453.5056	456.51	0.6581
		0.25 (4-Erlang)	24.5345	24.6258	0.3707	487.8748	492.15	0.8687
		3 (2-HyperEx)	41.2059	41.0384	0.4082	805.7456	806.45	0.0873
			AVERAGE ERROR		0.3873	AVERAGE ERROR		0.5380
	5	0 (Det.)	19.8576	19.9327	0.3768	396.7444	400.47	0.9303
		0.25 (4-Erlang)	21.6457	21.7429	0.4470	431.0278	437.67	1.5176
		3 (2-HyperEx)	37.6634	37.3751	0.7714	735.4609	736.64	0.1601
			AVERAGE ERROR		0.5317	AVERAGE ERROR		0.8693
	6	0 (Det.)	19.8734	19.9256	0.2620	397.7982	400.6	0.6994
		0.25 (4-Erlang)	21.6585	21.8132	0.7092	431.9097	439.27	1.6756
		3 (2-HyperEx)	37.4744	37.1985	0.7417	731.4916	705.5	3.6841
			AVERAGE ERROR		0.5710	AVERAGE ERROR		2.0197
	ERROR				0.4967			1.1424
4	4	0 (Det.)	18.8282	18.9059	0.4110	506.4109	511.19	0.9349
		0.25 (4-Erlang)	20.1458	20.2606	0.5666	541.2939	547.52	1.1371
		3 (2-HyperEx)	32.66	32.4407	0.6760	859.6778	859.78	0.0119
			AVERAGE ERROR		0.5512	AVERAGE ERROR		0.6946
	5	0 (Det.)	16.3349	16.4307	0.5831	434.6722	438.75	0.9294
		0.25 (4-Erlang)	17.6359	17.6003	0.2023	467.1511	451.65	3.4321
		3 (2-HyperEx)	29.7293	29.6142	0.3887	770.0156	776.54	0.8402
			AVERAGE ERROR		0.3913	AVERAGE ERROR		1.7339
	6	0 (Det.)	16.3595	16.4426	0.5054	435.1468	442.65	1.6951
		0.25 (4-Erlang)	17.6617	17.7133	0.2913	467.9082	473.4	1.1601
		3 (2-HyperEx)	29.6364	29.3777	0.8806	766.8501	760.5	0.8350
			AVERAGE ERROR		0.5591	AVERAGE ERROR		1.2300
	ERROR				0.5005			1.2195
5	4	0 (Det.)	16.8729	16.9816	0.6401	451.4434	459.04	1.6549
		0.25 (4-Erlang)	17.896	17.9595	0.3536	477.4882	482.16	0.9689
		3 (2-HyperEx)	27.8876	27.8149	0.2614	735.9063	742.05	0.8279
			AVERAGE ERROR		0.4183	AVERAGE ERROR		1.1506
	5	0 (Det.)	14.5243	14.6105	0.5900	390.1925	392.92	0.6942
		0.25 (4-Erlang)	15.5364	15.5786	0.2709	416.2461	412.51	0.9057
		3 (2-HyperEx)	25.2192	25.1363	0.3298	667.062	661.87	0.7844
			AVERAGE ERROR		0.3969	AVERAGE ERROR		0.7948
	6	0 (Det.)	14.5604	14.6019	0.2842	391.9365	395.74	0.9611
		0.25 (4-Erlang)	15.5729	15.6413	0.4373	417.7998	413.71	0.9886
		3 (2-HyperEx)	25.191	25.1195	0.2846	666.801	671.52	0.7027
			AVERAGE ERROR		0.3354	AVERAGE ERROR		0.8841
	ERROR				0.3835			0.9432

5.3.2 IMPACT OF DOWNTIME VARIABILITY

As the squared coefficient of variation of the downtimes, $Cv_Y^{\ 2}$, increases, the average waiting time of a highest priority customer, $E[W_1]$, and a lowest priority customer, $E[W_n]$, also increase as seen in Figures 5.3 and 5.4. On the other hand, $E[W_1]$ and $E[W_n]$ decrease when the number of interruptions, *k*, increases. This is due to the fact that we kept the same down time probability as we have increased the number of interruptions resulting in smaller downtimes per interruption which in turn reduced customer waiting times.

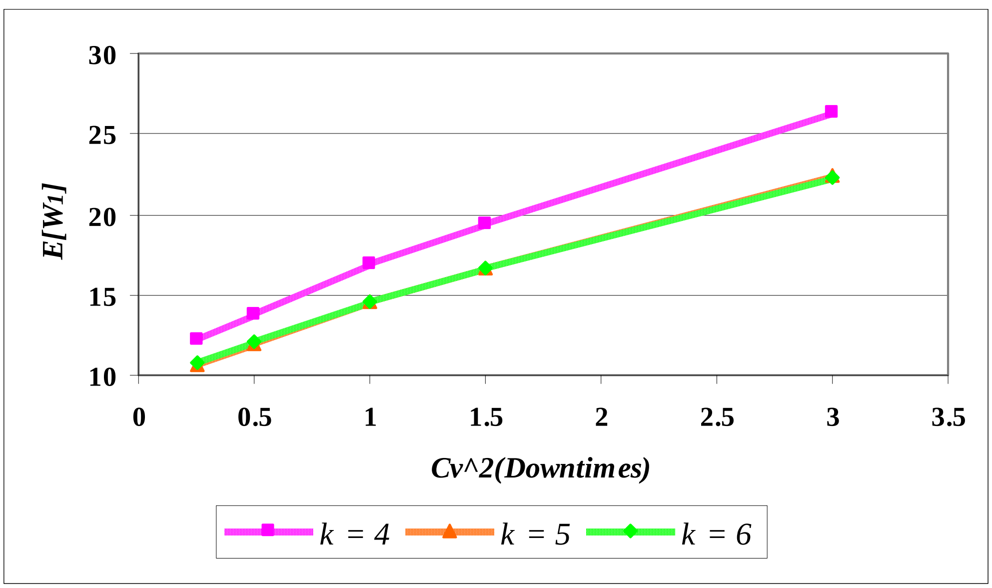

Figure 5.3 Impact of $Cv_Y^{\ 2}$ on $E[W_1]$ in the case of 5 priority classes

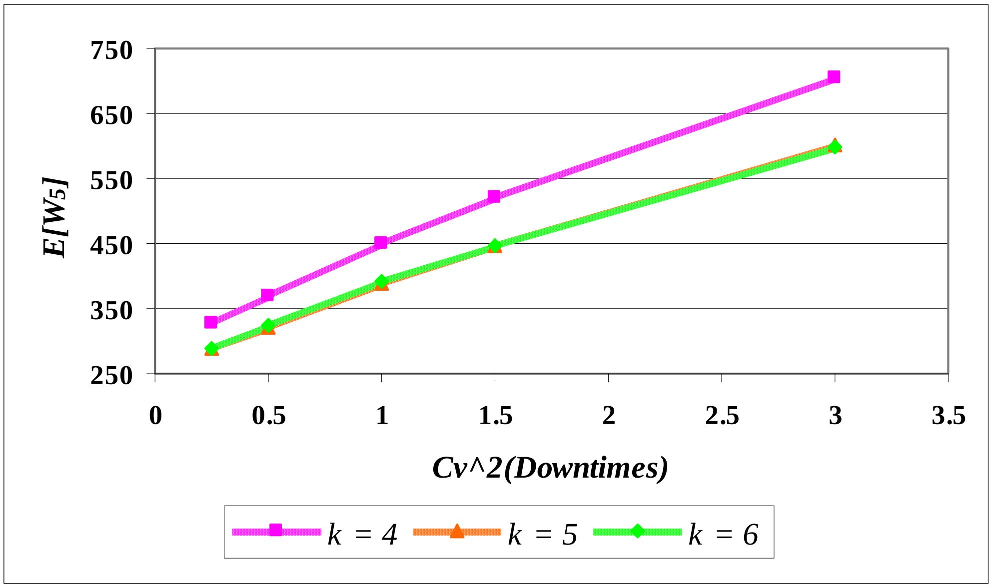

Figure 5.4 Impact of $Cv_Y{}^2$ on $E[W_5]$ in the case of 5 priority classes

The detailed analytical and simulated results obtained by changing $Cv_{Y_i}{}^2$ for $i = (1,\ldots,k)$, the number of priority classes, *n*, and the number of interruptions, *k*, are shown in Table 5.3.

The error levels for $E[W_n]$ remain below 7% as we increase the squared coefficient of variation of the downtimes, $Cv_{Y_i}{}^2$ for $i = (1,\ldots,k)$, from 0.25 to 3, the number of priority classes, *n*, from 3 to 5, and the number of interruptions, *k*, from 4 to 6.

On the other hand, the error for the average waiting time of a highest priority customer, $E[W_1]$, is less than 5% for all the values of $Cv_{Y_i}{}^2$ except $Cv_{Y_i}{}^2 = 3$. When we increase $Cv_{Y_i}{}^2$ to 3, the error level reaches 10%, because the value of the portion of the average waiting time that we exclude in our approximation increases significantly as the downtime variability increases.

The error levels do not show a distinct pattern as we increase the values of $Cv_{Y_i}{}^2$, n and k.

Table 5.3 $E[W_j]$ in the case of multiple priority classes when changing $Cv_Y{}^2$

n	k	$Cv^2(Y)$	$E[W_1]$ Analytical	$E[W_1]$ Simulation	$E[W_1]$ Error	$E[W_n]$ Analytical	$E[W_n]$ Simulation	$E[W_n]$ Error
3	4	0.25 (4-Erlang)	17.1078	17.0154	0.543	340.8097	341.21	0.1173
		0.5 (2-Erlang)	19.0091	19.0034	0.03	378.7174	380.6	0.4946
		1 (Expo)	22.7283	22.8157	0.3831	453.5056	456.51	0.6581
		1.5 (2-HyperEx)	25.8651	26.6616	2.9874	515.3688	532.44	3.2062
		3 (2-HyperEx)	34.2332	38.0752	10.091	682.5652	728.45	6.299
			AVERAGE ERROR		4.487	AVERAGE ERROR		3.3878
	5	0.25 (4-Erlang)	15.2588	15.2041	0.3598	304.6659	306.29	0.5302
		0.5 (2-Erlang)	16.8155	16.8076	0.047	335.7776	336.14	0.1078
		1 (Expo)	19.8576	19.9327	0.3768	396.7444	400.47	0.9303
		1.5 (2-HyperEx)	22.4386	23.0618	2.7023	448.1718	454.66	1.427
		3 (2-HyperEx)	29.3214	32.2577	9.1026	585.78	609.6	3.9075
			AVERAGE ERROR		4.0606	AVERAGE ERROR		2.0883
	6	0.25 (4-Erlang)	15.289	15.2245	0.4237	305.7284	305.65	0.0257
		0.5 (2-Erlang)	16.8419	16.786	0.333	336.7797	336.93	0.0446
		1 (Expo)	19.8734	19.9256	0.262	397.7982	400.6	0.6994
		1.5 (2-HyperEx)	22.3976	23.0602	2.8733	447.9518	457.17	2.0164
		3 (2-HyperEx)	29.1138	32.2166	9.6311	582.512	604.96	3.7107
			AVERAGE ERROR		4.2555	AVERAGE ERROR		2.1421
	AVERAGE ERROR				2.327			1.4042
4	4	0.25 (4-Erlang)	13.8958	13.81	0.6213	373.8354	375.6	0.4698
		0.5 (2-Erlang)	15.5604	15.5095	0.3282	418.5761	421.69	0.7384
		1 (Expo)	18.8282	18.9059	0.411	507.4109	511.19	0.7393
		1.5 (2-HyperEx)	21.5886	22.1688	2.6172	581.3841	591.38	1.6903
		3 (2-HyperEx)	28.9428	32.3684	10.583	779.8832	837.45	6.8741
			AVERAGE ERROR		4.5371	AVERAGE ERROR		3.1012
	5	0.25 (4-Erlang)	12.2825	12.2241	0.4777	326.0571	327.7	0.5013
		0.5 (2-Erlang)	13.6528	13.6372	0.1144	362.4683	366.3	1.0461
		1 (Expo)	16.3349	16.4307	0.5831	434.6722	438.75	0.9294
		1.5 (2-HyperEx)	18.6053	19.1501	2.8449	494.4123	509.2	2.9041
		3 (2-HyperEx)	24.67	27.2236	9.3801	656.3596	690.35	4.9236
			AVERAGE ERROR		4.2693	AVERAGE ERROR		2.9191
	6	0.25 (4-Erlang)	12.3191	12.2258	0.7631	327.2144	327.64	0.1299
		0.5 (2-Erlang)	13.688	13.6224	0.4816	363.6405	366.46	0.7694
		1 (Expo)	16.3595	16.4426	0.5054	435.1468	442.65	1.6951
		1.5 (2-HyperEx)	18.5843	19.1845	3.1286	493.7272	509.91	3.1737
		3 (2-HyperEx)	24.5079	27.324	10.306	651.8959	682.81	4.5275
			AVERAGE ERROR		4.6468	AVERAGE ERROR		3.1321
	AVERAGE ERROR				2.5041			2.2685
5	4	0.25 (4-Erlang)	12.221	12.1423	0.6481	326.4207	325.64	0.2397
		0.5 (2-Erlang)	13.7946	13.7443	0.366	368.4161	367.44	0.2656
		1 (Expo)	16.8729	16.9816	0.6401	451.4434	459.04	1.6549
		1.5 (2-HyperEx)	19.4727	20.1265	3.2485	520.3658	535.62	2.848
		3 (2-HyperEx)	26.4021	29.6073	10.826	705.8834	756.65	6.7094
			AVERAGE ERROR		4.9048	AVERAGE ERROR		3.7374
	5	0.25 (4-Erlang)	10.7057	10.6325	0.6885	287.2692	287.78	0.1775
		0.5 (2-Erlang)	11.998	11.968	0.2507	321.9753	323.46	0.459
		1 (Expo)	14.5243	14.6105	0.59	390.1925	392.92	0.6942
		1.5 (2-HyperEx)	16.6656	17.1641	2.9043	447.0928	460.3	2.8693
		3 (2-HyperEx)	22.3856	24.6148	9.0563	601.2667	622.99	3.4869
			AVERAGE ERROR		4.1835	AVERAGE ERROR		2.3501
	6	0.25 (4-Erlang)	10.7492	10.6578	0.8576	288.8986	288.61	0.1
		0.5 (2-Erlang)	12.0404	11.9981	0.3526	323.658	326.35	0.8249
		1 (Expo)	14.5604	14.6019	0.2842	391.9365	395.74	0.9611
		1.5 (2-HyperEx)	16.6597	17.1903	3.0866	447.9199	456.57	1.8946
		3 (2-HyperEx)	22.2488	24.8539	10.482	598.914	627.49	4.554
			AVERAGE ERROR		4.6175	AVERAGE ERROR		2.4699
	AVERAGE ERROR				3.343			2.0547

5.3.3 IMPACT OF SYSTEM UTILIZATION

As seen in Figures 5.5 and 5.6, the average waiting time of a highest priority customer $E[W_1]$, and a lowest priority customer $E[W_n]$ increase as the system utilization, $P(B)$, increases. Also, $E[W_1]$ and $E[W_n]$ decrease as the number of interruptions experienced by the system, k, increases.

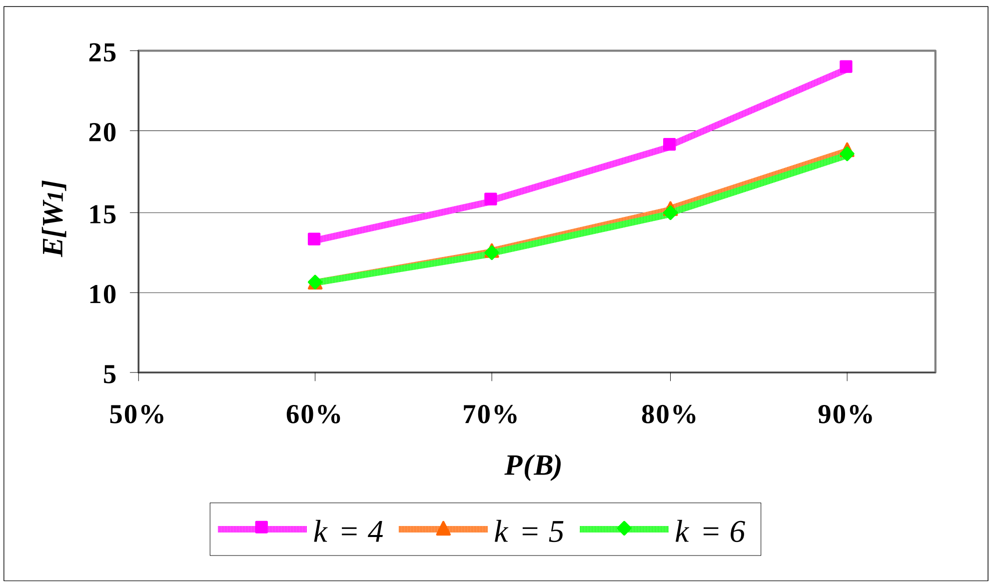

Figure 5.5 Impact of $P(B)$ on $E[W_1]$ in the case of 5 priority classes

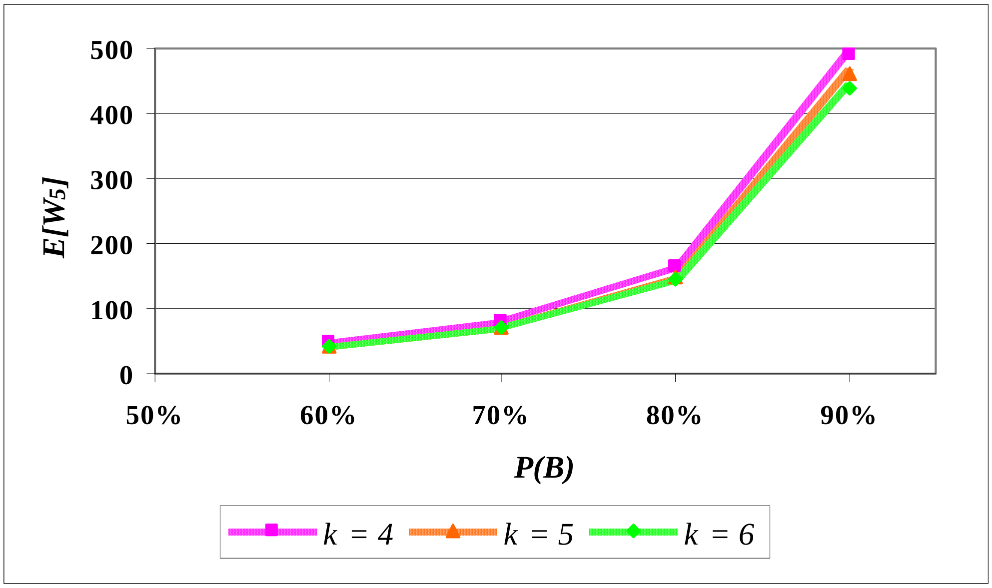

Figure 5.6 Impact of $P(B)$ on $E[W_5]$ in the case of 5 priority classes

According to the detailed results shown in Table 5.4, the error levels for $E[W_1]$ and $E[W_n]$ remain below 1% and 2%, respectively, as we increase the system utilization, $P(B)$, from 60% to 90%, the number of priority classes, *n*, from 3 to 5, and the number of interruptions, *k*, from 4 to 6.

The average error for the average waiting time of a highest priority customer $E[W_1]$ increases as the total number of priority classes, *n*, increases. However, the error levels do not show a distinct pattern as we increase $P(B)$ and *k*.

Table 5.4 $E[W_j]$ in the case of multiple priority classes when changing $P(B)$

n	k	P(B)	E[W 1] Analytical	E[W 1] Simulation	E[W 1] Error	E[W n] Analytical	E[W n] Simulation	E[W n] Error
3	4	60%	15.009	15.0646	0.3691	51.7307	51.8749	0.278
		70%	18.1193	18.2061	0.4768	88.8879	89.3525	0.52
		80%	22.4694	22.6079	0.6126	182.5142	184.53	1.0924
		90%	28.9934	29.1442	0.5174	557.9354	566.6	1.5292
		AVERAGE ERROR			0.5356	AVERAGE ERROR		1.0472
	5	60%	13.6108	13.6564	0.3339	46.0955	46.2265	0.2834
		70%	16.7292	16.7893	0.358	80.5725	81.1736	0.7405
		80%	21.1834	21.3038	0.5652	169.1407	170.62	0.867
		90%	28.069	28.1639	0.337	535.6098	539.62	0.7432
		AVERAGE ERROR			0.42	AVERAGE ERROR		0.7836
	6	60%	13.6712	13.7035	0.2357	46.2893	46.5279	0.5128
		70%	16.8042	16.8667	0.3706	80.9161	81.2238	0.3788
		80%	21.2797	21.3697	0.4212	169.8723	170.77	0.5257
		90%	28.1988	28.3196	0.4266	537.9122	547.63	1.7745
		AVERAGE ERROR			0.4061	AVERAGE ERROR		0.893
	ERROR				0.4312			0.772
4	4	60%	14.2875	14.3527	0.4543	53.2839	53.7199	0.8116
		70%	17.1461	17.2094	0.3678	92.6261	93.2424	0.661
		80%	21.1002	21.2311	0.6165	194.0878	196.37	1.1622
		90%	26.947	27.0908	0.5308	620.2237	625.41	0.8293
		AVERAGE ERROR			0.5051	AVERAGE ERROR		0.8841
	5	60%	12.151	12.2267	0.6191	45.2778	45.7038	0.9321
		70%	14.6716	14.7692	0.6608	79.19	79.9652	0.9694
		80%	18.1586	18.2425	0.4599	166.8587	168.59	1.0269
		90%	23.3201	23.4203	0.4278	536.3439	542.92	1.2112
		AVERAGE ERROR			0.5162	AVERAGE ERROR		1.0692
	6	60%	12.2055	12.2659	0.4924	45.4709	45.8332	0.7905
		70%	14.7366	14.8288	0.6218	79.5096	80.4158	1.1269
		80%	18.2413	18.3415	0.5463	167.5753	168.85	0.7549
		90%	23.4244	23.4916	0.2861	538.145	541.94	0.7003
		AVERAGE ERROR			0.4847	AVERAGE ERROR		0.8607
	ERROR				0.4931			0.938
5	4	60%	13.2706	13.36	0.6692	48.006	48.3706	0.7538
		70%	15.7419	15.8441	0.645	81.4895	82.2463	0.9202
		80%	19.0977	19.1515	0.2809	164.6051	165.43	0.4986
		90%	23.9228	23.9865	0.2656	489.9261	494.17	0.8588
		AVERAGE ERROR			0.3972	AVERAGE ERROR		0.7592
	5	60%	10.6562	10.6779	0.2032	41.8433	41.9102	0.1596
		70%	12.6028	12.6524	0.392	71.9956	72.2124	0.3002
		80%	15.217	15.3067	0.586	148.5799	149.65	0.7151
		90%	18.9142	19.0546	0.7368	460.1768	468.22	1.7178
		AVERAGE ERROR			0.5716	AVERAGE ERROR		0.911
	6	60%	10.5597	10.5935	0.3191	41.1864	41.3874	0.4857
		70%	12.4514	12.5021	0.4055	70.4424	70.9557	0.7234
		80%	14.9843	15.0481	0.424	144.1567	145.06	0.6227
		90%	18.5477	18.6504	0.5507	439.6056	445.24	1.2655
		AVERAGE ERROR			0.4601	AVERAGE ERROR		0.8705
	ERROR				0.5193			0.8469

5.3.4 IMPACT OF DOWNTIME PROBABILITY

Figures 5.7 and 5.8 show that the average waiting time of a highest priority customer, $E[W_1]$, and a lowest priority customer, $E[W_n]$**,** increase as the downtime probability of the system, P_d, increases. Conversely, $E[W_1]$ and $E[W_n]$ decrease as the number of interruptions, *k*, increases.

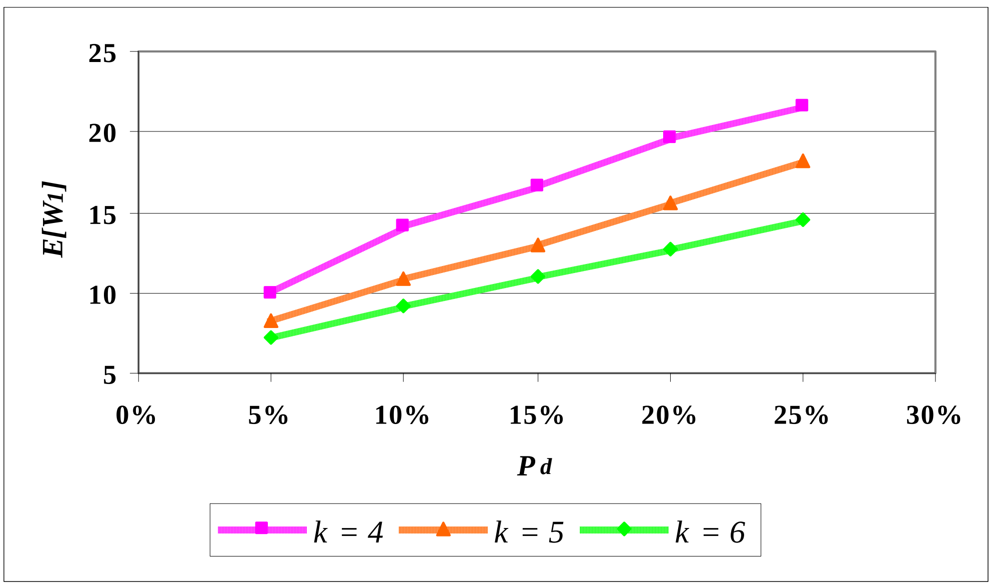

Figure 5.7 Impact of P_d on $E[W_1]$ in the case of 5 priority classes

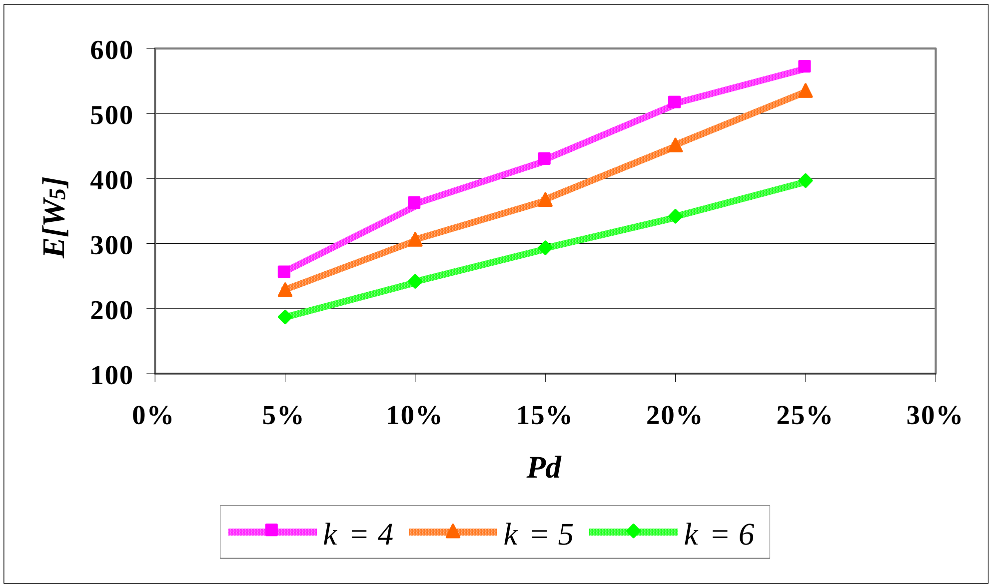

Figure 5.8 Impact of P_d on $E[W_5]$ in the case of 5 priority classes

According to the results shown in Table 5.5, the error for the average waiting time of a highest priority customer and a lowest priority customer are less than 1% and 4%, respectively, for all values of P_d, *n* and *k*.

The error levels for $E[W_1]$ and $E[W_n]$ increase as the downtime probability, P_d, increases. The average error for $E[W_1]$ and $E[W_n]$ increases as the number of priority classes, *n*, increases. On the other hand, the error levels do not show a distinct pattern as we increase the total number of interruptions, *k*.

Table 5.5 $E[W_j]$ in the case of multiple priority classes when changing P_d

n	k	Pd	E[W 1] Analytical	E[W 1] Simulation	E[W 1] Error	E[W n] Analytical	E[W n] Simulation	E[W n] Error
3	4	5%	13.0229	13.0569	0.2604	264.5539	265.94	0.5212
		10%	17.6481	17.7014	0.3011	361.046	359.063	0.5523
		15%	20.477	20.5749	0.4758	422.1496	425.29	0.7384
		20%	23.997	24.1838	0.7724	498.0786	504.61	1.2943
		25%	26.2271	26.5094	1.0649	548.1682	566.76	3.2804
		AVERAGE ERROR			0.771	AVERAGE ERROR		1.771
	5	5%	11.9532	11.9395	0.1147	232.4804	233.15	0.2872
		10%	14.9475	14.9723	0.1656	293.4201	294	0.1972
		15%	17.3253	17.3614	0.2079	342.6912	342.82	0.0376
		20%	20.4574	20.5551	0.4753	408.0668	410.15	0.5079
		25%	23.5136	23.6757	0.6847	472.6452	480.83	1.7022
		AVERAGE ERROR			0.456	AVERAGE ERROR		0.7492
	6	5%	11.3674	11.3753	0.0694	221.4799	221.55	0.0316
		10%	13.6453	13.6336	0.0858	267.7581	267.96	0.0753
		15%	15.7778	15.8262	0.3058	311.694	314.27	0.8197
		20%	17.7931	17.8539	0.3405	353.8494	356.3	0.6878
		25%	20.0186	20.1696	0.7487	401.3676	409.77	2.0505
		AVERAGE ERROR			0.465	AVERAGE ERROR		1.186
	ERROR				0.342			0.7066
4	4	5%	11.4635	11.463	0.0044	294.9056	294.21	0.2364
		10%	15.7581	15.8247	0.4209	409.8176	410.16	0.0835
		15%	18.372	18.4441	0.3909	483.5722	458.73	5.4154
		20%	21.6246	21.7608	0.6259	575.5249	585.81	1.7557
		25%	23.6708	23.7863	0.4856	637.5572	650.06	1.9233
		AVERAGE ERROR			0.5008	AVERAGE ERROR		3.0315
	5	5%	9.548	9.5338	0.1489	235.3888	234.89	0.2124
		10%	12.3287	12.3337	0.0405	307.4742	309.23	0.5678
		15%	14.5049	14.4977	0.0497	365.5649	366.73	0.3177
		20%	17.364	17.4573	0.5344	443.3421	448.25	1.0949
		25%	20.1433	20.3375	0.9549	520.772	530.91	1.9096
		AVERAGE ERROR			0.513	AVERAGE ERROR		1.1074
	6	5%	8.9555	8.9462	0.104	210.9232	210.35	0.2725
		10%	11.6221	11.6187	0.0293	287.7799	286.43	0.4713
		15%	13.6658	13.7184	0.3834	341.9005	344.74	0.8237
		20%	15.5941	15.669	0.478	394.4042	397.63	0.8113
		25%	17.7184	17.8429	0.6978	454.0439	462.28	1.7816
		AVERAGE ERROR			0.5197	AVERAGE ERROR		1.1388
	ERROR				0.2838			0.9017
5	4	5%	10.0241	9.9724	0.5184	253.739	253.04	0.2762
		10%	14.1038	14.1525	0.3441	360.884	362.95	0.5692
		15%	16.5833	16.5847	0.0084	429.6025	427.71	0.4425
		20%	19.6655	19.7933	0.6457	515.378	524.07	1.6586
		25%	21.5752	21.7694	0.8921	571.8276	587.12	2.6046
		AVERAGE ERROR			0.5154	AVERAGE ERROR		1.1102
	5	5%	8.2129	8.2103	0.0317	228.2265	227.8	0.1872
		10%	10.8589	10.8342	0.228	305.7629	305.09	0.2206
		15%	12.9283	12.9892	0.4689	368.9173	372.94	1.0786
		20%	15.6365	15.6969	0.3848	452.7643	457.8	1.1
		25%	18.2614	18.3865	0.6804	536.1357	545.88	1.7851
		AVERAGE ERROR			0.5113	AVERAGE ERROR		1.3212
	6	5%	7.2488	7.2549	0.0841	188.2474	188.94	0.3666
		10%	9.1933	9.2012	0.0859	241.4141	242.07	0.271
		15%	11.0065	11.0338	0.2474	292.3634	293.31	0.3227
		20%	12.7124	12.7792	0.5227	341.9984	347.33	1.535
		25%	14.5805	14.6963	0.788	397.2468	407.1	2.4203
		AVERAGE ERROR			0.5194	AVERAGE ERROR		1.426
	ERROR				0.4207			0.9323

5.3.5 CONCLUSION

In this chapter, we consider a single-server, multi-class queueing system subject to multiple types of possibly simultaneous interruptions motivated by the transit vessel entrances in the Istanbul Strait. Since the complexity of the system makes the exact analysis difficult, an analytical model is developed to approximate the expected waiting time of a class j customer in the aforementioned queueing model.

The numerical results show that the approximation works reasonably well for the expected waiting time of a highest priority customer, $E[W_1]$, and a lowest priority customer, $E[W_n]$, for a wide range of system parameters. In addition, we conclude that it is not the service time, arrival process, times-to-interruption, or the number of interruptions, but the variability of downtime processes and the number of priority classes that determine the accuracy of the approximation.

We also analyze the impact of various key parameters on the system behavior. We observe that an increase in all of the system parameters except number of interruptions, k, lead to an increase in the expected waiting time of a customer in the queue. On the other hand, $E[W_j]$ decreases as k increases.

The main contribution of our work is that we incorporate the notion of priority classes into a queueing model with multiple types of possibly simultaneous interruptions, which has never been done before.

The main use of this model will be in predicting the impact of various system parameters on the congestion levels in waterway entrances. In particular, the impact of various closure profiles (due to construction projects or traffic management strategies) and an increase in vessel traffic on vessel delays are crucial in long range capacity planning in waterways.

From a critical standpoint, even though we assume class-independent interruptions, in reality some interruptions may only affect a distinct class of customers (class-dependent interruptions) in multi-class settings. The proposed model cannot handle these situations. We extend our current model in the next chapter in order to analyze these more realistic scenarios.

6 MULTI-CLASS QUEUES WITH MULTIPLE TYPES OF CLASS-DEPENDENT INTERRUPTIONS

In queueing systems where different types of customers are served and the server is subject to multiple types of interruptions, some interruptions may only affect a distinct class of customers but not others. This is especially true for the vessel traffic at waterway entrances. The passage of some vessel classes may be suspended by a set of interruptions while other classes may be stopped due to a different set of interruptions.

A case in point is the Istanbul Strait. According to the 1998 Regulations, vessels exceeding 200 meters can only pass during daytime. Therefore, while sunset interrupts the passage of these vessels, it has no affect on other vessels. Also, while surface currents greater than 4 knots/hr suspend the traffic of large, deep-draft vessels carrying dangerous cargo, they have no affect on other vessel classes. In addition, some interruptions may affect all vessels classes. For example, when the visibility is less than 0.5 miles, the transit vessel traffic is suspended regardless of the vessel class.

In this chapter, we propose a queueing analysis to estimate the average vessel waiting times at the waterway entrances. These problems can be studied as queues with multiple types of class-dependent service interruptions, as discussed in detail in Section 6.1.

6.1 A QUEUEING MODEL

The incoming vessels form customer arrival streams, which can be identified by the time intervals between consecutive arrivals. We assume that class *j* customers arrive from a Poisson process with rate λ_j per unit time and that there are two classes of customers receiving service at the system.

After a vessel enters the Strait, a second vessel starts its passage as soon as the first one traverses the minimum required distance between two consecutive vessels. Therefore, the time it takes for a vessel to traverse the required distance before the next vessel may enter the Strait is considered the *service time* of a customer in the queueing model. At the end of the service time, the next vessel in line (if any) is allowed to enter the Strait. This is typically a short period of time due to the fact that the distance to be maintained between consecutive vessels is about 0.5-1 nautical miles. The practice in Istanbul results in about 2.5 minutes. In this study, we assume that the service time of a class *j* customer, S_j, has an arbitrary distribution, and the two classes of customers are served according to the **non-preemptive** priority discipline where class 1 has the higher priority. When the server becomes idle, a class 1 customer is always served prior to a class 2 customer even if the class 2 customer arrives before the other. Within each priority class, the "first come, first served" policy determines the order of service. The non-preemptive discipline allows the lower priority customer to complete its service when a higher priority customer arrives during its service time. In reality, the priority structure is decided upon by the resident Vessel Traffic Services system and it may change from one location to another.

Service may be interrupted and the waterway may be closed due to poor visibility, storms, high currents or other random stoppages. We assume that the server is subject to *k* different types of operation-independent, non-identical, possibly simultaneous interruptions. The interruptions are independent and the downtimes do not affect each other. That is, it is possible to have a number of downtimes progressing simultaneously. Note that this is common in many other systems modeled using queues such as manufacturing and communication systems.

Also, we assume that the interruption processes are **class-dependent**, that is different priority classes are affected by different sets of interruptions. These sets may be overlapping. A *down cycle* starts either when an interruption occurs while the server is idle or when an interruption that affects the current customer in service occurs during an uptime. The down cycle ends either when the system becomes operational again or a vessel that is not affected by the current interruption(s) arrives.

Typically, the vessel that is given the go-ahead and proceeding to the entrance does not get interrupted even if a condition that would normally stop the traffic erupts. That is, the current customer is not affected by an interruption that started during the current service. However, this interruption would stop the following vessels from entering the Strait if it belongs to the set of interruptions that affect their service. We assume that time to interruption of type *i*, Z_i, follows an exponential distribution with rate δ_i, while its downtime, Y_i, has an arbitrary distribution. A point of observation is that due to the nature of closures in waterways, the downtimes are much longer than the service times.

Thus, the vessel traffic at the entrance points of waterways may very well be considered a two-class priority queueing model with a single-server and an infinite queue, which is subject to multiple types of class-dependent possibly simultaneous interruptions. Classes can be identified on lengths, types of cargo and it is not too difficult to make two classes out of many. Ideally, we would like to consider larger number of classes; however, the problem becomes too difficult to handle analytically. Therefore, we have kept the number of classes at two, for convenience.

In this dissertation, we propose an approximation method to obtain the expected waiting time of two classes of customers in the queue using the "completion-time approach". The *service completion time*, C_j, is defined as the time interval between the service start time of a class *j* customer, which corresponds to a vessel entry, and the time the next customer may start its service, that is, the instance the next vessel is allowed to enter. It is equal to the service time of the current customer, if no interruptions occur. In case of interruptions, the service completion time is longer than the service time due to downtimes since the service is available to the next customer in line only after the system becomes operational for that customer.

Taking into account the three facts that the aforementioned service times are much shorter than downtimes, the vessels continue their passage during the interruption, and the remaining service times are over by the time the down cycle ends, the queueing model is equivalent to one with scrapping where the customer is assumed to be scrapped upon an interruption. This is only a modeling convenience to keep track of the time until the first interruption occurs, which is referred to as the *actual service time* of a customer in the model.

In the following sections, we focus our attention to the queueing system and refer to vessels as customers.

6.2 WAITING TIME

Consider a single-server queueing system with two classes of customers. We assume that class j customers arrive from a Poisson process with rate λ_j per unit time. Service time, S_j, of a class j customer follows an arbitrary distribution. The server is subject to k operation-independent, non-identical, class-dependent, possibly simultaneous interruptions. Let $\mathcal{F}_j$ be the set of interruptions that affect class j customers. The time to interruption of type i, Z_i, follows an exponential distribution with rate δ_i, while its downtime, Y_i, has an arbitrary distribution.

Some of the interruptions may affect only one class while others may affect both classes. If the server is down due to an interruption i that affect both classes ($i \in \mathcal{F}_1 \cap \mathcal{F}_2$), no customer is taken to service. This is also true if there is a class 1 customer at the head of the queue and the server is down due an interruption h that only affects class 1 ($h \in \mathcal{F}_1$). In such a situation, we assume that lower priority class 2 customers can not bypass the class 1 customers waiting in the queue. On the other hand, if the server is down due to an interruption l that only affects class 2 ($l \in \mathcal{F}_2$) and there are no class 1 customers in the queue, the system remains down until either interruption l ends or a class 1 customer arrives.

Below, we will base our analysis on what a customer observes in the system at the point of its arrival. Let an arriving class j customer observe N_m customers of class m waiting in the queue and W_j be its waiting time in the queue until its service starts.

If the server is busy upon arrival, an arriving class 1 customer waits until the service time of the current customer is completed. If the class 1 customer arrives when the server is down due to an interruption i affecting class 1 ($i \in \mathcal{F}_1$), it waits until it is up again. The arriving customer also has to wait until all the class 1 customers that arrived earlier are served, and the downtimes of the possible interruptions that affect class 1 that may occur during their services are completed. Class 2 customers do not interfere with this class, since it has lower priority. Thus, the waiting time of an arriving class 1 customer can be expressed as follows:

$$E[W_1] = E[N_1]E[C_1] + E[C_r] + E[T_{RD_1}] \tag{6.1}$$

which, coupled with $E[N] = \lambda E[W]$ gives us

$$E[W_1] = \frac{E[C_r] + E[T_{RD_1}]}{1 - \lambda_1 E[C_1]}. \tag{6.2}$$

where C_1, C_r, and T_{RD_1} represent the service completion time of a class 1 customer, the remaining service completion time of the current customer found in the server upon arrival, and the total remaining downtime of the system when it is down upon arrival of a class 1 customer, respectively.

A class 2 customer first waits until the current customer leaves the server if the server is busy upon arrival. Then, it waits until all the class 1 and class 2 customers that arrived earlier are served and the downtimes of the possible interruptions that may occur during their services are completed. It also waits for the class 1 customers arriving during its delay in the queue. The customer may also have to wait for the remaining system downtime if the server is down upon its arrival. Thus, using the expected length of the busy period presented in [Altıok, 1997], we can write

$$E[W_2] = \frac{E[N_1]E[C_1] + E[N_2]E[C_2] + E[C_r] + E[T_{RD_1}]}{1 - \rho_1} \tag{6.3}$$

with $\rho_1 = \lambda_1 E[C_1]$ resulting in

$$E[W_2] = \frac{\lambda_1 E[W_1]\, E[C_1] + E[C_r] + E[T_{RD_1}]}{1 - \lambda_1\, E[C_1] - \lambda_2 E[C_2]}. \tag{6.4}$$

where C_j is the service completion time of a class *j* customer. $E[C_j]$ can be viewed as the service time of a class *j* customer in an imaginary server that does not experience interruptions during service time. Notice that this is the same server mentioned in Chapter 4, which experiences downtime only when it is idle. In this case, the server serves two types of customers. Recall that the service dynamics such as scrapings are hidden in the service time (the completion time process). The $\lambda_1\, E[C_1] + \lambda_2 E[C_2]$ expression in (6.4) represents the utilization of this imaginary server, denoted by $P(B)$, which is the percentage of the time the imaginary server is busy. The server is stable if and only if $P(B) = \lambda_1\, E[C_1] + \lambda_2 E[C_2] < 1$.

6.2.1 SERVICE COMPLETION TIME (C_j)

Here we discuss the characteristics of the service completion time of a class *j* customer, C_j, in the case of two priority classes and *k* class-dependent interruptions. Note that C_j is similar to C discussed in Section 4.4.1 and consists of two parts; the actual service time of a class *j* customer, S_{a_j}, and the downtime experienced by that customer during its service T_{DS_j}. We have

$$E\left[C_j\right] = E\left[S_{a_j}\right] + E\left[T_{DS_j}\right]. \tag{6.5}$$

Note that in the case of k class-dependent interruptions, the actual service time of a customer of class j, S_{a_j}, is identical to the one explained in Section 5.2.1. The LST of the density function of S_{a_j} is presented in (5.10)

Unlike the previous models, in the case of k class-dependent interruptions, the expected downtime experienced by a class j customer during its service, $E[T_{DS_j}]$, depends not only on the class of the customer in service, but also the class of the next customer waiting at the head of the queue. Thus, $E[T_{DS_j}]$ is given by

$$E\left[T_{DS_j}\right] = \sum_{m=1}^{2} q^m E\left[T_{DS_j}^m\right] \tag{6.6}$$

where

$$q^m = \Pr\left(\text{Class } m \text{ customer at the head of the queue} \middle| \text{at least one customer in the queue}\right) \tag{6.7}$$

and is approximated by

$$q^j = \frac{\lambda_j}{\sum \lambda}. \tag{6.8}$$

Furthermore, $T_{DS_j}^{m}$ is the expected downtime experienced by a class *j* customer during its service while a class *m* customer is waiting at the head of the queue. $T_{DS_j}^{m}$ consists of the downtime experienced due to an interruption affecting class *m* ($i \in \mathcal{F}_m$), and the downtime experienced due to an interruption that does not affect class *m* ($i \in \mathcal{F} - \mathcal{F}_m$). We have

$$\begin{aligned} E[T_{DS_j}^{m}] = & \sum_{i \in \mathcal{F}_m} P\left(Z_i \leq \min\left(S_j, \mathcal{Z}\text{-}\{i\}\right)\right) E[T_{DS_j|i \in \mathcal{F}_m}^{m}] \\ & + \sum_{i \in \mathcal{F}\text{-}\mathcal{F}_m} P\left(Z_i \leq \min\left(S_j, \mathcal{Z}\text{-}\{i\}\right)\right) E[T_{DS_j|i \in \mathcal{F}\text{-}\mathcal{F}_m}^{m}] \end{aligned} . \tag{6.9}$$

$E[T_{DS_j|i \in \mathcal{F}_m}^{m}]$ is equal to the downtime of the current interruption *i* that affects class *m* if a higher class customer does not arrive or no other interruption occurs during this time. If a higher class *t* customer ($t \neq m$) arrives during the downtime, $E[T_{DS_j|i \in \mathcal{F}_m}^{m}]$ equals the sum of the downtimes of all possible interruptions affecting class *t*. Note that in the case of $m = 1$, this term does not exist since class 1 is the highest priority class. Otherwise, if another interruption *h* ($h \neq i$) occurs, the total downtime depends on the possible higher class vessel arrivals and other interruption occurrences during the downtime of *h*.

Similar to the previous models, for practical purposes, we assume that each interruption type may occur **at most once** during the service of a customer and that there may be **at most three** interruptions occurring consecutively during a down cycle. Thus using an approximation, we have obtained an expression for $E[T^1_{DS_j}|_{i\in\mathcal{F}_1}]$ and $E[T^2_{DS_j}|_{i\in\mathcal{F}_2}]$ are given in (6.10) and (6.12), respectively. $E[T^m_{DS_j}|_{i\in\mathcal{F}\text{-}\mathcal{F}_m}]$ is evaluated similarly with minor changes and $E[T^1_{DS_j}|_{i\in\mathcal{F}\text{-}\mathcal{F}_1}]$ and $E[T^2_{DS_j}|_{i\in\mathcal{F}\text{-}\mathcal{F}_2}]$ are given in (6.11) and (6.13), respectively.

Note that in the case of expected waiting time of a class 1 customer using (6.2), we need to calculate the time it waits until all the class 1 customers that arrived earlier are served, which is represented by $E[N_1]E[C_1]$. We know for fact that when any of these N_1 customers is in service, there is at least one class 1 customer at the head of the queue. Therefore, in this case we have $E[T_{DS_1}] = E[T^1_{DS_1}]$.

$$E\left[T^{1}_{DS_j|i\in\mathcal{F}_1}\right]=\left(\begin{array}{l} P\left(Y_i\le\min\left(\mathcal{Z}(\mathcal{F}_1)\text{-}\{i\}\right)\right)E\left[Y_i\mid Y_i\le\min\left(\mathcal{Z}(\mathcal{F}_1)\text{-}\{i\}\right)\right] \\ +\sum\limits_{\substack{h\in\mathcal{F}_1\\ h\ne i}}P\left(Z_h\le\min\left(Y_i,\mathcal{Z}(\mathcal{F}_1)\text{-}\{i,h\}\right)\right)\left[\begin{array}{l} E\left[Z_h\mid Z_h\le\min\left(Y_i,\mathcal{Z}(\mathcal{F}_1)\text{-}\{i,h\}\right)\right]+\left(\begin{array}{l} P\left(\max\left(Y_{r_i},Y_h\right)\le\min\left(\mathcal{Z}(\mathcal{F}_1)\text{-}\{i,h\}\right)\right) \\ \times E\left[\max\left(Y_{r_i},Y_h\right)\mid\max\left(Y_{r_i},Y_h\right)\le\min\left(\mathcal{Z}(\mathcal{F}_1)\text{-}\{i,h\}\right)\right]\end{array}\right) \\ +\sum\limits_{\substack{l\in\mathcal{F}\\ l\ne h\ne i}}P\left(Z_l\le\min\left(\max\left(Y_{r_i},Y_h\right),\mathcal{Z}(\mathcal{F}_1)\text{-}\{i,h,l\}\right)\right)\left(\begin{array}{l} E\left[Z_l\mid Z_l\le\min\left(\max\left(Y_{r_i},Y_h\right),\mathcal{Z}(\mathcal{F}_1)\text{-}\{i,h,l\}\right)\right] \\ +E\left[\max\left(Y_{r_i},Y_{r_h},Y_l\right)\right]\end{array}\right)\end{array}\right]\end{array}\right) \tag{6.10}$$

where $\mathcal{Z}(\mathcal{F})\text{-}\{i,h,l\}=\{Z_1,...,Z_{i-1},Z_{i+1},Z_{h-1},Z_{h+1},Z_{l-1},Z_{l+1},...,Z_k\}$.

$$E\left[T^{1}_{DS_j|i\in\mathcal{F}\text{-}\mathcal{F}_1}\right]=\left(\begin{array}{l} P\left(S_{r_j}\le\min\left(\mathcal{Z}(\mathcal{F})\text{-}\{i\}\right)\right)E\left[S_{r_j}\mid S_{r_j}\le\min\left(\mathcal{Z}(\mathcal{F}_1)\right)\right] \\ +\sum\limits_{\substack{h\in\mathcal{F}_1\\ h\ne i}}P\left(Z_h\le\min\left(S_{r_j},\mathcal{Z}(\mathcal{F}_1)\text{-}\{h\}\right)\right)\left[\begin{array}{l} E\left[Z_h\mid Z_h\le\min\left(S_{r_j},\mathcal{Z}(\mathcal{F}_1)\text{-}\{h\}\right)\right] \\ +\mathbf{1}_{\mathcal{F}_m}(h)\left(\begin{array}{l} P\left(Y_h\le\min\left(\mathcal{Z}(\mathcal{F})\text{-}\{h\}\right)\right)E\left[Y_h\mid Y_h\le\min\left(\mathcal{Z}(\mathcal{F}_1)\text{-}\{h\}\right)\right] \\ +\sum\limits_{\substack{l\in\mathcal{F}_1\\ l\ne h\ne i}}P\left(Z_l\le\min\left(Y_h,\mathcal{Z}(\mathcal{F}_1)\text{-}\{h,l\}\right)\right)\left[E\left[Z_l\mid Z_l\le\min\left(Y_h,\mathcal{Z}(\mathcal{F}_1)\text{-}\{h,l\}\right)\right]+E\left[\max\left(Yr_h,Y_l\right)\right]\right]\end{array}\right)\end{array}\right]\end{array}\right) \tag{6.11}$$

$$
E\left[T^2_{DS_j|i\in\mathcal{F}_2}\right]=\left(\begin{array}{l}
P\left(Y_i\le\min\left(A_1,\mathcal{Z}(\mathcal{F})\text{-}\{i\}\right)\right)E\left[Y_i\mid Y_i\le\min\left(A_1,\mathcal{Z}(\mathcal{F})\text{-}\{i\}\right)\right]\\
+P\left(A_1\le\min\left(Y_i,\mathcal{Z}(\mathcal{F})\text{-}\{i\}\right)\right)\left[E\left[A_1\mid A_1\le\min\left(Y_i,\mathcal{Z}(\mathcal{F})\text{-}\{i\}\right)\right]+\mathbf{1}_{\mathcal{F}_1}(i)\left(\begin{array}{l}
P\left(Y_{r_i}\le\min\left(\mathcal{Z}(\mathcal{F}_1)\text{-}\{i\}\right)\right)E\left[Y_{r_i}\mid Y_{r_i}\le\min\left(\mathcal{Z}(\mathcal{F}_1)\text{-}\{i\}\right)\right]\\
+\sum\limits_{\substack{h\in\mathcal{F}_1\\ h\ne i}}P\left(Z_h\le\min\left(Y_{r_i},\mathcal{Z}(\mathcal{F}_1)\text{-}\{i,h\}\right)\right)\left[\begin{array}{l}
E\left[Z_h\mid Z_h\le\min\left(Y_{r_i},\mathcal{Z}(\mathcal{F}_1)\text{-}\{i,h\}\right)\right]\\
+\left[\begin{array}{l}P\left(\max(Y_{r_i},Y_h)\le\min\left(\mathcal{Z}(\mathcal{F}_1)\text{-}\{i,h\}\right)\right)\\ \times E\left[\max(Y_{r_i},Y_h)\mid\max(Y_{r_i},Y_h)\le\min\left(\mathcal{Z}(\mathcal{F}_1)\text{-}\{i,h\}\right)\right]\end{array}\right]\\
+\sum\limits_{\substack{l\in\mathcal{F}_t\\ l\ne h\ne i}}\left[\begin{array}{l}P\left(Z_l\le\min\left(\max(Y_{r_i},Y_h),\mathcal{Z}(\mathcal{F}_1)\text{-}\{i,h,l\}\right)\right)\\ \times\left[E\left[Z_l\mid Z_l\le\min\left(\max(Y_{r_i},Y_h),\mathcal{Z}(\mathcal{F}_1)\text{-}\{i,h,l\}\right)\right]+E\left[\max\left(Y_{r_i},Y_{r_h},Y_l\right)\right]\right]\end{array}\right]
\end{array}\right]
\end{array}\right)\right]\\
+\sum\limits_{\substack{h\in\mathcal{F}\\ h\ne i}}P\left(Z_h\le\min\left(Y_i,A_1,\mathcal{Z}(\mathcal{F})\text{-}\{i,h\}\right)\right)\left[\begin{array}{l}
E\left[Z_h\mid Z_h\le\min\left(Y_i,A_1,\mathcal{Z}(\mathcal{F})\text{-}\{i,h\}\right)\right]+\left(\begin{array}{l}P\left(\max\left(Y_{r_i},\mathbf{1}_{\mathcal{F}_2}(h)Y_h\right)\le\min\left(A_1,\mathcal{Z}(\mathcal{F})\text{-}\{i,h\}\right)\right)\\ \times E\left[\max\left(Y_{r_i},\mathbf{1}_{\mathcal{F}_2}(h)Y_h\right)\mid\max\left(Y_{r_i},\mathbf{1}_{\mathcal{F}_2}(h)Y_h\right)\le\min\left(A_1,\mathcal{Z}(\mathcal{F})\text{-}\{i,h\}\right)\right]\end{array}\right)\\
+P\left(A_1\le\min\left(\max\left(Y_{r_i},\mathbf{1}_{\mathcal{F}_2}(h)Y_h\right),\mathcal{Z}(\mathcal{F})\text{-}\{i,h\}\right)\right)\left[\begin{array}{l}
E\left[A_1\mid A_1\le\min\left(\max\left(Y_{r_i},\mathbf{1}_{\mathcal{F}_2}(h)Y_h\right),\mathcal{Z}(\mathcal{F})\text{-}\{i,h\}\right)\right]\\
+\left(\mathbf{1}_{\mathcal{F}_1}(i)+\mathbf{1}_{\mathcal{F}_1}(h)\right)\left(\begin{array}{l}
\left(\begin{array}{l}P\left(\max\left(\mathbf{1}_{\mathcal{F}_1}(i)Y_{r_i},\mathbf{1}_{\mathcal{F}_1}(h)Y_{r_h}\right)\le\min\left(\mathcal{Z}(\mathcal{F}_1)\text{-}\left\{\{i,h\}\in\mathcal{F}_t\right\}\right)\right)\\ \times E\left[\max\left(\mathbf{1}_{\mathcal{F}_1}(i)Y_{r_i},\mathbf{1}_{\mathcal{F}_1}(h)Y_{r_h}\right)\mid\max\left(Y_{r_i},Y_{r_h}\right)\le\min\left(\mathcal{Z}(\mathcal{F}_1)\text{-}\left\{\{i,h\}\in\mathcal{F}_1\right\}\right)\right]\end{array}\right)\\
+\sum\limits_{\substack{l\in\mathcal{F}_1\\ l\ne h\ne i}}\left(\begin{array}{l}P\left(Z_l\le\min\left(\max\left(\mathbf{1}_{\mathcal{F}_1}(i)Y_{r_i},\mathbf{1}_{\mathcal{F}_1}(h)Y_{r_h}\right),\mathcal{Z}(\mathcal{F}_1)\text{-}\left\{\{i,h\}\in\mathcal{F}_1,l\right\}\right)\right)\\ \times\left[\begin{array}{l}E\left[Z_l\mid Z_l\le\min\left(\max\left(\mathbf{1}_{\mathcal{F}_1}(i)Y_{r_i},\mathbf{1}_{\mathcal{F}_1}(h)Y_{r_h}\right),\mathcal{Z}(\mathcal{F}_1)\text{-}\left\{\{i,h\}\in\mathcal{F}_1,l\right\}\right)\right]\\ +E\left[\max\left(\mathbf{1}_{\mathcal{F}_1}(i)Y_{r_i},\mathbf{1}_{\mathcal{F}_1}(h)Y_{r_h},Y_l\right)\right]\end{array}\right]\end{array}\right)
\end{array}\right)
\end{array}\right]\\
+\sum\limits_{\substack{l\in\mathcal{F}\\ l\ne h\ne i}}P\left(Z_l\le\min\left(\max\left(Y_{r_i},\mathbf{1}_{\mathcal{F}_2}(h)Y_h\right),A_1,\mathcal{Z}(\mathcal{F})\text{-}\{i,h,l\}\right)\right)\left[\begin{array}{l}
E\left[Z_l\mid Z_l\le\min\left(\max\left(Y_{r_i},\mathbf{1}_{\mathcal{F}_2}(h)Y_h\right),A_1,\mathcal{Z}(\mathcal{F})\text{-}\{i,h,l\}\right)\right]\\
+\left(\begin{array}{l}P\left(\max\left(Y_{r_i},\mathbf{1}_{\mathcal{F}_2}(h)Y_{r_h},\mathbf{1}_{\mathcal{F}_2}(l)Y_l\right)\le A_1\right)\\ \times E\left[\max\left(Y_{r_i},\mathbf{1}_{\mathcal{F}_2}(h)Y_{r_h},\mathbf{1}_{\mathcal{F}_2}(l)Y_l\right)\mid\mathrm{K}\le A_1\right]\end{array}\right)\\
+\left(\begin{array}{l}P\left(A_1,\le\min\left(\max\left(Y_{r_i},\mathbf{1}_{\mathcal{F}_2}(h)Y_{r_h},\mathbf{1}_{\mathcal{F}_2}(l)Y_l\right)\right)\right)\\ \times\left[\begin{array}{l}E\left[A_1,\mid A_1,\le\min\left(\max\left(Y_{r_i},\mathbf{1}_{\mathcal{F}_2}(h)Y_{r_h},\mathbf{1}_{\mathcal{F}_2}(l)Y_l\right)\right)\right]\\ +E\left[\max\left(\mathbf{1}_{\mathcal{F}_1}(i)Y_{r_i},\mathbf{1}_{\mathcal{F}_1}(h)Y_{r_h},\mathbf{1}_{\mathcal{F}_1}(l)Y_{r_l}\right)\right]\end{array}\right]\end{array}\right)
\end{array}\right]
\end{array}\right]
\end{array}\right) \tag{6.12}
$$

where A_1 is the time until the next class 1 customer arrival and $\mathbf{1}_{\mathcal{F}_j}(i)=\begin{cases}1 & \text{if } i\in\mathcal{F}_j,\\ 0 & \text{if } i\notin\mathcal{F}_j.\end{cases}$.

$$
E\left[T^2_{DS_j|i\in\mathcal{F}\text{-}\mathcal{F}_2}\right]=\left(\begin{array}{l}
P\left(S_{r_j}\le\min\left(A_1,\mathcal{Z}(\mathcal{F})\text{-}\{i\}\right)\right)E\left[S_{r_j}\mid S_{r_j}\le\min\left(A_1,\mathcal{Z}(\mathcal{F})\text{-}\{i\}\right)\right]\\
+P\left(A_1\le\min\left(S_{r_j},\mathcal{Z}(\mathcal{F})\text{-}\{i\}\right)\right)\left[\begin{array}{l}
E\left[A_1\mid A_1\le\min\left(S_{r_j},\mathcal{Z}(\mathcal{F})\text{-}\{i\}\right)\right]\\
+\mathbf{1}_{\mathcal{F}_1}(i)\left(\begin{array}{l}
P\left(Y_{r_i}\le\min\left(\mathcal{Z}(\mathcal{F}_1)\text{-}\{i\}\right)\right)E\left[Y_{r_i}\mid Y_{r_i}\le\min\left(\mathcal{Z}(\mathcal{F}_1)\text{-}\{i\}\right)\right]\\
+\sum\limits_{\substack{h\in\mathcal{F}_1\\ h\ne i}}P\left(Z_h\le\min\left(Y_{r_i},\mathcal{Z}(\mathcal{F}_1)\text{-}\{i,h\}\right)\right)\left[\begin{array}{l}
E\left[Z_h\mid Z_h\le\min\left(Y_{r_i},\mathcal{Z}(\mathcal{F}_1)\text{-}\{i,h\}\right)\right]\\
+\left(\begin{array}{l}
P\left(\max(Y_{r_i},Y_h)\le\min\left(\mathcal{Z}(\mathcal{F}_1)\text{-}\{i,h\}\right)\right)\\
\times E\left[\max(Y_{r_i},Y_h)\mid\max(Y_{r_i},Y_h)\le\min\left(\mathcal{Z}(\mathcal{F}_1)\text{-}\{i,h\}\right)\right]
\end{array}\right)\\
+\sum\limits_{\substack{l\in\mathcal{F}_1\\ l\ne h\ne i}}\left(\begin{array}{l}
P\left(Z_l\le\min\left(\max(Y_{r_i},Y_h),\mathcal{Z}(\mathcal{F}_1)\text{-}\{i,h,l\}\right)\right)\\
\times\left(E\left[Z_l\mid Z_l\le\min\left(\max(Y_{r_i},Y_h),\mathcal{Z}(\mathcal{F}_1)\text{-}\{i,h,l\}\right)\right]+E\left[\max\left(Y_{r_i},Y_{r_h},Y_l\right)\right]\right)
\end{array}\right)
\end{array}\right]
\end{array}\right)\\
+\left(1-\mathbf{1}_{\mathcal{F}_1}(i)\right)\left(\begin{array}{l}
P\left(S_{r_j}\le\min\left(\mathcal{Z}(\mathcal{F}_1)\right)\right)E\left[S_{r_j}\mid S_{r_j}\le\min\left(\mathcal{Z}(\mathcal{F}_1)\right)\right]\\
+\sum\limits_{h\in\mathcal{F}_1}P\left(Z_h\le\min\left(S_{r_j},\mathcal{Z}(\mathcal{F}_1)\text{-}\{h\}\right)\right)\left[\begin{array}{l}
E\left[Z_h\mid Z_h\le\min\left(S_{r_j},\mathcal{Z}(\mathcal{F}_1)\text{-}\{h\}\right)\right]\\
+P\left(Y_h\le\min\left(\mathcal{Z}(\mathcal{F}_1)\text{-}\{h\}\right)\right)E\left[Y_h\mid Y_h\le\min\left(\mathcal{Z}(\mathcal{F}_1)\text{-}\{h\}\right)\right]\\
+\sum\limits_{\substack{l\in\mathcal{F}_1\\ l\ne h}}\left(\begin{array}{l}
P\left(Z_l\le\min\left(Y_h,\mathcal{Z}(\mathcal{F}_1)\text{-}\{h,l\}\right)\right)\\
\times\left(E\left[Z_l\mid Z_l\le\min\left(Y_h,\mathcal{Z}(\mathcal{F}_1)\text{-}\{h,l\}\right)\right]+E\left[\max\left(Y_{r_h},Y_l\right)\right]\right)
\end{array}\right)
\end{array}\right]
\end{array}\right)
\end{array}\right]\\
+\sum\limits_{\substack{h\in\mathcal{F}\\ h\ne i}}P\left(Z_h\le\min\left(S_{r_j},A_1,\mathcal{Z}(\mathcal{F})\text{-}\{i,h\}\right)\right)\left(E\left[Z_h\mid Z_h\le\min\left(S_{r_j},A_1,\mathcal{Z}(\mathcal{F})\text{-}\{i,h\}\right)\right]+\mathbf{1}_{\mathcal{F}_2}(h)\psi_1+\left(1-\mathbf{1}_{\mathcal{F}_2}(h)\right)\psi_2\right)
\end{array}\right)\quad(6.13)
$$

where ψ_1 and ψ_2 are given in (6.17) and (6.18), respectively.

$$\psi_1 = \left(\begin{array}{l} P\left(Y_h \le \min\left(A_1, \mathcal{Z}(\boldsymbol{\mathcal{F}})\text{-}\{i,h\}\right)\right) E\left[Y_h \mid Y_h \le \min\left(A_1, \mathcal{Z}(\boldsymbol{\mathcal{F}})\text{-}\{i,h\}\right)\right] \\ +P\left(A_1 \le \min\left(Y_h, \mathcal{Z}(\boldsymbol{\mathcal{F}})\text{-}\{i,h\}\right)\right) \left[\begin{array}{l} E\left[A_1 \mid A_1 \le \min\left(Y_h, \mathcal{Z}(\boldsymbol{\mathcal{F}})\text{-}\{i,h\}\right)\right] \\ + \left(\begin{array}{l} P\left(\max\left(\mathbf{1}_{\boldsymbol{\mathcal{F}}_1}(i) Y_{r_i}, \mathbf{1}_{\boldsymbol{\mathcal{F}}_1}(h) Y_{r_h}\right) \le \min\left(\mathcal{Z}(\boldsymbol{\mathcal{F}}_1)\text{-}\left\{\mathbf{1}_{\boldsymbol{\mathcal{F}}_1}(i) i, \mathbf{1}_{\boldsymbol{\mathcal{F}}_1}(h) h\right\}\right)\right) \\ \times E\left[\max\left(\mathbf{1}_{\boldsymbol{\mathcal{F}}_1}(i) Y_{r_i}, \mathbf{1}_{\boldsymbol{\mathcal{F}}_1}(h) Y_{r_h}\right) \mid \max\left(\mathbf{1}_{\boldsymbol{\mathcal{F}}_1}(i) Y_{r_i}, \mathbf{1}_{\boldsymbol{\mathcal{F}}_1}(h) Y_{r_h}\right) \le \min\left(\mathcal{Z}(\boldsymbol{\mathcal{F}}_1)\text{-}\left\{\mathbf{1}_{\boldsymbol{\mathcal{F}}_1}(i) i, \mathbf{1}_{\boldsymbol{\mathcal{F}}_1}(h) h\right\}\right)\right] \end{array} \right) \\ + \sum_{\substack{l \in \boldsymbol{\mathcal{F}}_t \\ l \ne i}} \left(\begin{array}{l} P\left(Z_l \le \min\left(\max\left(\mathbf{1}_{\boldsymbol{\mathcal{F}}_1}(i) Y_{r_i}, \mathbf{1}_{\boldsymbol{\mathcal{F}}_1}(h) Y_{r_h}\right), \mathcal{Z}(\boldsymbol{\mathcal{F}}_1)\text{-}\left\{\mathbf{1}_{\boldsymbol{\mathcal{F}}_1}(i) i, \mathbf{1}_{\boldsymbol{\mathcal{F}}_1}(h) h_t, l\right\}\right)\right) \\ \times\left[E\left[Z_l \mid Z_l \le \min\left(\max\left(\mathbf{1}_{\boldsymbol{\mathcal{F}}_1}(i) Y_{r_i}, \mathbf{1}_{\boldsymbol{\mathcal{F}}_1}(h) Y_{r_h}\right), \mathcal{Z}(\boldsymbol{\mathcal{F}}_1)\text{-}\left\{\mathbf{1}_{\boldsymbol{\mathcal{F}}_1}(i) i, \mathbf{1}_{\boldsymbol{\mathcal{F}}_1}(h) h, l\right\}\right)\right] + E\left[\max\left(\mathbf{1}_{\boldsymbol{\mathcal{F}}_1}(i) Y_{r_i}, \mathbf{1}_{\boldsymbol{\mathcal{F}}_1}(h) Y_{r_h}, Y_l\right)\right]\right] \end{array} \right) \end{array} \right] \\ + \sum_{\substack{l \in \boldsymbol{\mathcal{F}} \\ l \ne h \ne i}} P\left(Z_l \le \min\left(Y_h, A_1, \mathcal{Z}(\boldsymbol{\mathcal{F}})\text{-}\{i,h,l\}\right)\right) \left[\begin{array}{l} E\left[Z_l \mid Z_l \le \min\left(Y_h, A_1, \mathcal{Z}(\boldsymbol{\mathcal{F}})\text{-}\{i,h,l\}\right)\right] + \left(P\left(\max\left(Yr_h, \mathbf{1}_{\boldsymbol{\mathcal{F}}_2}(l) Y_l\right) \le A_1\right) E\left[\max\left(Yr_h, \mathbf{1}_{\boldsymbol{\mathcal{F}}_2}(l) Y_l\right) \mid \max\left(Yr_h, \mathbf{1}_{\boldsymbol{\mathcal{F}}_2}(l) Y_l\right) \le A_1\right]\right) \\ + \left(P\left(A_1 \le \max\left(Yr_h, \mathbf{1}_{\boldsymbol{\mathcal{F}}_2}(l) Y_l\right)\right)\left[E\left[A_1 \mid A_1 \le \max\left(Yr_h, \mathbf{1}_{\boldsymbol{\mathcal{F}}_2}(l) Y_l\right)\right] + E\left[\max\left(\mathbf{1}_{\boldsymbol{\mathcal{F}}_1}(i) Y_{r_i}, \mathbf{1}_{\boldsymbol{\mathcal{F}}_1}(h) Y_{r_h}, \mathbf{1}_{\boldsymbol{\mathcal{F}}_1}(l) Y_{r_l}\right)\right]\right]\right) \end{array} \right] \end{array} \right) \tag{6.14}$$

$$\psi_2 = \left(\begin{array}{l} P\left(S_{r_j} \le \min\left(A_1, \mathcal{Z}(\boldsymbol{\mathcal{F}})\text{-}\{i,h\}\right)\right) E\left[S_{r_j} \mid S_{r_j} \le \min\left(A_1, \mathcal{Z}(\boldsymbol{\mathcal{F}})\text{-}\{i,h\}\right)\right] \\ +P\left(A_1 \le \min\left(S_{r_j}, \mathcal{Z}(\boldsymbol{\mathcal{F}})\text{-}\{i,h\}\right)\right) \left[\begin{array}{l} E\left[A_1 \mid A_1 \le \min\left(S_{r_j}, \mathcal{Z}(\boldsymbol{\mathcal{F}})\text{-}\{i,h\}\right)\right] \\ + \left(\begin{array}{l} P\left(\max\left(\mathbf{1}_{\boldsymbol{\mathcal{F}}_1}(i) Y_{r_i}, \mathbf{1}_{\boldsymbol{\mathcal{F}}_1}(h) Y_{r_h}\right) \le \min\left(\mathcal{Z}(\boldsymbol{\mathcal{F}}_t)\text{-}\left\{\mathbf{1}_{\boldsymbol{\mathcal{F}}_1}(i) i, \mathbf{1}_{\boldsymbol{\mathcal{F}}_1}(h) h\right\}\right)\right) \\ \times E\left[\max\left(\mathbf{1}_{\boldsymbol{\mathcal{F}}_1}(i) Y_{r_i}, \mathbf{1}_{\boldsymbol{\mathcal{F}}_1}(h) Y_{r_h}\right) \mid \max\left(Yr_i, Yr_h\right) \le \min\left(\mathcal{Z}(\boldsymbol{\mathcal{F}}_t)\text{-}\left\{\mathbf{1}_{\boldsymbol{\mathcal{F}}_1}(i) i, \mathbf{1}_{\boldsymbol{\mathcal{F}}_1}(h) h\right\}\right)\right] \end{array} \right) \\ + \sum_{\substack{l \in \boldsymbol{\mathcal{F}}_t \\ l \ne i}} \left(\begin{array}{l} P\left(Z_l \le \min\left(\max\left(\mathbf{1}_{\boldsymbol{\mathcal{F}}_1}(i) Y_{r_i}, \mathbf{1}_{\boldsymbol{\mathcal{F}}_1}(h) Y_{r_h}\right), \mathcal{Z}(\boldsymbol{\mathcal{F}}_t)\text{-}\left\{\mathbf{1}_{\boldsymbol{\mathcal{F}}_1}(i) i, \mathbf{1}_{\boldsymbol{\mathcal{F}}_1}(h) h, l\right\}\right)\right) \\ \times\left[E\left[Z_l \mid Z_l \le \min\left(\max\left(\mathbf{1}_{\boldsymbol{\mathcal{F}}_1}(i) Y_{r_i}, \mathbf{1}_{\boldsymbol{\mathcal{F}}_1}(h) Y_{r_h}\right), \mathcal{Z}(\boldsymbol{\mathcal{F}}_t)\text{-}\left\{\mathbf{1}_{\boldsymbol{\mathcal{F}}_1}(i) i, \mathbf{1}_{\boldsymbol{\mathcal{F}}_1}(h) h, l\right\}\right)\right] + E\left[\max\left(\mathbf{1}_{\boldsymbol{\mathcal{F}}_1}(i) Y_{r_i}, \mathbf{1}_{\boldsymbol{\mathcal{F}}_1}(h) Y_{r_h}, Y_l\right)\right]\right] \end{array} \right) \end{array} \right] \\ + \sum_{\substack{l \in \boldsymbol{\mathcal{F}} \\ l \ne h \ne i}} P\left(Z_l \le \min\left(S_{r_j}, A_1, \mathcal{Z}(\boldsymbol{\mathcal{F}})\text{-}\{i,h,l\}\right)\right) \left[\begin{array}{l} E\left[Z_l \mid Z_l \le \min\left(S_{r_j}, A_1, \mathcal{Z}(\boldsymbol{\mathcal{F}})\text{-}\{i,h,l\}\right)\right] \\ +\left(l \in \boldsymbol{\mathcal{F}}_m\right)\left(\left(P\left(Y_l \le A_1\right) E\left[Y_l \mid Y_l \le A_1\right]\right) + P\left(A_1 \le Y_l\right)\left[E\left[A_1 \mid A_1 \le Y_l\right] + E\left[\max\left(\mathbf{1}_{\boldsymbol{\mathcal{F}}_1}(i) Y_{r_i}, \mathbf{1}_{\boldsymbol{\mathcal{F}}_1}(h) Y_{r_h}, \mathbf{1}_{\boldsymbol{\mathcal{F}}_1}(l) Y_{r_l}\right)\right]\right]\right) \\ +\left(l \notin \boldsymbol{\mathcal{F}}_m\right)\left(\left(P\left(S_{r_j} \le A_1\right) E\left[S_{r_j} \mid S_{r_j} \le A_1\right]\right) + P\left(A_1 \le S_{r_j}\right)\left(E\left[A_1 \mid A_1 \le S_{r_j}\right] + E\left[\max\left(\mathbf{1}_{\boldsymbol{\mathcal{F}}_1}(i) Y_{r_i}, \mathbf{1}_{\boldsymbol{\mathcal{F}}_1}(h) Y_{r_h}, \mathbf{1}_{\boldsymbol{\mathcal{F}}_1}(l) Y_{r_l}\right)\right]\right)\right) \end{array} \right] \end{array} \right) \tag{6.15}$$

6.2.2 REMAINING SERVICE COMPLETION TIME (C_r)

The remaining service completion time of the current customer in service as observed by an arrival, C_r, is the time until the next customer (if any) may start its service. It consists of the remaining actual service time of the customer, $S_{r_{a_j}}$, and the downtime experienced by the customer during its remaining service completion time, T_{DRS_j}. In the case of two priority classes and *k* class-dependent interruptions, an arriving customer can find a customer from either one of the two priority classes in the server. Therefore, expected remaining service completion time can be expressed as follows:

$$E\left[C_r\right] = \sum_{j=1}^{2} \rho_j \left(E[S_{r_{a_j}}] + E[T_{DRS_j}] \right) \tag{6.16}$$

where ρ_j is the probability that the arriving customer finds a class *j* customer in the server at the time of its arrival.

The remaining actual service time of a customer of class *j*, $S_{r_{a_j}}$, can be evaluated using (4.21) and (5.10).

Similar to $E[T_{DS_j}]$ explained in Section 6.2.1, the expected downtime experienced by a class *j* customer during its remaining service, $E[T_{DRS_j}]$, depends not only on the class of the customer in service, but also the class of the next customer waiting at the head of the queue. Thus, $E[T_{DRS_j}]$ is given by

$$E\left[T_{DRS_j}\right] = \sum_{m=1}^{2} q^m E\left[T_{DRS_j}^m\right] \tag{6.17}$$

where q^m is evaluated using (6.10).

Using arguments similar to $E[T_{DS_j}]$, we have

$$\begin{aligned} E\left[T_{DRS_j}^m\right] &= \sum_{i \in \mathcal{F}_m} P\left(Z_i \le \min\left(S_{r_j}, \mathcal{Z}\text{-}\{i\}\right)\right) E\left[T_{DRS_j|i \in \mathcal{F}_m}^m\right] \\ &\quad + \sum_{i \in \mathcal{F}\text{-}\mathcal{F}_m} P\left(Z_i \le \min\left(S_{r_j}, \mathcal{Z}\text{-}\{i\}\right)\right) E\left[T_{DRS_j|i \in \mathcal{F}\text{-}\mathcal{F}_m}^m\right] \end{aligned} \tag{6.18}$$

where $E\left[T_{DRS_j|i \in \mathcal{F}_m}^m\right] = E\left[T_{DS_j|i \in \mathcal{F}_m}^m\right]$ and $E\left[T_{DRS_j|i \in \mathcal{F}\text{-}\mathcal{F}_m}^m\right] = E\left[T_{DS_j|i \in \mathcal{F}\text{-}\mathcal{F}_m}^m\right]$.

6.2.3 REMAINING SYSTEM DOWNTIME (T_{RD})

In this section, we present the remaining system downtime as observed by an arriving customer. We define the remaining system downtime as the remaining duration of a down cycle.

Since, based on our approximation, we limit the number of interruptions that can occur during a service time to three, the server may be down due to at most three different interruptions upon a customer arrival. If the system is down due to one type of interruption, one or two more types of interruptions may still occur during the down cycle. Conversely, if the system is experiencing two interruptions simultaneously, then the third may still occur during the same down cycle.

In this case, the remaining system downtime when it is down upon arrival of a class *j* customer, T_{RD_j}, depends on the class of the customer waiting at the head of the queue. Therefore, T_{RD_j} is defined by

$$E\left[T_{RD_j}\right] = \sum_{m=1}^{j} q^m \, E\left[T_{RD_j}^m\right] \tag{6.19}$$

where $T_{RD_j}^m$ is the remaining system downtime when a class *m* customer is waiting at the head of the queue. $E\left[T_{RD_j}^1\right]$ can be obtained using (6.23).

$$
\begin{aligned}
E\left[T_{RD_j}^{1}\right] = {} & \sum_{i\in\mathcal{F}_1} P_{d,i}\left(\prod_{\substack{m\in\mathcal{F}_1\\ m\neq i}}\left(1-P_{d,m}\right)\right)
\left[\begin{array}{l}
P\left(Y_{r_i}\leq \min\left(\mathcal{Z}(\mathcal{F}_1)\text{-}\{i\}\right)\right)E\left[Y_{r_i}\mid Y_{r_i}\leq \min\left(\mathcal{Z}(\mathcal{F}_1)\text{-}\{i\}\right)\right]\\
+\sum\limits_{\substack{h\in\mathcal{F}_1\\ h\neq i}} P\left(Z_h\leq \min\left(Y_{r_i},\mathcal{Z}(\mathcal{F}_1)\text{-}\{i\}\right)\right)
\left[\begin{array}{l}
E\left[Z_h\mid Z_h\leq \min\left(Y_{r_i},\mathcal{Z}(\mathcal{F}_1)\text{-}\{i\}\right)\right]\\
+\left[P\left(\max(Y_{r_i},Y_h)\leq \min\left(\mathcal{Z}(\mathcal{F}_1)\text{-}\{i,h\}\right)\right)\times E\left[\max(Y_{r_i},Y_h)\mid \max(Y_{r_i},Y_h)\leq \min\left(\mathcal{Z}(\mathcal{F}_1)\text{-}\{i,h\}\right)\right]\right]\\
+\sum\limits_{\substack{l\in\mathcal{F}_1\\ l\neq h\neq i}}
\left[\begin{array}{l}
P\left(Z_l\leq \min\left(\max(Y_{r_i},Y_h),\mathcal{Z}(\mathcal{F}_1)\text{-}\{i,h,l\}\right)\right)\\
\times\left[\begin{array}{l}
+\left(P\left(Y_{r_i}>\max(Y_{r_h},Y_l)\right)\times\left(\begin{array}{l}E\left[Z_l\mid Z_l\leq \min\left(Y_{r_i},\mathcal{Z}(\mathcal{F}_1)\text{-}\{i,h,l\}\right)\right]\\ +E\left[Y_{r_i}\mid Y_{r_i}>\max(Y_{r_h},Y_h)\right]\end{array}\right)\right)\\
+\left(P\left(Yr_h>\max(Yr_i,Y_l)\right)\times\left(\begin{array}{l}E\left[Z_l\mid Z_l\leq \min\left(Y_{r_h},\mathcal{Z}(\mathcal{F}_1)\text{-}\{i,h,l\}\right)\right]\\ +E\left[Y_{r_h}\mid Y_{r_h}>\max(Yr_i,Y_l)\right]\end{array}\right)\right)\\
+\left(P\left(Y_l>\max(Y_{r_i},Y_{r_h})\right)\left(\begin{array}{l}E\left[Z_l\mid Z_l\leq \min\left(\max(Y_{r_i},Y_h),\mathcal{Z}(\mathcal{F}_1)\text{-}\{i,h,l\}\right)\right]\\ +E\left[Y_l\mid Y_l>\max(Y_{r_i},Y_{r_h})\right]\end{array}\right)\right)
\end{array}\right]
\end{array}\right]
\end{array}\right]
\end{array}\right]\\
& +\sum_{i\in\mathcal{F}_1} P_{d,i}\sum_{\substack{h\in\mathcal{F}_1\\ h\neq i}} P_{d,h}\left(\prod_{\substack{m\in\mathcal{F}_1\\ m\neq h\neq i}}\left(1-P_{d,m}\right)\right)
\left[\begin{array}{l}
P\left(\max(Y_{r_i},Y_{r_h})\leq \min\left(\mathcal{Z}(\mathcal{F}_1)\text{-}\{i,h\}\right)\right)\times E\left[\max(Y_{r_i},Y_{r_h})\middle|\max(Y_{r_i},Y_{r_h})\leq \min\left(\mathcal{Z}(\mathcal{F}_1)\text{ - }\{i,h\}\right)\right]\\
+\sum\limits_{\substack{l\in\mathcal{F}_1\\ l\neq h\neq i}}
\left[\begin{array}{l}
P\left(Z_l\leq \min\left(\max(Y_{r_i},Y_{r_h}),\mathcal{Z}(\mathcal{F}_1)\text{-}\{i,h,l\}\right)\right)\\
\times\left[\begin{array}{l}
P\left(Y_{r_i}>\max(Y_{r_h},Y_l)\right)\left(E\left[Z_l\mid Z_l\leq \min\left(Y_{r_i},\mathcal{Z}(\mathcal{F}_1)\text{ - }\{i,h\}\right)\right]+E\left[Y_{r_i}\mid Y_{r_i}>\max(Y_{r_h},Y_l)\right]\right)\\
+P\left(Y_{r_h}>\max(Y_{r_i},Y_l)\right)\left(E\left[Z_l\mid Z_l\leq \min\left(Y_{r_h},\mathcal{Z}(\mathcal{F}_1)\text{ - }\{i,h\}\right)\right]+E\left[Y_{r_h}\mid Y_{r_h}>\max(Y_{r_i},Y_l)\right]\right)\\
+P\left(Y_l>\max(Y_{r_i},Y_{r_h})\right)\left(\begin{array}{l}E\left[Z_l\mid Z_l\leq \min\left(\max(Y_{r_i},Y_{r_h}),\mathcal{Z}(\mathcal{F}_1)\text{ - }\{i,h\}\right)\right]\\ +E\left[Y_l\mid Y_l>\max(Y_{r_i},Y_{r_h})\right]\end{array}\right)
\end{array}\right]
\end{array}\right]
\end{array}\right]\\
& +\sum_{i\in\mathcal{F}_1} P_{d,i}\sum_{\substack{h\in\mathcal{F}_1\\ h\neq i}} P_{d,h}\sum_{\substack{l\in\mathcal{F}_1\\ l\neq h\neq i}} P_{d,l}\left(\prod_{\substack{m\in\mathcal{F}_1\\ m\neq l\neq h\neq i}}\left(1-P_{d,m}\right)\right)E\left[\max(Y_{r_i},Y_{r_h},Y_{r_l})\right]
\end{aligned}
\tag{6.20}
$$

Furthermore, $E\left[T_{RD_j}^2\right]$ is defined by

$$E\left[T_{RD_j}^2\right]=\left(\begin{array}{l}\sum_{i\in\mathcal{F}_2} P_{d,i}\left(\prod_{\substack{m\in\mathcal{F}\\ m\neq i}}\left(1-P_{d,m}\right)\right)\xi_1 \\ +\sum_{i=1}^{k-1} P_{d,i}\sum_{h=i+1}^{k} P_{d,h}\left(\left(i\in\mathcal{F}_j\right)\vee\left(h\in\mathcal{F}_j\right)\right)\left(\prod_{\substack{m=1\\ m\neq i\neq h}}^{k}\left(1-P_{d,m}\right)\right)\xi_2 \\ +\sum_{i=1}^{k-2} P_{d,i}\sum_{h=i+1}^{k-1} P_{d,h}\sum_{l=h+1}^{k} P_{d,l}\left(\prod_{\substack{m=1\\ m\neq i\neq h\neq l}}^{k}\left(1-Pd_m\right)\right)\xi_3\end{array}\right) \tag{6.21}$$

where ξ_1, ξ_2, and ξ_3 are obtained using (6.25), (6.26) and (6.27), respectively.

$$
\xi_1 = \left[\begin{array}{l}
P\left(Y_{r_i} \le \min\left(A_1, \mathcal{Z}(\mathcal{F})\text{-}\{i\}\right)\right) E\left[Y_{r_i} \mid Y_{r_i} \le \min\left(A_1, \mathcal{Z}(\mathcal{F})\text{-}\{i\}\right)\right] \\
+P\left(A_1 \le \min\left(Y_{r_i}, \mathcal{Z}(\mathcal{F})\text{-}\{i\}\right)\right) \left[\begin{array}{l}
E\left[A_1 \mid A_1 \le \min\left(Y_{r_i}, \mathcal{Z}(\mathcal{F})\text{-}\{i\}\right)\right] \\
+\mathbf{1}_{\mathcal{F}_1}(i) \left(\begin{array}{l}
P\left(Y_{r_i} \le \min\left(\mathcal{Z}(\mathcal{F}_1)\text{-}\{i\}\right)\right) E\left[Y_{r_i} \mid Y_{r_i} \le \min\left(\mathcal{Z}(\mathcal{F}_1)\text{-}\{i\}\right)\right] \\
+\sum\limits_{\substack{h \in \mathcal{F}_1 \\ h \ne i}} P\left(Z_h \le \min\left(Y_{r_i}, \mathcal{Z}(\mathcal{F}_1)\text{-}\{i,h\}\right)\right) \left[\begin{array}{l}
E\left[Z_h \mid Z_h \le \min\left(Y_{r_i}, \mathcal{Z}(\mathcal{F}_1)\text{-}\{i,h\}\right)\right] + \left[\begin{array}{l}
P\left(\max(Y_{r_i}, Y_h) \le \min\left(\mathcal{Z}(\mathcal{F}_1)\text{-}\{i,h\}\right)\right) \\
\times E\left[\max(Y_{r_i}, Y_h) \mid \max(Y_{r_i}, Y_h) \le \min\left(\mathcal{Z}(\mathcal{F}_1)\text{-}\{i,h\}\right)\right]
\end{array} \right] \\
+\sum\limits_{\substack{l \in \mathcal{F}_1 \\ l \ne h \ne i}} P\left(Z_l \le \min\left(\max(Y_{r_i}, Y_h), \mathcal{Z}(\mathcal{F}_1)\text{-}\{i,h,l\}\right)\right) \left[\begin{array}{l}
E\left[Z_l \mid Z_l \le \min\left(\max(Y_{r_i}, Y_h), \mathcal{Z}(\mathcal{F}_1)\text{-}\{i,h,l\}\right)\right] \\
+E\left[\max\left(Y_{r_i}, Y_{r_h}, Y_l\right)\right]
\end{array} \right]
\end{array} \right]
\end{array} \right)
\end{array} \right] \\
+\sum\limits_{\substack{h \in \mathcal{F} \\ h \ne i}} P\left(Z_h \le \min\left(Y_{r_i}, A_1, \mathcal{Z}(\mathcal{F})\text{-}\{i,h\}\right)\right) \left[\begin{array}{l}
E\left[Z_h \mid Z_h \le \min\left(Y_{r_i}, A_1, \mathcal{Z}(\mathcal{F})\text{-}\{i,h\}\right)\right] \\
+\left[P\left(\max(Y_{r_i}, \mathbf{1}_{\mathcal{F}_2}(h) Y_h) \le \min\left(A_1, \mathcal{Z}(\mathcal{F})\text{-}\{i,h\}\right)\right) \times E\left[\max(Y_{r_i}, \mathbf{1}_{\mathcal{F}_2}(h) Y_h) \mid \max(Y_{r_i}, \mathbf{1}_{\mathcal{F}_2}(h) Y_h) \le \min\left(A_1, \mathcal{Z}(\mathcal{F})\text{-}\{i,h\}\right)\right]\right] \\
+P\left(A_1 \le \min\left(\max(Y_{r_i}, \mathbf{1}_{\mathcal{F}_2}(h) Y_h), \mathcal{Z}(\mathcal{F})\text{-}\{i,h\}\right)\right) \left(\begin{array}{l}
E\left[A_1 \mid A_1 \le \min\left(\max(Y_{r_i}, \mathbf{1}_{\mathcal{F}_2}(h) Y_h), \mathcal{Z}(\mathcal{F})\text{-}\{i,h\}\right)\right] \\
+\left(\begin{array}{l}
\left(\mathbf{1}_{\mathcal{F}_1}(i) + \mathbf{1}_{\mathcal{F}_1}(h)\right) \\
\times \left(\begin{array}{l}
\left(\begin{array}{l}
P\left(\max\left(\mathbf{1}_{\mathcal{F}_1}(i) Y_{r_i}, \mathbf{1}_{\mathcal{F}_1}(h) Y_{r_h}\right) \le \min\left(\mathcal{Z}(\mathcal{F}_t)\text{-}\left\{\mathbf{1}_{\mathcal{F}_1}(i) i, \mathbf{1}_{\mathcal{F}_1}(h) h\right\}\right)\right) \\
\times E\left[\max\left(\mathbf{1}_{\mathcal{F}_1}(i) Y_{r_i}, \mathbf{1}_{\mathcal{F}_1}(h) Y_{r_h}\right) \mid \max\left(\mathbf{1}_{\mathcal{F}_1}(i) Y_{r_i}, \mathbf{1}_{\mathcal{F}_1}(h) Y_{r_h}\right) \le \min\left(\mathcal{Z}(\mathcal{F}_t)\text{-}\left\{\mathbf{1}_{\mathcal{F}_1}(i) i, \mathbf{1}_{\mathcal{F}_1}(h) h\right\}\right)\right]
\end{array} \right) \\
+\sum\limits_{\substack{l \in \mathcal{F}_1 \\ l \ne h \ne i}} \left[\begin{array}{l}
P\left(Z_l \le \min\left(\max\left(\mathbf{1}_{\mathcal{F}_1}(i) Y_{r_i}, \mathbf{1}_{\mathcal{F}_1}(h) Y_{r_h}\right), \mathcal{Z}(\mathcal{F}_t)\text{-}\left\{\mathbf{1}_{\mathcal{F}_1}(i) i, \mathbf{1}_{\mathcal{F}_1}(h) h\right\}\right)\right) \\
\times \left[\begin{array}{l}
E\left[Z_l \mid Z_l \le \min\left(\max\left(\mathbf{1}_{\mathcal{F}_1}(i) Y_{r_i}, \mathbf{1}_{\mathcal{F}_1}(h) Y_{r_h}\right), \mathcal{Z}(\mathcal{F}_t)\text{-}\left\{\mathbf{1}_{\mathcal{F}_1}(i) i, \mathbf{1}_{\mathcal{F}_1}(h) h\right\}\right)\right] \\
+E\left[\max\left(\mathbf{1}_{\mathcal{F}_1}(i) Y_{r_i}, \mathbf{1}_{\mathcal{F}_1}(h) Y_{r_h}, Y_l\right)\right]
\end{array} \right]
\end{array} \right]
\end{array} \right)
\end{array} \right)
\end{array} \right) \\
+\sum\limits_{\substack{l \in \mathcal{F} \\ l \ne h \ne i}} P\left(Z_l \le \min\left(\max\left(Y_{r_i}, \mathbf{1}_{\mathcal{F}_2}(h) Y_h\right), A_1, \mathcal{Z}(\mathcal{F})\text{-}\{i,h,l\}\right)\right) \left[\begin{array}{l}
E\left[Z_l \mid Z_l \le \min\left(\max\left(Y_{r_i}, \mathbf{1}_{\mathcal{F}_2}(h) Y_h\right), A_1, \mathcal{Z}(\mathcal{F})\text{-}\{i,h,l\}\right)\right] \\
+\left(\begin{array}{l}
P\left(\max\left(Y_{r_i}, \mathbf{1}_{\mathcal{F}_2}(h) Y_{r_h}, \mathbf{1}_{\mathcal{F}_2}(l) Y_l\right) \le A_1\right) \\
\times E\left[\max\left(Y_{r_i}, \mathbf{1}_{\mathcal{F}_2}(h) Y_{r_h}, \mathbf{1}_{\mathcal{F}_2}(l) Y_l\right) \mid \max\left(Y_{r_i}, \mathbf{1}_{\mathcal{F}_2}(h) Y_{r_h}, \mathbf{1}_{\mathcal{F}_2}(l) Y_l\right) \le A_1\right]
\end{array} \right) \\
+\left(P\left(A_1 \le \max\left(Y_{r_i}, \mathbf{1}_{\mathcal{F}_2}(h) Y_{r_h}, \mathbf{1}_{\mathcal{F}_2}(l) Y_l\right)\right) \left[\begin{array}{l}
E\left[A_1 \mid A_1 \le \max\left(Y_{r_i}, \mathbf{1}_{\mathcal{F}_2}(h) Y_{r_h}, \mathbf{1}_{\mathcal{F}_2}(l) Y_l\right)\right] \\
+E\left[\max\left(\mathbf{1}_{\mathcal{F}_1}(i) Y_{r_i}, \mathbf{1}_{\mathcal{F}_1}(h) Y_{r_h}, \mathbf{1}_{\mathcal{F}_1}(l) Y_{r_l}\right)\right]
\end{array} \right] \right)
\end{array} \right]
\end{array} \right]
\end{array} \right] \tag{6.22}
$$

$$
\begin{aligned}
\xi_2 = \Bigg[& P\left(\max\left(\mathbf{1}_{\mathcal{F}_2}(i)Y_{r_i},\mathbf{1}_{\mathcal{F}_2}(h)Y_{r_h}\right) \le \min\left(A_1,\mathcal{Z}\text{-}\{i,h\}\right)\right) \times E\left[\max\left(\mathbf{1}_{\mathcal{F}_2}(i)Y_{r_i},\mathbf{1}_{\mathcal{F}_2}(h)Y_{r_h}\right) \Big| \max\left(\mathbf{1}_{\mathcal{F}_2}(i)Y_{r_i},\mathbf{1}_{\mathcal{F}_2}(h)Y_{r_h}\right) \le \min\left(A_1,\mathcal{Z}\text{-}\{i,h\}\right)\right] \\
& +\sum_{t=1}^{j-1} P\left(A_1 \le \min\left(\max\left(\mathbf{1}_{\mathcal{F}_2}(i)Y_{r_i},\mathbf{1}_{\mathcal{F}_2}(h)Y_{r_h}\right),\mathcal{Z}(\mathcal{F})\text{-}\{i,h\}\right)\right) \Bigg(E\left[A_1 \mid A_1 \le \min\left(\max\left(\mathbf{1}_{\mathcal{F}_2}(i)Y_{r_i},\mathbf{1}_{\mathcal{F}_2}(h)Y_{r_h}\right),\mathcal{Z}(\mathcal{F})\text{-}\{i,h\}\right)\right] \\
& \quad + \Bigg(\left(\mathbf{1}_{\mathcal{F}_1}(i)+\mathbf{1}_{\mathcal{F}_1}(h)\right) \times \Bigg(\Bigg(P\left(\max\left(\mathbf{1}_{\mathcal{F}_1}(i)Y_{r_i},\mathbf{1}_{\mathcal{F}_1}(h)Y_{r_h}\right) \le \min\left(\mathcal{Z}(\mathcal{F}_t)\text{-}\left\{\mathbf{1}_{\mathcal{F}_1}(i)i,\mathbf{1}_{\mathcal{F}_1}(h)h\right\}\right)\right) \\
& \quad\quad \times E\left[\max\left(\mathbf{1}_{\mathcal{F}_1}(i)Y_{r_i},\mathbf{1}_{\mathcal{F}_1}(h)Y_{r_h}\right) \mid \max\left(\mathbf{1}_{\mathcal{F}_1}(i)Y_{r_i},\mathbf{1}_{\mathcal{F}_1}(h)Y_{r_h}\right) \le \min\left(\mathcal{Z}(\mathcal{F}_t)\text{-}\left\{\mathbf{1}_{\mathcal{F}_1}(i)i,\mathbf{1}_{\mathcal{F}_1}(h)h\right\}\right)\right] \Bigg) \\
& \quad\quad + \sum_{\substack{l\in\mathcal{F}_1 \\ l\ne h\ne i}} \Bigg[P\left(Z_l \le \min\left(\max\left(\mathbf{1}_{\mathcal{F}_1}(i)Y_{r_i},\mathbf{1}_{\mathcal{F}_1}(h)Y_{r_h}\right),\mathcal{Z}(\mathcal{F}_t)\text{-}\left\{\mathbf{1}_{\mathcal{F}_1}(i)i,\mathbf{1}_{\mathcal{F}_1}(h)h,l\right\}\right)\right) \\
& \quad\quad\quad \times \Bigg[E\left[Z_l \mid Z_l \le \min\left(\max\left(\mathbf{1}_{\mathcal{F}_1}(i)Y_{r_i},\mathbf{1}_{\mathcal{F}_1}(h)Y_{r_h}\right),\mathcal{Z}(\mathcal{F}_t)\text{-}\left\{\mathbf{1}_{\mathcal{F}_1}(i)i,\mathbf{1}_{\mathcal{F}_1}(h)h,l\right\}\right)\right] + E\left[\max\left(\mathbf{1}_{\mathcal{F}_1}(i)Y_{r_i},\mathbf{1}_{\mathcal{F}_1}(h)Y_{r_h},Y_l\right)\right] \Bigg] \Bigg] \Bigg) \Bigg) \Bigg) \\
& +\sum_{\substack{l=1 \\ l\ne h\ne i}}^{k} P\left(Z_l \le \min\left(\max\left(\mathbf{1}_{\mathcal{F}_2}(i)Y_{r_i},\mathbf{1}_{\mathcal{F}_2}(h)Y_{r_h}\right),A_1,\mathcal{Z}(\mathcal{F})\text{-}\{i,h,l\}\right)\right) \Bigg[E\left[Z_l \mid Z_l \le \min\left(\max\left(\mathbf{1}_{\mathcal{F}_2}(i)Y_{r_i},\mathbf{1}_{\mathcal{F}_2}(h)Y_{r_h}\right),A_1,\mathcal{Z}(\mathcal{F})\text{-}\{i,h,l\}\right)\right] \\
& \quad + \Bigg(P\left(\max\left(\mathbf{1}_{\mathcal{F}_2}(i)Y_{r_i},\mathbf{1}_{\mathcal{F}_2}(h)Y_{r_h},\mathbf{1}_{\mathcal{F}_2}(l)Y_{r_l}\right) \le \min\left(A_1,\mathcal{Z}(\mathcal{F})\text{-}\{i,h,l\}\right)\right) \\
& \quad\quad \times E\left[\max\left(\mathbf{1}_{\mathcal{F}_2}(i)Y_{r_i},\mathbf{1}_{\mathcal{F}_2}(h)Y_{r_h},\mathbf{1}_{\mathcal{F}_2}(l)Y_{r_l}\right) \Big| \max\left(\mathbf{1}_{\mathcal{F}_2}(i)Y_{r_i},\mathbf{1}_{\mathcal{F}_2}(h)Y_{r_h},\mathbf{1}_{\mathcal{F}_2}(l)Y_{r_l}\right) \le \min\left(A_1,\mathcal{Z}(\mathcal{F})\text{-}\{i,h,l\}\right)\right] \Bigg) \\
& \quad + \Bigg[P\left(A_1 \le \min\left(\max\left(\mathbf{1}_{\mathcal{F}_2}(i)Y_{r_i},\mathbf{1}_{\mathcal{F}_2}(h)Y_{r_h},\mathbf{1}_{\mathcal{F}_2}(l)Y_{r_l}\right),\mathcal{Z}(\mathcal{F})\text{-}\{i,h,l\}\right)\right) \\
& \quad\quad \times \Bigg(E\left[A_1 \Big| A_1 \le \min\left(\max\left(\mathbf{1}_{\mathcal{F}_2}(i)Y_{r_i},\mathbf{1}_{\mathcal{F}_2}(h)Y_{r_h},\mathbf{1}_{\mathcal{F}_2}(l)Y_{r_l}\right),\mathcal{Z}(\mathcal{F})\text{-}\{i,h,l\}\right)\right] + E\left[\max\left(\mathbf{1}_{\mathcal{F}_1}(i)Y_{r_i},\mathbf{1}_{\mathcal{F}_1}(h)Y_{r_h},\mathbf{1}_{\mathcal{F}_1}(l)Y_{r_l}\right)\right] \Bigg) \Bigg] \Bigg] \Bigg]
\end{aligned}
\qquad (6.23)
$$

$$\xi_3 = \left[\begin{array}{l} \left(\begin{array}{l} P\left(\max\left(\mathbf{1}_{\mathcal{F}_2}(i) Y_{r_i}, \mathbf{1}_{\mathcal{F}_2}(h) Y_{r_h}, \mathbf{1}_{\mathcal{F}_2}(l) Y_{r_l} \right) \leq A_1 \right) \\ \times E\left[\max\left(\mathbf{1}_{\mathcal{F}_2}(i) Y_{r_i}, \mathbf{1}_{\mathcal{F}_2}(h) Y_{r_h}, \mathbf{1}_{\mathcal{F}_2}(l) Y_{r_l} \right) \middle| \max\left(\Upsilon r\left(\{i,h,l\} \in \mathcal{F}_j \right) \right) \leq A_1 \right] \end{array} \right) \\ + \left(\begin{array}{l} P\left(A_1 \leq \max\left(\mathbf{1}_{\mathcal{F}_2}(i) Y_{r_i}, \mathbf{1}_{\mathcal{F}_2}(h) Y_{r_h}, \mathbf{1}_{\mathcal{F}_2}(l) Y_{r_l} \right) \right) \\ \times \left[\begin{array}{l} E\left[A_1 \middle| A_1 \leq \max\left(\mathbf{1}_{\mathcal{F}_2}(i) Y_{r_i}, \mathbf{1}_{\mathcal{F}_2}(h) Y_{r_h}, \mathbf{1}_{\mathcal{F}_2}(l) Y_{r_l} \right) \right] \\ + E\left[\max\left(\mathbf{1}_{\mathcal{F}_2}(i) Y_{r_i}, \mathbf{1}_{\mathcal{F}_2}(h) Y_{r_h}, \mathbf{1}_{\mathcal{F}_2}(l) Y_{r_l} \right) \right] \end{array} \right] \end{array} \right) \end{array} \right] \tag{6.24}$$

6.3 NUMERICAL RESULTS

In this section, the accuracy of the approximation method for two-class systems with possibly simultaneous class-dependent interruptions is evaluated by comparing its results to the results of a simulation model representing the queueing system under discussion in a number of different scenarios. The simulation model is developed using the ARENA© simulation tool. The simulated results were obtained from 10 replications, each simulating 3.5 million customers. The average waiting time of a class j ($j = 1, 2$) customer, $E[W_j]$, is obtained in both approaches.

In addition, we present the impact of a change in different system parameters such as service time variability, downtime variability, system utilization, downtime probability, and number of interruptions on $E[C]$ and $E[W]$ in different scenarios.

© ARENA is a trademark of Rockwell software.

We use the following assumptions common to all scenarios:

- Poisson customer arrivals
- Exponential times to interruption

We conduct five sets of experiments changing the following key variables:

i. Cv^2 of service time

ii. Cv^2 of downtime

iii. System utilization *(P(B))*

iv. Downtime probability *(Pd)*

v. Number of interruptions *(k)*

In each experiment, we vary one parameter while keeping all the others invariant at their base values as shown in Table 6.1, where the shaded areas indicate the base values.

Table 6.1 Parameters used in experiments in the class-dependent interruptions case

Parameter	**Values**				
Cv^2(Service Time)	0	0.25	3		
Cv^2(Downtime)	0.25	0.5	1	1.5	3
System Utilization (*P(B)*)	60%	70%	80%	90%	
Downtime Probability (P_d)	5%	10%	15%	20%	25%
Number of Interruptions (*k*)	3	4	5	6	

6.3.1 IMPACT OF SERVICE TIME VARIABILITY

Figures 6.1 and 6.2 show the impact of the squared coefficient of variation of the service times, $Cv_S^{\,2}$, on the average waiting time of a high priority customer, $E[W_1]$, and a low priority customer, $E[W_2]$, respectively, in the case of class-dependent interruptions. Higher $Cv_S^{\,2}$ values result in higher expected waiting time values for both of the classes. In addition, the average waiting times decrease in general when the total number of interruptions, k, increases. This is due to the fact that we kept the same down time probability as we have increased the number of interruptions resulting in smaller downtimes per interruption which in turn reduced customer waiting times.

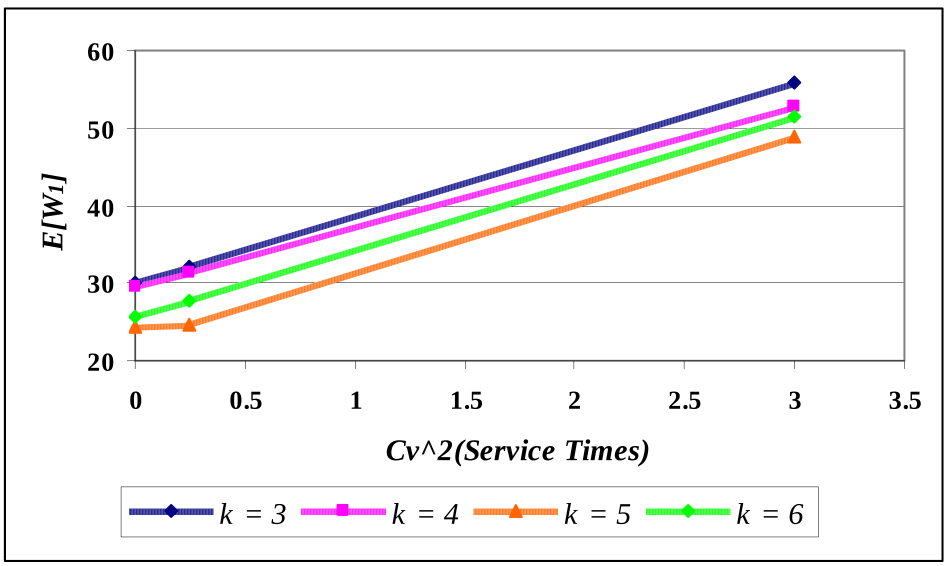

Figure 6.1 Impact of $Cv_S^{\,2}$ on $E[W_1]$ in the class-dependent interruptions case

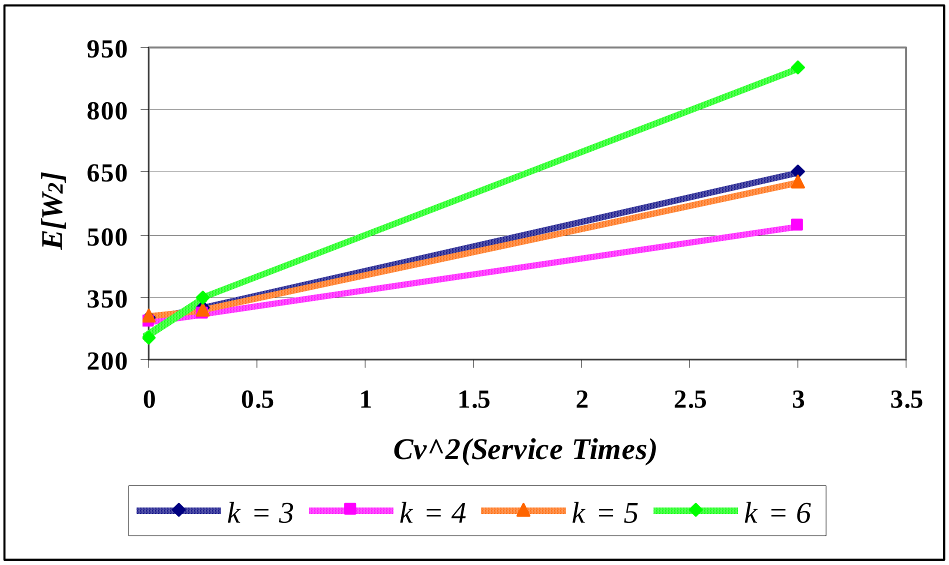

Figure 6.2 Impact of $Cv_S^{\,2}$ on $E[W_2]$ in the class-dependent interruptions case

The detailed results obtained by changing $Cv_S^{\,2}$ and k are shown in Table 6.2 including the relative errors comparing the analytical and simulation results for the expected waiting time of the high priority class, $E[W_1]$ and the low priority class, $E[W_2]$.

We observe that the error levels associated with $E[W_1]$ and $E[W_2]$ remain below 3% as we increase the squared coefficient of variation of the service time, $Cv_S^{\,2}$, from 0 to 3, and the number of interruptions, k, from 3 to 6.

The error levels increase in general as we increase the values for $Cv_S^{\,2}$ and k. Also, the average error for the average waiting time across different values of $Cv_S^{\,2}$ increases as the number of interruptions increases.

Table 6.2 $E[W_j]$ in the class-dependent interruptions case when changing $Cv_S^{\ 2}$

k	***$Cv^2(S)$***	***E[W₁]***			***E[W₂]***		
		Analytical	**Simulation**	**Error**	**Analytical**	**Simulation**	**Error**
3	0 (Det.)	29.9452	29.6920	0.8528	302.7870	305.0600	0.7451
	0.25 (4-Erlang)	32.1068	32.4022	0.9117	323.8389	327.7700	1.1993
	3 (2-HyperEx)	55.7428	56.6475	1.5971	653.3737	662.2600	1.3418
			AVERAGE ERROR	1.1205		AVERAGE ERROR	1.0954
4	0 (Det.)	29.5602	29.0988	1.5856	292.4250	296.9800	1.5338
	0.25 (4-Erlang)	31.3182	31.8326	1.6160	309.3650	314.8900	1.7546
	3 (2-HyperEx)	52.8020	53.7341	1.7347	523.2591	533.5000	1.9196
			AVERAGE ERROR	1.6454		AVERAGE ERROR	1.7360
5	0 (Det.)	24.3846	24.7970	1.6631	304.1408	309.4400	1.7125
	0.25 (4-Erlang)	24.6264	25.0947	1.8661	321.1755	327.7400	2.0030
	3 (2-HyperEx)	48.9737	50.0123	2.0767	626.3289	642.2000	2.4714
			AVERAGE ERROR	1.8686		AVERAGE ERROR	2.0623
6	0 (Det.)	25.7910	26.1707	1.4509	255.1220	259.8000	1.8006
	0.25 (4-Erlang)	27.6883	28.2225	1.8928	349.3831	357.5900	2.2951
	3 (2-HyperEx)	51.4696	52.5633	2.0807	904.1117	927.6500	2.5374
			AVERAGE ERROR	1.8081		AVERAGE ERROR	2.2110

6.3.2 IMPACT OF DOWNTIME VARIABILITY

As the squared coefficient of variation of the downtimes, $Cv_Y^{\ 2}$**,** increases, the average waiting time of a high priority customer, $E[W_1]$, and a low priority customer, $E[W_2]$, also increase as seen in Figures 6.3 and 6.4. On the other hand, $E[W_1]$ and $E[W_2]$ decrease in general as the number of interruptions, *k*, increases.

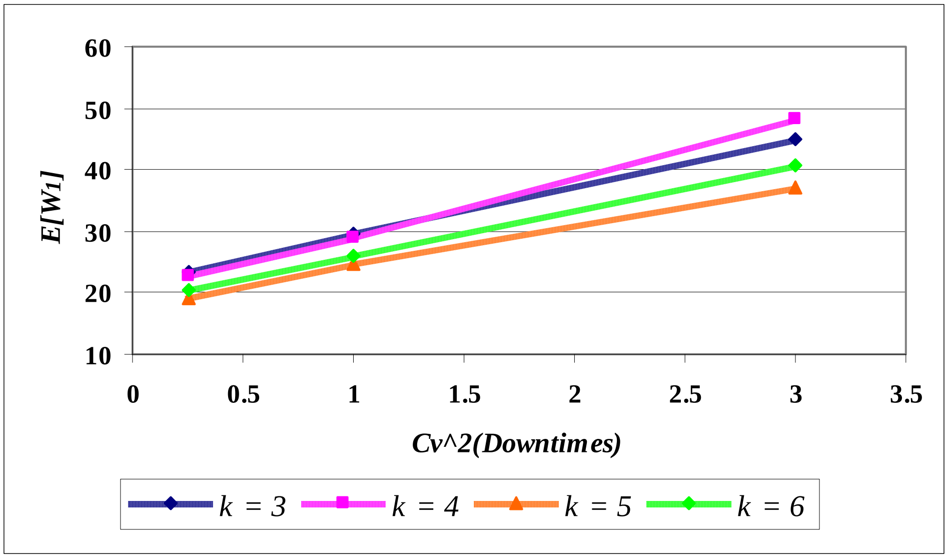

Figure 6.3 Impact of $Cv_Y^{\ 2}$ on $E[W_1]$ in the class-dependent interruptions case

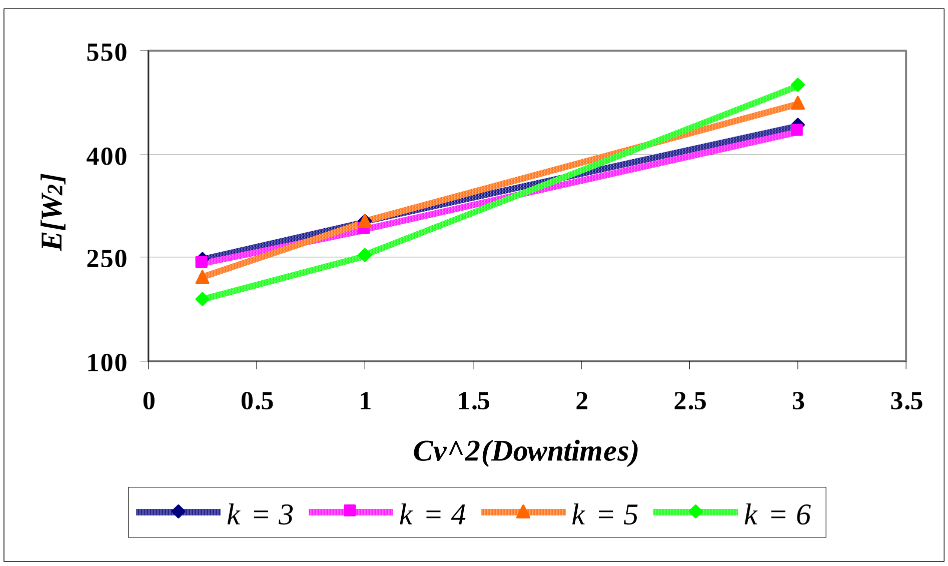

Figure 6.4 Impact of $Cv_Y^{\ 2}$ on $E[W_2]$ in the class-dependent interruptions case

The detailed analytical and simulated results obtained by changing $Cv_{Y_i}^{\ 2}$ for $i = (1, \ldots, k)$, and the number of interruptions, *k*, are shown in Table 6.3.

The error levels for $E[W_1]$ and $E[W_2]$ remain below 3.5% as we increase the squared coefficient of variation of the downtimes, ${Cv_{Y_i}}^2$ for $i = (1,\ldots,k)$, from 0.25 to 3, and the number of interruptions, *k*, from 3 to 6.

The error levels increase in general as we increase the values of ${Cv_{Y_i}}^2$ and *k*. Also, the average error for the average waiting time across different values of ${Cv_{Y_i}}^2$ increases in general as the number of interruptions increases.

Table 6.3 $E[W_j]$ in the class-dependent interruptions case when changing ${Cv_Y}^2$

k	***Cv²(Y)***	***E[W₁]***			***E[W₂]***		
		Analytical	**Simulation**	**Error**	**Analytical**	**Simulation**	**Error**
3	0.25 (4-Erlang)	23.3622	23.5077	0.6189	247.4654	249.0300	0.6283
	1 (Expo)	29.9452	29.6920	0.8528	302.7870	305.0600	0.7451
	3 (2-HyperEx)	44.4781	45.0512	1.2721	441.7317	448.7700	1.5684
			AVERAGE ERROR	0.9146		AVERAGE ERROR	0.9806
4	0.25 (4-Erlang)	22.5470	22.7416	0.8557	243.6079	246.1800	1.0448
	1 (Expo)	29.5602	29.0988	1.5856	292.4250	296.9800	1.5338
	3 (2-HyperEx)	47.4393	48.2905	1.7627	434.5574	443.1600	1.9412
			AVERAGE ERROR	1.4013		AVERAGE ERROR	1.5066
5	0.25 (4-Erlang)	18.9805	19.2026	1.1566	222.5504	225.8300	1.4522
	1 (Expo)	24.3846	24.7970	1.6631	304.1408	309.4400	1.7125
	3 (2-HyperEx)	36.5445	37.2501	1.8942	473.3597	484.1400	2.2267
			AVERAGE ERROR	1.5713		AVERAGE ERROR	1.7971
6	0.25 (4-Erlang)	20.4255	20.5040	0.3829	189.1873	192.1480	1.5408
	1 (Expo)	25.7910	26.1707	1.4509	255.1220	259.8000	1.8006
	3 (2-HyperEx)	39.6481	40.5788	2.2936	501.1205	517.5700	3.1782
			AVERAGE ERROR	1.3758		AVERAGE ERROR	2.1732

6.3.3 IMPACT OF SYSTEM UTILIZATION

As seen in Figures 6.5 and 6.6, the average waiting time of a high priority customer, $E[W_1]$, and a low priority customer, $E[W_2]$, increase as the system utilization, $P(B)$, increases.

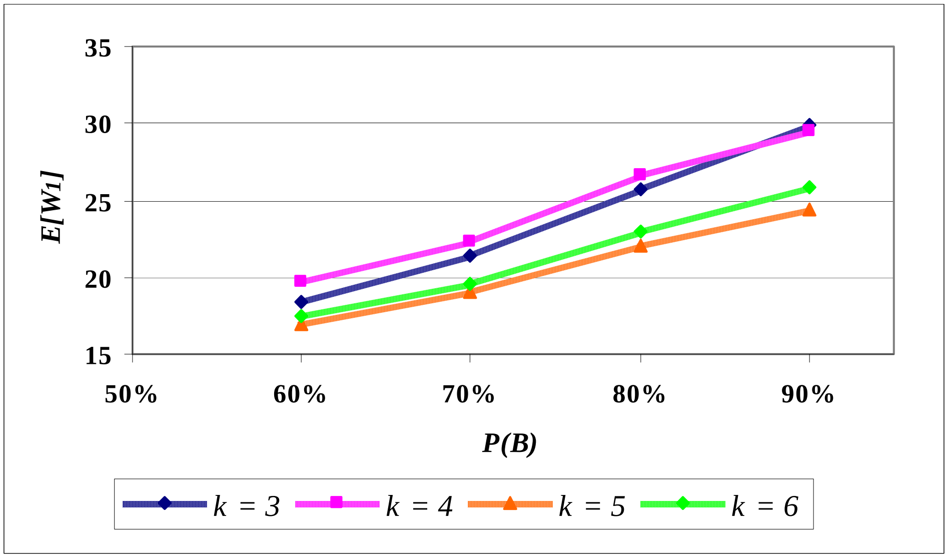

Figure 6.5 Impact of $P(B)$ on $E[W_1]$ in the class-dependent interruptions case

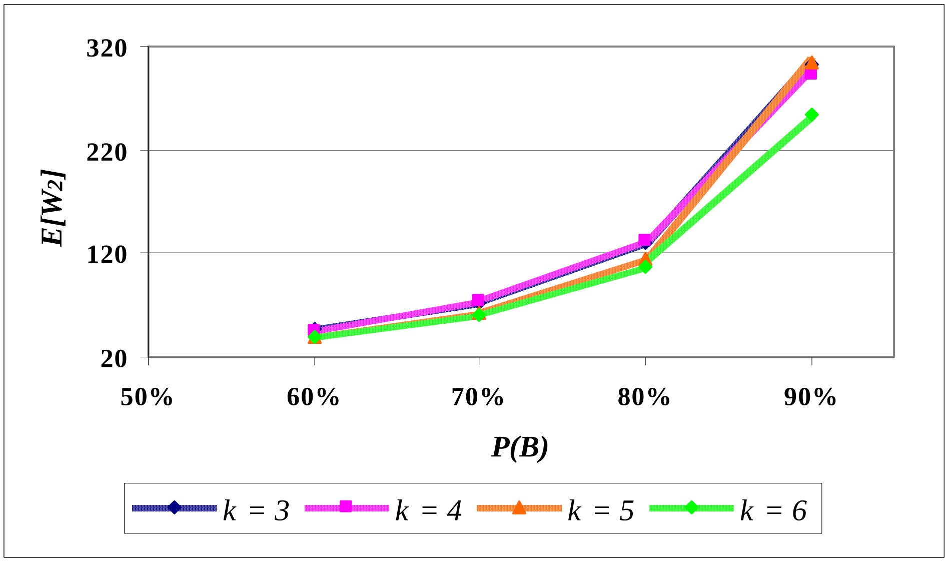

Figure 6.6 Impact of $P(B)$ on $E[W_2]$ in the class-dependent interruptions case

According to the detailed results shown in Table 6.4, the error levels for $E[W_1]$ and $E[W_2]$ both remain below 2%, as we increase the system utilization, $P(B)$, from 60% to 90%, and the number of interruptions, *k*, from 3 to 6.

The average error for the average waiting time increases in general as $P(B)$ and k increase.

Table 6.4 $E[W_j]$ in the class-dependent interruptions case when changing $P(B)$

k	**P(B)**	**E[W₁]** Analytical	Simulation	Error	**E[W₂]** Analytical	Simulation	Error
3	60%	18.3834	18.4798	0.5217	47.1439	47.4422	0.6288
	70%	21.3808	21.5144	0.6210	72.6788	73.1453	0.6378
	80%	25.6541	25.8209	0.6460	130.0946	131.0100	0.6987
	90%	29.9452	29.6920	0.8528	302.7870	305.4600	0.8751
			AVERAGE ERROR	0.7066		AVERAGE ERROR	0.7372
4	60%	19.6588	19.7707	0.5660	44.2768	44.6375	0.8081
	70%	22.3155	22.5148	0.8852	74.3054	75.0035	0.9308
	80%	26.6613	27.0158	1.3122	133.1867	134.9900	1.3359
	90%	29.5602	29.0988	1.5856	292.4250	296.9800	1.5338
			AVERAGE ERROR	1.2610		AVERAGE ERROR	1.2668
5	60%	17.0161	17.1683	0.8865	40.0280	40.4542	1.0535
	70%	19.0182	19.2042	0.9685	62.5045	63.3563	1.3445
	80%	22.1143	22.4342	1.4259	115.4946	117.5000	1.7067
	90%	24.3846	24.7970	1.6631	304.1408	309.4400	1.7125
			AVERAGE ERROR	1.3525		AVERAGE ERROR	1.5879
6	60%	17.4587	17.6181	0.9048	38.8722	39.3429	1.1964
	70%	19.6022	19.8229	1.1134	60.7348	61.6853	1.5409
	80%	22.9144	23.2461	1.4269	107.8647	109.8240	1.7840
	90%	25.7910	26.1707	1.4509	255.1220	259.8000	1.8006
			AVERAGE ERROR	1.3304		AVERAGE ERROR	1.7085

6.3.4 IMPACT OF DOWNTIME PROBABILITY

Figures 6.7 and 6.8 show that the average waiting time of a high priority customer, $E[W_1]$, and a low priority customer, $E[W_2]$, increase as the system downtime probability, P_d, increases. Conversely, $E[W_1]$ and $E[W_2]$ decrease as the number of interruptions, *k*, increases from 3 to 6.

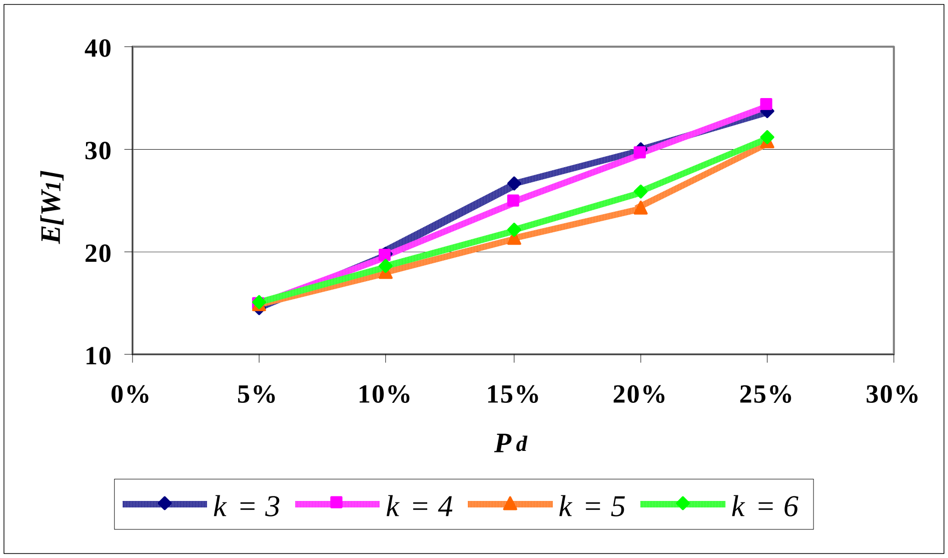

Figure 6.7 Impact of P_d on $E[W_1]$ in the class-dependent interruptions case

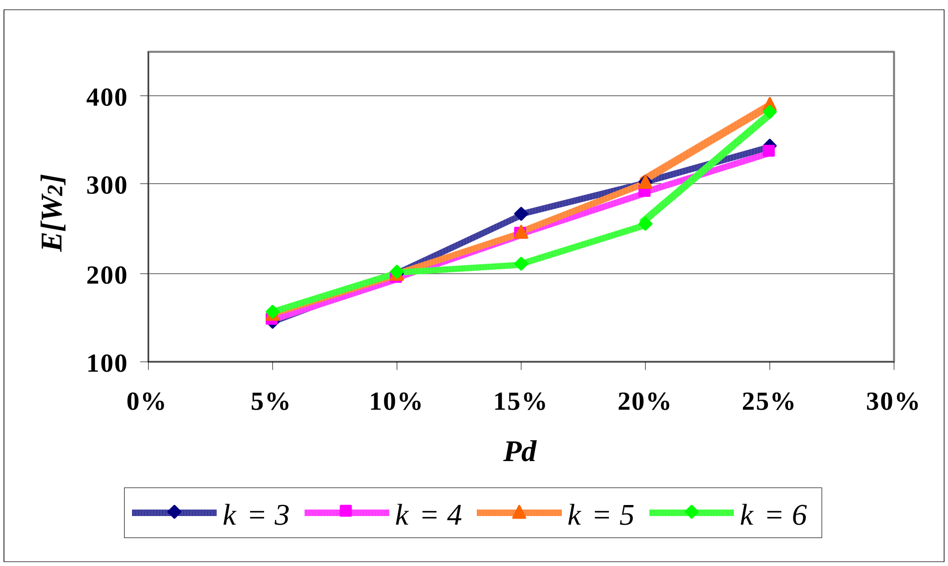

Figure 6.8 Impact of P_d on $E[W_2]$ in the class-dependent interruptions case

According to the detailed results shown in Table 6.5, the error for the average waiting time of a customer is less than 3.5% for all values of P_d and k.

The error levels for $E[W_1]$ and $E[W_2]$ increase in general as the system downtime probability, P_d, and the total number of interruptions, *k*, increase.

Table 6.5 $E[W_j]$ in the class-dependent interruptions case when changing P_d

k	Pd	*E[W₁]*			*E[W₂]*		
		Analytical	**Simulation**	**Error**	**Analytical**	**Simulation**	**Error**
3	0.05	14.4316	14.4412	0.0665	144.3220	144.8600	0.3714
	0.10	19.7204	19.7452	0.1256	198.6779	200.0700	0.6958
	0.15	26.5769	26.6797	0.3853	267.1957	269.1300	0.7187
	0.20	29.9452	29.6920	0.8528	302.7870	305.4600	0.8751
	0.25	33.7190	33.3775	1.0231	343.9813	347.6400	1.0524
			AVERAGE ERROR	0.7537		AVERAGE ERROR	0.8821
4	0.05	14.9079	14.8429	0.4379	147.7309	148.9100	0.7918
	0.10	19.6904	19.4311	1.3345	194.9117	197.0600	1.0902
	0.15	24.9906	24.6322	1.4550	245.5446	249.3100	1.5103
	0.20	29.5602	29.0988	1.5856	292.4250	296.9800	1.5338
	0.25	34.2247	33.5682	1.9557	338.0494	345.9800	2.2922
			AVERAGE ERROR	1.6655		AVERAGE ERROR	1.7788
5	0.05	14.8943	15.0553	1.0694	154.7956	156.4600	1.0638
	0.10	17.9704	18.2557	1.5628	199.9276	202.6400	1.3385
	0.15	21.4323	21.7781	1.5878	246.9880	251.0500	1.6180
	0.20	24.3846	24.7970	1.6631	304.1408	309.4400	1.7125
	0.25	30.7541	31.3496	1.8995	390.4208	403.2700	3.1863
			AVERAGE ERROR	1.7168		AVERAGE ERROR	2.1723
6	0.05	15.1338	15.3274	1.2631	156.7795	159.2890	1.5754
	0.10	18.6003	18.8990	1.5805	201.8903	204.9500	1.4929
	0.15	22.1831	22.5480	1.6183	210.9300	214.5400	1.6827
	0.20	25.7910	26.1707	1.4509	255.1220	259.8000	1.8006
	0.25	31.2049	31.9107	2.2118	381.3134	394.3200	3.2985
			AVERAGE ERROR	1.7603		AVERAGE ERROR	2.2606

6.3.5 CONCLUSION

In this chapter, we have considered a single-server, two-class queueing system subject to multiple types of possibly simultaneous, class-dependent interruptions motivated by the transit vessel entrances in the Istanbul Strait. Since the complexity of the system makes the exact analysis difficult, an analytical model is developed to approximate the expected waiting time of a class j customer in the aforementioned queueing model.

The numerical results show that the approximation works reasonably well for the expected waiting time of a high priority customer, $E[W_1]$, and a low priority customer, $E[W_2]$, for a wide range of system parameters. In addition, we conclude that it is not the service time or the arrival process, but the times-to-interruption, the variability of downtime processes, and the number of interruptions that determine the accuracy of the approximation.

We also analyze the impact of various key parameters on the system behavior. We observe that an increase in any of the system parameters except number of interruptions, k, leads to an increase in the expected waiting time of a customer in the queue. On the other hand, $E[W_j]$ decreases as k increases.

The main contribution of our work is that we consider multiple types of class-dependent possibly simultaneous interruptions in a priority queueing model, which has never been studied before.

The main use of this model will be in predicting the impact of various systems parameters on the congestion level in waterway entrances. In particular, the impact of various closure profiles (due to construction projects or traffic management strategies) and and increase in vessel traffic on vessel delays are crucial in long range capacity planning in waterways.

From a critical standpoint, even though we assume a two-class priority queueing model, in reality there may be more than two classes of customers. The proposed model cannot handle these situations. We will extend our current model in our future work to be able to analyze these more realistic scenarios.

7 CONCLUSION

Istanbul is the only city in the world that stands astride two continents. Europe is separated from Asia by the Istanbul Strait in the northwestern corner of Turkey. It holds a strategic importance as it links the states of Black Sea to the Mediterranean and the world beyond.

The Istanbul Strait is considered not only one of the world's most dangerous waterways to navigate but also one of the most congested maritime traffic regions in the world. More than 50,000 transit vessels pass through the Strait annually, 20% of which are tankers, dangerous cargo vessels, and LNG-LPG carriers. Currently, the oil and gas from the newly independent energy-rich states along the Caspian Sea reach the western markets through the Istanbul Strait. Consequently, more than 3 million barrels of oil pass through the Strait every day.

The nature of the global economy dictates that the tanker traffic in the Istanbul Strait cannot be eliminated. Nonetheless, the economic aspirations and environmental awareness need not to be mutually exclusive goals in the Strait as stated in [Joyner, 2002]. The risk involving the transit traffic can be mitigated by operational policies and restrictions that adequately regulate the transit vessel traffic while maintaining the freedom of passage. Until then, the environment, the priceless historical monuments and the health and safety of the city's residents will be at jeopardy.

In view of this, we have studied both the practical and analytical aspects of the transit vessel traffic in the Istanbul Strait. While a mathematical risk analysis based on simulation modeling constitutes our practical contribution, our analysis of a single-server queueing model motivated by the transit vessel traffic in the Istanbul Strait represents the analytical aspect of our research.

In this research, we have developed a mathematical risk analysis model to analyze the risks involved in the transit vessel traffic system in the Istanbul Strait. In the first step of the risk analysis, the transit vessel traffic system was analyzed and a simulation model was developed to mimic and study the system. In addition to vessel traffic and geographical conditions, the current vessel scheduling practices were modeled using a scheduling algorithm. This algorithm was developed through discussions with the Turkish Straits Vessel Traffic Services (VTS) to mimic their decisions on sequencing vessel entrances as well as coordinating vessel traffic in both directions.

Furthermore, a scenario analysis was performed to evaluate the impact of several parameters on the system performance. The results showed that the arrival rate and the number of available pilots and tugboats highly influence the average waiting time of the vessels. The arrival rate also affects the number of vessels passing through the Strait. Consequently, even a slight increase in the incoming traffic results in severe traffic congestion and longer waiting times.

Risk analysis was performed by incorporating a probabilistic accident risk model into the simulation model. The framework of this risk model was established taking into account the attributes that influence the occurrence of an accident as well as the consequences and their impact. The mathematical accident risk model was developed based on probabilistic arguments and utilized historical accident data and subject matter expert opinions.

We have also performed a scenario analysis to understand and evaluate the characteristics of the accident risk. This analysis allowed us to investigate how various factors impact risks in the Strait. These factors include vessel arrivals, scheduling policies, pilotage, overtaking, and local traffic density.

The numerical results showed that local traffic density and pilotage are the two main factors that affect slice risk the most. A 50% decrease in local traffic density results in an average of 50% decrease in slice risk. The importance of the local traffic density is also highlighted by the fact that the majority of the vessels observe the maximum risk at slice 19, which has a heavier local traffic density than other slices. Moreover, changing the local traffic density does not impact the vessel waiting times. Therefore, to reduce risk significantly, the scheduling procedure should be revised to move more of the dangerous cargo vessels to nighttime traffic. This requires further research on what kind of modifications can be done to the nighttime scheduling practice to control vessel delays.

Moreover, the model indicates that pilots are of utmost importance for safe passage and lack of pilotage significantly increases the risks in the Strait. In the current practice, vessels greater than 300 m. in length are mandated to take a pilot and it is voluntary for the rest. Thus, we recommend mandatory pilotage for vessels greater than 150 m. in length.

Conversely, changing the scheduling policy by increasing the required time gaps between consecutive vessels, thereby reducing the number of scheduled vessels decreases the average slice risk. However, in such scenarios the resulting average vessel waiting times are unacceptable. Therefore, they are rendered infeasible even though they result in lower average slice risks. On the other hand, in the future major decreases in dangerous cargo traffic may occur due to alternative transport modes such as pipelines and other routes. In this case, scheduling changes can be made to take lesser number of vessels into the Strait and can still be justified due to the resultant insignificant increases in delays. Additionally, scheduling decisions to balance out delays vs. risks should be made based on extensive experimentation with the model developed in this study.

Even though vessel arrival rates are directly proportional to the average slice risk, they have a small impact as long as the scheduling policies are not changed. Thus, the change in the arrival rates must be substantial in order to obtain a significant impact. In the wake of increase in arrival rates, the scheduling regime should be kept as is to maintain the risks at the current levels. A 10% increase in the dangerous cargo vessel arrival rates results in rather acceptable waiting times at the entrance. However, further increases in vessel traffic may result in discouraging shippers away from the Strait due to excessive waiting times.

Note that in the scenario where both the vessel arrival rates and the number of scheduled vessels are decreased, the combination of the two factors results in a greater decrease in average and maximum slice risks. This scenario also provides acceptable waiting times.

Finally, complexity of the operations at the Istanbul Strait motivated us to model congestion at the waterway entrances through queueing analysis. We have developed single-server queueing models subject to multiple types of operation-independent interruptions. We have used waiting time arguments and service completion time analysis to approximate the expected waiting time of a customer (vessel) in the aforementioned queue for various cases of service interruptions. These cases include the single-class models with non-simultaneous and possibly simultaneous interruptions, the multi-class priority queueing model with k possibly simultaneous class-independent interruptions, and the two-class priority queueing model with k possibly simultaneous class-dependent interruptions.

The numerical results showed that the approximation for the single-class model works reasonably well for the average completion time and the average waiting time for a wide range of system parameters. Similarly, the approximation for the multi-class models works reasonably well for the expected waiting time of a highest priority customer, and a lowest priority customer. In addition, we concluded that it is not the service time, arrival process, times-to-interruption, or the number of interruptions, but the variability of downtime processes and the number of priority classes that determine the accuracy of the approximation.

We have also analyzed the impact of various key parameters on the system behavior. We observed that an increase in any of the parameters except number of interruptions, *k*, leads to an increase in the expected waiting time of a customer in the queue. On the other hand, average waiting times decrease as *k* increases.

The main contribution of our work is that contrary to the previous studies on queueing models with multiple interruptions, in our model the downtime experienced by a customer is not simply the sum of the downtimes of all possible interruptions during its service. Interruption types are operation-independent, that is they may occur at anytime, and their downtime processes start immediately after their occurrences. Therefore, the expected waiting time of a customer in the queue involves complicated scenarios of common downtimes rather than a simple summation, requiring an involved approach including approximations. We have also incorporated the notions of priority classes and class-dependent interruptions into a queueing model with multiple types of possibly simultaneous interruptions, which had never been done before.

The main use of these analytical models will be in predicting the impact of various system parameters on the congestion level in waterway entrances. In particular, the impact of various closure profiles (due to construction projects or traffic management strategies) and the impact of an increase in vessel traffic on vessel delays are crucial in long range capacity planning in waterways.

APPENDIX A: Scale Values of Situational Attributes Influencing Accident Occurrence

In this appendix, we provide scale values of situational attributes influencing accident occurrence obtained from the experts.

x_1 : 1st Interacting Vessel Class - x_2 : 2nd Interacting Vessel Class

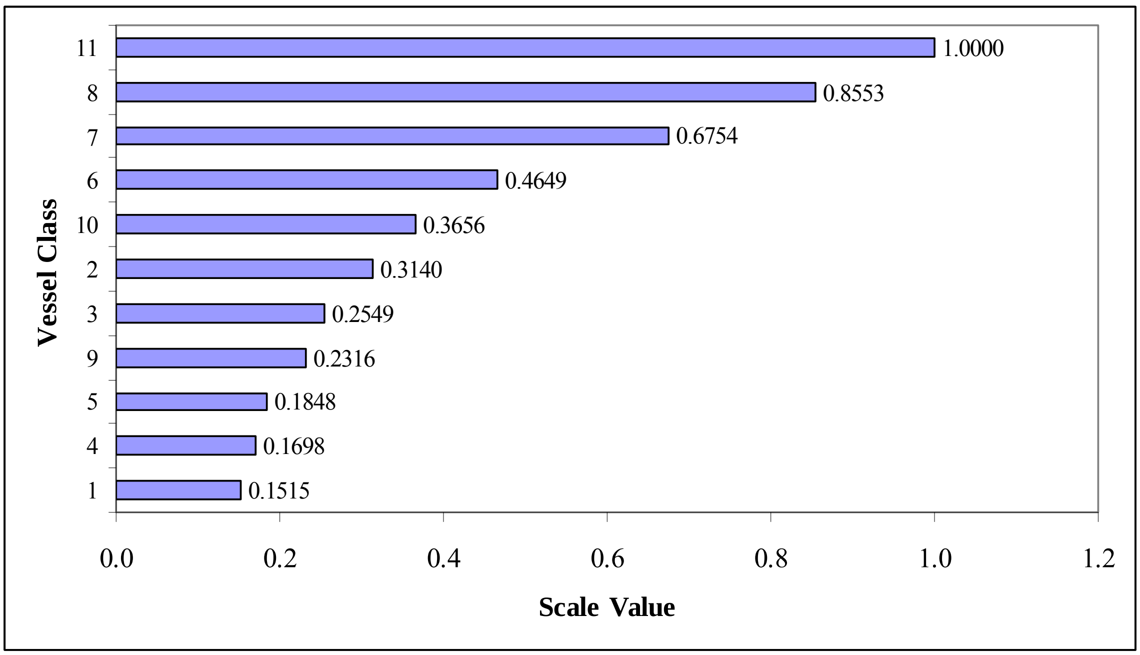

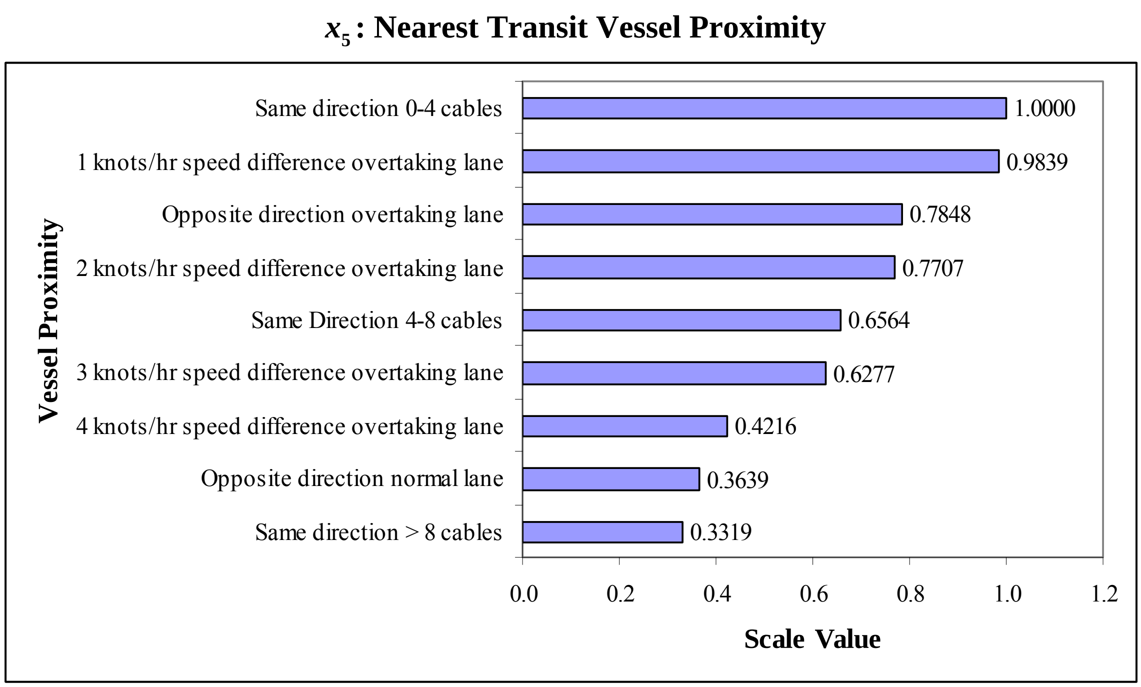
x_5 : Nearest Transit Vessel Proximity
Vessel Proximity
Same direction 0-4 cables
1 knots/hr speed difference overtaking lane
Opposite direction overtaking lane
2 knots/hr speed difference overtaking lane
Same Direction 4-8 cables
3 knots/hr speed difference overtaking lane
4 knots/hr speed difference overtaking lane
Opposite direction normal lane
Same direction > 8 cables
1.0000
0.9839
0.7848
0.7707
0.6564
0.6277
0.4216
0.3639
0.3319
0.0
0.2
0.4
0.6
0.8
1.0
1.2
Scale Value

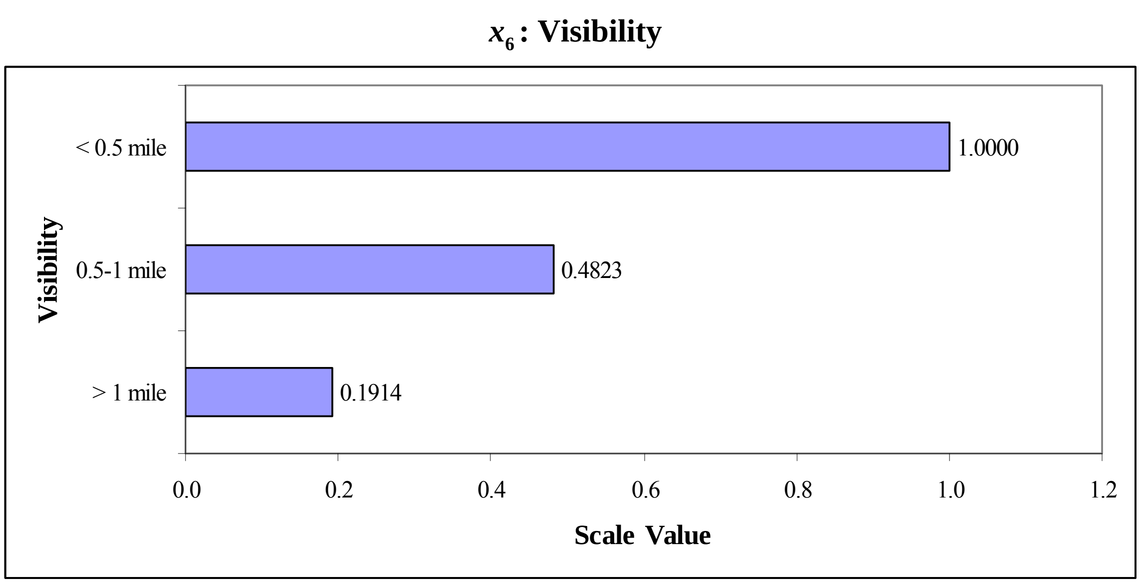
x_6 : Visibility
Visibility
< 0.5 mile
0.5-1 mile
> 1 mile
1.0000
0.4823
0.1914
0.0
0.2
0.4
0.6
0.8
1.0
1.2
Scale Value

x_7 : Current

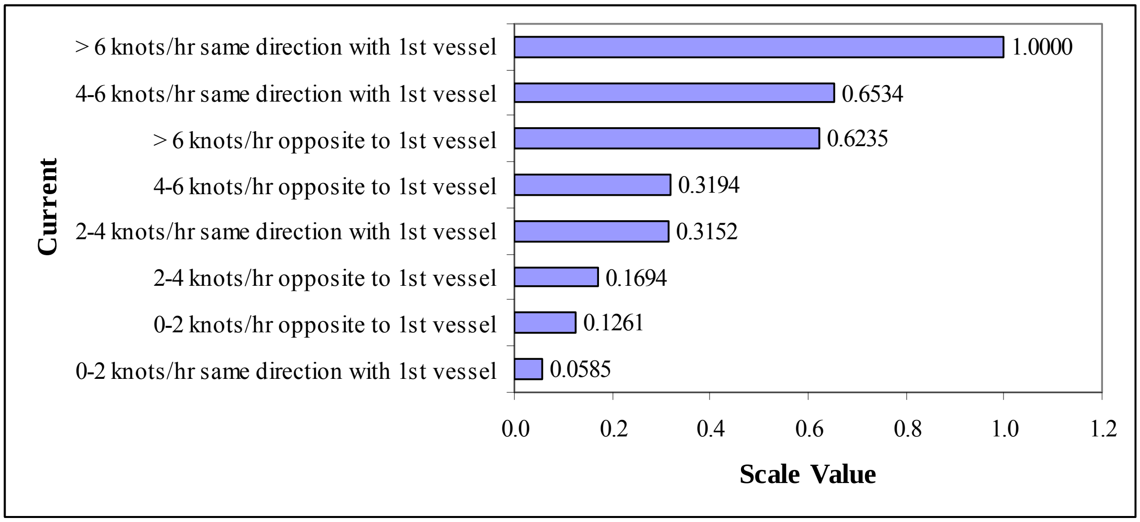

x_8 : Local Traffic Density

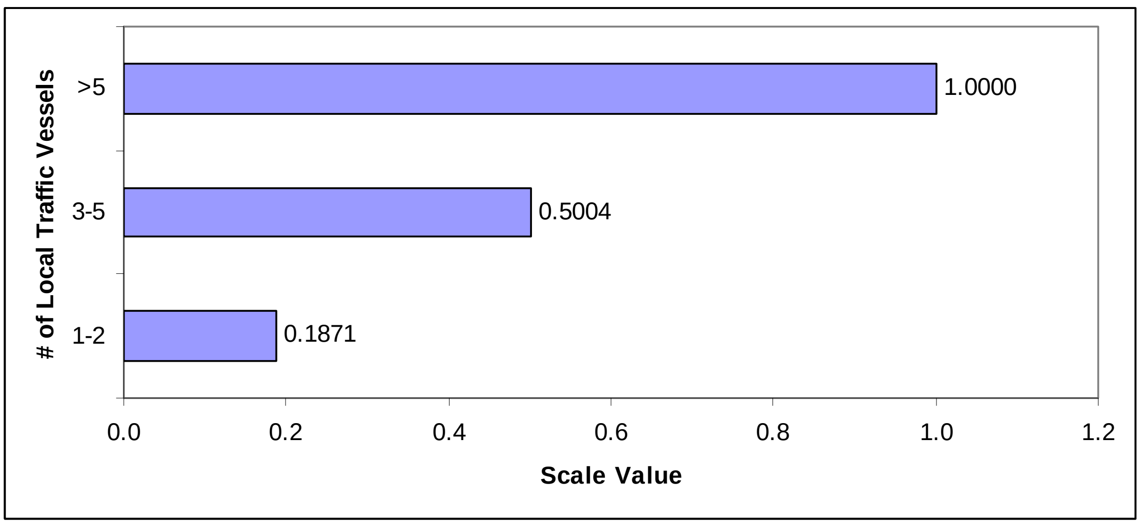

x_9 : Zone

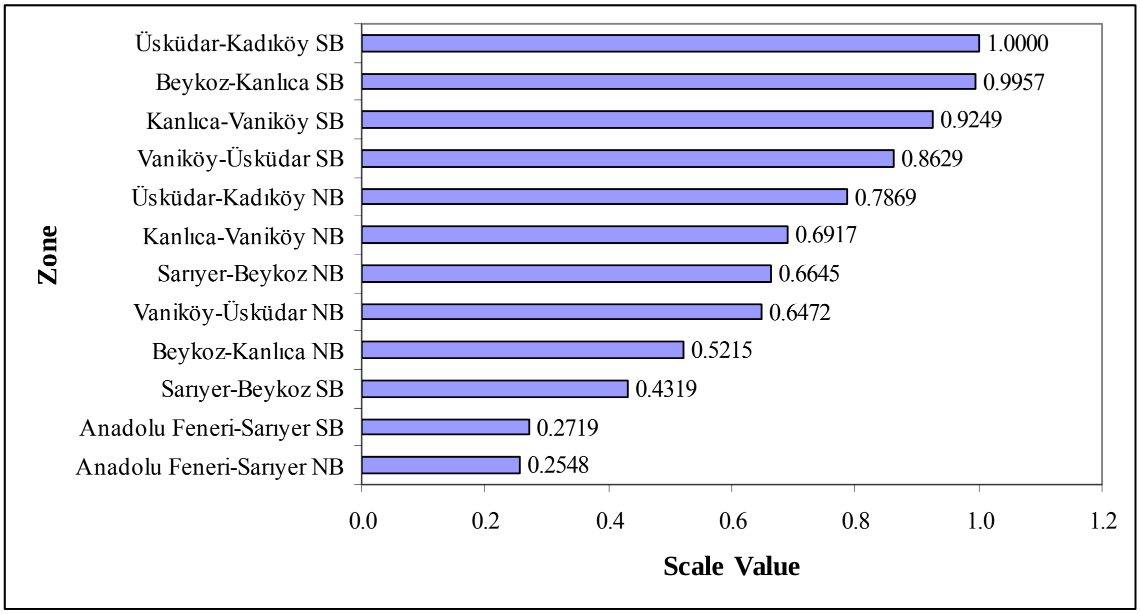

x_{10} : Vessel Reliability

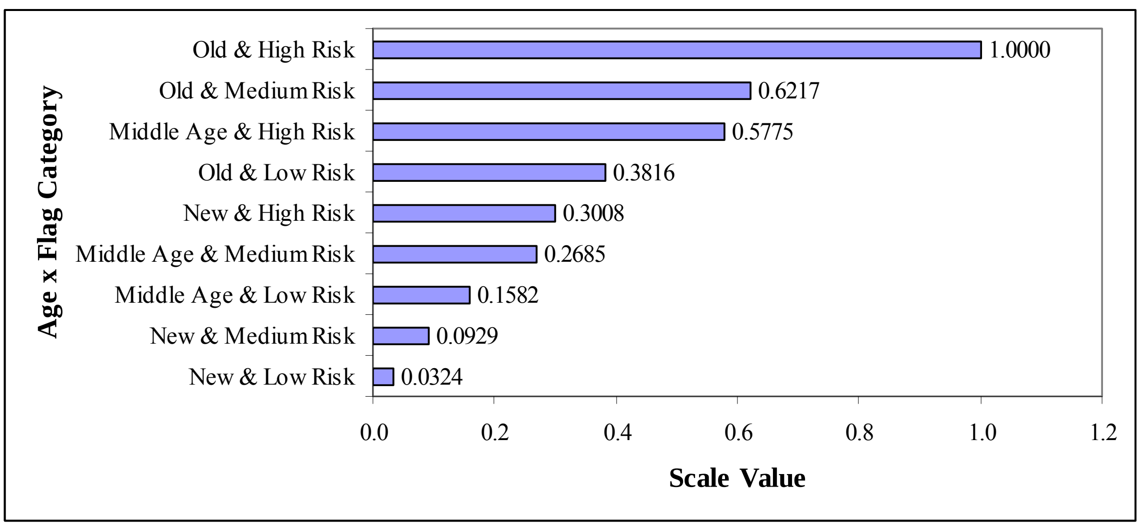

APPENDIX B: Regression Results of the Accident Probability Questionnaires

$\Pr\left(\text{Collision} \middle| \text{Human Error}, \underline{S}^1\right)$

Summary

R^2	R	Adj. R^2	S.E. of Estimate
0.934	0.966	0.893	0.400

ANOVA

Source	Sum Sq.	D.F.	Mean Sq.	F	Prob.
Regression	54.336	15	3.622	22.601	0.000
Residual	3.847	24	0.160		
Total	58.182	39			

Regression Coefficients

Source	Coefficient	Std Error	Std Beta	-95% C.I.	+95% C.I.	t	Prob.
Intercept	0.216	0.080		0.052	0.380	2.721	0.012
X1	1.726	0.322	0.281	1.062	2.390	5.361	0.000
X2	2.046	0.318	0.338	1.390	2.702	6.435	0.000
X3	1.680	0.597	0.435	0.447	2.912	2.813	0.010
X4	1.633	0.204	0.423	1.212	2.055	8.004	0.000
X5	1.401	0.338	0.217	0.703	2.099	4.142	0.000
X6	1.415	0.649	0.239	0.076	2.754	2.181	0.039
X7	3.430	0.936	0.492	1.498	5.363	3.663	0.001
X8	1.244	0.633	0.211	-0.062	2.551	1.966	0.061
X10	1.255	0.204	0.325	0.834	1.676	6.151	0.000
X15	-2.564	1.301	-0.490	-5.249	0.121	-1.971	0.060
X16	2.410	0.947	0.442	0.455	4.364	2.545	0.018
X19	-3.937	1.537	-0.547	-7.109	-0.764	-2.561	0.017
X20	-3.842	1.347	-0.617	-6.621	-1.062	-2.853	0.009
X21	4.264	1.380	0.621	1.415	7.113	3.089	0.005
X22	4.201	1.383	0.584	1.346	7.056	3.037	0.006

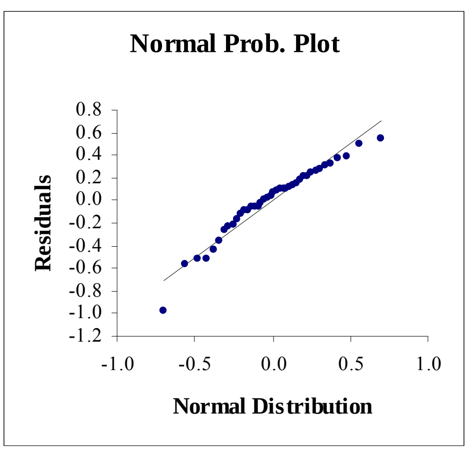

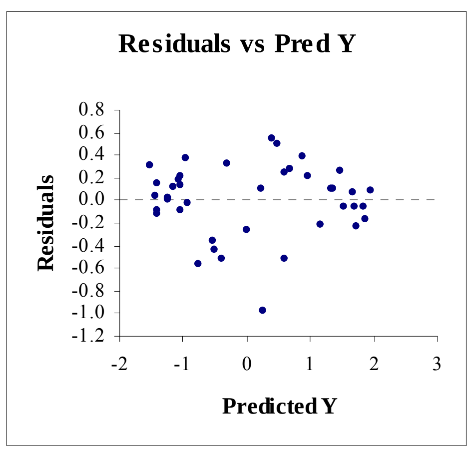

$\Pr\left(\text{Collision}\,\middle|\,\text{Steering Failure}, \underline{S}^1\right)$

Summary

R^2	R	Adj. R^2	S.E. of Estimate
0.928	0.964	0.888	0.470

ANOVA

Source	Sum Sq.	D.F.	Mean Sq.	F	Prob.
Regression	71.591	14	5.114	23.159	0.000
Residual	5.520	25	0.221		
Total	77.111	39			

Regression Coefficients

Source	Coefficient	Std Error	Std Beta	-95% C.I.	+95% C.I.	t	Prob.
Intercept	0.243	0.091		0.055	0.430	2.661	0.013
X1	1.976	0.378	0.280	1.197	2.754	5.228	0.000
X2	2.384	0.373	0.342	1.615	3.153	6.387	0.000
X3	2.105	0.616	0.473	0.835	3.374	3.414	0.002
X4	1.328	0.526	0.299	0.245	2.411	2.525	0.018
X5	1.655	0.397	0.223	0.837	2.473	4.169	0.000
X6	2.200	0.365	0.323	1.449	2.952	6.029	0.000
X7	2.645	0.697	0.330	1.210	4.081	3.795	0.001
X8	1.911	0.364	0.281	1.162	2.661	5.254	0.000
X9	2.306	0.799	0.208	0.660	3.952	2.886	0.008
X10	1.388	0.239	0.312	0.895	1.881	5.801	0.000
X13	-1.994	0.886	-0.315	-3.818	-0.169	-2.250	0.033
X14	2.046	1.016	0.355	-0.047	4.139	2.013	0.055
X15	-2.115	1.259	-0.351	-4.708	0.478	-1.680	0.105
X16	1.506	0.912	0.240	-0.373	3.385	1.650	0.111

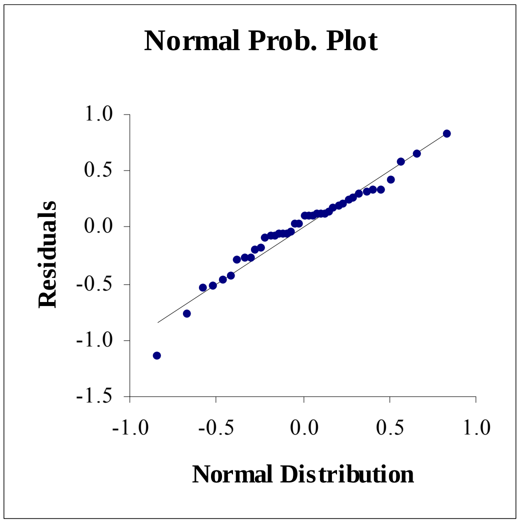

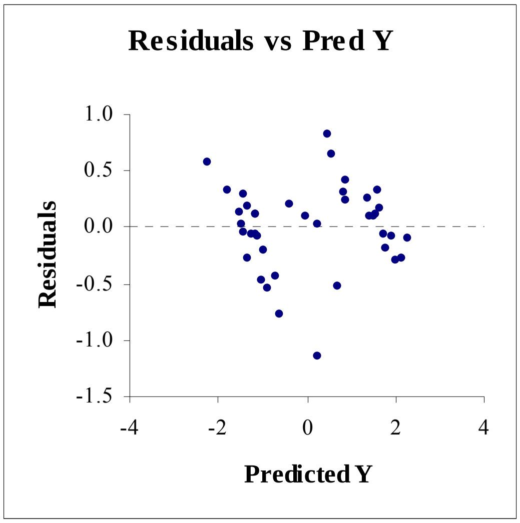

$\Pr\left(\text{Collision}\,\middle|\,\text{Propulsion Failure}, \underline{S}^1\right)$

Summary

R^2	R	Adj. R^2	S.E. of Estimate
0.928	0.963	0.883	0.474

ANOVA

Source	Sum Sq.	D.F.	Mean Sq.	F	Prob.
Regression	69.451	15	4.630	20.566	0.000
Residual	5.403	24	0.225		
Total	74.854	39			

Regression Coefficients

Source	Coefficient	Std Error	Std Beta	-95% C.I.	+95% C.I.	t	Prob.
Intercept	0.231	0.094		0.036	0.425	2.448	0.022
X1	1.938	0.382	0.279	1.150	2.725	5.079	0.000
X2	2.344	0.377	0.341	1.566	3.122	6.219	0.000
X3	2.341	0.708	0.534	0.880	3.801	3.308	0.003
X4	1.772	0.242	0.404	1.273	2.271	7.325	0.000
X5	1.548	0.401	0.212	0.721	2.376	3.862	0.001
X6	1.641	0.769	0.244	0.054	3.227	2.134	0.043
X7	4.161	1.110	0.526	1.871	6.452	3.749	0.001
X8	1.466	0.750	0.219	-0.082	3.014	1.954	0.062
X10	1.383	0.242	0.316	0.884	1.882	5.717	0.000
X15	-3.139	1.542	-0.529	-6.322	0.043	-2.036	0.053
X16	2.477	1.122	0.400	0.160	4.793	2.207	0.037
X19	-4.512	1.822	-0.553	-8.272	-0.752	-2.476	0.021
X20	-4.596	1.596	-0.651	-7.890	-1.302	-2.879	0.008
X21	4.886	1.636	0.627	1.510	8.263	2.987	0.006
X22	4.895	1.639	0.600	1.511	8.278	2.986	0.006

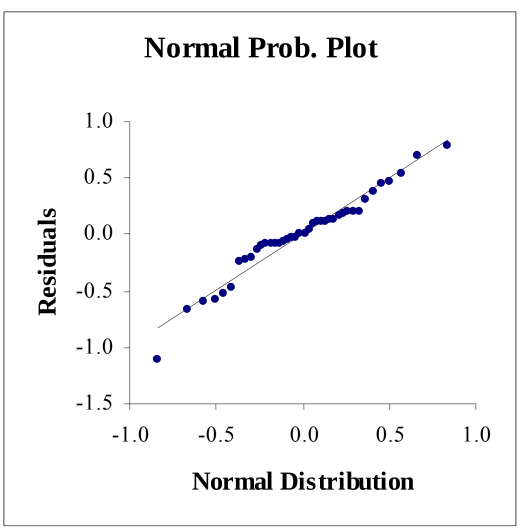

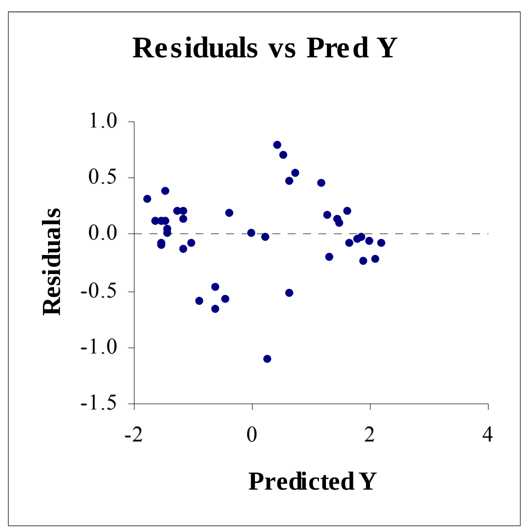

$\Pr\left(\text{Collision} \middle| \text{Communication/Navigation Equipment Failure}, \underline{S}^1\right)$

Summary

R^2	R	Adj. R^2	S.E. of Estimate
0.936	0.968	0.901	0.383

ANOVA

Source	Sum Sq.	D.F.	Mean Sq.	F	Prob.
Regression	54.008	14	3.858	26.322	0.000
Residual	3.664	25	0.147		
Total	57.672	39			

Regression Coefficients

Source	Coefficient	Std Error	Std Beta	-95% C.I.	+95% C.I.	t	Prob.
Intercept	0.208	0.074		0.055	0.361	2.797	0.010
X1	1.570	0.308	0.257	0.936	2.204	5.101	0.000
X2	1.754	0.304	0.291	1.128	2.380	5.769	0.000
X3	1.602	0.502	0.417	0.568	2.637	3.190	0.004
X4	1.156	0.429	0.301	0.273	2.039	2.697	0.012
X5	1.380	0.323	0.215	0.714	2.047	4.268	0.000
X6	2.174	0.297	0.369	1.561	2.786	7.311	0.000
X7	2.138	0.568	0.308	0.968	3.307	3.764	0.001
X8	1.766	0.296	0.300	1.156	2.377	5.959	0.000
X9	2.022	0.651	0.211	0.681	3.363	3.105	0.005
X10	1.321	0.195	0.344	0.920	1.723	6.777	0.000
X13	-1.602	0.722	-0.293	-3.089	-0.116	-2.220	0.036
X14	1.740	0.828	0.349	0.035	3.446	2.102	0.046
X15	-1.554	1.026	-0.298	-3.667	0.558	-1.515	0.142
X16	1.229	0.743	0.226	-0.302	2.760	1.653	0.111

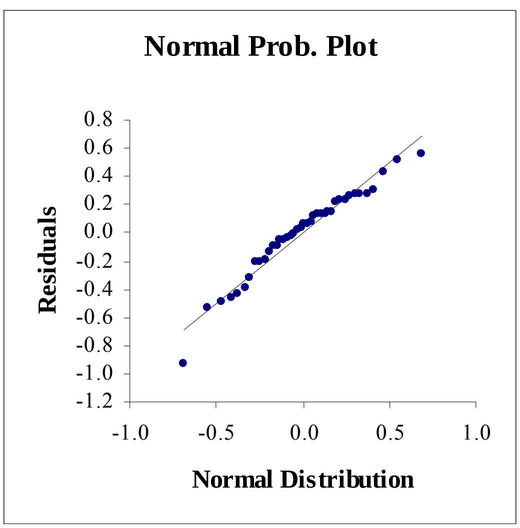

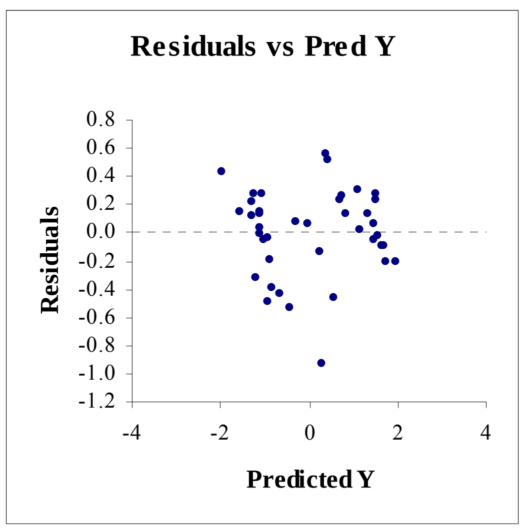

$\Pr\left(\text{Grounding} \middle| \text{Human Error}, \underline{S}^{1}\right)$

Summary

R^2	R	Adj. R^2	S.E. of Estimate
0.933	0.966	0.877	0.389

ANOVA

Source	Sum Sq.	D.F.	Mean Sq.	F	Prob.
Regression	40.103	16	2.506	16.585	0.000
Residual	2.871	19	0.151		
Total	42.974	35			

Regression Coefficients

Source	Coefficient	Std Error	Std Beta	-95% C.I.	+95% C.I.	t	Prob.
Intercept	0.383	0.091		0.192	0.574	4.197	0.000
X1	1.847	0.313	0.351	1.193	2.502	5.909	0.000
X3	2.311	0.605	0.695	1.044	3.577	3.818	0.001
X4	0.943	0.465	0.284	-0.030	1.916	2.028	0.057
X5	1.193	0.328	0.215	0.505	1.880	3.631	0.002
X6	1.124	0.637	0.221	-0.209	2.456	1.765	0.094
X7	3.236	0.920	0.540	1.310	5.163	3.516	0.002
X8	1.433	0.628	0.282	0.118	2.748	2.281	0.034
X10	0.881	0.200	0.265	0.463	1.299	4.413	0.000
X13	-1.300	0.803	-0.275	-2.980	0.380	-1.619	0.122
X14	1.806	0.902	0.420	-0.081	3.694	2.003	0.060
X15	-3.807	1.345	-0.842	-6.622	-0.993	-2.831	0.011
X16	2.819	0.956	0.599	0.818	4.821	2.948	0.008
X19	-3.150	1.609	-0.509	-6.518	0.218	-1.958	0.065
X20	-3.253	1.377	-0.607	-6.134	-0.371	-2.363	0.029
X21	3.621	1.416	0.613	0.659	6.584	2.558	0.019
X22	3.220	1.426	0.520	0.235	6.204	2.258	0.036

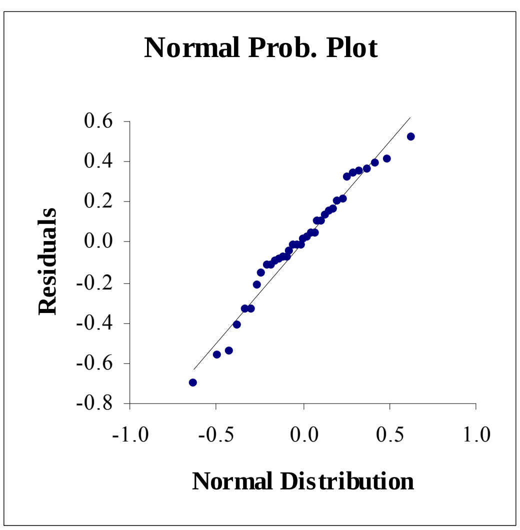

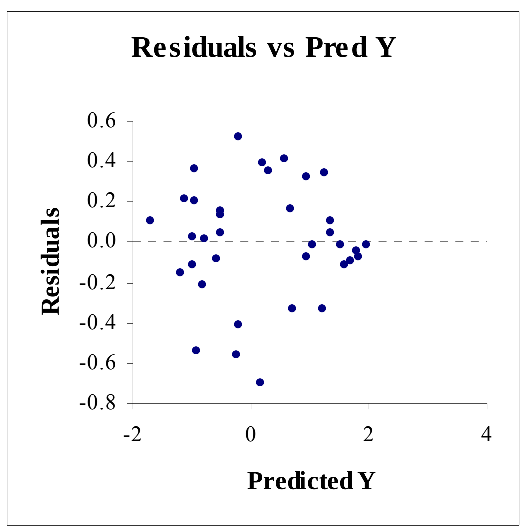

$\Pr\left(\text{Grounding} \middle| \text{Steering Failure}, \underline{S}^1\right)$

Summary

R^2	R	Adj. R^2	S.E. of Estimate
0.913	0.955	0.867	0.473

ANOVA

Source	Sum Sq.	D.F.	Mean Sq.	F	Prob.
Regression	53.663	12	4.472	20.028	0.000
Residual	5.136	23	0.223		
Total	58.799	35			

Regression Coefficients

Source	Coefficient	Std Error	Std Beta	-95% C.I.	+95% C.I.	t	Prob.
Intercept	0.366	0.097		0.165	0.568	3.761	0.001
X1	2.210	0.380	0.358	1.424	2.996	5.816	0.000
X3	2.534	0.608	0.652	1.276	3.792	4.167	0.000
X5	1.420	0.399	0.219	0.594	2.246	3.556	0.002
X6	1.991	0.367	0.334	1.232	2.750	5.426	0.000
X7	2.564	0.695	0.366	1.127	4.001	3.692	0.001
X8	1.718	0.366	0.289	0.961	2.474	4.694	0.000
X9	1.751	0.789	0.181	0.120	3.383	2.221	0.036
X10	0.949	0.241	0.244	0.450	1.448	3.932	0.001
X13	-2.782	0.895	-0.504	-4.633	-0.931	-3.109	0.005
X14	4.138	0.724	0.822	2.639	5.636	5.712	0.000
X15	-3.419	1.228	-0.647	-5.960	-0.879	-2.784	0.011
X16	2.303	0.888	0.418	0.466	4.140	2.593	0.016

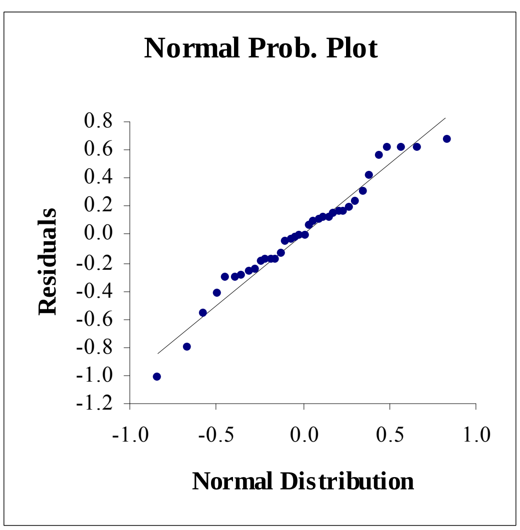

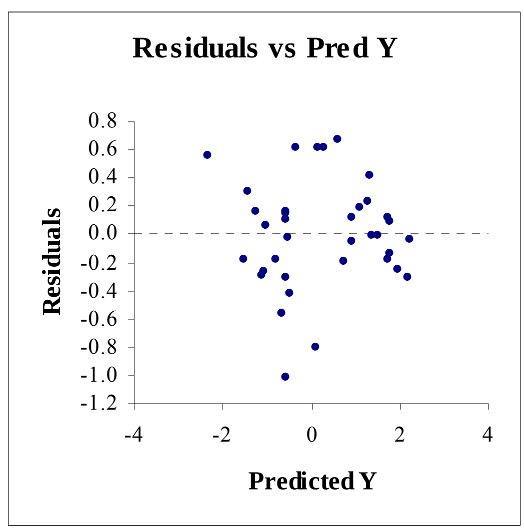

$\Pr\left(\text{Grounding} \middle| \text{Propulsion Failure}, \underline{S}^1\right)$

Summary

R^2	R	Adj. R^2	S.E. of Estimate
0.916	0.957	0.867	0.481

ANOVA

Source	Sum Sq.	D.F.	Mean Sq.	F	Prob.
Regression	55.603	13	4.277	18.475	0.000
Residual	5.093	22	0.232		
Total	60.697	35			

Regression Coefficients

Source	Coefficient	Std Error	Std Beta	-95% C.I.	+95% C.I.	t	Prob.
Intercept	0.396	0.101		0.186	0.606	3.909	0.001
X1	2.190	0.387	0.350	1.387	2.992	5.659	0.000
X3	2.330	0.636	0.590	1.010	3.650	3.661	0.001
X4	0.852	0.540	0.216	-0.269	1.972	1.577	0.129
X5	1.440	0.407	0.219	0.597	2.283	3.543	0.002
X6	2.073	0.374	0.343	1.298	2.848	5.548	0.000
X7	2.908	0.715	0.408	1.425	4.390	4.067	0.001
X8	1.720	0.373	0.285	0.947	2.492	4.615	0.000
X9	1.854	0.821	0.188	0.152	3.556	2.259	0.034
X10	1.013	0.246	0.256	0.503	1.523	4.121	0.000
X13	-2.622	0.918	-0.467	-4.525	-0.718	-2.857	0.009
X14	3.001	1.042	0.587	0.839	5.162	2.879	0.009
X15	-2.743	1.303	-0.511	-5.446	-0.040	-2.105	0.047
X16	1.772	0.936	0.317	-0.169	3.713	1.893	0.072

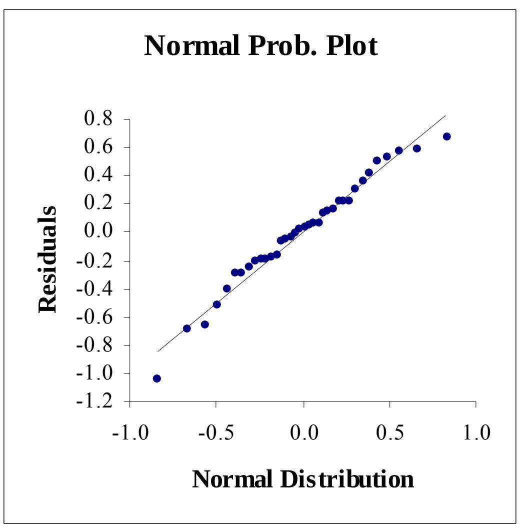

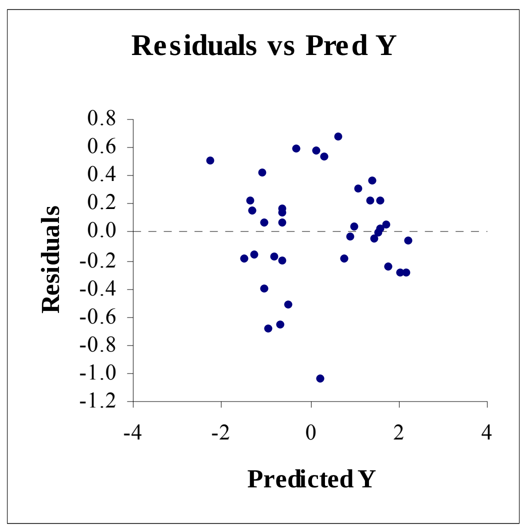

$$\Pr\left(\text{Grounding} \middle| \text{Communication/Navigation Equipment Failure}, \underline{S}^1\right)$$

Summary

R^2	R	Adj. R^2	S.E. of Estimate
0.929	0.964	0.887	0.358

ANOVA

Source	Sum Sq.	D.F.	Mean Sq.	F	Prob.
Regression	36.633	13	2.818	22.046	0.000
Residual	2.812	22	0.128		
Total	39.445	35			

Regression Coefficients

Source	Coefficient	Std Error	Std Beta	-95% C.I.	+95% C.I.	t	Prob.
Intercept	0.314	0.075		0.158	0.470	4.168	0.000
X1	1.625	0.288	0.322	1.028	2.221	5.651	0.000
X3	1.503	0.473	0.472	0.523	2.484	3.179	0.004
X4	0.836	0.401	0.262	0.003	1.668	2.082	0.049
X5	1.094	0.302	0.206	0.468	1.721	3.622	0.002
X6	1.759	0.278	0.361	1.183	2.334	6.334	0.000
X7	2.194	0.531	0.382	1.092	3.296	4.130	0.000
X8	1.431	0.277	0.294	0.857	2.005	5.170	0.000
X9	1.503	0.610	0.189	0.238	2.767	2.464	0.022
X10	0.939	0.183	0.295	0.560	1.317	5.138	0.000
X13	-1.707	0.682	-0.377	-3.122	-0.293	-2.503	0.020
X14	2.081	0.774	0.505	0.475	3.687	2.687	0.013
X15	-1.684	0.968	-0.389	-3.692	0.325	-1.738	0.096
X16	1.235	0.696	0.274	-0.208	2.677	1.775	0.090

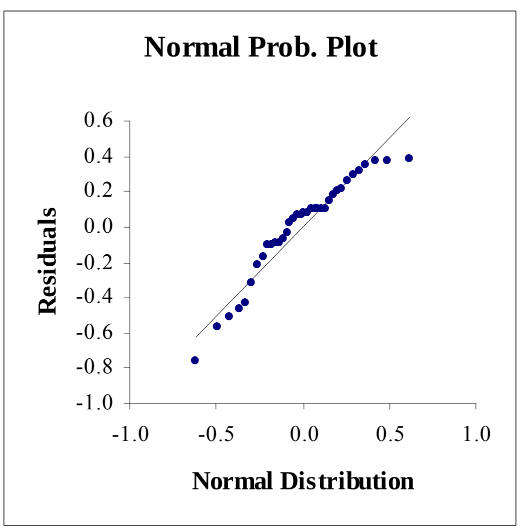

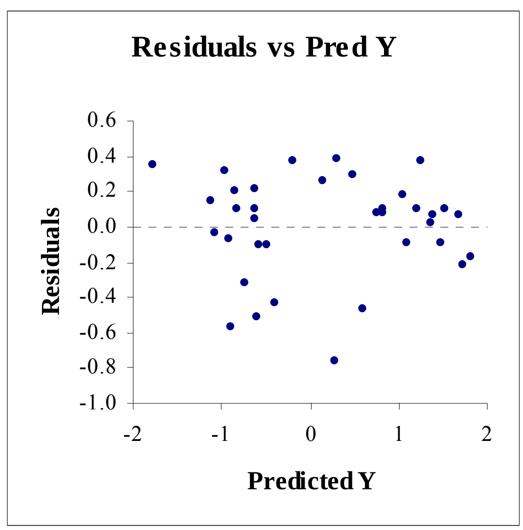

$\Pr\left(\text{Ramming}\middle|\text{Human Error}, \underline{S}^1\right)$

Summary

R^2	R	Adj. R^2	S.E. of Estimate
0.923	0.961	0.877	0.440

ANOVA

Source	Sum Sq.	D.F.	Mean Sq.	F	Prob.
Regression	50.787	13	3.907	20.173	0.000
Residual	4.260	22	0.194		
Total	55.047	35			

Regression Coefficients

Source	Coefficient	Std Error	Std Beta	-95% C.I.	+95% C.I.	t	Prob.
Intercept	0.278	0.096		0.079	0.478	2.890	0.009
X1	1.853	0.354	0.311	1.119	2.587	5.236	0.000
X3	2.180	0.661	0.580	0.810	3.551	3.299	0.003
X4	1.440	0.225	0.383	0.973	1.907	6.395	0.000
X6	1.518	0.619	0.264	0.235	2.801	2.453	0.023
X7	3.496	0.842	0.515	1.749	5.242	4.150	0.000
X8	1.165	0.641	0.203	-0.166	2.495	1.816	0.083
X10	1.391	0.225	0.370	0.924	1.858	6.176	0.000
X15	-3.766	1.528	-0.736	-6.934	-0.597	-2.464	0.022
X16	3.037	1.126	0.570	0.702	5.372	2.697	0.013
X17	5.829	1.521	0.959	2.675	8.984	3.833	0.001
X18	-4.522	1.587	-0.728	-7.812	-1.231	-2.850	0.009
X20	-5.118	1.606	-0.844	-8.448	-1.788	-3.188	0.004
X22	5.990	1.526	0.854	2.826	9.154	3.926	0.001

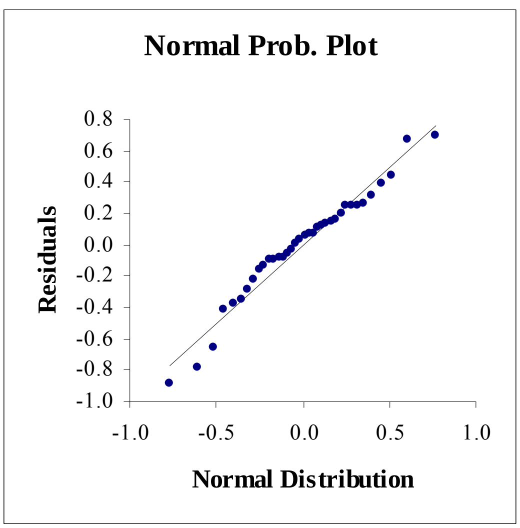

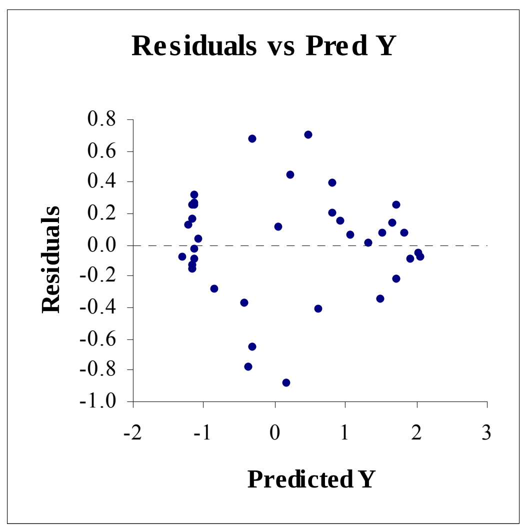

$\Pr\left(\text{Ramming}\,\middle|\,\text{Steering Failure}, \underline{S}^1\right)$

Summary

R^2	R	Adj. R^2	S.E. of Estimate
0.919	0.959	0.871	0.492

ANOVA

Source	Sum Sq.	D.F.	Mean Sq.	F	Prob.
Regression	60.463	13	4.651	19.222	0.000
Residual	5.323	22	0.242		
Total	65.786	35			

Regression Coefficients

Source	Coefficient	Std Error	Std Beta	-95% C.I.	+95% C.I.	t	Prob.
Intercept	0.302	0.108		0.079	0.526	2.806	0.010
X1	1.974	0.396	0.303	1.154	2.794	4.990	0.000
X3	2.833	0.739	0.689	1.301	4.365	3.834	0.001
X4	1.414	0.252	0.344	0.891	1.936	5.614	0.000
X6	1.795	0.692	0.285	0.360	3.229	2.594	0.017
X7	4.434	0.942	0.598	2.481	6.387	4.709	0.000
X8	1.445	0.717	0.230	-0.042	2.932	2.015	0.056
X10	1.436	0.252	0.349	0.913	1.958	5.702	0.000
X15	-4.734	1.708	-0.846	-8.276	-1.191	-2.771	0.011
X16	3.637	1.258	0.624	1.027	6.247	2.890	0.009
X17	7.243	1.700	1.089	3.717	10.769	4.260	0.000
X18	-5.810	1.774	-0.856	-9.488	-2.132	-3.276	0.003
X20	-6.829	1.795	-1.030	-10.551	-3.107	-3.805	0.001
X22	7.282	1.705	0.950	3.746	10.819	4.270	0.000

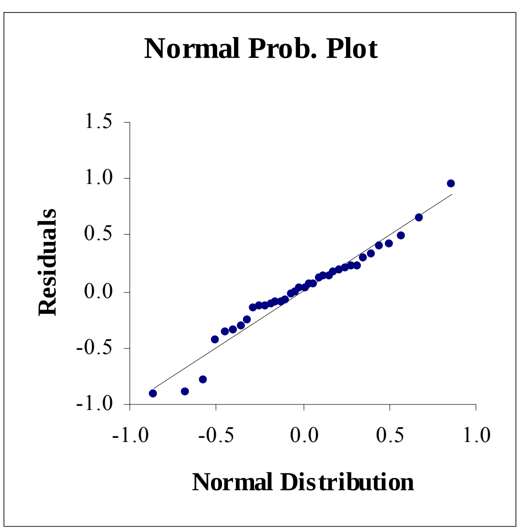

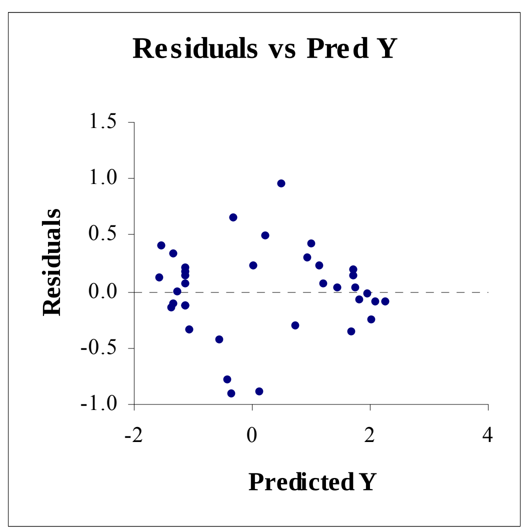

$\Pr\left(\text{Ramming} \middle| \text{Propulsion Failure}, \underline{S}^{1}\right)$

Summary

R^2	R	Adj. R^2	S.E. of Estimate
0.921	0.960	0.874	0.495

ANOVA

Source	Sum Sq.	D.F.	Mean Sq.	F	Prob.
Regression	62.698	13	4.823	19.662	0.000
Residual	5.396	22	0.245		
Total	68.094	35			

Regression Coefficients

Source	Coefficient	Std Error	Std Beta	-95% C.I.	+95% C.I.	t	Prob.
Intercept	0.269	0.108		0.044	0.493	2.476	0.021
X1	2.010	0.398	0.303	1.184	2.836	5.048	0.000
X3	2.767	0.744	0.661	1.224	4.310	3.720	0.001
X4	1.462	0.253	0.349	0.936	1.988	5.768	0.000
X6	1.698	0.696	0.265	0.254	3.142	2.438	0.023
X7	4.468	0.948	0.592	2.502	6.434	4.713	0.000
X8	1.321	0.722	0.207	-0.176	2.818	1.829	0.081
X10	1.458	0.253	0.349	0.933	1.984	5.753	0.000
X15	-4.483	1.720	-0.788	-8.050	-0.917	-2.607	0.016
X16	3.593	1.267	0.606	0.966	6.221	2.836	0.010
X17	7.255	1.712	1.073	3.705	10.805	4.238	0.000
X18	-5.759	1.786	-0.834	-9.462	-2.056	-3.225	0.004
X20	-6.705	1.807	-0.994	-10.452	-2.958	-3.711	0.001
X22	7.269	1.717	0.932	3.708	10.830	4.233	0.000

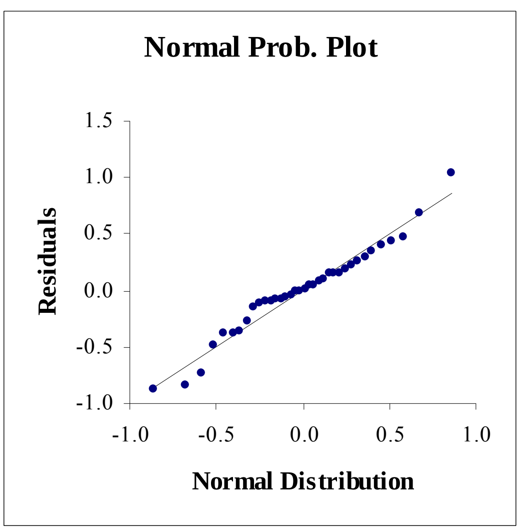

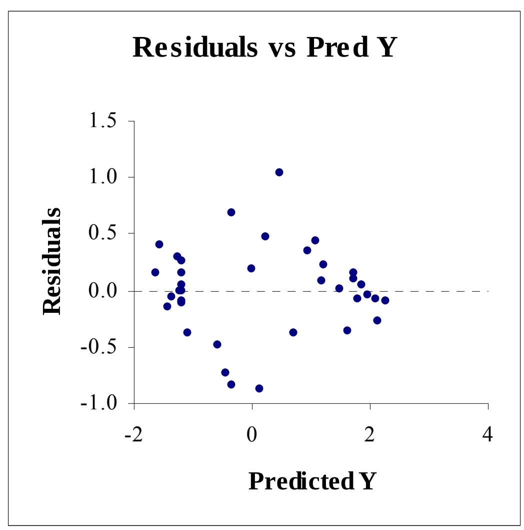

$\Pr\left(\text{Ramming}\,\middle|\,\text{Communication/Navigation Equipment Failure}, \underline{S}^{1}\right)$

Summary

R^2	R	Adj. R^2	S.E. of Estimate
0.931	0.965	0.891	0.445

ANOVA

Source	Sum Sq.	D.F.	Mean Sq.	F	Prob.
Regression	59.077	13	4.544	22.934	0.000
Residual	4.359	22	0.198		
Total	63.436	35			

Regression Coefficients

Source	Coefficient	Std Error	Std Beta	-95% C.I.	+95% C.I.	t	Prob.
Intercept	0.280	0.097		0.077	0.482	2.868	0.009
X1	1.847	0.358	0.288	1.105	2.590	5.160	0.000
X3	2.567	0.669	0.636	1.181	3.954	3.840	0.001
X4	1.405	0.228	0.348	0.932	1.877	6.166	0.000
X6	2.077	0.626	0.336	0.779	3.375	3.319	0.003
X7	3.971	0.852	0.545	2.204	5.738	4.660	0.000
X8	1.547	0.649	0.251	0.201	2.893	2.384	0.026
X10	1.532	0.228	0.379	1.059	2.004	6.722	0.000
X15	-4.353	1.546	-0.793	-7.559	-1.148	-2.817	0.010
X16	3.282	1.139	0.574	0.920	5.643	2.882	0.009
X17	6.639	1.539	1.017	3.448	9.829	4.315	0.000
X18	-5.197	1.605	-0.779	-8.525	-1.868	-3.238	0.004
X20	-6.338	1.624	-0.974	-9.706	-2.970	-3.903	0.001
X22	6.855	1.543	0.911	3.655	10.056	4.442	0.000

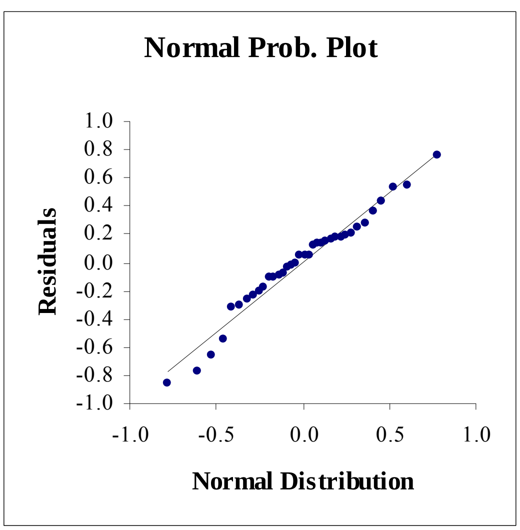

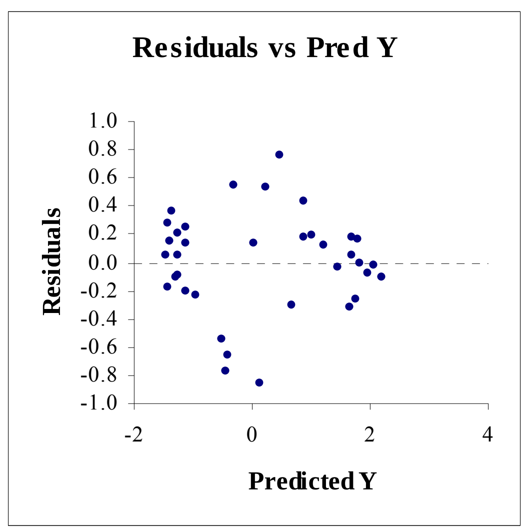

$\Pr\left(\text{Fire/Explosion} \middle| \text{Human Error}, \underline{S}^1\right)$

Summary

R^2	R	Adj. R^2	S.E. of Estimate
0.963	0.981	0.948	0.179

ANOVA

Source	Sum Sq.	D.F.	Mean Sq.	F	Prob.
Regression	4.171	2	2.085	65.186	0.000
Residual	0.160	5	0.032		
Total	4.331	7			

Regression Coefficients

Source	Coefficient	Std Error	Std Beta	-95% C.I.	+95% C.I.	t	Prob.
Intercept	0.116	0.068		-0.058	0.290	1.710	0.148
X1	1.043	0.144	0.623	0.673	1.413	7.243	0.001
X10	0.859	0.096	0.772	0.613	1.105	8.980	0.000

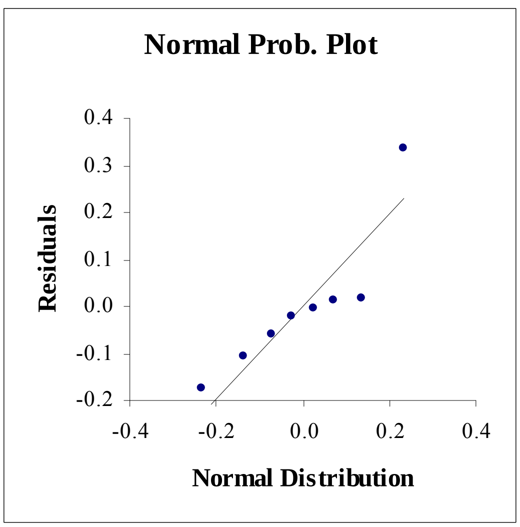

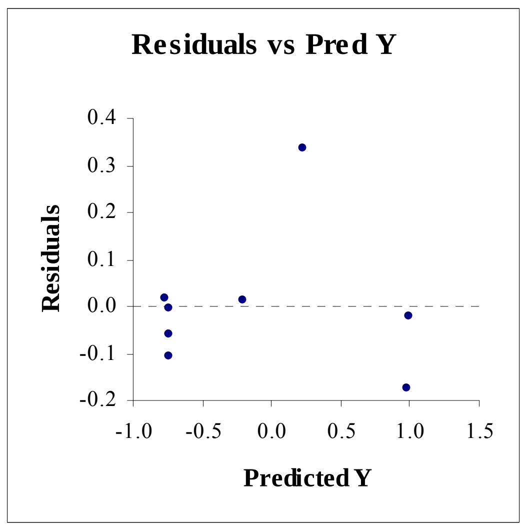

$\Pr\left(\text{Fire/Explosion} \middle| \text{Mechanical/Electrical Failure}, \underline{S}^1\right)$

Summary

R^2	R	Adj. R^2	S.E. of Estimate
0.971	0.985	0.959	0.166

ANOVA

Source	Sum Sq.	D.F.	Mean Sq.	F	Prob.
Regression	4.547	2	2.274	82.313	0.000
Residual	0.138	5	0.028		
Total	4.685	7			

Regression Coefficients

Source	Coefficient	Std Error	Std Beta	-95% C.I.	+95% C.I.	t	Prob.
Intercept	0.113	0.063		-0.048	0.275	1.801	0.132
X1	1.191	0.134	0.683	0.847	1.535	8.898	0.000
X10	0.838	0.089	0.724	0.610	1.067	9.432	0.000

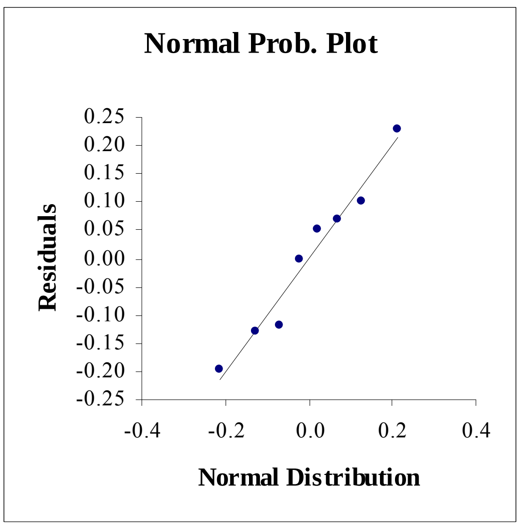

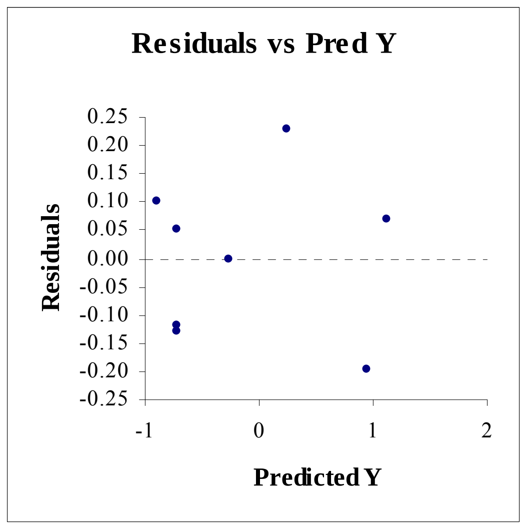

APPENDIX C: Regression Results of the Human Error Probability Questionnaire

Summary

R^2	R	Adj. R^2	S.E. of Estimate
0.756	0.870	0.634	0.308

ANOVA

Source	Sum Sq.	D.F.	Mean Sq.	F	Prob.
Regression	7.634	13	0.587	6.207	0.000
Residual	2.460	26	0.095		
Total	10.094	39			

Regression Coefficients

Source	Coefficient	Std Error	Std Beta	-95% C.I.	+95% C.I.	t	Prob.
Intercept	-0.045	0.061		-0.171	0.081	-0.733	0.470
X2	0.292	0.244	0.116	-0.211	0.794	1.194	0.243
X3	0.595	0.415	0.370	-0.257	1.448	1.435	0.163
X6	0.462	0.418	0.187	-0.398	1.322	1.105	0.279
X7	0.657	0.403	0.287	-0.171	1.484	1.630	0.115
X10	0.324	0.173	0.201	-0.031	0.678	1.875	0.072
X12	0.375	0.328	0.138	-0.300	1.051	1.143	0.263
X15	-2.411	0.927	-1.174	-4.317	-0.505	-2.600	0.015
X16	2.545	0.704	1.160	1.097	3.993	3.613	0.001
X17	3.291	0.958	1.265	1.321	5.260	3.434	0.002
X18	-2.305	0.983	-0.915	-4.324	-0.285	-2.346	0.027
X20	-2.617	1.002	-1.009	-4.676	-0.557	-2.612	0.015
X22	3.179	0.944	1.172	1.238	5.120	3.367	0.002
X23	0.650	0.249	0.282	0.139	1.161	2.616	0.015

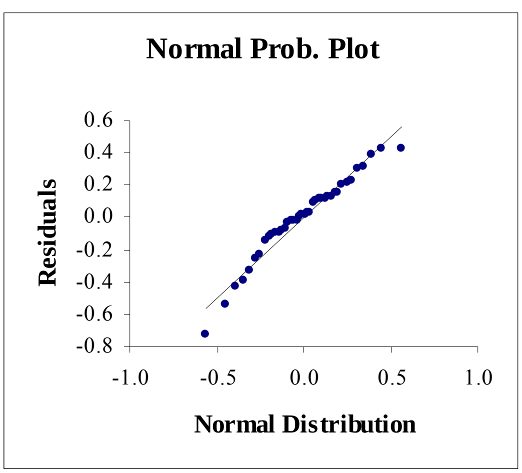

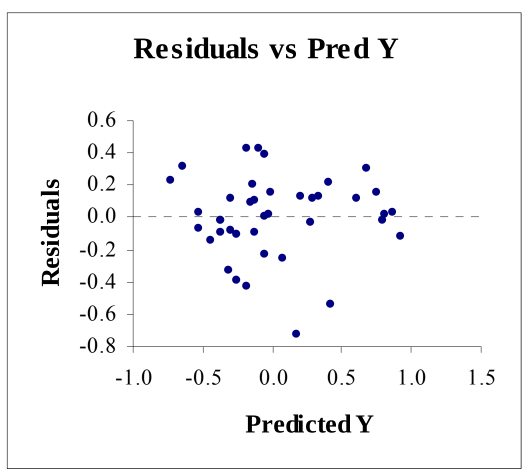

APPENDIX D: Regression Results For Consequence Questionnaires

$\Pr\left(\text{Human Casualty}\left(\text{Low Impact}\right)\middle|\text{Collision}, \underline{S}^2\right)$

Summary

R^2	R	Adj. R^2	S.E. of Estimate
0.751	0.867	0.661	0.466

ANOVA

Source	Sum Sq.	D.F.	Mean Sq.	F	Prob.
Regression	7.200	4	1.800	8.305	0.002
Residual	2.384	11	0.217		
Total	9.584	15			

Regression Coefficients

Source	Coefficient	Std Error	Std Beta	-95% C.I.	+95% C.I.	t	Prob.
Intercept	0.098	0.125		-0.178	0.373	0.782	0.451
W1	1.848	0.531	0.524	0.680	3.015	3.482	0.005
W2	1.595	0.548	0.438	0.389	2.802	2.910	0.014
W3	0.657	0.241	0.411	0.126	1.187	2.724	0.020
W4	0.509	0.241	0.319	-0.021	1.040	2.114	0.058

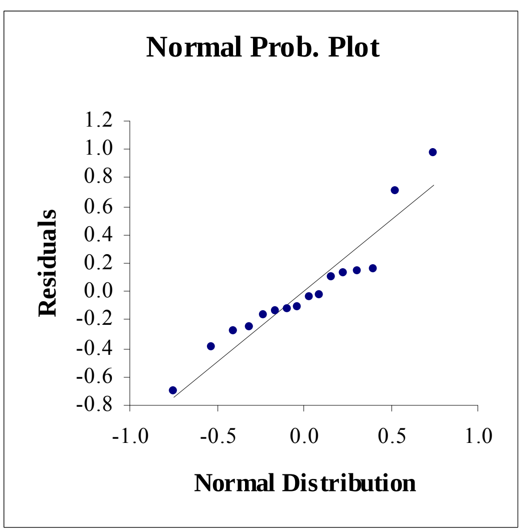

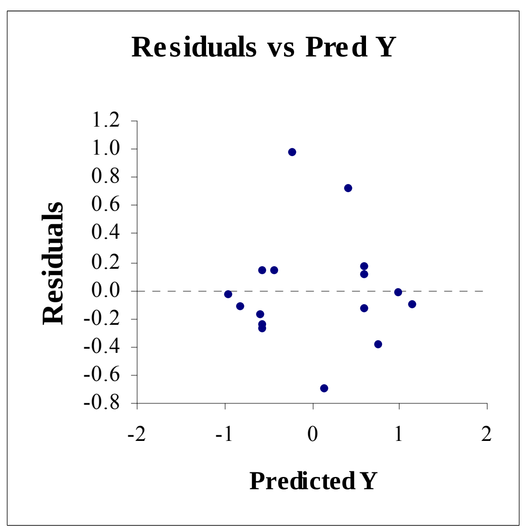

$\Pr\left(\text{Human Casualty}\left(\text{Medium Impact}\right)\middle|\text{Collision}, \underline{S}^2\right)$

Summary

R^2	R	Adj. R^2	S.E. of Estimate
0.837	0.915	0.778	0.374

ANOVA

Source	Sum Sq.	D.F.	Mean Sq.	F	Prob.
Regression	7.885	4	1.971	14.129	0.000
Residual	1.535	11	0.140		
Total	9.420	15			

Regression Coefficients

Source	Coefficient	Std Error	Std Beta	-95% C.I.	+95% C.I.	t	Prob.
Intercept	0.053	0.100		-0.167	0.274	0.533	0.605
W1	2.044	0.426	0.585	1.107	2.981	4.801	0.001
W2	1.653	0.440	0.457	0.684	2.621	3.757	0.003
W3	0.623	0.193	0.393	0.197	1.049	3.222	0.008
W4	0.539	0.193	0.340	0.113	0.964	2.785	0.018

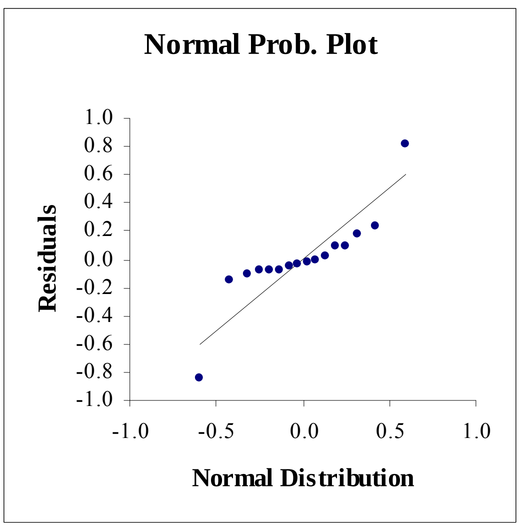

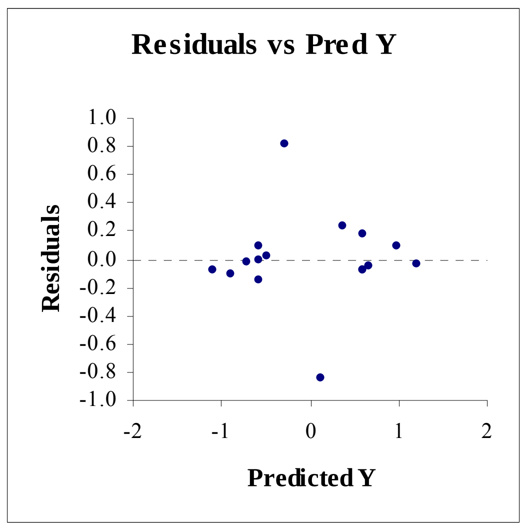

$\Pr\left(\text{Human Casualty}\left(\text{Low Impact}\right)\middle|\text{Ramming}, \underline{S}^2\right)$

Summary

R^2	R	Adj. R^2	S.E. of Estimate
0.767	0.876	0.679	0.333

ANOVA

Source	Sum Sq.	D.F.	Mean Sq.	F	Prob.
Regression	2.913	3	0.971	8.754	0.007
Residual	0.887	8	0.111		
Total	3.801	11			

Regression Coefficients

Source	Coefficient	Std Error	Std Beta	-95% C.I.	+95% C.I.	t	Prob.
Intercept	0.181	0.101		-0.051	0.414	1.804	0.109
W1	1.198	0.404	0.507	0.267	2.129	2.967	0.018
W3	0.404	0.174	0.397	0.003	0.805	2.323	0.049
W5	0.867	0.253	0.587	0.285	1.450	3.433	0.009

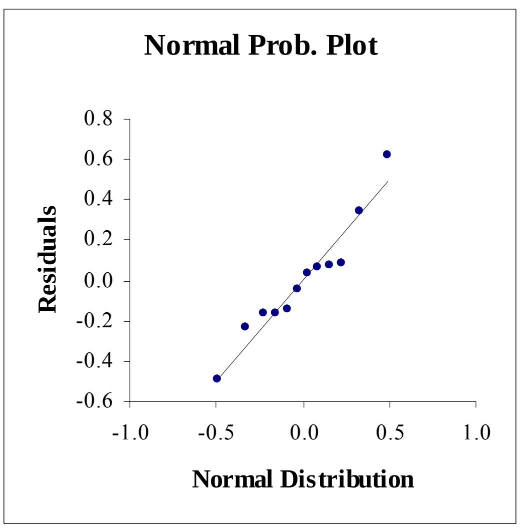

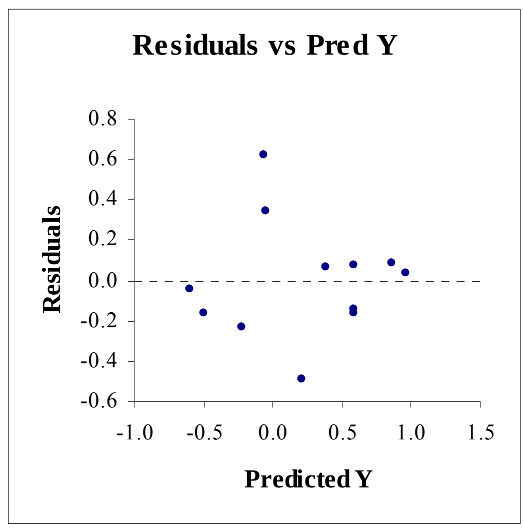

$\Pr\left(\text{Human Casualty}\left(\text{Medium Impact}\right)\middle|\text{Ramming}, \underline{S}^2\right)$

Summary

R^2	R	Adj. R^2	S.E. of Estimate
0.683	0.827	0.564	0.464

ANOVA

Source	Sum Sq.	D.F.	Mean Sq.	F	Prob.
Regression	3.716	3	1.239	5.750	0.021
Residual	1.723	8	0.215		
Total	5.439	11			

Regression Coefficients

Source	Coefficient	Std Error	Std Beta	-95% C.I.	+95% C.I.	t	Prob.
Intercept	0.203	0.140		-0.120	0.526	1.448	0.186
W1	1.262	0.563	0.447	-0.035	2.560	2.243	0.055
W3	0.602	0.242	0.495	0.043	1.161	2.485	0.038
W5	0.849	0.352	0.480	0.038	1.661	2.413	0.042

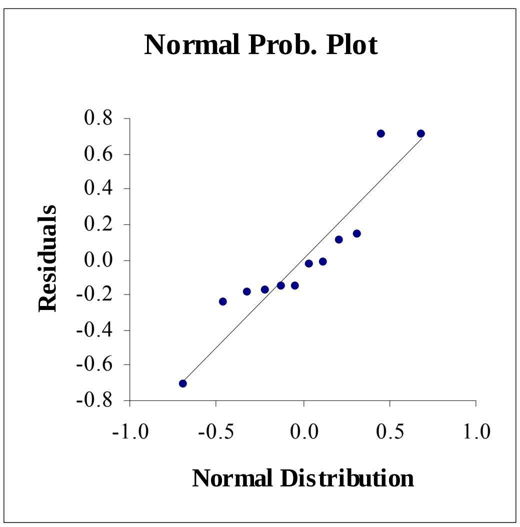

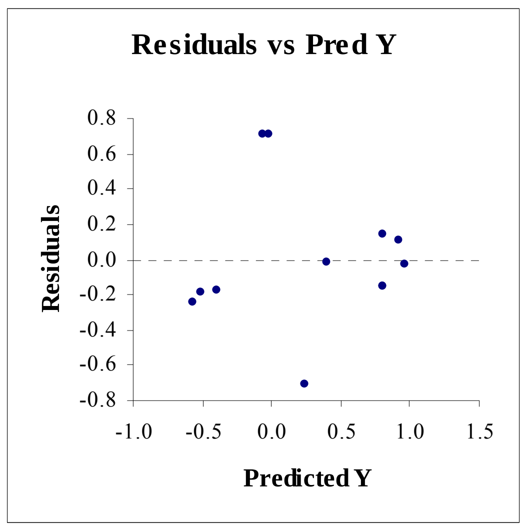

$\Pr\left(\text{Human Casualty}\left(\text{Low Impact}\right)\middle|\text{Fire/Explosion}, \underline{S}^2\right)$

Summary

R^2	R	Adj. R^2	S.E. of Estimate
0.818	0.904	0.749	0.444

ANOVA

Source	Sum Sq.	D.F.	Mean Sq.	F	Prob.
Regression	7.081	3	2.360	11.949	0.003
Residual	1.580	8	0.198		
Total	8.661	11			

Regression Coefficients

Source	Coefficient	Std Error	Std Beta	-95% C.I.	+95% C.I.	t	Prob.
Intercept	0.056	0.134		-0.254	0.365	0.415	0.689
W1	2.731	0.539	0.765	1.488	3.973	5.067	0.001
W3	0.452	0.232	0.294	-0.083	0.988	1.948	0.087
W5	0.826	0.337	0.370	0.048	1.603	2.449	0.040

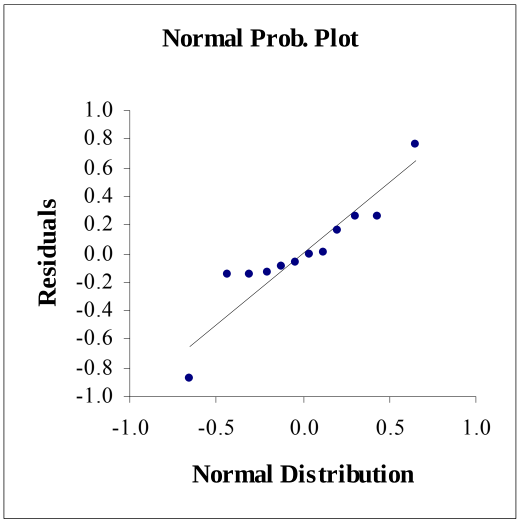

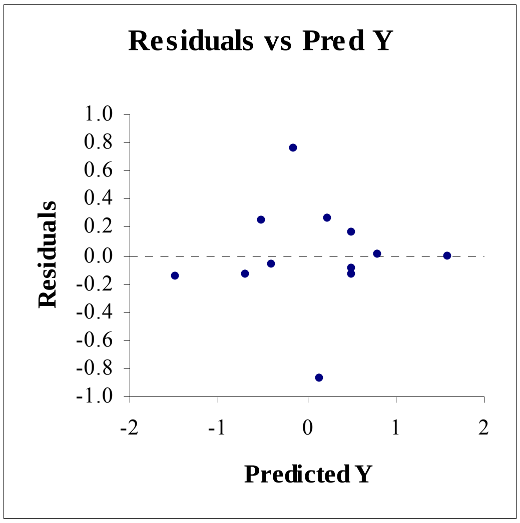

$\Pr\left(\text{Human Casualty}\left(\text{Medium Impact}\right)\middle|\text{Fire/Explosion}, \underline{S}^2\right)$

Summary

R^2	R	Adj. R^2	S.E. of Estimate
0.842	0.918	0.783	0.410

ANOVA

Source	Sum Sq.	D.F.	Mean Sq.	F	Prob.
Regression	7.162	3	2.387	14.196	0.001
Residual	1.345	8	0.168		
Total	8.507	11			

Regression Coefficients

Source	Coefficient	Std Error	Std Beta	-95% C.I.	+95% C.I.	t	Prob.
Intercept	0.171	0.124		-0.114	0.457	1.383	0.204
W1	2.678	0.497	0.758	1.532	3.825	5.387	0.001
W3	0.444	0.214	0.291	-0.050	0.938	2.072	0.072
W5	0.925	0.311	0.418	0.208	1.642	2.974	0.018

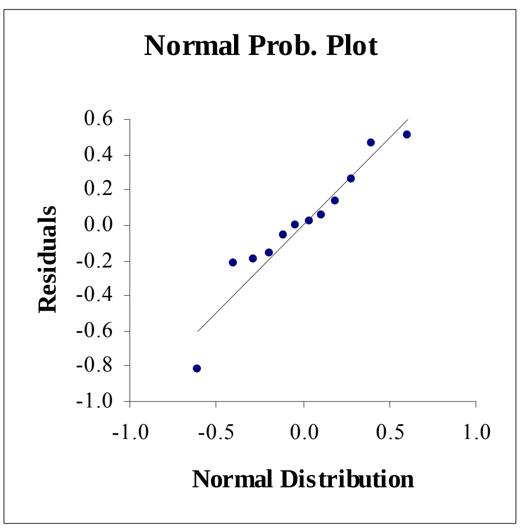

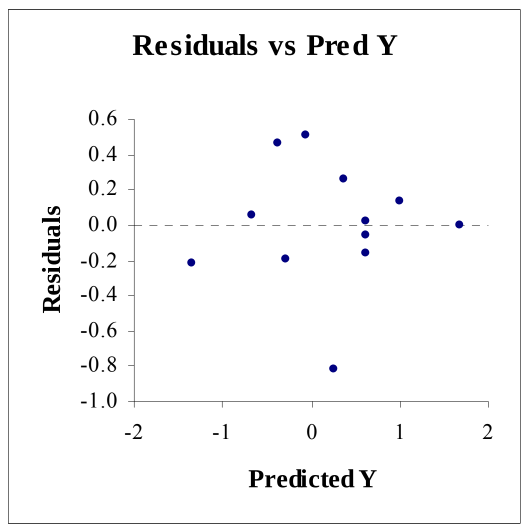

$\Pr\left(\text{Human Casualty}\left(\text{High Impact}\right)\middle|\text{Fire/Explosion}, \underline{S}^2\right)$

Summary

R^2	R	Adj. R^2	S.E. of Estimate
0.849	0.921	0.792	0.479

ANOVA

Source	Sum Sq.	D.F.	Mean Sq.	F	Prob.
Regression	10.319	3	3.440	14.976	0.001
Residual	1.837	8	0.230		
Total	12.156	11			

Regression Coefficients

Source	Coefficient	Std Error	Std Beta	-95% C.I.	+95% C.I.	t	Prob.
Intercept	0.177	0.145		-0.157	0.511	1.225	0.256
W1	3.200	0.581	0.757	1.861	4.540	5.508	0.001
W3	0.639	0.250	0.351	0.062	1.216	2.552	0.034
W5	0.998	0.363	0.377	0.160	1.836	2.745	0.025

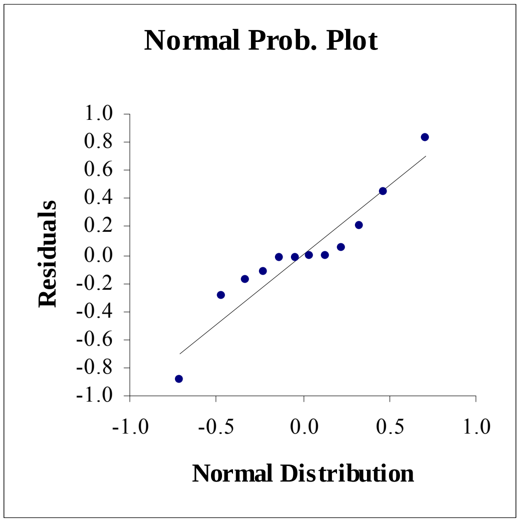

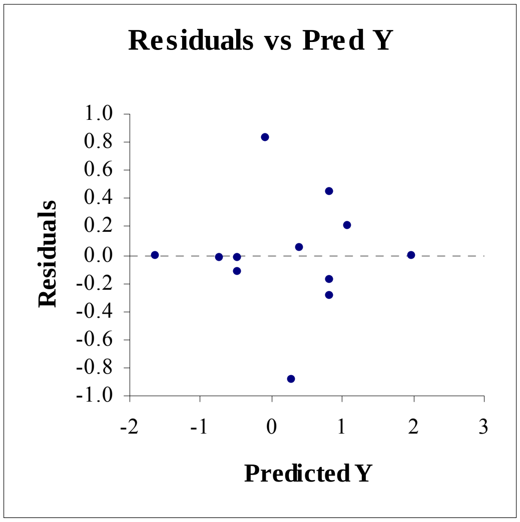

$\Pr\left(\text{Human Casualty}\left(\text{Low Impact}\right)\middle|\text{Grounding}, \underline{S}^2\right)$

Summary

R^2	R	Adj. R^2	S.E. of Estimate
0.634	0.796	0.488	0.542

ANOVA

Source	Sum Sq.	D.F.	Mean Sq.	F	Prob.
Regression	2.549	2	1.274	4.335	0.081
Residual	1.470	5	0.294		
Total	4.019	7			

Regression Coefficients

Source	Coefficient	Std Error	Std Beta	-95% C.I.	+95% C.I.	t	Prob.
Intercept	0.174	0.209		-0.362	0.711	0.835	0.442
W1	2.452	1.051	0.633	-0.250	5.154	2.333	0.067
W3	0.567	0.291	0.529	-0.180	1.314	1.952	0.108

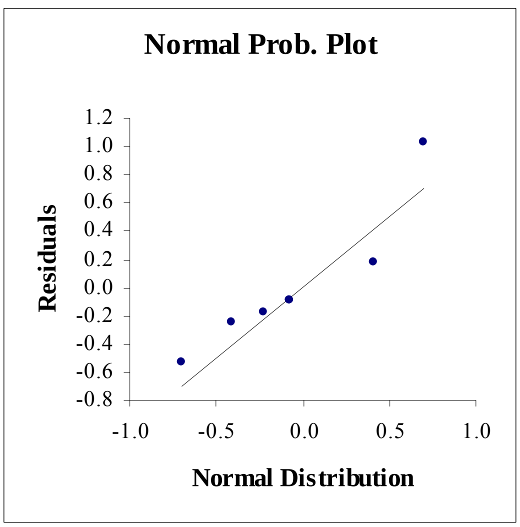

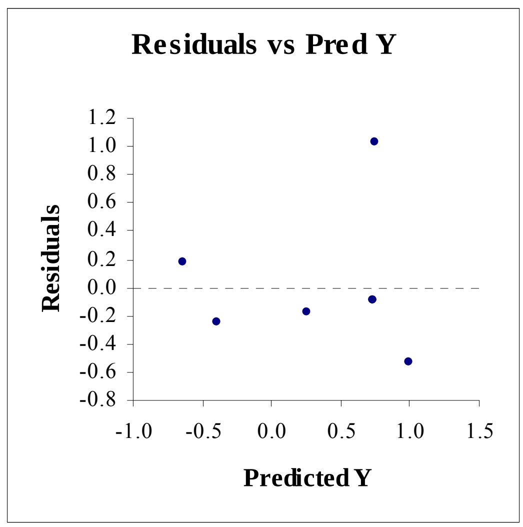

$\Pr\left(\text{Human Casualty}\left(\text{Medium Impact}\right)\middle|\text{Grounding}, \underline{S}^2\right)$

Summary

R^2	R	Adj. R^2	S.E. of Estimate
0.670	0.818	0.537	0.555

ANOVA

Source	Sum Sq.	D.F.	Mean Sq.	F	Prob.
Regression	3.121	2	1.560	5.067	0.063
Residual	1.540	5	0.308		
Total	4.661	7			

Regression Coefficients

Source	Coefficient	Std Error	Std Beta	-95% C.I.	+95% C.I.	t	Prob.
Intercept	0.173	0.214		-0.376	0.722	0.810	0.455
W1	2.736	1.076	0.655	-0.029	5.501	2.543	0.052
W3	0.620	0.297	0.537	-0.145	1.384	2.084	0.092

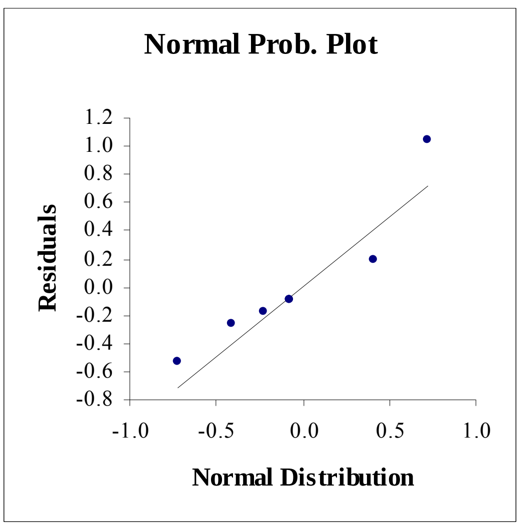

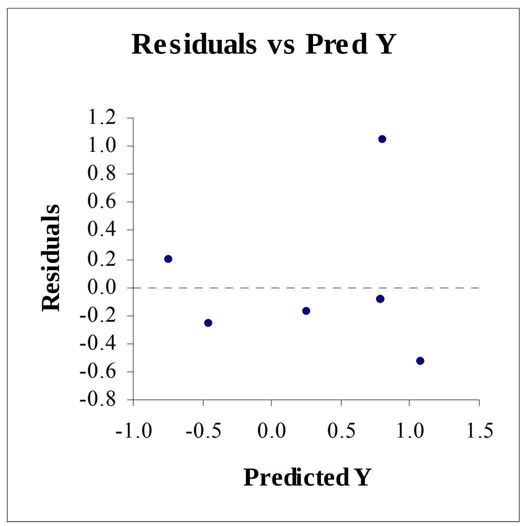

$\Pr\left(\text{Environmental Damage}\left(\text{Low Impact}\right)\middle|\text{Collision},\underline{S}^2\right)$

Summary

R^2	R	Adj. R^2	S.E. of Estimate
0.928	0.963	0.902	0.388

ANOVA

Source	Sum Sq.	D.F.	Mean Sq.	F	Prob.
Regression	21.286	4	5.321	35.437	0.000
Residual	1.652	11	0.150		
Total	22.938	15			

Regression Coefficients

Source	Coefficient	Std Error	Std Beta	-95% C.I.	+95% C.I.	t	Prob.
Intercept	-0.038	0.104		-0.266	0.191	-0.363	0.724
W1	2.448	0.330	0.601	1.722	3.174	7.422	0.000
W2	2.492	0.320	0.630	1.788	3.196	7.789	0.000
W3	0.712	0.201	0.288	0.270	1.153	3.548	0.005
W4	0.689	0.201	0.278	0.247	1.130	3.433	0.006

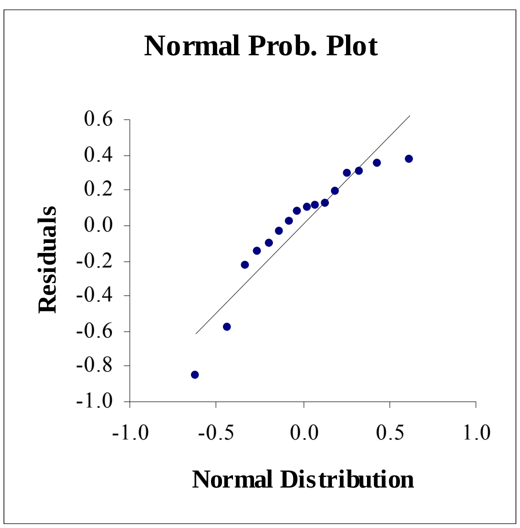

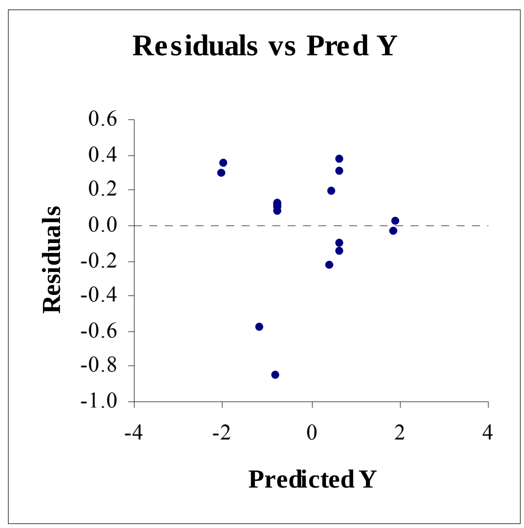

$$\Pr\left(\text{Environmental Damage}\left(\text{Medium Impact}\right)\middle|\text{Collision}, \underline{S}^2\right)$$

Summary

R^2	R	Adj. R^2	S.E. of Estimate
0.956	0.978	0.940	0.345

ANOVA

Source	Sum Sq.	D.F.	Mean Sq.	F	Prob.
Regression	28.375	4	7.094	59.436	0.000
Residual	1.313	11	0.119		
Total	29.688	15			

Regression Coefficients

Source	Coefficient	Std Error	Std Beta	-95% C.I.	+95% C.I.	t	Prob.
Intercept	-0.026	0.092		-0.229	0.178	-0.279	0.785
W1	2.754	0.294	0.594	2.106	3.401	9.365	0.000
W2	2.874	0.285	0.639	2.247	3.502	10.078	0.000
W3	0.825	0.179	0.293	0.432	1.219	4.615	0.001
W4	0.876	0.179	0.311	0.482	1.269	4.896	0.000

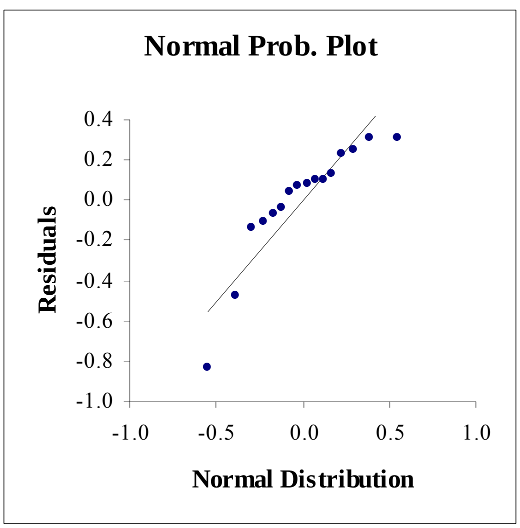

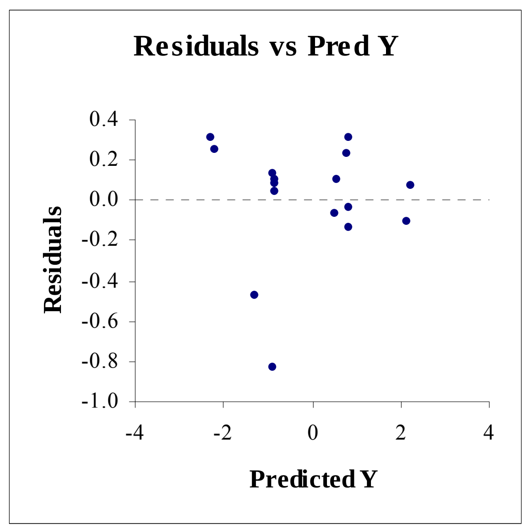

$$\Pr\left(\text{Environmental Damage}\left(\text{Low Impact}\right)\middle|\text{Grounding}, \underline{S}^2\right)$$

Summary

R^2	R	Adj. R^2	S.E. of Estimate
0.961	0.980	0.945	0.266

ANOVA

Source	Sum Sq.	D.F.	Mean Sq.	F	Prob.
Regression	8.633	2	4.316	61.086	0.000
Residual	0.353	5	0.071		
Total	8.986	7			

Regression Coefficients

Source	Coefficient	Std Error	Std Beta	-95% C.I.	+95% C.I.	t	Prob.
Intercept	0.012	0.100		-0.244	0.269	0.123	0.907
W1	2.223	0.221	0.893	1.655	2.790	10.062	0.000
W3	0.645	0.149	0.385	0.263	1.027	4.337	0.007

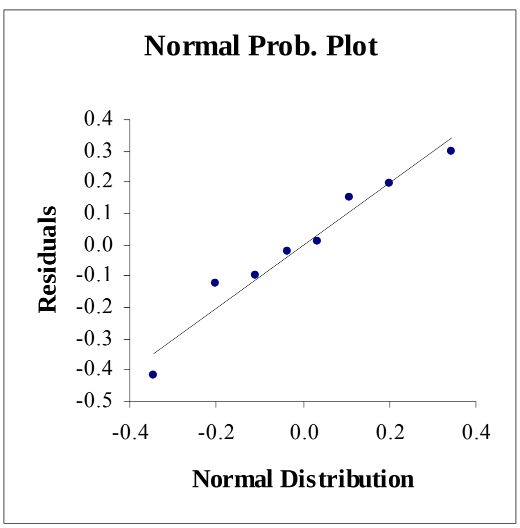

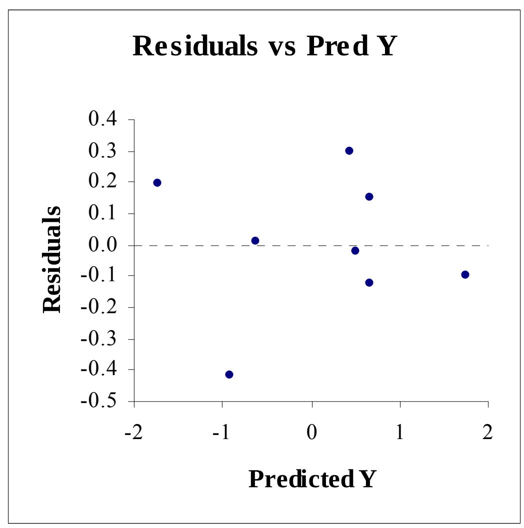

$\Pr\left(\text{Environmental Damage}\left(\text{Medium Impact}\right)\middle|\text{Grounding}, \underline{S}^2\right)$

Summary

R^2	R	Adj. R^2	S.E. of Estimate
0.951	0.975	0.931	0.376

ANOVA

Source	Sum Sq.	D.F.	Mean Sq.	F	Prob.
Regression	13.679	2	6.840	48.495	0.001
Residual	0.705	5	0.141		
Total	14.384	7			

Regression Coefficients

Source	Coefficient	Std Error	Std Beta	-95% C.I.	+95% C.I.	t	Prob.
Intercept	0.012	0.141		-0.350	0.375	0.088	0.933
W1	2.574	0.312	0.817	1.772	3.377	8.250	0.000
W3	1.089	0.210	0.513	0.549	1.629	5.184	0.004

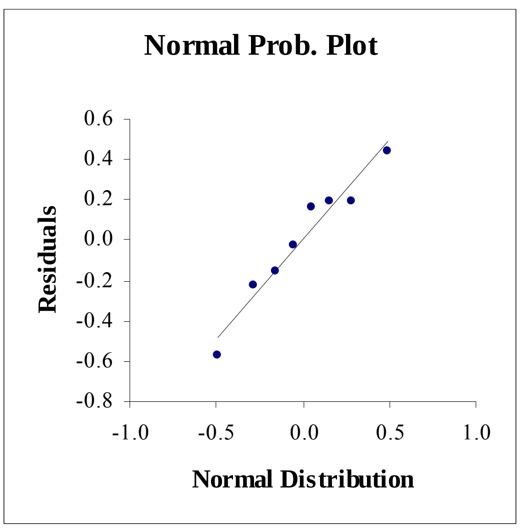

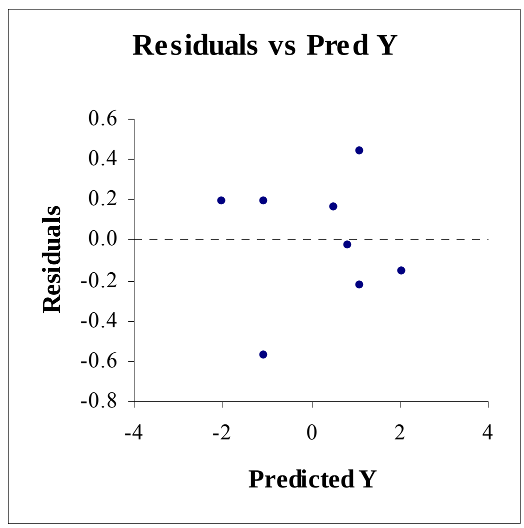

$\Pr\left(\text{Environmental Damage}\left(\text{Low Impact}\right)\middle|\text{Ramming}, \underline{S}^2\right)$

Summary

R^2	R	Adj. R^2	S.E. of Estimate
0.927	0.963	0.898	0.419

ANOVA

Source	Sum Sq.	D.F.	Mean Sq.	F	Prob.
Regression	11.212	2	5.606	31.926	0.001
Residual	0.878	5	0.176		
Total	12.090	7			

Regression Coefficients

Source	Coefficient	Std Error	Std Beta	-95% C.I.	+95% C.I.	t	Prob.
Intercept	0.058	0.159		-0.350	0.466	0.365	0.730
W1	2.462	0.348	0.853	1.567	3.358	7.072	0.001
W3	0.793	0.224	0.427	0.217	1.369	3.540	0.017

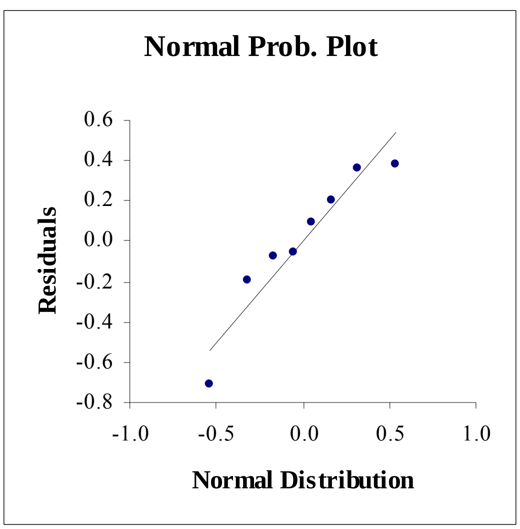

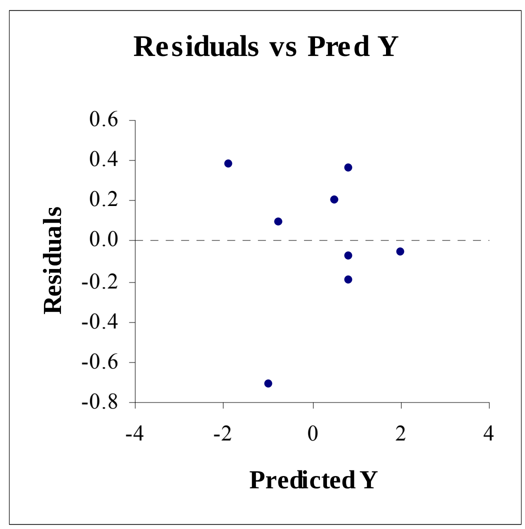

$\Pr\left(\text{Environmental Damage}\left(\text{Medium Impact}\right)\middle|\text{Ramming}, \underline{S}^2\right)$

Summary

R^2	R	Adj. R^2	S.E. of Estimate
0.955	0.977	0.936	0.378

ANOVA

Source	Sum Sq.	D.F.	Mean Sq.	F	Prob.
Regression	15.018	2	7.509	52.496	0.000
Residual	0.715	5	0.143		
Total	15.733	7			

Regression Coefficients

Source	Coefficient	Std Error	Std Beta	-95% C.I.	+95% C.I.	t	Prob.
Intercept	-0.022	0.143		-0.391	0.346	-0.156	0.882
W1	2.783	0.314	0.845	1.975	3.591	8.856	0.000
W3	0.996	0.202	0.470	0.477	1.516	4.927	0.004

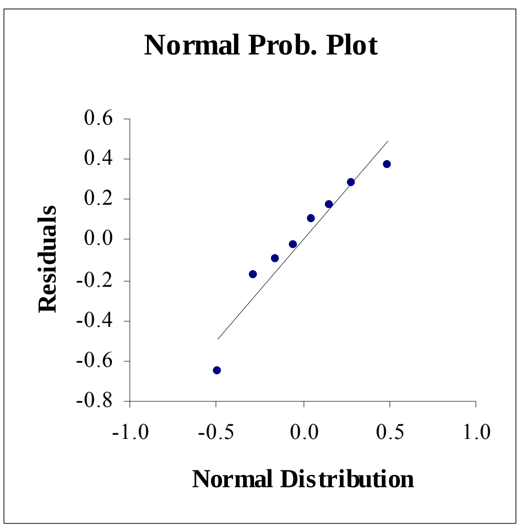

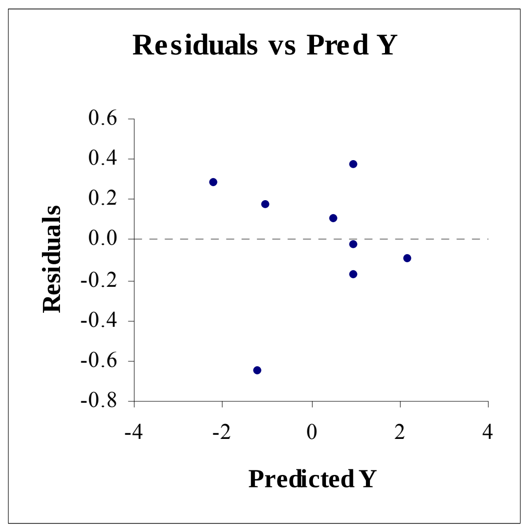

$\Pr\left(\text{Environmental Damage}\left(\text{Low Impact}\right)\middle|\text{Fire/Explosion}, \underline{S}^2\right)$

Summary

R^2	R	Adj. R^2	S.E. of Estimate
0.883	0.939	0.856	0.432

ANOVA

Source	Sum Sq.	D.F.	Mean Sq.	F	Prob.
Regression	12.634	2	6.317	33.812	0.000
Residual	1.681	9	0.187		
Total	14.316	11			

Regression Coefficients

Source	Coefficient	Std Error	Std Beta	-95% C.I.	+95% C.I.	t	Prob.
Intercept	0.070	0.131		-0.226	0.365	0.534	0.606
W1	2.675	0.359	0.852	1.863	3.487	7.454	0.000
W3	0.756	0.226	0.383	0.246	1.267	3.350	0.009

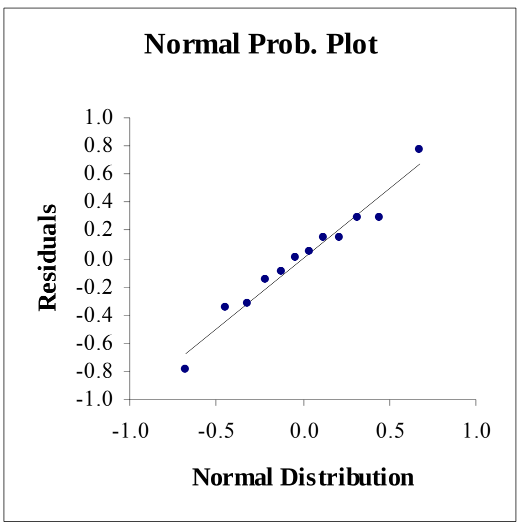

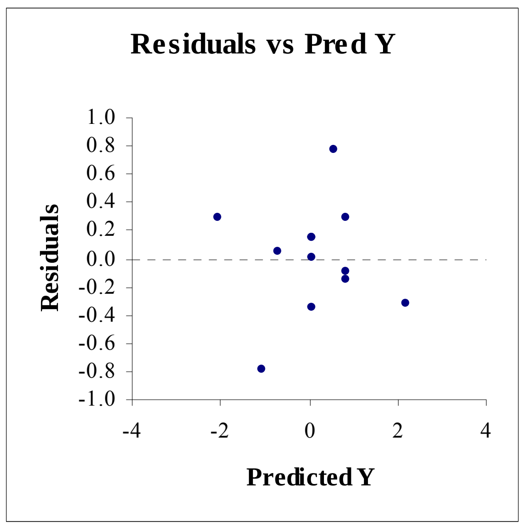

$\Pr\left(\text{Environmental Damage}\left(\text{Medium Impact}\right)\middle|\text{Fire/Explosion}, \underline{S}^2\right)$

Summary

R^2	R	Adj. R^2	S.E. of Estimate
0.927	0.963	0.911	0.364

ANOVA

Source	Sum Sq.	D.F.	Mean Sq.	F	Prob.
Regression	15.174	2	7.587	57.375	0.000
Residual	1.190	9	0.132		
Total	16.364	11			

Regression Coefficients

Source	Coefficient	Std Error	Std Beta	-95% C.I.	+95% C.I.	t	Prob.
Intercept	-0.023	0.112		-0.277	0.231	-0.206	0.842
W1	2.750	0.302	0.819	2.067	3.433	9.108	0.000
W9	1.430	0.262	0.490	0.837	2.023	5.454	0.000

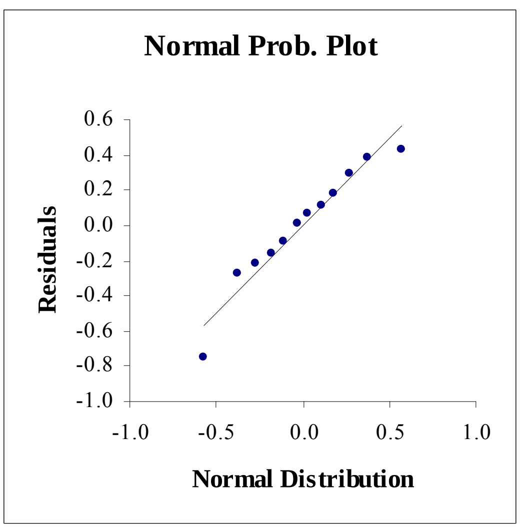

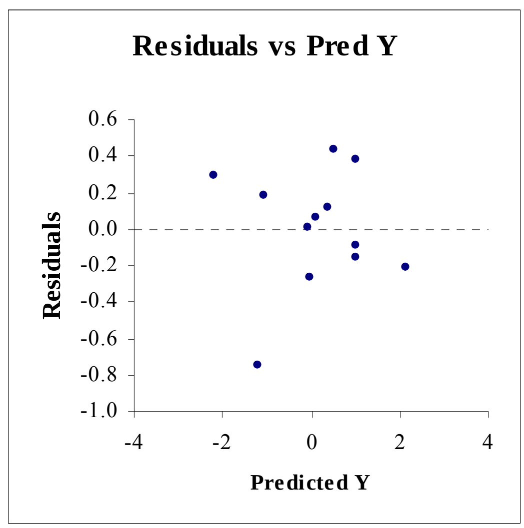

$$\Pr\left(\text{Environmental Damage}\left(\text{High Impact}\right)\middle|\text{Fire/Explosion}, \underline{S}^2\right)$$

Summary

R^2	R	Adj. R^2	S.E. of Estimate
0.928	0.963	0.900	0.465

ANOVA

Source	Sum Sq.	D.F.	Mean Sq.	F	Prob.
Regression	22.143	3	7.381	34.147	0.000
Residual	1.729	8	0.216		
Total	23.873	11			

Regression Coefficients

Source	Coefficient	Std Error	Std Beta	-95% C.I.	+95% C.I.	t	Prob.
Intercept	0.152	0.141		-0.172	0.476	1.085	0.310
W1	3.463	0.386	0.854	2.573	4.353	8.973	0.000
W3	0.909	0.243	0.356	0.349	1.469	3.745	0.006
W5	3.049	1.162	0.250	0.371	5.728	2.625	0.030

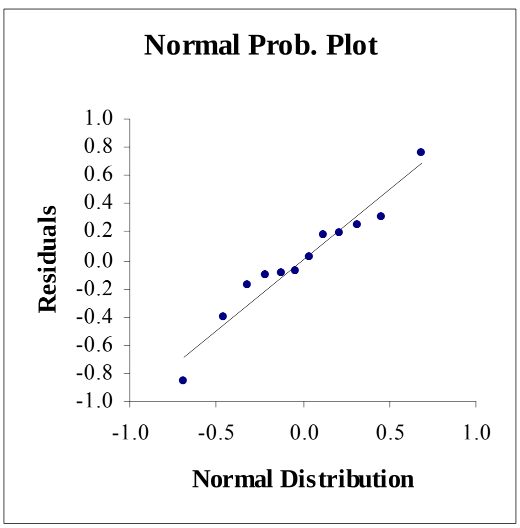

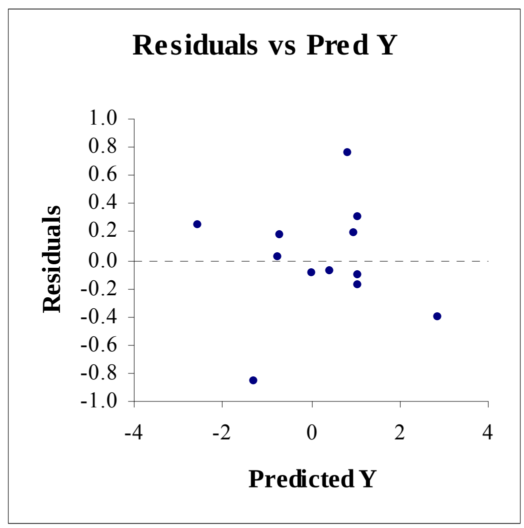

$\Pr\left(\text{Environmental Damage}\left(\text{Low Impact}\right)\middle|\text{Sinking}, \underline{S}^2\right)$

Summary

R^2	R	Adj. R^2	S.E. of Estimate
0.933	0.966	0.906	0.454

ANOVA

Source	Sum Sq.	D.F.	Mean Sq.	F	Prob.
Regression	14.290	2	7.145	34.693	0.001
Residual	1.030	5	0.206		
Total	15.320	7			

Regression Coefficients

Source	Coefficient	Std Error	Std Beta	-95% C.I.	+95% C.I.	t	Prob.
Intercept	0.037	0.172		-0.405	0.479	0.218	0.836
W1	2.832	0.377	0.871	1.862	3.801	7.509	0.001
W3	0.828	0.243	0.396	0.205	1.452	3.414	0.019

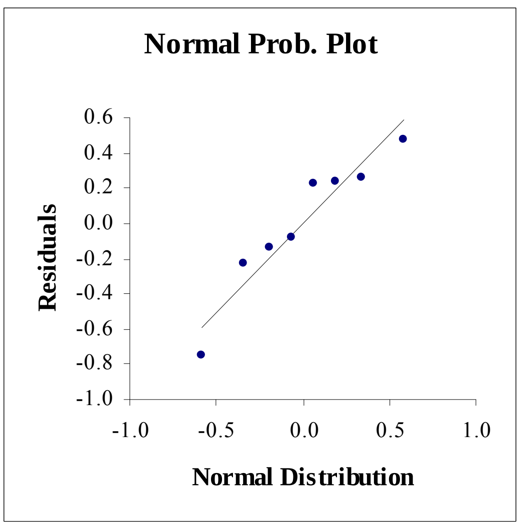

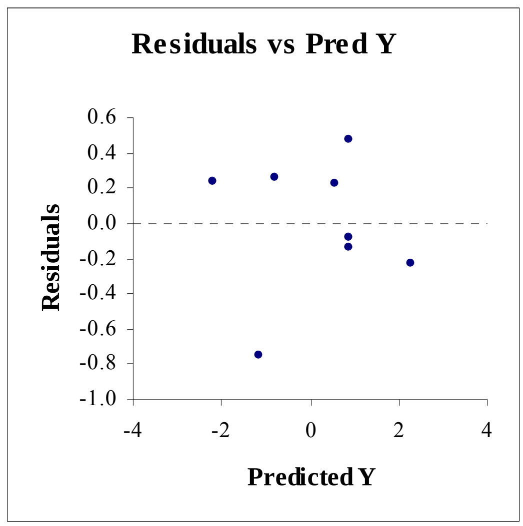

$\Pr\left(\text{Environmental Damage}\left(\text{Medium Impact}\right)\middle|\text{Sinking}, \underline{S}^2\right)$

Summary

R^2	R	Adj. R^2	S.E. of Estimate
0.957	0.978	0.940	0.436

ANOVA

Source	Sum Sq.	D.F.	Mean Sq.	F	Prob.
Regression	21.192	2	10.596	55.776	0.000
Residual	0.950	5	0.190		
Total	22.142	7			

Regression Coefficients

Source	Coefficient	Std Error	Std Beta	-95% C.I.	+95% C.I.	t	Prob.
Intercept	-0.023	0.165		-0.448	0.402	-0.139	0.895
W1	3.381	0.362	0.865	2.450	4.312	9.334	0.000
W3	1.096	0.233	0.436	0.497	1.695	4.704	0.005

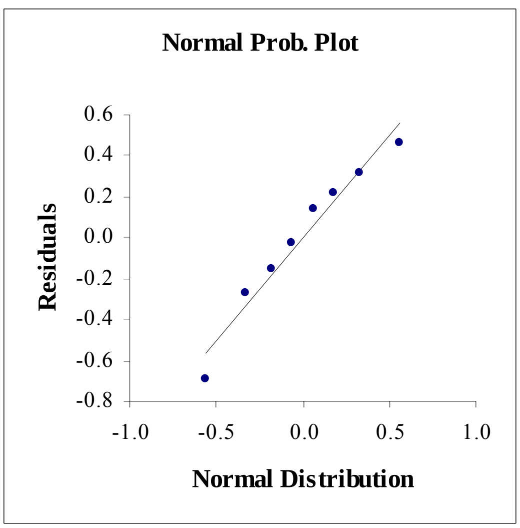

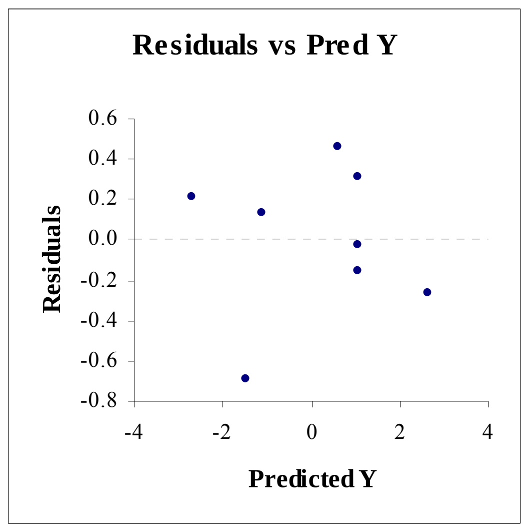

$\Pr\left(\text{Traffic Effectiveness}\left(\text{Low Impact}\right)\middle|\text{Collision}, \underline{S}^2\right)$

Summary

R^2	R	Adj. R^2	S.E. of Estimate
0.956	0.978	0.936	0.235

ANOVA

Source	Sum Sq.	D.F.	Mean Sq.	F	Prob.
Regression	15.722	6	2.620	47.390	0.000
Residual	0.719	13	0.055		
Total	16.441	19			

Regression Coefficients

Source	Coefficient	Std Error	Std Beta	-95% C.I.	+95% C.I.	t	Prob.
Intercept	0.137	0.061		0.006	0.268	2.255	0.042
W1	2.120	0.255	0.483	1.568	2.671	8.305	0.000
W2	2.025	0.255	0.462	1.474	2.577	7.936	0.000
W3	1.918	0.404	0.922	1.045	2.791	4.747	0.000
W4	0.834	0.121	0.401	0.572	1.097	6.872	0.000
W5	2.069	0.410	0.561	1.184	2.954	5.052	0.000
W9	-1.110	0.442	-0.548	-2.065	-0.155	-2.511	0.026

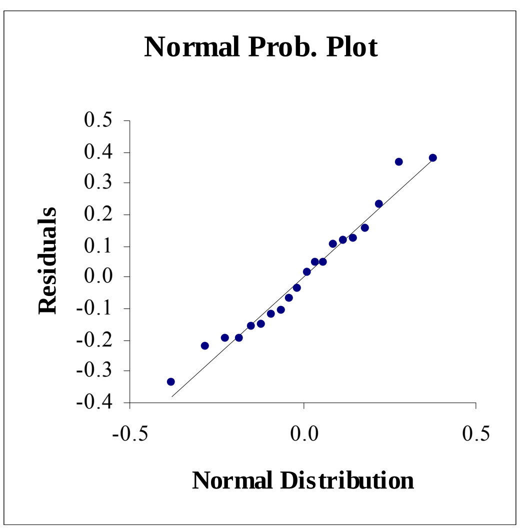

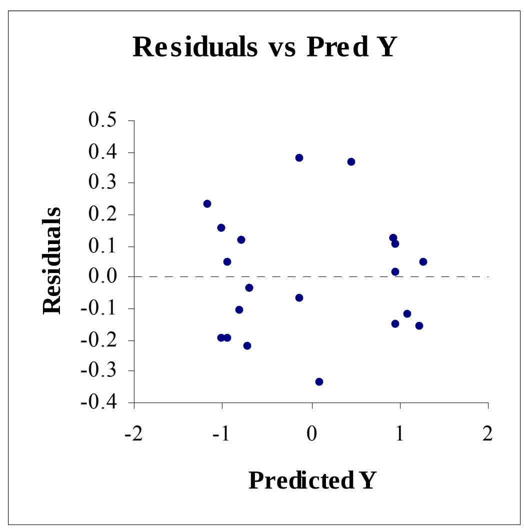

$\Pr\left(\text{Traffic Effectiveness}\left(\text{Medium Impact}\right)\middle|\text{Collision}, \underline{S}^2\right)$

Summary

R^2	R	Adj. R^2	S.E. of Estimate
0.945	0.972	0.925	0.321

ANOVA

Source	Sum Sq.	D.F.	Mean Sq.	F	Prob.
Regression	24.693	5	4.939	47.812	0.000
Residual	1.446	14	0.103		
Total	26.139	19			

Regression Coefficients

Source	Coefficient	Std Error	Std Beta	-95% C.I.	+95% C.I.	t	Prob.
Intercept	0.044	0.079		-0.125	0.213	0.563	0.582
W1	2.740	0.348	0.496	1.993	3.487	7.868	0.000
W2	2.783	0.348	0.503	2.036	3.530	7.990	0.000
W3	1.031	0.165	0.393	0.677	1.386	6.234	0.000
W4	0.939	0.165	0.358	0.584	1.294	5.676	0.000
W5	1.775	0.293	0.381	1.146	2.403	6.056	0.000

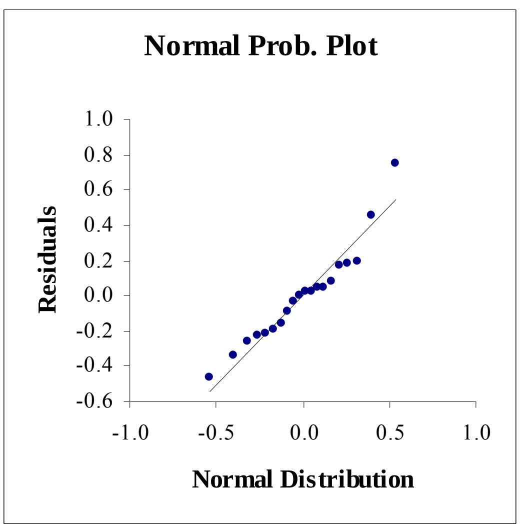

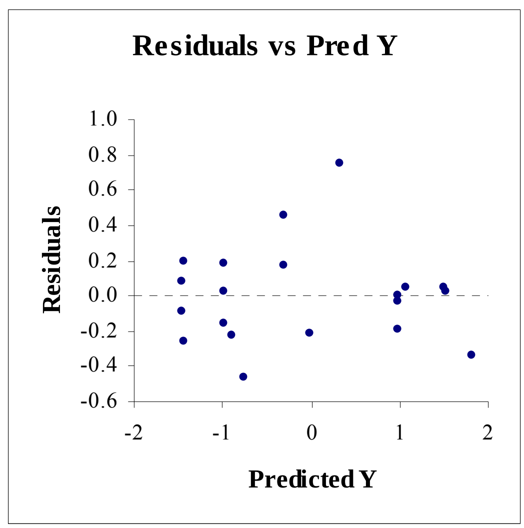

$\Pr\left(\text{Traffic Effectiveness}\left(\text{Low Impact}\right)\middle|\text{Grounding}, \underline{S}^2\right)$

Summary

R^2	R	Adj. R^2	S.E. of Estimate
0.946	0.973	0.926	0.224

ANOVA

Source	Sum Sq.	D.F.	Mean Sq.	F	Prob.
Regression	7.031	3	2.344	46.643	0.000
Residual	0.402	8	0.050		
Total	7.433	11			

Regression Coefficients

Source	Coefficient	Std Error	Std Beta	-95% C.I.	+95% C.I.	t	Prob.
Intercept	0.131	0.069		-0.029	0.291	1.893	0.095
W1	1.662	0.245	0.559	1.097	2.227	6.782	0.000
W3	0.924	0.117	0.649	0.653	1.194	7.873	0.000
W5	2.033	0.341	0.490	1.246	2.819	5.960	0.000

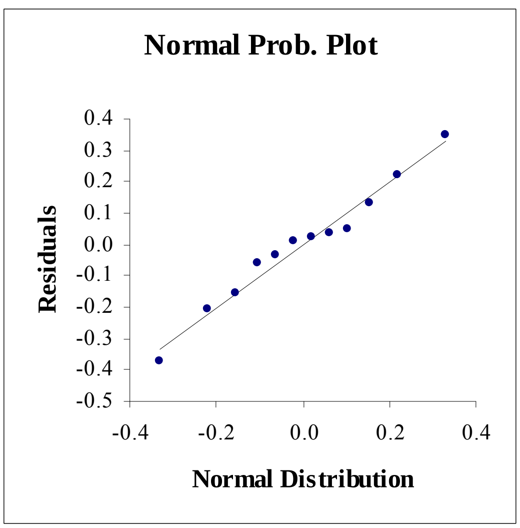

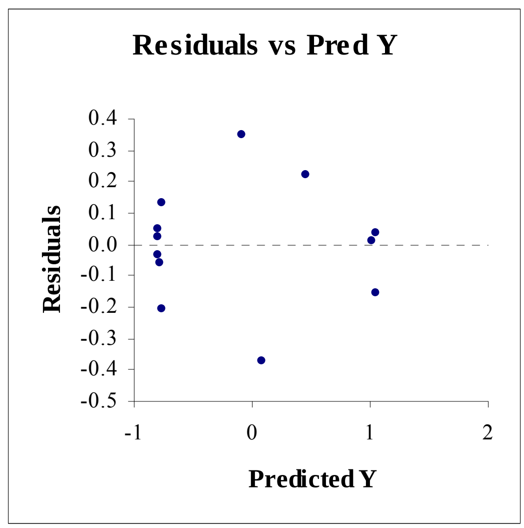

$\Pr\left(\text{Traffic Effectiveness}\left(\text{Medium Impact}\right)\middle|\text{Grounding}, \underline{S}^2\right)$

Summary

R^2	R	Adj. R^2	S.E. of Estimate
0.952	0.976	0.934	0.275

ANOVA

Source	Sum Sq.	D.F.	Mean Sq.	F	Prob.
Regression	12.011	3	4.004	52.965	0.000
Residual	0.605	8	0.076		
Total	12.616	11			

Regression Coefficients

Source	Coefficient	Std Error	Std Beta	-95% C.I.	+95% C.I.	t	Prob.
Intercept	0.180	0.085		-0.016	0.376	2.114	0.067
W1	2.162	0.300	0.558	1.469	2.855	7.195	0.000
W3	1.257	0.144	0.678	0.925	1.589	8.734	0.000
W5	2.485	0.418	0.460	1.521	3.450	5.941	0.000

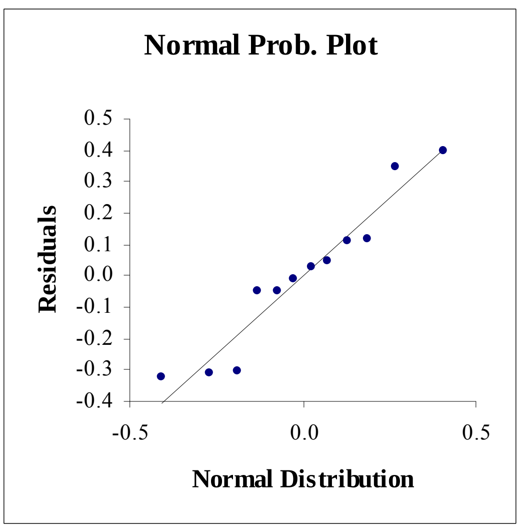

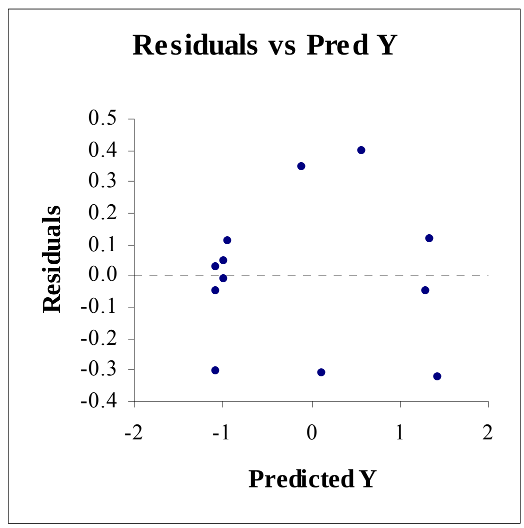

$\Pr\left(\text{Traffic Effectiveness}\left(\text{Low Impact}\right)\middle|\text{Ramming}, \underline{S}^2\right)$

Summary

R^2	R	Adj. R^2	S.E. of Estimate
0.921	0.960	0.892	0.308

ANOVA

Source	Sum Sq.	D.F.	Mean Sq.	F	Prob.
Regression	8.858	3	2.953	31.210	0.000
Residual	0.757	8	0.095		
Total	9.615	11			

Regression Coefficients

Source	Coefficient	Std Error	Std Beta	-95% C.I.	+95% C.I.	t	Prob.
Intercept	0.127	0.095		-0.093	0.346	1.332	0.220
W1	1.795	0.336	0.531	1.020	2.570	5.340	0.001
W3	1.015	0.161	0.627	0.644	1.387	6.308	0.000
W5	2.449	0.468	0.519	1.370	3.529	5.234	0.001

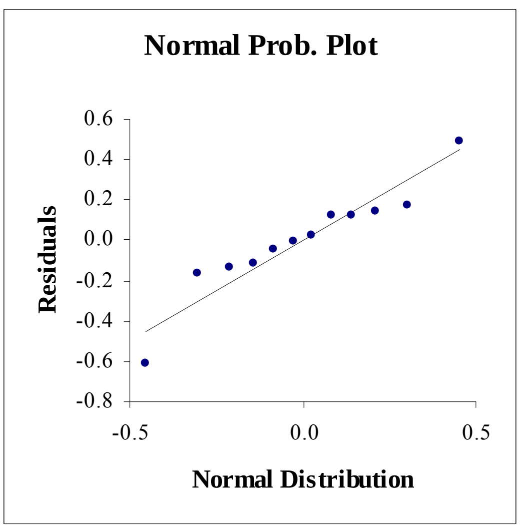

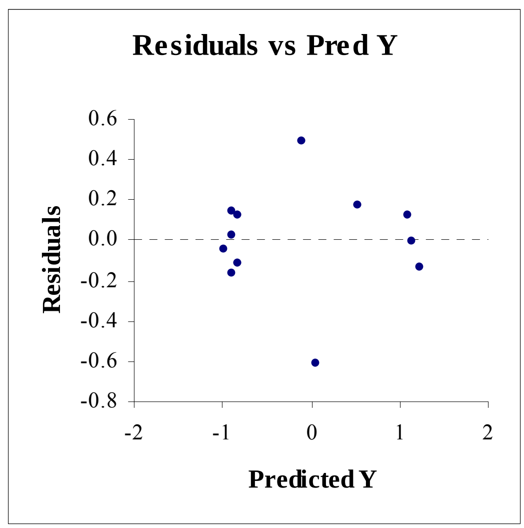

$$\Pr\left(\text{Traffic Effectiveness}\left(\text{Medium Impact}\right)\middle|\text{Ramming}, \underline{S}^2\right)$$

Summary

R^2	R	Adj. R^2	S.E. of Estimate
0.934	0.967	0.910	0.340

ANOVA

Source	Sum Sq.	D.F.	Mean Sq.	F	Prob.
Regression	13.123	3	4.374	37.924	0.000
Residual	0.923	8	0.115		
Total	14.046	11			

Regression Coefficients

Source	Coefficient	Std Error	Std Beta	-95% C.I.	+95% C.I.	t	Prob.
Intercept	0.176	0.105		-0.066	0.418	1.677	0.132
W1	2.409	0.371	0.589	1.553	3.265	6.489	0.000
W3	1.192	0.178	0.609	0.782	1.602	6.704	0.000
W5	2.814	0.517	0.494	1.622	4.005	5.445	0.001

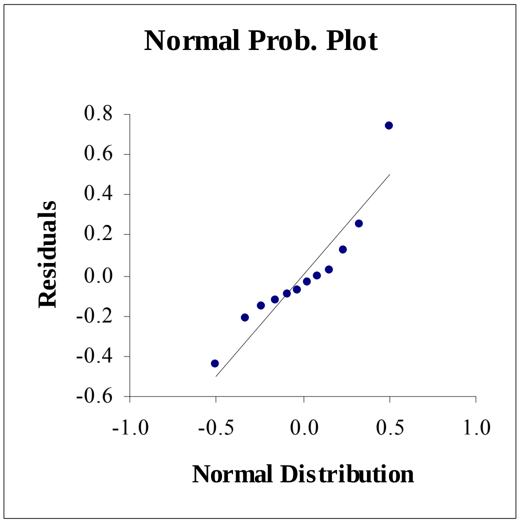

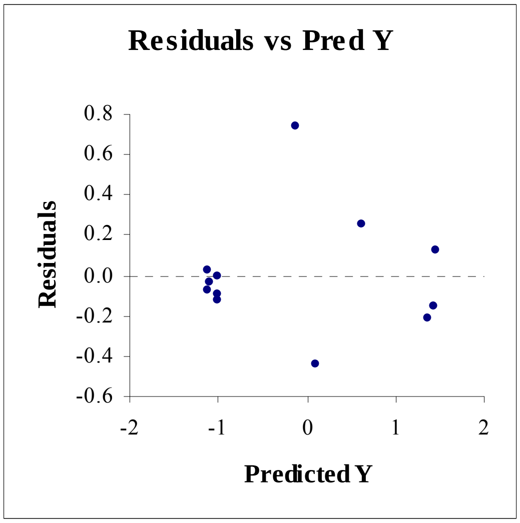

$$\Pr\left(\text{Traffic Effectiveness}\left(\text{Low Impact}\right)\middle|\text{Fire/Explosion}, \underline{S}^2\right)$$

Summary

R^2	R	Adj. R^2	S.E. of Estimate
0.967	0.984	0.955	0.193

ANOVA

Source	Sum Sq.	D.F.	Mean Sq.	F	Prob.
Regression	8.858	3	2.953	79.018	0.000
Residual	0.299	8	0.037		
Total	9.157	11			

Regression Coefficients

Source	Coefficient	Std Error	Std Beta	-95% C.I.	+95% C.I.	t	Prob.
Intercept	0.061	0.059		-0.074	0.196	1.036	0.331
W1	2.894	0.295	0.627	2.214	3.574	9.812	0.000
W3	0.959	0.101	0.607	0.726	1.192	9.497	0.000
W5	2.117	0.294	0.460	1.438	2.795	7.197	0.000

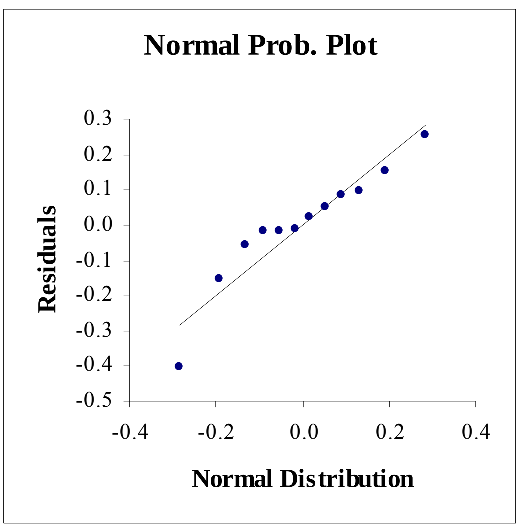

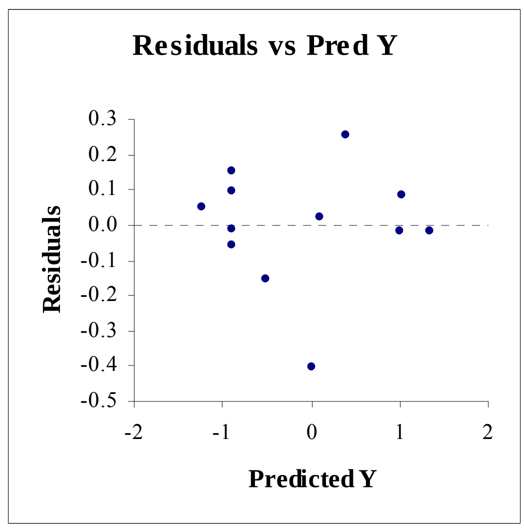

$\Pr\left(\text{Traffic Effectiveness}\left(\text{Medium Impact}\right)\middle|\text{Fire/Explosion}, \underline{S}^2\right)$

Summary

R^2	R	Adj. R^2	S.E. of Estimate
0.975	0.987	0.965	0.196

ANOVA

Source	Sum Sq.	D.F.	Mean Sq.	F	Prob.
Regression	11.903	3	3.968	103.505	0.000
Residual	0.307	8	0.038		
Total	12.210	11			

Regression Coefficients

Source	Coefficient	Std Error	Std Beta	-95% C.I.	+95% C.I.	t	Prob.
Intercept	0.135	0.059		-0.002	0.272	2.279	0.052
W1	3.715	0.299	0.697	3.027	4.404	12.436	0.000
W3	0.874	0.102	0.479	0.638	1.110	8.541	0.000
W5	2.729	0.298	0.514	2.042	3.416	9.163	0.000

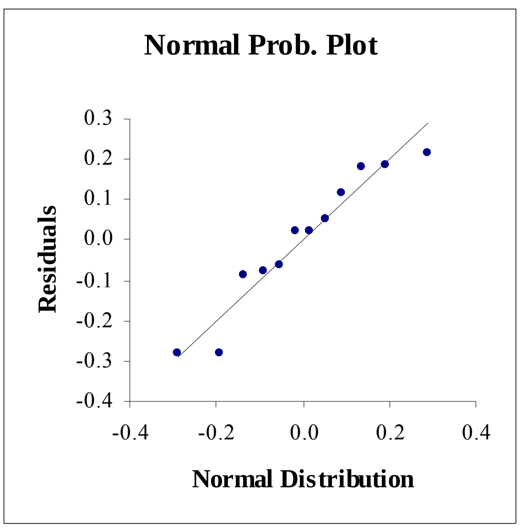

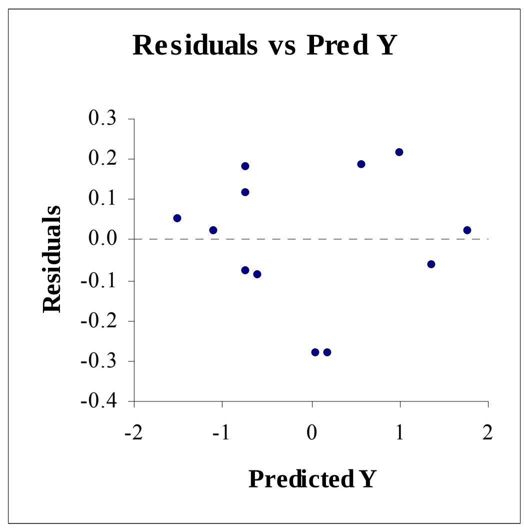

$\Pr\left(\text{Traffic Effectiveness}\left(\text{High Impact}\right)\middle|\text{Fire/Explosion}, \underline{S}^2\right)$

Summary

R^2	R	Adj. R^2	S.E. of Estimate
0.962	0.981	0.948	0.280

ANOVA

Source	Sum Sq.	D.F.	Mean Sq.	F	Prob.
Regression	16.061	3	5.354	68.089	0.000
Residual	0.629	8	0.079		
Total	16.690	11			

Regression Coefficients

Source	Coefficient	Std Error	Std Beta	-95% C.I.	+95% C.I.	t	Prob.
Intercept	0.057	0.085		-0.139	0.253	0.666	0.524
W1	4.119	0.428	0.661	3.133	5.106	9.627	0.000
W3	1.106	0.147	0.518	0.768	1.444	7.549	0.000
W5	3.172	0.427	0.510	2.188	4.156	7.435	0.000

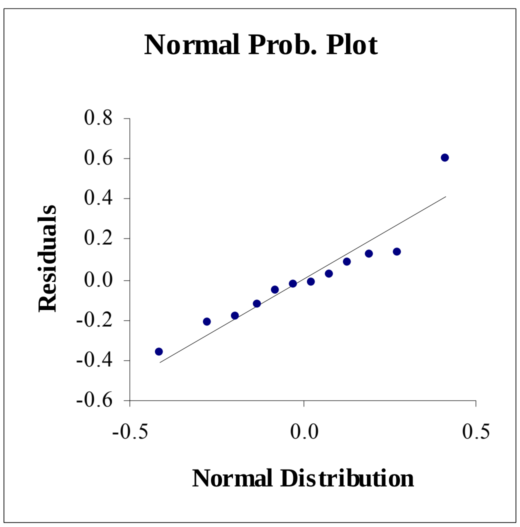

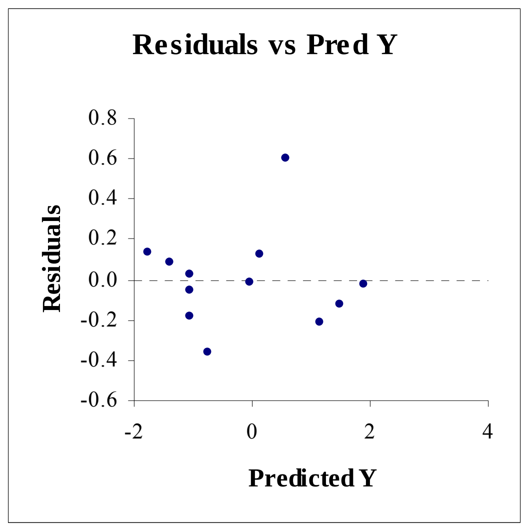

$\Pr\left(\text{Traffic Effectiveness}\left(\text{Low Impact}\right)\middle|\text{Sinking}, \underline{S}^2\right)$

Summary

R^2	R	Adj. R^2	S.E. of Estimate
0.943	0.971	0.922	0.202

ANOVA

Source	Sum Sq.	D.F.	Mean Sq.	F	Prob.
Regression	5.404	3	1.801	44.347	0.000
Residual	0.325	8	0.041		
Total	5.729	11			

Regression Coefficients

Source	Coefficient	Std Error	Std Beta	-95% C.I.	+95% C.I.	t	Prob.
Intercept	0.091	0.062		-0.052	0.235	1.467	0.181
W1	1.833	0.220	0.702	1.325	2.341	8.323	0.000
W3	0.656	0.105	0.525	0.413	0.899	6.219	0.000
W5	1.648	0.307	0.453	0.940	2.355	5.373	0.001

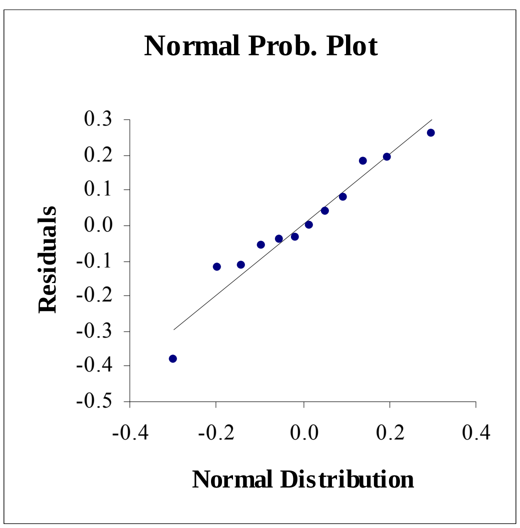

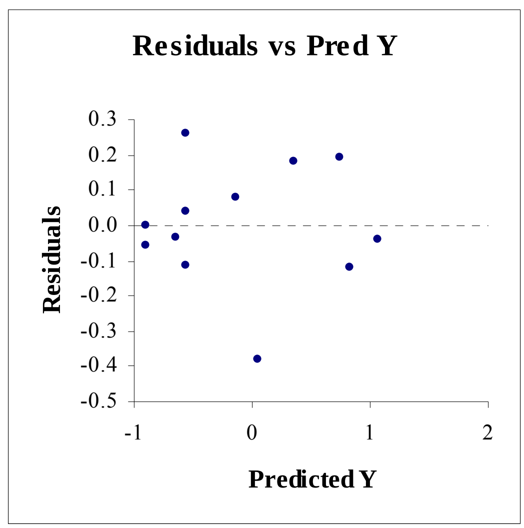

$\Pr\left(\text{Traffic Effectiveness}\left(\text{Medium Impact}\right)\middle|\text{Sinking}, \underline{S}^2\right)$

Summary

R^2	R	Adj. R^2	S.E. of Estimate
0.962	0.981	0.948	0.273

ANOVA

Source	Sum Sq.	D.F.	Mean Sq.	F	Prob.
Regression	15.163	3	5.054	67.742	0.000
Residual	0.597	8	0.075		
Total	15.760	11			

Regression Coefficients

Source	Coefficient	Std Error	Std Beta	-95% C.I.	+95% C.I.	t	Prob.
Intercept	0.078	0.084		-0.117	0.273	0.925	0.382
W1	3.006	0.299	0.694	2.317	3.694	10.068	0.000
W3	1.040	0.143	0.502	0.711	1.370	7.276	0.000
W5	3.047	0.416	0.505	2.089	4.005	7.332	0.000

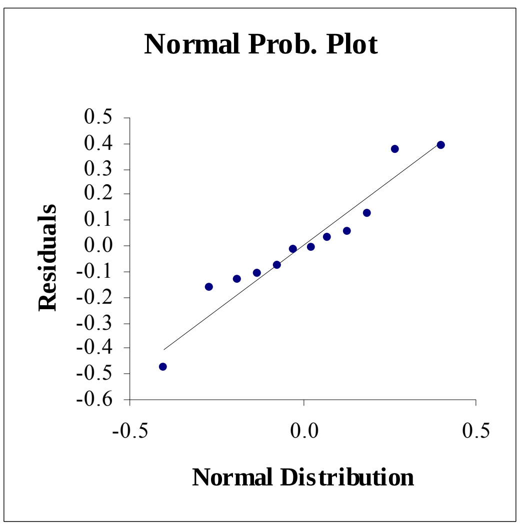

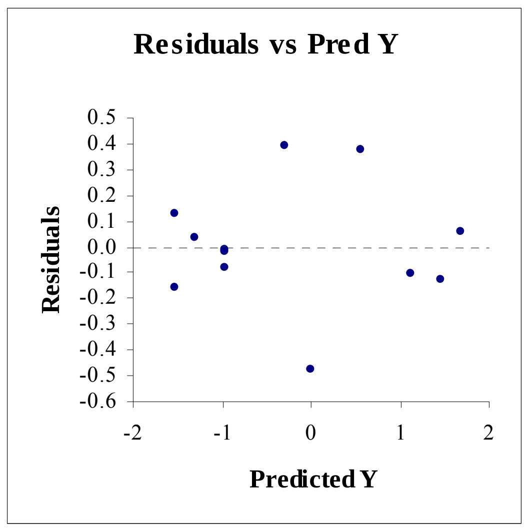

$$\Pr\left(\text{Property/Infrastructure Damage}\left(\text{Low Impact}\right)\middle|\text{Ramming}, \underline{S}^2\right)$$

Summary

R^2	R	Adj. R^2	S.E. of Estimate
0.825	0.908	0.755	0.420

ANOVA

Source	Sum Sq.	D.F.	Mean Sq.	F	Prob.
Regression	4.163	2	2.082	11.798	0.013
Residual	0.882	5	0.176		
Total	5.046	7			

Regression Coefficients

Source	Coefficient	Std Error	Std Beta	-95% C.I.	+95% C.I.	t	Prob.
Intercept	0.109	0.149		-0.273	0.491	0.731	0.497
W1	1.258	0.362	0.650	0.328	2.188	3.477	0.018
W5	1.146	0.338	0.634	0.277	2.015	3.389	0.019

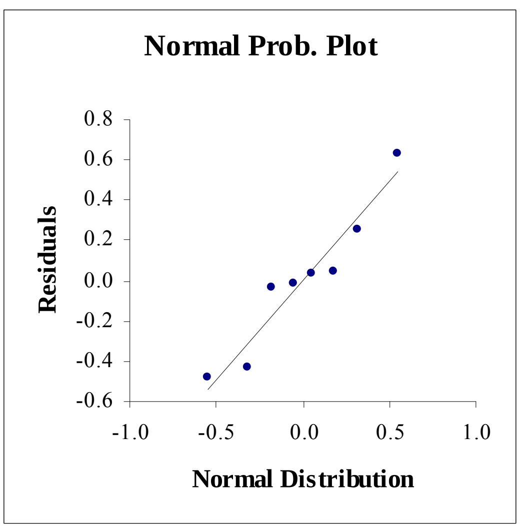

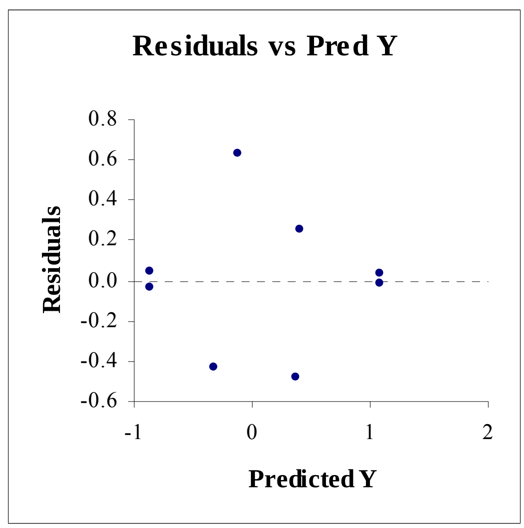

$$\Pr\left(\text{Property/Infrastructure Damage}\left(\text{Medium Impact}\right)\middle|\text{Ramming}, \underline{S}^2\right)$$

Summary

R^2	R	Adj. R^2	S.E. of Estimate
0.869	0.932	0.817	0.534

ANOVA

Source	Sum Sq.	D.F.	Mean Sq.	F	Prob.
Regression	9.464	2	4.732	16.610	0.006
Residual	1.424	5	0.285		
Total	10.888	7			

Regression Coefficients

Source	Coefficient	Std Error	Std Beta	-95% C.I.	+95% C.I.	t	Prob.
Intercept	0.082	0.189		-0.403	0.568	0.436	0.681
W1	1.890	0.460	0.665	0.709	3.071	4.113	0.009
W5	1.734	0.430	0.653	0.629	2.838	4.035	0.010

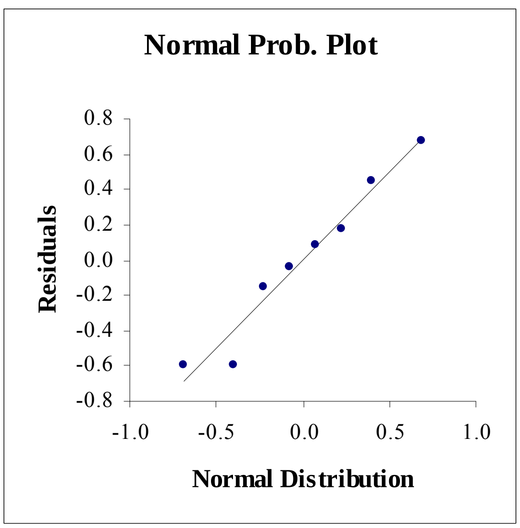

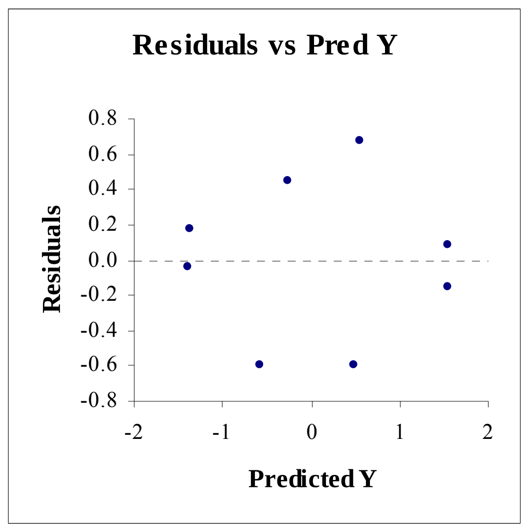

$$\Pr\left(\text{Property/Infrastructure Damage}\left(\text{Low Impact}\right)\middle|\text{Fire/Explosion}, \underline{S}^2\right)$$

Summary

R^2	R	Adj. R^2	S.E. of Estimate
0.929	0.964	0.902	0.416

ANOVA

Source	Sum Sq.	D.F.	Mean Sq.	F	Prob.
Regression	17.982	3	5.994	34.687	0.000
Residual	1.382	8	0.173		
Total	19.365	11			

Regression Coefficients

Source	Coefficient	Std Error	Std Beta	-95% C.I.	+95% C.I.	t	Prob.
Intercept	0.156	0.125		-0.134	0.445	1.241	0.250
W1	2.567	0.358	0.678	1.742	3.392	7.172	0.000
W3	1.117	0.217	0.486	0.617	1.618	5.146	0.001
W5	1.724	0.335	0.487	0.952	2.495	5.151	0.001

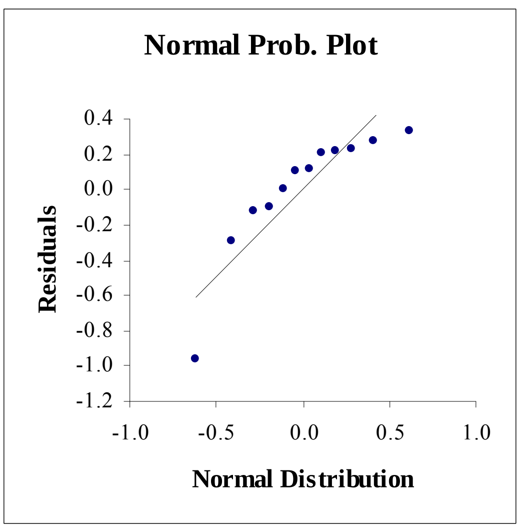

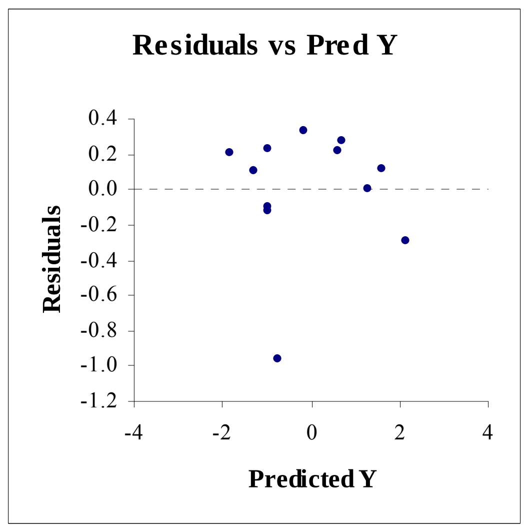

$\Pr\left(\text{Property/Infrastructure Damage}\left(\text{Medium Impact}\right)\middle|\text{Fire/Explosion}, \underline{S}^2\right)$

Summary

R^2	R	Adj. R^2	S.E. of Estimate
0.939	0.969	0.917	0.415

ANOVA

Source	Sum Sq.	D.F.	Mean Sq.	F	Prob.
Regression	21.409	3	7.136	41.354	0.000
Residual	1.381	8	0.173		
Total	22.790	11			

Regression Coefficients

Source	Coefficient	Std Error	Std Beta	-95% C.I.	+95% C.I.	t	Prob.
Intercept	0.164	0.125		-0.125	0.453	1.311	0.226
W1	2.779	0.358	0.676	1.954	3.603	7.769	0.000
W3	1.074	0.217	0.431	0.574	1.574	4.950	0.001
W5	2.103	0.334	0.547	1.332	2.874	6.289	0.000

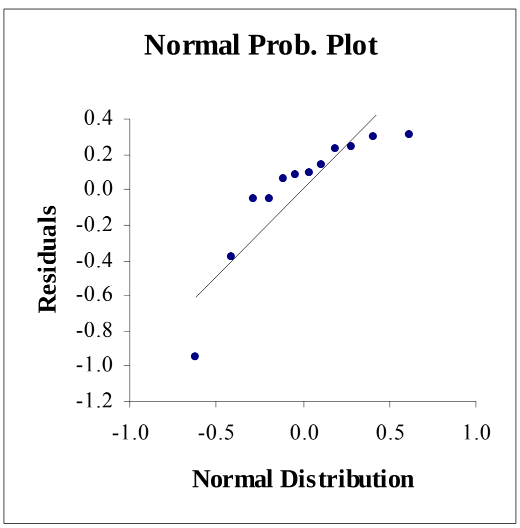

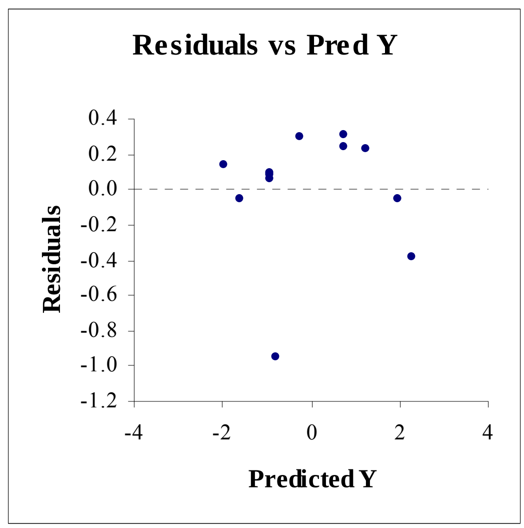

$\Pr\left(\text{Property/Infrastructure Damage}\left(\text{High Impact}\right)\middle|\text{Fire/Explosion}, \underline{S}^2\right)$

Summary

R^2	R	Adj. R^2	S.E. of Estimate
0.909	0.953	0.875	0.583

ANOVA

Source	Sum Sq.	D.F.	Mean Sq.	F	Prob.
Regression	27.148	3	9.049	26.650	0.000
Residual	2.717	8	0.340		
Total	29.865	11			

Regression Coefficients

Source	Coefficient	Std Error	Std Beta	-95% C.I.	+95% C.I.	t	Prob.
Intercept	0.216	0.176		-0.189	0.622	1.231	0.253
W1	3.051	0.502	0.648	1.894	4.207	6.081	0.000
W3	1.435	0.304	0.503	0.733	2.137	4.715	0.002
W5	2.151	0.469	0.489	1.070	3.233	4.586	0.002

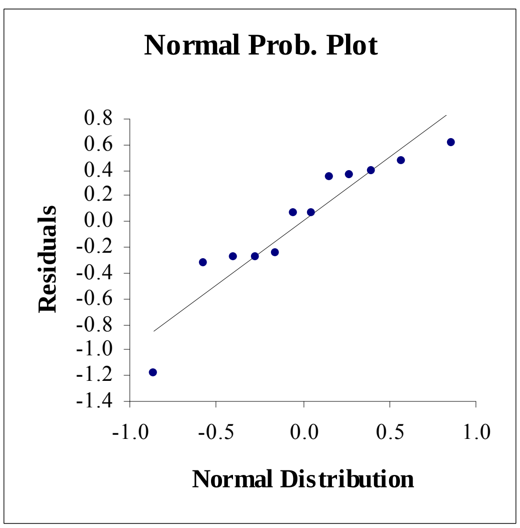

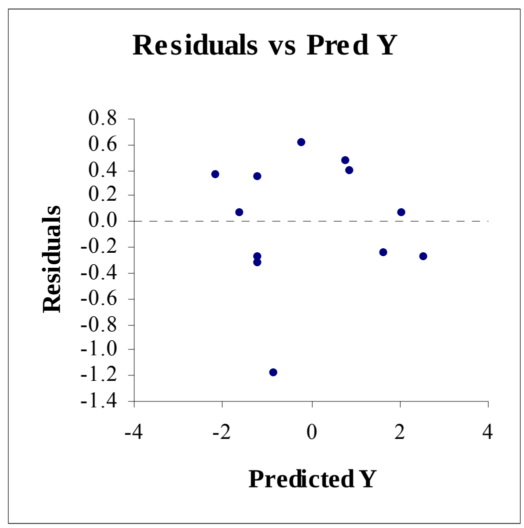

$\Pr\left(\text{Property/Infrastructure Damage}\left(\text{Low Impact}\right)\middle|\text{Sinking}, \underline{S}^2\right)$

Summary

R^2	R	Adj. R^2	S.E. of Estimate
0.838	0.915	0.811	0.366

ANOVA

Source	Sum Sq.	D.F.	Mean Sq.	F	Prob.
Regression	4.155	1	4.155	31.045	0.001
Residual	0.803	6	0.134		
Total	4.958	7			

Regression Coefficients

Source	Coefficient	Std Error	Std Beta	-95% C.I.	+95% C.I.	t	Prob.
Intercept	-0.338	0.139		-0.679	0.002	-2.430	0.051
W8	1.817	0.326	0.915	1.019	2.615	5.572	0.001

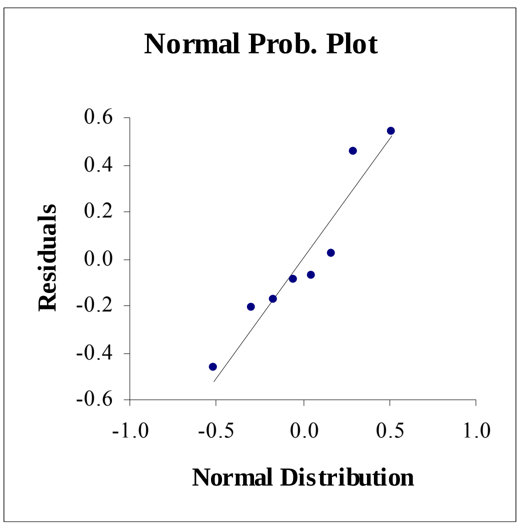

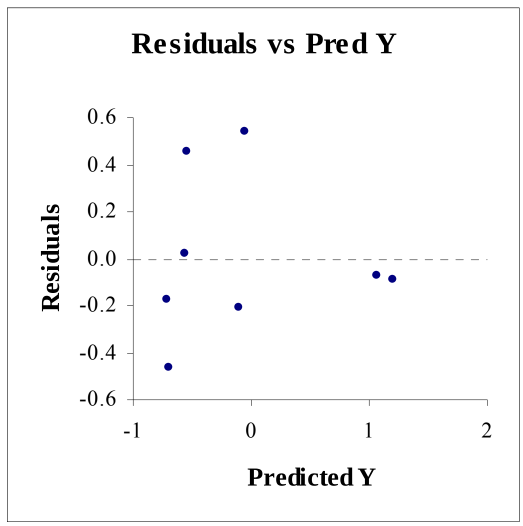

$\Pr\left(\text{Property/Infrastructure Damage}\left(\text{Medium Impact}\right)\middle|\text{Sinking}, \underline{S}^2\right)$

Summary

R^2	R	Adj. R^2	S.E. of Estimate
0.960	0.980	0.943	0.283

ANOVA

Source	Sum Sq.	D.F.	Mean Sq.	F	Prob.
Regression	9.527	2	4.764	59.387	0.000
Residual	0.401	5	0.080		
Total	9.928	7			

Regression Coefficients

Source	Coefficient	Std Error	Std Beta	-95% C.I.	+95% C.I.	t	Prob.
Intercept	0.016	0.100		-0.242	0.274	0.161	0.879
W1	1.931	0.244	0.712	1.304	2.558	7.918	0.001
W5	1.706	0.228	0.672	1.120	2.292	7.482	0.001

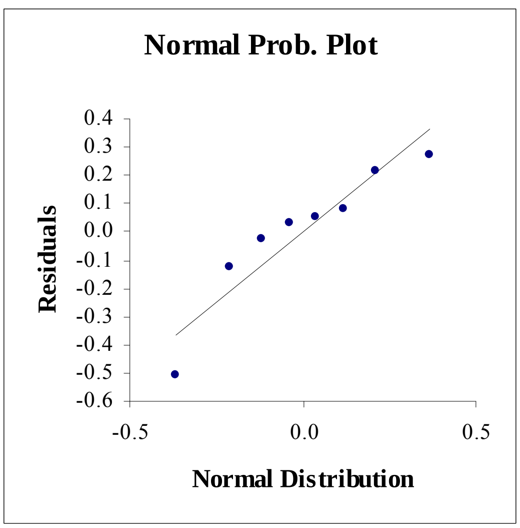

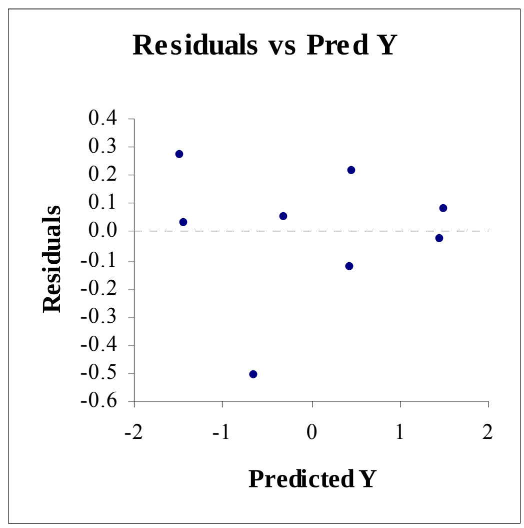

APPENDIX E: LST of the Density Function of the Actual Service Time

$$S_a = \begin{cases} S & \text{w.p. } P(\text{The server does not fail during the service of the job}) \\ Z_1 & \text{w.p. } P\left(\text{The server fails during the service due to failure type } 1\right) \\ Z_2 & \text{w.p. } P\left(\text{The server fails during the service due to failure type } 2\right) \\ \vdots & \vdots \\ Z_k & \text{w.p. } P\left(\text{The server fails during the service due to failure type } k\right) \end{cases}$$

Under the deterministic service time assumption $\left(S = x\right)$,

$$F^*_{S_a}(s) = F^*_S(s)\,P\left(\min\left(Z_1,\ldots,Z_k\right) > x\right) + \sum_{i=1}^{k} E\left[e^{-sZ_i}\,\middle|\,Z_i \le \min\left(x,Z_1,\ldots,Z_{i-1},Z_{i+1},\ldots,Z_k\right)\right]P\left(Z_i \le \min\left(x,Z_1,\ldots,Z_{i-1},Z_{i+1},\ldots,Z_k\right)\right)$$

where

$$F^*_S(s) = e^{-sx}$$

$$P\left(\min\left(Z_1,\ldots,Z_k\right) > x\right) = e^{-\sum_{j=1}^{k}\delta_j x}$$

$$E\left[e^{-sZ_i}\,\middle|\,Z_i \le \min\left(x,Z_1,\ldots,Z_{i-1},Z_{i+1},\ldots,Z_k\right)\right] = \int_0^\infty e^{-sz} f_{Z_i|Z_i\le\min\left(x,Z_1,\ldots,Z_{i-1},Z_{i+1},\ldots,Z_k\right)}(z)\,dz$$

Let $T = \min\left(x,Z_1,\ldots,Z_{i-1},Z_{i+1},\ldots,Z_k\right)$

$$f_{Z_i \left| Z_i \leq \min\left(x, Z_1, \ldots, Z_{i-1}, Z_{i+1}, \ldots, Z_k \right) \right.}(z) = \frac{dF_{Z_i \left| Z_i \leq \min\left(x, Z_1, \ldots, Z_{i-1}, Z_{i+1}, \ldots, Z_k \right) \right.}(z)}{dz}$$

$$\begin{aligned} F_{Z_i \left| \min\left(x, Z_1, \ldots, Z_{i-1}, Z_{i+1}, \ldots, Z_k \right) \right.}(z) &= P\left(Z_i \leq z \middle| Z_i \leq \min\left(x, Z_1, \ldots, Z_{i-1}, Z_{i+1}, \ldots, Z_k \right) \right) \\ &= \frac{P\left(Z_i \leq z, Z_i \leq \min\left(x, Z_1, \ldots, Z_{i-1}, Z_{i+1}, \ldots, Z_k \right) \right)}{P\left(Z_i \leq T \right)} \\ &= \frac{P\left(Z_i \leq \min\left(z, x, Z_1, \ldots, Z_{i-1}, Z_{i+1}, \ldots, Z_k \right) \right)}{P\left(Z_i \leq T \right)} \end{aligned}$$

Let $T' = \min\left(z, x, Z_1, \ldots, Z_{i-1}, Z_{i+1}, \ldots, Z_k \right)$

$$f_{T'}(t) = \begin{cases} \sum\limits_{\substack{j=1 \\ j \neq i}}^{k} \delta_j e^{-\sum\limits_{\substack{j=1 \\ j \neq i}}^{k} \delta_j t} & t < \min(z, x) \\ e^{-\sum\limits_{\substack{j=1 \\ j \neq i}}^{k} \delta_j \min(z, x)} & t = \min(z, x) \end{cases}$$

$$P\left(Z_i \le T'\right) = \int P\left(Z_i \le u\right) f_{T'}(u)\,du = \int_0^{\min(z,x)} P\left(Z_i \le u\right) f_T(u)\,du + P\left(Z_i \le \min(z,x)\right) e^{-\sum_{\substack{m=1 \\ m\neq i}}^{k} \delta_m \min(z,x)}$$

$$= -e^{-\left(\delta_i + \sum_{\substack{m=1 \\ m\neq i}}^{k} \delta_m\right)\min(z,x)} + \frac{\delta_i + e^{-\left(\delta_i + \sum_{\substack{m=1 \\ m\neq i}}^{k} \delta_m\right)\min(z,x)} \sum_{\substack{m=1 \\ m\neq i}}^{k} \delta_m}{\delta_i + \sum_{\substack{m=1 \\ m\neq i}}^{k} \delta_m}$$

$$= \frac{\delta_i}{\sum_{m=1}^{k} \delta_m} \left(1 - e^{-\left(\sum_{m=1}^{k} \delta_m\right)\min(z,x)}\right)$$

Thus,

$$F_{Z_i \mid \min\left(x, Z_1, \ldots, Z_{i-1}, Z_{i+1}, \ldots, Z_k\right)}(z) = \frac{P\left(Z_i \le T'\right)}{P\left(Z_i \le T\right)}$$

$$= \frac{\frac{\delta_i}{\sum_{m=1}^{k} \delta_m} \left(1 - e^{-\left(\sum_{m=1}^{k} \delta_m\right)\min(z,x)}\right)}{\frac{\delta_i}{\sum_{m=1}^{k} \delta_m} \left(1 - e^{-\left(\sum_{m=1}^{k} \delta_m\right)x}\right)}$$

$$F_{Z_i \mid \min\left(x, Z_1, \ldots, Z_{i-1}, Z_{i+1}, \ldots, Z_k\right)}(z) = \frac{1 - e^{-\left(\sum_{m=1}^{k} \delta_m\right)\min(z,x)}}{1 - e^{-\left(\sum_{m=1}^{k} \delta_m\right)x}}.$$

and

$$f_{Z_i|Z_i\le\min\left(x,Z_1,\ldots,Z_{i-1},Z_{i+1},\ldots,Z_k\right)}(z)=\frac{dF_{Z_i|Z_i\le\min\left(x,Z_1,\ldots,Z_{i-1},Z_{i+1},\ldots,Z_k\right)}(z)}{dz}$$

$$=\frac{\min^{(1,0)}(z,x)\;e^{-\left(\sum_{m=1}^{k}\delta_m\right)\min(z,x)}\left(\sum_{m=1}^{k}\delta_m\right)}{1-e^{-\left(\sum_{m=1}^{k}\delta_m\right)x}}$$

where

$$\min^{(1,0)}(z,x)=\begin{cases}1 & z\le x\\ 0 & z>x\end{cases}.$$

Then,

$$E\left[e^{-sZ_i}\middle|Z_i\le\min\left(x,Z_1,\ldots,Z_{i-1},Z_{i+1},\ldots,Z_k\right)\right]=\int_0^\infty e^{-sz}\,f_{Z_i|Z_i\le\min\left(x,Z_1,\ldots,Z_{i-1},Z_{i+1},\ldots,Z_k\right)}(z)\,dz$$

$$=\int_0^x e^{-sz}\left(\frac{e^{-\left(\sum_{m=1}^{k}\delta_m\right)z}\left(\sum_{m=1}^{k}\delta_m\right)}{1-e^{-\left(\sum_{m=1}^{k}\delta_m\right)x}}\right)dz$$

$$E\left[e^{-sZ_i}\middle|Z_i\le\min\left(x,Z_1,\ldots,Z_{i-1},Z_{i+1},\ldots,Z_k\right)\right]=\frac{\left(1-e^{-\left(s+\sum_{m=1}^{k}\delta_m\right)x}\right)\left(\sum_{m=1}^{k}\delta_m\right)}{\left(1-e^{-\left(\sum_{m=1}^{k}\delta_m\right)x}\right)\left(s+\sum_{m=1}^{k}\delta_m\right)}.$$

Therefore the LST of the density function of the actual service time is equal to

$$F_{S_a}^{*}(s) = e^{-x\left(s+\sum_{m=1}^{k}\delta_m\right)} + \sum_{i=1}^{k}\left(\frac{\delta_i}{\left(s+\sum_{m=1}^{k}\delta_m\right)}\left(1-e^{-x\left(s+\sum_{m=1}^{k}\delta_m\right)}\right)\right).$$

APPENDIX F: First Two Moments of S_a for the 4-Phase Erlang Case

In the case where the service time follows a **4-phase Erlang** distribution with rate α and a density function of $\left(f_S(u)=\frac{\alpha^4}{6}u^3 e^{-\alpha u}\right)$, the first two moments of S_a are

$$m_1=\frac{4\alpha^4}{\left(\alpha+\sum_{m=1}^{k}\delta_m\right)^5}-\sum_{i=1}^{k}\left(\begin{array}{c}\dfrac{\delta_i\left(2\alpha+\sum_{m=1}^{k}\delta_m\right)\left(2\alpha^2+2\alpha\sum_{m=1}^{k}\delta_m+\left(\sum_{m=1}^{k}\delta_m\right)^2\right)}{\left(\alpha+\sum_{m=1}^{k}\delta_m\right)^4\left(4\alpha^3+6\alpha^2\sum_{m=1}^{k}\delta_m+4\alpha\left(\sum_{m=1}^{k}\delta_m\right)^2+\left(\sum_{m=1}^{k}\delta_m\right)^3\right)}\\ \times\left(\begin{array}{c}\left(\alpha^2+2\alpha\left(\alpha+\sum_{m=1}^{k}\delta_m\right)+3\left(\alpha+\sum_{m=1}^{k}\delta_m\right)^2\right)\\ -\dfrac{4\left(\alpha^3+\alpha^2\left(\alpha+\sum_{m=1}^{k}\delta_m\right)+\alpha\left(\alpha+\sum_{m=1}^{k}\delta_m\right)^2+\left(\alpha+\sum_{m=1}^{k}\delta_m\right)^3\right)}{\alpha+\sum_{m=1}^{k}\delta_m}\end{array}\right)\end{array}\right)$$

$$m_2 = \frac{20\alpha^4}{\left(\alpha + \sum_{m=1}^{k}\delta_m\right)^6} + \sum_{i=1}^{k}\left(\begin{array}{l} \dfrac{\delta_i\left(2\alpha + \sum_{m=1}^{k}\delta_m\right)\left(2\alpha^2 + 2\alpha\sum_{m=1}^{k}\delta_m + \left(\sum_{m=1}^{k}\delta_m\right)^2\right)}{\left(\alpha + \sum_{m=1}^{k}\delta_m\right)^4\left(4\alpha^3 + 6\alpha^2\sum_{m=1}^{k}\delta_m + 4\alpha\left(\sum_{m=1}^{k}\delta_m\right)^2 + \left(\sum_{m=1}^{k}\delta_m\right)^3\right)} \\ \times\left(\begin{array}{l} \left(2\alpha + 6\left(\alpha + \sum_{m=1}^{k}\delta_m\right)\right) - \dfrac{8\left(\alpha^2 + 2\alpha\left(\alpha + \sum_{m=1}^{k}\delta_m\right) + 3\left(\alpha + \sum_{m=1}^{k}\delta_m\right)^2\right)}{\alpha + \sum_{m=1}^{k}\delta_m} \\ + \dfrac{20\left(\alpha^3 + \alpha^2\left(\alpha + \sum_{m=1}^{k}\delta_m\right) + \alpha\left(\alpha + \sum_{m=1}^{k}\delta_m\right)^2 + \left(\alpha + \sum_{m=1}^{k}\delta_m\right)^3\right)}{\left(\alpha + \sum_{m=1}^{k}\delta_m\right)^2} \end{array} \right) \end{array} \right).$$

APPENDIX G: Some Key Components of the Expression for the Completion Time

$E\left[e^{-sZ_h}\middle| Z_h \le \min\left(Y_i, \mathcal{Z}\text{-}\{i,h\}\right)\right]$: Laplace transform of a time to interruption given it is less than a downtime and the rest of the times to interruptions

---

$$E\left[e^{-sZ_h}\middle| Z_h \le \min\left(Y_i, \mathcal{Z}\text{-}\{i,h\}\right)\right] = \int_0^\infty e^{-sz} f_{Z_h|Z_h \le \min\left(Y_i, \mathcal{Z}\text{-}\{i,h\}\right)}(z)\,dz$$

Let $T = \min\left(Y_i, \mathcal{Z}\text{-}\{i,h\}\right)$

$$f_{Z_h|Z_h \le \min\left(Y_i, \mathcal{Z}\text{-}\{i,h\}\right)}(z) = \frac{dF_{Z_h|Z_h \le \min\left(Y_i, \mathcal{Z}\text{-}\{i,h\}\right)}(z)}{dz}$$

$$F_{Z_h|Z_h \le \min\left(Y_i, \mathcal{Z}\text{-}\{i,h\}\right)}(z) = P\left(Z_h \le z \middle| Z_h \le \min\left(Y_i, \mathcal{Z}\text{-}\{i,h\}\right)\right)$$

$$= \frac{P\left(Z_h \le z, Z_h \le \min\left(Y_i, \mathcal{Z}\text{-}\{i,h\}\right)\right)}{P\left(Z_h \le T\right)}$$

$$= \frac{P\left(Z_h \le \min\left(z, Y_i, \mathcal{Z}\text{-}\{i,h\}\right)\right)}{P\left(Z_h \le T\right)}$$

Let $T' = \min\left(z, Y_i, \mathcal{Z}\text{-}\{i,h\}\right)$

$$f_{T'}(t) = \begin{cases} \left(\gamma_i + \sum\limits_{\substack{m=1 \\ m\neq i\neq h}}^{k} \delta_m \right) e^{-\left(\gamma_i + \sum\limits_{\substack{m=1 \\ m\neq i\neq h}}^{k} \delta_m \right) t} & t < z \\ e^{-\left(\gamma_i + \sum\limits_{\substack{m=1 \\ m\neq i\neq h}}^{k} \delta_m \right) z} & t = z \end{cases}$$

$$P\left(Z_h \leq T'\right) = \int P\left(Z_h \leq u\right) f_{T'}(u)\, du = \int\limits_0^z P\left(Z_h \leq u\right) f_{T'}(u)\, du + P\left(Z_h \leq z\right) e^{-\left(\gamma_i + \sum\limits_{\substack{m=1 \\ m\neq i\neq h}}^{k} \delta_m \right) z}$$

$$= -e^{-\left(\gamma_i + \sum\limits_{\substack{m=1 \\ m\neq i\neq h}}^{k} \delta_m \right) z} \left(1 - e^{-\delta_h z}\right)$$

$$+ \frac{\delta_h + \left(\gamma_i + \sum\limits_{\substack{m=1 \\ m\neq i\neq h}}^{k} \delta_m \right) e^{-\left(\gamma_i + \delta_h + \sum\limits_{\substack{m=1 \\ m\neq i\neq h}}^{k} \delta_m \right) z} - \left(\gamma_i + \delta_h + \sum\limits_{\substack{m=1 \\ m\neq i\neq h}}^{k} \delta_m \right) e^{-\left(\gamma_i + \sum\limits_{\substack{m=1 \\ m\neq i\neq h}}^{k} \delta_m \right) z}}{\gamma_i + \delta_h + \sum\limits_{\substack{m=1 \\ m\neq i\neq h}}^{k} \delta_m}$$

$$= \frac{\delta_h}{\gamma_i + \sum\limits_{\substack{m=1 \\ m\neq i}}^{k} \delta_m} \left(1 - e^{-\left(\gamma_i + \sum\limits_{\substack{m=1 \\ m\neq i}}^{k} \delta_m \right) z} \right).$$

Thus,

$$F_{Z_h \mid Z_h \le \min\left(Y_i, \mathcal{Z}\text{-}\{i,h\}\right)}(z) = \frac{P\left(Z_h \le T'\right)}{P\left(Z_h \le T\right)}$$

$$= \frac{\dfrac{\delta_h}{\gamma_i + \sum\limits_{\substack{m=1 \\ m \ne i}}^{k} \delta_m}\left(1 - e^{-\left(\gamma_i + \sum\limits_{\substack{m=1 \\ m \ne i}}^{k} \delta_m\right) z}\right)}{\dfrac{\delta_h}{\gamma_i + \sum\limits_{\substack{m=1 \\ m \ne i}}^{k} \delta_m}}$$

$$F_{Z_h \mid Z_h \le \min\left(Y_i, \mathcal{Z}\text{-}\{i,h\}\right)}(z) = 1 - e^{-\left(\gamma_i + \sum\limits_{\substack{m=1 \\ m \ne i}}^{k} \delta_m\right) z}.$$

and

$$f_{Z_h \mid Z_h \le \min\left(Y_i, \mathcal{Z}\text{-}\{i,h\}\right)}(z) = \frac{dF_{Z_h \mid Z_h \le \min\left(Y_i, \mathcal{Z}\text{-}\{i,h\}\right)}(z)}{dz}$$

$$= \left(\gamma_i + \sum_{\substack{m=1 \\ m \ne i}}^{k} \delta_m\right) e^{-\left(\gamma_i + \sum\limits_{\substack{m=1 \\ m \ne i}}^{k} \delta_m\right) z}.$$

Then,

$$E\left[e^{-sZ_h}\middle|Z_h \le \min\left(Y_i, \mathcal{Z}\text{-}\{i,h\}\right)\right] = \int_0^\infty e^{-sz} f_{Z_h|Z_h \le \min\left(Y_i,\mathcal{Z}\text{-}\{i,h\}\right)}(z)\,dz$$

$$= \int_0^\infty e^{-sz}\left(\left(\gamma_i + \sum_{\substack{m=1\\m\ne i}}^{k}\delta_m\right)e^{-\left(\gamma_i+\sum_{\substack{m=1\\m\ne i}}^{k}\delta_m\right)z}\right)dz$$

$$E\left[e^{-sZ_h}\middle|Z_h \le \min\left(Y_i, \mathcal{Z}\text{-}\{i,h\}\right)\right] = \frac{\left(\gamma_i + \sum_{\substack{m=1\\m\ne i}}^{k}\delta_m\right)}{\left(s+\gamma_i + \sum_{\substack{m=1\\m\ne i}}^{k}\delta_m\right)}.$$

$E\left[e^{-s\max(Y_{r_i},Y_h)} \mid \max(Y_{r_i},Y_h) \le \min\left(\mathcal{Z}\text{-}\{i,h\}\right)\right]$: Laplace transform of the maximum of two downtimes given it is less than the rest of the times to interruptions

---

$$E\left[e^{-s\max(Y_{r_i},Y_h)} \mid \max(Y_{r_i},Y_h) \le \min\left(\mathcal{Z}\text{-}\{i,h\}\right)\right] = \int_0^\infty e^{-sy} f_{\max(Y_{r_i},Y_h)|\max(Y_{r_i},Y_h)\le\min\left(\mathcal{Z}\text{-}\{i,h\}\right)}(y)\,dy$$

$$f_{\max(Y_{r_i},Y_h)|\max(Y_{r_i},Y_h)\le\min\left(\mathrm{Z}\text{-}\{i,h\}\right)}(y) = \frac{dF_{\max(Y_{r_i},Y_h)|\max(Y_{r_i},Y_h)\le\min\left(\mathrm{Z}\text{-}\{i,h\}\right)}(y)}{dy}$$

$$F_{\max(Y_{r_i},Y_h)|\max(Y_{r_i},Y_h)\le\min\left(\mathcal{Z}\text{-}\{i,h\}\right)}(y) = P\left(\max(Y_{r_i},Y_h)\le y \,\middle|\, \max(Y_{r_i},Y_h)\le \min\left(\mathcal{Z}\text{-}\{i,h\}\right)\right)$$

$$= \frac{P\left(\max(Y_{r_i},Y_h)\le y, \max(Y_{r_i},Y_h)\le \min\left(\mathcal{Z}\text{-}\{i,h\}\right)\right)}{P\left(\max(Y_{r_i},Y_h)\le \min\left(\mathcal{Z}\text{-}\{i,h\}\right)\right)}$$

$$= \frac{P\left(\max(Y_{r_i},Y_h)\le \min\left(y,\mathcal{Z}\text{-}\{i,h\}\right)\right)}{P\left(\max(Y_{r_i},Y_h)\le \min\left(\mathcal{Z}\text{-}\{i,h\}\right)\right)}$$

Let $T = \min\left(y, \mathcal{Z}\text{-}\{i,h\}\right)$ and $Y' = \max(Y_{r_i}, Y_h)$

$$f_T(t) = \begin{cases} \left(\sum\limits_{\substack{m=1\\ m\ne i\ne h}}^{k} \delta_m\right) e^{-\left(\sum\limits_{\substack{m=1\\ m\ne i\ne h}}^{k} \delta_m\right)t} & t<y \\ e^{-\left(\sum\limits_{\substack{m=1\\ m\ne i\ne h}}^{k} \delta_m\right)y} & t=y \end{cases}$$

$$P\left(Y'\le T\right) = \int P\left(Y'\le u\right) f_T(u)\,du = \int_0^y P\left(Y'\le u\right) f_T(u)\,du + P\left(Y'\le y\right) e^{-\left(\sum\limits_{\substack{m=1\\ m\ne i\ne h}}^{k} \delta_m\right)y}$$

$$= \frac{\gamma_i}{\gamma_i + \sum\limits_{\substack{m=1\\ m\ne i\ne h}}^{k} \delta_m}\left(1 - e^{-\left(\gamma_i + \sum\limits_{\substack{m=1\\ m\ne i\ne h}}^{k} \delta_m\right)y}\right) + \frac{\gamma_h}{\gamma_h + \sum\limits_{\substack{m=1\\ m\ne i\ne h}}^{k} \delta_m}\left(1 - e^{-\left(\gamma_h + \sum\limits_{\substack{m=1\\ m\ne i\ne h}}^{k} \delta_m\right)y}\right)$$

$$- \frac{\left(\gamma_i + \gamma_h\right)}{\gamma_i + \gamma_h + \sum\limits_{\substack{m=1\\ m\ne i\ne h}}^{k} \delta_m}\left(1 - e^{-\left(\gamma_i + \gamma_h + \sum\limits_{\substack{m=1\\ m\ne i\ne h}}^{k} \delta_m\right)y}\right).$$

Thus,

$$F_{Y'|Y'\le\min(Z\text{-}\{i,h\})}(y)=\frac{P(Z_h\le T')}{P(Z_h\le T)}$$

$$F_{Y'|Y'\le\min(Z\text{-}\{i,h\})}(y)=\frac{\left(\begin{array}{l}\dfrac{\gamma_i}{\gamma_i+\sum\limits_{\substack{m=1\\m\ne i\ne h}}^{k}\delta_m}\left(1-e^{-\left(\gamma_i+\sum\limits_{\substack{m=1\\m\ne i\ne h}}^{k}\delta_m\right)y}\right)+\dfrac{\gamma_h}{\gamma_h+\sum\limits_{\substack{m=1\\m\ne i\ne h}}^{k}\delta_m}\left(1-e^{-\left(\gamma_h+\sum\limits_{\substack{m=1\\m\ne i\ne h}}^{k}\delta_m\right)y}\right)\\ -\dfrac{(\gamma_i+\gamma_h)}{\gamma_i+\gamma_h+\sum\limits_{\substack{m=1\\m\ne i\ne h}}^{k}\delta_m}\left(1-e^{-\left(\gamma_i+\gamma_h+\sum\limits_{\substack{m=1\\m\ne i\ne h}}^{k}\delta_m\right)y}\right)\end{array}\right)}{\left(1-\sum\limits_{\substack{m=1\\m\ne i\ne h}}^{k}\delta_m\left(\dfrac{1}{\gamma_i+\sum\limits_{\substack{m=1\\m\ne i\ne h}}^{k}\delta_m}+\dfrac{1}{\gamma_h+\sum\limits_{\substack{m=1\\m\ne i\ne h}}^{k}\delta_m}-\dfrac{1}{\gamma_i+\gamma_h+\sum\limits_{\substack{m=1\\m\ne i\ne h}}^{k}\delta_m}\right)\right)}$$

and

$$f_{Y'|Y'\le\min\left(\mathcal{Z}\text{-}\{i,h\}\right)}(y)=\frac{dF_{Y'|Y'\le\min\left(\mathcal{Z}\text{-}\{i,h\}\right)}(y)}{dz}$$

$$=\frac{\left(\gamma_i e^{-\left(\gamma_i+\sum\limits_{\substack{m=1\\m\ne i\ne h}}^{k}\delta_m\right)y}+\gamma_h e^{-\left(\gamma_h+\sum\limits_{\substack{m=1\\m\ne i\ne h}}^{k}\delta_m\right)y}-\left(\gamma_i+\gamma_h\right)e^{-\left(\gamma_i+\gamma_h+\sum\limits_{\substack{m=1\\m\ne i\ne h}}^{k}\delta_m\right)y}\right)}{\left(1-\sum\limits_{\substack{m=1\\m\ne i\ne h}}^{k}\delta_m\left(\frac{1}{\gamma_i+\sum\limits_{\substack{m=1\\m\ne i\ne h}}^{k}\delta_m}+\frac{1}{\gamma_h+\sum\limits_{\substack{m=1\\m\ne i\ne h}}^{k}\delta_m}-\frac{1}{\gamma_i+\gamma_h+\sum\limits_{\substack{m=1\\m\ne i\ne h}}^{k}\delta_m}\right)\right)}.$$

Then,

$$E\left[e^{-s\max(Y_{r_i},Y_h)}\,|\max(Y_{r_i},Y_h)\le\min\left(\mathcal{Z}\text{-}\{i,h\}\right)\right]=\int_0^\infty e^{-sy}f_{\max(Y_{r_i},Y_h)|\max(Y_{r_i},Y_h)\le\min\left(\mathcal{Z}\text{-}\{i,h\}\right)}(y)dy$$

$$E\left[e^{-s\max(Y_{r_i},Y_h)}\,|\max(Y_{r_i},Y_h)\le\min\left(\mathcal{Z}\text{-}\{i,h\}\right)\right]$$

$$=\frac{\left(\gamma_i+\sum\limits_{\substack{m=1\\m\ne i\ne h}}^{k}\delta_m\right)\left(\gamma_h+\sum\limits_{\substack{m=1\\m\ne i\ne h}}^{k}\delta_m\right)\left(\gamma_i+\gamma_h+\sum\limits_{\substack{m=1\\m\ne i\ne h}}^{k}\delta_m\right)}{\left(\gamma_i+\gamma_h+2\sum\limits_{\substack{m=1\\m\ne i\ne h}}^{k}\delta_m\right)}\left(\frac{2s+\gamma_i+\gamma_h+2\sum\limits_{\substack{m=1\\m\ne i\ne h}}^{k}\delta_m}{\left(s+\gamma_i+\sum\limits_{\substack{m=1\\m\ne i\ne h}}^{k}\delta_m\right)\left(s+\gamma_h+\sum\limits_{\substack{m=1\\m\ne i\ne h}}^{k}\delta_m\right)\left(s+\gamma_i+\gamma_h+\sum\limits_{\substack{m=1\\m\ne i\ne h}}^{k}\delta_m\right)}\right).$$

$E\left[e^{-sZ_l} \mid Z_l \le \min\left(Y_{r_i}, \mathcal{Z}\text{-}\{i,h,l\}\right)\right]$: Laplace transform of a time to interruption given it is less than a remaining downtime and the rest of the times to interruptions

---

$$E\left[e^{-sZ_l} \mid Z_l \le \min\left(Y_{r_i}, \mathcal{Z}\text{-}\{i,h,l\}\right)\right] = \int_0^{\infty} e^{-sz} f_{Z_l \mid Z_l \le \min\left(Y_{r_i}, \mathcal{Z}\text{-}\{i,h,l\}\right)}(z)\, dz$$

Let $T = \min\left(Y_{r_i}, \mathcal{Z}\text{-}\{i,h,l\}\right)$

$$f_{Z_l \mid Z_l \le \min\left(Y_{r_i}, \mathcal{Z}\text{-}\{i,h,l\}\right)}(z) = \frac{dF_{Z_l \mid Z_l \le \min\left(Y_{r_i}, \mathcal{Z}\text{-}\{i,h,l\}\right)}(z)}{dz}$$

$$\begin{aligned}
F_{Z_l \mid Z_l \le \min\left(Y_{r_i}, \mathcal{Z}\text{-}\{i,h,l\}\right)}(z) &= P\left(Z_l \le z \mid Z_l \le \min\left(Y_{r_i}, \mathcal{Z}\text{-}\{i,h,l\}\right)\right) \\
&= \frac{P\left(Z_l \le z, Z_l \le \min\left(Y_{r_i}, \mathcal{Z}\text{-}\{i,h,l\}\right)\right)}{P\left(Z_l \le T\right)} \\
&= \frac{P\left(Z_l \le \min\left(z, Y_{r_i}, \mathcal{Z}\text{-}\{i,h,l\}\right)\right)}{P\left(Z_l \le T\right)}
\end{aligned}$$

Let $T' = \min\left(z, Y_{r_i}, \mathcal{Z}\text{-}\{i,h,l\}\right)$

$$f_{T'}(t) = \begin{cases} \left(\gamma_i + \sum\limits_{\substack{m=1 \\ m \neq i \neq h \neq l}}^{k} \delta_m \right) e^{-\left(\gamma_i + \sum\limits_{\substack{m=1 \\ m \neq i \neq h \neq l}}^{k} \delta_m \right) t} & t < z \\ e^{-\left(\gamma_i + \sum\limits_{\substack{m=1 \\ m \neq i \neq h \neq l}}^{k} \delta_m \right) z} & t = z \end{cases}$$

$$P\left(Z_l \leq T'\right) = \int P\left(Z_l \leq u\right) f_{T'}(u)\, du = \int_0^z P\left(Z_l \leq u\right) f_{T'}(u)\, du + P\left(Z_l \leq z\right) e^{-\left(\gamma_i + \sum\limits_{\substack{m=1 \\ m \neq i \neq h \neq l}}^{k} \delta_m \right) z}$$

$$P\left(Z_l \leq T'\right) = \frac{\delta_l}{\gamma_i + \sum\limits_{\substack{m=1 \\ m \neq i \neq h}}^{k} \delta_m} \left(1 - e^{-\left(\gamma_i + \sum\limits_{\substack{m=1 \\ m \neq i \neq h}}^{k} \delta_m \right) z} \right).$$

Thus,

$$F_{Z_l \middle| Z_l \leq \min\left(Y_{r_i}, \mathcal{Z} - \{i,h,l\}\right)}(z) = \frac{P\left(Z_l \leq T'\right)}{P\left(Z_l \leq T\right)}$$

$$= \frac{\dfrac{\delta_l}{\gamma_i + \sum\limits_{\substack{m=1 \\ m \neq i \neq h}}^{k} \delta_m} \left(1 - e^{-\left(\gamma_i + \sum\limits_{\substack{m=1 \\ m \neq i \neq h}}^{k} \delta_m \right) z} \right)}{\dfrac{\delta_l}{\gamma_i + \sum\limits_{\substack{m=1 \\ m \neq i \neq h}}^{k} \delta_m}}$$

$$F_{Z_l \middle| Z_l \leq \min\left(Y_{r_i}, \mathcal{Z} - \{i,h,l\}\right)}(z) = 1 - e^{-\left(\gamma_i + \sum\limits_{\substack{m=1 \\ m \neq i \neq h}}^{k} \delta_m \right) z}.$$

and

$$f_{Z_l \left| Z_l \le \min\left(Yr_i, \mathcal{Z}\text{-}\{i,h,l\} \right)\right.}(z) = \frac{dF_{Z_l \left| Z_l \le \min\left(Yr_i, \mathcal{Z}\text{-}\{i,h,l\} \right)\right.}(z)}{dz} = \left(\gamma_i + \sum_{\substack{m=1 \\ m \ne i \ne h}}^{k} \delta_m \right) e^{-\left(\gamma_i + \sum_{\substack{m=1 \\ m \ne i \ne h}}^{k} \delta_m \right) z}.$$

Then,

$$E\left[e^{-sZ_l} \mid Z_l \le \min\left(Y_{r_i}, \mathcal{Z}\text{-}\{i,h,l\} \right) \right] = \int_0^\infty e^{-sz} f_{Z_l \left| Z_l \le \min\left(Y_{r_i}, \mathcal{Z}\text{-}\{i,h,l\} \right)\right.}(z)\, dz = \frac{\left(\gamma_i + \sum_{\substack{m=1 \\ m \ne i \ne h}}^{k} \delta_m \right)}{\left(s + \gamma_i + \sum_{\substack{m=1 \\ m \ne i \ne h}}^{k} \delta_m \right)}.$$

$E\left[e^{-sZ_l} \mid Z_l \le \min\left(\max(Y_{r_i}, Y_h), \mathcal{Z}\text{-}\{i,h,l\} \right) \right]$: Laplace transform of a time to interruption given it is less than the maximum of two downtimes and the rest of the times to interruptions

---

$$E\left[e^{-sZ_l} \mid Z_l \le \min\left(\max(Y_{r_i}, Y_h), \mathcal{Z}\text{-}\{i,h,l\} \right) \right] = \int_0^\infty e^{-sz} f_{Z_l \left| Z_l \le \min\left(\max(Y_{r_i}, Y_h), \mathcal{Z}\text{-}\{i,h,l\} \right)\right.}(z)\, dz$$

Let $T = \min\left(\max(Y_{r_i}, Y_h), \mathcal{Z}\text{-}\{i,h,l\} \right)$

$$f_{Z_l \left| Z_l \le \min\left(\max(Y_{r_i}, Y_h), \mathcal{Z}\text{-}\{i,h,l\} \right)\right.}(z) = \frac{dF_{Z_l \left| Z_l \le \min\left(\max(Y_{r_i}, Y_h), \mathcal{Z}\text{-}\{i,h,l\} \right)\right.}(z)}{dz}$$

$$F_{Z_l \left| Z_l \le \min\left(\max(Y_{r_i}, Y_h), \mathcal{Z}\text{-}\{i,h,l\}\right)\right.}(z) = P\left(Z_l \le z \middle| Z_l \le \min\left(\max(Y_{r_i}, Y_h), \mathcal{Z}\text{-}\{i,h,l\}\right)\right)$$

$$= \frac{P\left(Z_l \le z, Z_l \le \min\left(\max(Y_{r_i}, Y_h), \mathcal{Z}\text{-}\{i,h,l\}\right)\right)}{P\left(Z_l \le T\right)}$$

$$= \frac{P\left(Z_l \le \min\left(z, \max(Y_{r_i}, Y_h), \mathcal{Z}\text{-}\{i,h,l\}\right)\right)}{P\left(Z_l \le T\right)}$$

Let $T' = \min\left(z, \max(Y_{r_i}, Y_h), \mathcal{Z}\text{-}\{i,h,l\}\right)$

$$f_{T'}(t) = \begin{cases} \left(\begin{array}{l} \left(\gamma_i + \sum\limits_{\substack{m=1 \\ m\ne i\ne h\ne l}}^{k} \delta_m\right) e^{-\left(\gamma_i + \sum\limits_{\substack{m=1 \\ m\ne i\ne h\ne l}}^{k} \delta_m\right)t} + \left(\gamma_h + \sum\limits_{\substack{m=1 \\ m\ne i\ne h\ne l}}^{k} \delta_m\right) e^{-\left(\gamma_h + \sum\limits_{\substack{m=1 \\ m\ne i\ne h\ne l}}^{k} \delta_m\right)t} \\ + \left(\gamma_i + \gamma_h + \sum\limits_{\substack{m=1 \\ m\ne i\ne h\ne l}}^{k} \delta_m\right) e^{-\left(\gamma_i + \gamma_h + \sum\limits_{\substack{m=1 \\ m\ne i\ne h\ne l}}^{k} \delta_m\right)t} \end{array} \right) & t < z \\ e^{-\left(\gamma_i + \sum\limits_{\substack{m=1 \\ m\ne i\ne h\ne l}}^{k} \delta_m\right)z} + e^{-\left(\gamma_h + \sum\limits_{\substack{m=1 \\ m\ne i\ne h\ne l}}^{k} \delta_m\right)z} - e^{-\left(\gamma_i + \gamma_h + \sum\limits_{\substack{m=1 \\ m\ne i\ne h\ne l}}^{k} \delta_m\right)z} & t = z \end{cases}$$

$$P\left(Z_l \le T'\right) = \int P\left(Z_l \le u\right) f_{T'}(u)\, du$$

$$= \int_0^z P\left(Z_l \le u\right) f_{T'}(u)\, du + P\left(Z_l \le z\right) \left(\begin{array}{l} e^{-\left(\gamma_i + \sum\limits_{\substack{m=1 \\ m\ne i\ne h\ne l}}^{k} \delta_m\right)z} + e^{-\left(\gamma_h + \sum\limits_{\substack{m=1 \\ m\ne i\ne h\ne l}}^{k} \delta_m\right)z} \\ - e^{-\left(\gamma_i + \gamma_h + \sum\limits_{\substack{m=1 \\ m\ne i\ne h\ne l}}^{k} \delta_m\right)z} \end{array} \right)$$

Hence,

$$E\left[e^{-sZ_l} \mid Z_l \le \min\left(Y_{r_i}, \mathcal{Z}\text{-}\{i,h,l\}\right)\right] = \int_0^\infty e^{-sz} f_{Z_l \mid Z_l \le \min\left(Y_{r_i}, \mathcal{Z}\text{-}\{i,h,l\}\right)}(z)\,dz$$

$$E\left[e^{-sZ_l} \mid Z_l \le \min\left(Y_{r_i}, \mathcal{Z}\text{-}\{i,h,l\}\right)\right] = \left(\frac{\left(\gamma_i + \sum_{\substack{m=1 \\ m\neq i\neq h}}^{k} \delta_m\right)\left(\gamma_h + \sum_{\substack{m=1 \\ m\neq i\neq h}}^{k} \delta_m\right)\left(\gamma_i + \gamma_h + \sum_{\substack{m=1 \\ m\neq i\neq h}}^{k} \delta_m\right)}{s\left(\gamma_h\left(\gamma_i + \gamma_h + 2\sum_{\substack{m=1 \\ m\neq i\neq h}}^{k} \delta_m\right) + \left(\gamma_i + \sum_{\substack{m=1 \\ m\neq i\neq h}}^{k} \delta_m\right)^2\right)} \times \left(\frac{1}{s+\gamma_i + \sum_{\substack{m=1 \\ m\neq i\neq h}}^{k} \delta_m} + \frac{1}{s+\gamma_h + \sum_{\substack{m=1 \\ m\neq i\neq h}}^{k} \delta_m} - \frac{1}{s+\gamma_i + \gamma_h + \sum_{\substack{m=1 \\ m\neq i\neq h}}^{k} \delta_m} \right) \right).$$

$E\left[e^{-sYr_i} \mid Y_{r_i} > \max(Y_{r_h}, Y_l)\right]$: Laplace transform of a remaining downtime given it is greater than the maximum of two other downtimes

---

$$E\left[e^{-sYr_i} \mid Y_{r_i} > \max(Y_{r_h}, Y_l)\right] = \int_0^\infty e^{-sy} f_{Y_{r_i} \mid Y_{r_i} > \max(Y_{r_h}, Y_l)}(y)\,dy$$

$$f_{Y_{r_i} \mid Y_{r_i} > \max(Y_{r_h}, Y_l)}(y) = \frac{dF_{Y_{r_i} \mid Y_{r_i} > \max(Y_{r_h}, Y_l)}(y)}{dy}$$

$$F_{Y_{r_i}|Y_{r_i}>\max(Y_{r_h},Y_l)}(y) = P\left(Y_{r_i} \le y \middle| Y_{r_i} > \max(Y_{r_h},Y_l)\right)$$

$$\begin{aligned}P\left(Y_{r_i} \le y\right) &= P\left(Y_{r_i} \le y \middle| Y_{r_i} > \max(Y_{r_h},Y_l)\right)P\left(Y_{r_i} > \max(Y_h,Y_l)\right) \\ &+ P\left(Y_{r_i} \le y \middle| Y_{r_i} \le \max(Y_{r_h},Y_l)\right)P\left(Y_{r_i} \le \max(Y_{r_h},Y_l)\right)\end{aligned}$$

$$P\left(Y_{r_i} \le y \middle| Y_{r_i} > \max(Y_{r_h},Y_l)\right) = \frac{P\left(Y_{r_i} \le y\right) - P\left(Y_{r_i} \le y \middle| Y_{r_i} \le \max(Y_{r_h},Y_l)\right)P\left(Y_{r_i} \le \max(Y_{r_h},Y_l)\right)}{P\left(Y_{r_i} > \max(Y_{r_h},Y_l)\right)}$$

$$P\left(Y_{r_i} \le y \middle| Y_{r_i} \le \max(Y_{r_h},Y_l)\right) = \frac{P\left(Y_{r_i} \le y, Y_{r_i} \le \max(Y_{r_h},Y_l)\right)}{P\left(Y_{r_i} \le \max(Y_{r_h},Y_l)\right)} = \frac{P\left(Y_{r_i} \le \min\left(y, \max(Y_{r_h},Y_l)\right)\right)}{P\left(Y_{r_i} \le \max(Y_{r_h},Y_l)\right)}$$

$$\begin{aligned}P\left(Y_{r_i} \le y \middle| Y_{r_i} > \max(Y_{r_h},Y_l)\right) &= \frac{P\left(Y_{r_i} \le y\right) - \dfrac{P\left(Y_{r_i} \le \min\left(y, \max(Y_{r_h},Y_l)\right)\right)}{P\left(Y_{r_i} \le \max(Y_{r_h},Y_l)\right)}P\left(Y_{r_i} \le \max(Y_{r_h},Y_l)\right)}{P\left(Y_{r_i} > \max(Y_{r_h},Y_l)\right)} \\ &= \frac{P\left(Y_{r_i} \le y\right) - P\left(Y_{r_i} \le \min\left(y, \max(Y_{r_h},Y_l)\right)\right)}{P\left(Y_{r_i} > \max(Y_{r_h},Y_l)\right)}\end{aligned}$$

Let $T' = \min\left(y, \max(Y_{r_h},Y_l)\right)$

$$f_{T'}(t) = \begin{cases} \gamma_h e^{-\gamma_h t} + \gamma_l e^{-\gamma_l t} - \left(\gamma_h + \gamma_l\right)e^{-\left(\gamma_h+\gamma_l\right)t} & t < y \\ e^{-\gamma_h y} + e^{-\gamma_l y} - e^{-\left(\gamma_h+\gamma_l\right)y} & t = y \end{cases}$$

$$P\left(Y_{r_i} \le T'\right) = \int P\left(Y_{r_i} \le u\right) f_{T'}(u)\,du = \int_0^y P\left(Y_{r_i} \le u\right) f_{T'}(u)\,du + P\left(Y_{r_i} \le y\right)\left(e^{-\gamma_h y} + e^{-\gamma_l y} - e^{-\left(\gamma_h+\gamma_l\right)y}\right)$$

$$P\left(Y_{r_i} \le T'\right) = \left(e^{-\gamma_h y} + e^{-\gamma_l y} - e^{-\left(\gamma_h+\gamma_l\right)y}\right)$$
$$-\gamma_i\left(\frac{e^{-\left(\gamma_i+\gamma_h\right)y}}{\gamma_i+\gamma_h} - \frac{e^{-\left(\gamma_i+\gamma_l\right)y}}{\gamma_i+\gamma_l} + \frac{e^{-\left(\gamma_i+\gamma_l+\gamma_h\right)y}}{\gamma_i+\gamma_l+\gamma_h} + \frac{\gamma_h\left(2\gamma_i+\gamma_h+\gamma_l\right)+\left(\gamma_i+\gamma_l\right)^2}{\left(\gamma_i+\gamma_h\right)\left(\gamma_i+\gamma_l\right)\left(\gamma_i+\gamma_h+\gamma_l\right)}\right).$$

$$P\left(Y_{r_i} \le y \middle| Y_{r_i} > \max(Y_{r_h}, Y_l)\right) = \frac{P\left(Y_{r_i} \le y\right) - P\left(Y_{r_i} \le \min\left(y, \max(Y_{r_h}, Y_l)\right)\right)}{P\left(Y_{r_i} > \max(Y_{r_h}, Y_l)\right)}$$

$$= \frac{\left(1-e^{-\gamma_i y}\right) - \left(\begin{array}{l}\left(e^{-\gamma_h y} + e^{-\gamma_l y} - e^{-\left(\gamma_h+\gamma_l\right)y}\right) \\ -\gamma_i\left(\begin{array}{l}\dfrac{e^{-\left(\gamma_i+\gamma_h\right)y}}{\gamma_i+\gamma_h} - \dfrac{e^{-\left(\gamma_i+\gamma_l\right)y}}{\gamma_i+\gamma_l} + \dfrac{e^{-\left(\gamma_i+\gamma_l+\gamma_h\right)y}}{\gamma_i+\gamma_l+\gamma_h} \\ + \dfrac{\gamma_h\left(2\gamma_i+\gamma_h+\gamma_l\right)+\left(\gamma_i+\gamma_l\right)^2}{\left(\gamma_i+\gamma_h\right)\left(\gamma_i+\gamma_l\right)\left(\gamma_i+\gamma_h+\gamma_l\right)}\end{array}\right)\end{array}\right)}{\dfrac{\gamma_h}{\gamma_i+\gamma_h} + \dfrac{\gamma_l}{\gamma_i+\gamma_l} - \dfrac{\gamma_h+\gamma_l}{\gamma_i+\gamma_h+\gamma_l}}$$

Then,

$$f_{Z_l \middle| Z_l \le \min\left(Y_{r_i}, \mathcal{Z}-\{i,h,l\}\right)}(z) = \frac{dF_{Z_l \middle| Z_l \le \min\left(Y_{r_i}, \mathcal{Z}-\{i,h,l\}\right)}(z)}{dz} = \frac{d}{dz}\left(P\left(Y_{r_i} \le y \middle| Y_{r_i} > \max(Y_{r_h}, Y_l)\right)\right)$$

Thus,

$$E\left[e^{-sZ_l} \mid Z_l \le \min\left(Y_{r_i}, \mathcal{Z}\text{-}\{i,h,l\}\right)\right] = \int_0^\infty e^{-sz} f_{Z_l \mid Z_l \le \min\left(Y_{r_i}, \mathcal{Z}\text{-}\{i,h,l\}\right)}(z)\,dz$$

$$E\left[e^{-sZ_l} \mid Z_l \le \min\left(Y_{r_i}, \mathcal{Z}\text{-}\{i,h,l\}\right)\right]$$

$$= \frac{(\gamma_i + \gamma_h)(\gamma_i + \gamma_l)(\gamma_i + \gamma_h + \gamma_l)}{\gamma_l(2\gamma_i + \gamma_h + \gamma_l)} \left(\begin{array}{l} \dfrac{\gamma_l(2s + \gamma_h + \gamma_l)}{(s+\gamma_h)(s+\gamma_l)(s+\gamma_h+\gamma_l)} \\ +\gamma_i \left(\dfrac{1}{(s+\gamma_i)(s+\gamma_i+\gamma_h)} + \dfrac{1}{(s+\gamma_i+\gamma_l)(s+\gamma_i+\gamma_h+\gamma_l)} \right) \end{array} \right).$$

REFERENCES

[Almaz, 2006] Almaz, A.O., *Investigation of the Transit Maritime Traffic in the Strait of Istanbul through Simulation Modeling and Scenario Analysis*, M.S. Thesis, Department of Industrial Engineering, Boğaziçi University, Istanbul, Turkey, 2006.

[Almaz *et al*., 2006] Almaz, A.O., Or, I. and Özbaş, B., "Simulation of maritime transit traffic in the Istanbul channel", *20th European Conference on Modelling and Simulation ECMS 2006. Modelling Methodologies and Simulation Key Technologies in Academia and Industry*, 360-366, Saint Augustin, Germany, 2006.

[Altıok, 1997] Altıok, T., *Performance Analysis of Manufacturing Systems,* Springer-Verlag, New York, NY, 1997.

[APS, 1975] American Physical Society Study Group on Light Water Reactor Safety, "Report to the American Physical Society", *Reviews of Modern Physics*, **47**, no. 1, 1975.

[Amrozowicz, 1996] Amrozowicz, M.D., *Quantitative Risk of Oil Tanker Groundings*, Master's Thesis, Department of Ocean Engineering, Massachusetts Institute of Technology, Cambridge, MA, 1996.

[Amrozowicz *et al*., 1997] Amrozowicz, M.D., Brown, A. and Golay, M., "Probabilistic analysis of tanker groundings", *Proceedings of the 1997 7th International Offshore and Polar Engineering Conference,* 313-320, Honolulu, HI, 1997.

[Anderson and Talley, 1995] Anderson, E. and Talley, W.K., "The oil spill size of tanker and barge accidents: Determinants and policy implications", *Land Economy,* **71**, 216-228, 1995.

[Ansell and Wharton, 1992] Ansell, J. and Wharton, F., *Risk; Analysis, Assessment and Management*, John Wiley & Sons, Chichester, 1992.

[Apostolakis and Lemon, 2005] Apostolakis, G.E., Lemon, D.M., "A Screening Methodology for the Identification and Ranking of Infrastructure Vulnerabilities Due to Terrorism", *Risk Analysis*, **25**, no. 2, 361-376, 2005.

[Atallah and Athens, 1984] Atallah, S. and Athens, P., "Assessing The Risks Of Maritime Transport Operations", *MariChem83, Conference on the Marine Transportation, Handling and Storage of Bulk Chemicals*, 111-120, Gastech Ltd, Hamburg, Germany, 1984.

[Aven, 2003] Aven, T., *Foundations of Risk Analysis; A Knowledge and Decision-Oriented Perspective*, John Wiley & Sons, Chichester, 2003.

[Aybay and Oral, 2002] Aybay, G. and Oral, N., "Turkey's Authority to Regulate Passage of Vessels through the Turkish Straits", *Perceptions Journal of International Affairs,* **3**, no. 2, 2002.

[Ayyub, 2003] Ayyub, B.M., *Risk Analysis in Engineering and Economics*, Chapman & Hall, Boca Raton, 2003.

[Bedford and Cooke, 2001] Bedford, T. and Cooke, R., *Probabilistic Risk Analysis; Foundations and Methods*, Cambridge University Press, Cambridge, 2001.

[Biles *et al*., 2004] Biles, W.E., Bilbrey, J.K. and Sasso, D., "Integration of simulation and geographic information systems: modeling traffic flow in inland waterways", *Proceedings of the 2004 Winter Simulation Conference*, 1392-1398, Washington, DC, 2004.

[Birpınar *et al*., 2005] Birpınar, M.E., Talu, G., Su, G. and Gülbey, M., *The Effect of Dense Maritime Traffic on the Bosporus strait and Marmara Sea Pollution*, Ministry of Environment and Forestry the Regional Directorate of Istanbul, Istanbul, Turkey 2005.

[Bonnabry *et al*., 2005] Bonnabry, P., Cingria, L., Sadeghipour, F., Ing, H., Fonzo-Christe, C., Pfister, R.E., "Use of a systematic risk analysis method to improve safety in the production of paediatric parenteral nutrition solutions", *Qual Saf Health Care*, **14**, no. 2, 93-98, 2005.

[Bronzini, 1995] Bronzini, M.S., *Panama Canal capacity analysis*, Oak Ridge National Laboratory, TN, 1995.

[Clark *et al*., 1983] Clark, T.D.,Jr, Kabil, M.M. and Mostafa, M.I.M., "An analysis and simulation of an experimental Suez Canal traffic control system", *1983 Winter Simulation Conference Proceedings*, 311-318, Arlington, VA, 1983.

[Chang *et al*., 2000] Chang, S.E., Shinozuka, M. and Moore, J.E., "Probabilistic Earthquake Scenarios: Extending Risk Analysis Methodologies to Spatially Distributed Systems", *Earthquake Spectra*, **16**, no. 3, 557-572, 2000.

[Cohen, 2003] Cohen, B.L., "Probabilistic risk analysis for a high-level radioactive waste epository", *Risk Analysis*, **23**, no. 5, 909-15, 2003.

[Colglazier and Weatherwas, 1986] Colglazier E.W. and Weatherwas, R.K., "Failure estimates for the space shuttle", *Abstracts of the Society for Risk Analysis Annual Meeting*, Boston, MA, 80, 1986.

[Cooke, 1991] Cooke, R.M., *Experts in Uncertainty: Opinion and Subjective Probability in Science*, Oxford University Press, Oxford, U.K., 1991.

[Dai *et al*., 2005] Dai, Y., Xie, M. and Poh, K., "Modeling and analysis of correlated software failures of multiple types", *IEEE Transactions on Reliability,* **54**, no. 1, 100-106, 2005.

[Degre *et al*., 2003] Degre, T., Glansdorp, C.C. and Van Der Tak, C., "Importance of an approach of maritime safety based on risk assessment models", *Navigation*, **50**, 59-77, 2003.

[Dougligeris *et al*., 1997] Dougligeris, C., Iakovou, E. and Yudhbir, L., "Maritime route risk analysis for hazardous materials transportation", *Proceedings of the 8th IFAC/IFIP/IFORS*, *Transportation Systems*, **2**, 563-568, Chania, Greece, 1997.

[EIA, 2006] US Energy Information Administration, *World Oil Transit Chokepoints*, Available:http://www.eia.doe.gov/cabs/World_Oil_Transit_Chokepoints/Bosporus_TurkishStraits.html [2008, 02/01], 2006.

[Elsayed, 1981] Elsayed, E.A., "An Optimum Repair Policy for the Machine Interference Problem", *The Journal of the Operational Research Society*, **32**, no. 9, 793-801, 1981.

[EPA, 1976] Reactor Safety Study, oversight hearings before the Subcommittee on Energy and the Environment of the Committee on Interior and Insular Affairs, House of Representatives, 94th Congress, 2nd session, serial no. 94-61, Washington, DC, 11 June, 1976.

[Erkaya, 1998] Erkaya, G., *Turkish straits: Opportunity or Obstacle for New Trade Pattern?*, Presentation, ECMT Seminar, Altalya, Turkey, 1998.

[EyeforTransport, 2004] EyeforTransport, Logistics and Transportation information and services provider, *EyeforTransport Transportation Glossary*, Available: http://www.eyefortransport.com/glossary/ef.shtml [2007, 01/10], 2004.

[Fortson *et al*., 1973] Fortson, R.M., Holmboe, E.L., Brown, F.B., Kirkland, J.T. and Tullier, P.M., *Maritime Accidental Spill Risk Analysis. Phase I. Methodology Development and Planning*, Technical Report, Operations Research Inc., Silver Spring, MD, 1973.

[Fragola, 1995] Fragola, J.R., *Probabilitic Risk Assessment of the Space Shuttle*, SAIC doc. no. SAICNY95-02-25, New York, 1995.

[Franzese *et al*., 2004] Franzese, L.A.G., Abdenur, L.O., Botter, R.C., Starks, D. and Cano, A.R., "Simulating the Panama Canal: present and future", *Proceedings of the 2004 Winter Simulation Conference*, **2**, 1835-1838, Washington, DC, 2004.

[Freely, 1996] Freely, J., *Istanbul: The Imperial City,* 1st edn, Penguin Books, London, 1996.

[Garrick and Kaplan 1999] Garrick, B.J., Kaplan, S., "A decision theory perspective on the disposal of high-level radioactive waste", Risk Analysis, **19**, no. 5, 903-13, 1999.

[Golkar *et al*., 1998] Golkar, J., Shekhar, A. and Buddhavarapu, S., "Panama Canal Simulation Model", *Proceedings of 1998 Winter Simulation Conference*, **2**, 1229-1237, Washington, DC, 1998.

[Gray *et al.*, 2003] Gray, W.J., Wang, P.P. and Scott, M., "A queueing model with service breakdowns and multiple stages of repair", *Journal of Applied Statistical Science*, **12**, no. 1, 75-89, 2003.

[Gray *et al.*, 2004] Gray, W.J., Wang, P.P. and Scott, M., "A Queueing Model with Multiple Types of Server Breakdowns", *Quality Technology & Quantitative Management*, **1**, no. 2, 245-255, 2004.

[Guedes Soares and Teixeira, 2001] Guedes Soares, C. and Teixeira, A.P., "Risk assessment in maritime transportation", *Reliability Engineering and System Safety*, **74**, no. 3, 299-309, 2001.

[Hara and Nakamura, 1993] Hara, K. and Nakamura, S., "A comprehensive assessment system for the maritime traffic environment", *Navigation*, **41**, no. 163, 390-404, 1993.

[Haimes, 2004] Haimes, Y.Y., *Risk Modeling, Assessment, and Management*, 2nd Edition, John Wiley & Sons, Hoboken, NJ, 2004.

[Haimes, 2006] Haimes, Y.Y., "On the Definition of Vulnerabilities in Measuring Risks to Infrastructures", *Risk Analysis*, **26**, no. 2, 293-296, 2006.

[Haimes and Longstaff, 2002] Haimes, Y.Y., Longstaff, T., "The Role of Risk Analysis in the Protection of Critical Infrastructures against Terrorism", *Risk Analysis*, **22**, no. 3, 439-444, 2002.

[Hsieh and Andersland, 1995] Hsieh, Y. and Andersland, M.S., "Repairable single-server systems with multiple breakdown modes", *Microelectronics and Reliability*, **35**, no. 2, 309-318, 1995.

[Iakovou, 2001] Iakovou, E.T., "An interactive multiobjective model for the strategic maritime transportation of petroleum products: Risk analysis and routing", *Safety Science*, **39**, no. 1-2, 19-29, 2001.

[TUMPA, 2004] Turkish Maritime Pilot Association (TUMPA), *Strait of Istanbul: Statistics of Passages*, Available: http://www.turkishpilots.org/DOCUMENTS/Statistics/bosporusstats_general_figures.htm [2006, 11/12], 2004.

[Jaiswal and Thiruvengadam, 1963] Jaiswal, N.K. and Thiruvengadam, K., "Simple Machine Interference with Two Types of Failure", *Operations Research*, **11**, no. 4, 624-636, 1963.

[Kaczmarek, 2003] Kaczmarek, Z., "The Impact of Climate Variability on Flood Risk in Poland", *Risk Analysis*, **23**, no. 3, 559-66, 2003.

[Kaneko, 2002] Kaneko, F., "Methods for probabilistic safety assessments of ships", *Journal of Marine Science and Technology*, **7**, no. 1, 1-16, 2002.

[Kaplan, 1997] Kaplan, S., "The Words of Risk Analysis", *Risk Analysis*, **17**, no. 4, 407-417, 1997.

[Kaplan and Garrick, 1981] Kaplan, S. and Garrick, B.J., "On the Quantitative Definition of Risk", *Risk Analysis*, **l**, no. 1, 11-27, 1981.

[Keefer and Beccue, 2001] Keefer, D.L., Beccue, P., "Practice abstract", *Interfaces*, **31**, no. 5, 62-64, 2001.

[Kemeny *et al*. 1979] Kemeny, J., *et al*., *Report of the President's Commision on the Accident at Three Mile Island*, Washington, DC, 1979.

[Kite-Powell *et al*., 1998] Kite-Powell, H.L., Patrikalakis, N.M., Jin, D., Abrams, S.L., Jebsen, J., Papakonstantinou, V. and Lin, S.C., *Formulation of a Model for Ship Transit Risk*, Final Project Report, Massachusetts Institute of Technology, Sea Grant Coll. Program, Cambridge, MA, 1998.

[Koller, 1999] Koller, G., *Risk Assessment and Decision Making in Business and Industry*, Chapman & Hall, 1999.

[Koller, 2000] Koller, G., *Risk Modeling for Determining Value and Decision Making*, Chapman & Hall, 2000.

[Kornhauser and Clark, 1995] Kornhauser, A.L. and Clark, W.A., *Quantitative forecast of vessel casualties resulting from additional oil tanker traffic through the Bosphorus*, Report, ALK Associates, Princeton, NJ, 1995.

[Kose *et al*., 2003] Kose, E., Basar, E., Demirci, E., Guneroglu, A. and Erkebay, S., "Simulation of marine traffic in Istanbul Strait", *Simulation Modelling Practice and Theory*, **11**, no. 7-8, 597-608, 2003.

[Kuroda *et al*., 1982] Kuroda, K., Kita, H. and Kono, S., "Mathematical Model of Ship Collision Probability", *Memoirs of the Faculty of Engineering, Kyoto University*, **44**, no. 1, 135-157, 1982.

[Le Blanc *et al*., 2001] Le Blanc, L.A., Hashemi, R.R. and Rucks, C.T., "Pattern development for vessel accidents: A comparison of statistical and neural computing techniques", *Expert Systems with Applications*, **20**, no. 2, 163-171, 2001.

[Le Blanc and Rucks, 1996] Le Blanc, L.A. and Rucks, C.T., "Multiple discriminant analysis of vessel accidents", *Accident Analysis and Prevention*, **28**, no. 4, 501-510, 1996.

[Lewis *et al*., 1979] Lewis, H., *et al*., *Risk Assessment Review Group Report to the U.S. Nuclear Regulatory Commission*, NUREG/CR-04000, 1979.

[Mai and Zimmermann, 2003] Mai S, Zimmermann C., "Risk Analysis-Tool for Integrated Coastal Planning", *Proc. of the 6th Int. Conf. on Coastal and Port Engineering in Developing Countries COPEDEC*, Colombo, Sri Lanka, 2003.

[Maio *et al*., 1991] Maio, D., Ricci, R., Rossetti, M., Schwenk, J. and Liu, T., *Port Needs Study, Vol. 1, Report No. DOT-CG-N-01-91-1.2, USDOT/RSPA/VolpeTSC*, U.S. Department of Transportation, Washington, DC, 1991.

[Merrick *et al*., 2000] Merrick, J.R.W., Van Dorp, J.R., Harrald, J., Mazzuchi, T., Spahn, J.E. and Grabowski, M., "A systems approach to managing oil transportation risk in Prince William Sound", *Systems Engineering*, **3**, no. 3, 128-142, 2000.

[Merrick *et al*., 2001] Merrick, J.R.W., Van Dorp, J.R., Mazzuchi, T.A. and Harrald, J.R., "Modeling risk in the dynamic environment of maritime transportation", *Proceedings of the 2001 Winter Simulation Conference*, **2**, 1090-1098, Arlington, VA, 2001.

[Merrick *et al*., 2002] Merrick, J.R.W., Van Dorp, J.R., Mazzuchi, T., Harrald, J.R., Spahn, J.E. and Grabowski, M., "The Prince William Sound risk assessment", *Interfaces*, **32**, no. 6, 25-40, 2002.

[Merrick *et al*., 2003] Merrick, J.R.W., Van Dorp, J.R., Blackford, J.P., Shaw, G.L., Harrald, J. and Mazzuchi, T.A., "A traffic density analysis of proposed ferry service expansion in San Francisco bay using a maritime simulation model", *Reliability Engineering and System Safety*, **81**, no. 2, 119-132, 2003.

[Merrick and Van Dorp, 2006] Merrick, J.R.W. and Van Dorp, R. 2006, "Speaking the truth in maritime risk assessment", *Risk Analysis*, **26**, no. 1, 223-237.

[Mırık and Karayakalı, 2008] Mırık, İ. and Karayakalı, Ü., *Simulation of Local traffic in the Strait of Istanbul*, Senior Project Report, Department of Industrial Engineering, Boğaziçi University, Istanbul, Turkey, 2008.

[MISS, 2006] Maritime International Secretariat Services Ltd, *Shipping Industry Flag State Performance Table*, Available: http://www.marisec.org/flag-performance/FlagStatePerformanceTable06.pdf [2008, 03/05], 2006.

[Modarres, 2006] Modarres, M., *Risk Analysis in Engineering: Probabilistic Techniques, Tools and Trends*, CRC Press, 2006.

[Moller *et al*., 2005] Moller, T.H., Molloy, F.C. and Thomas, H.M., "Oil spill risks and the state of preparedness in the Regional Seas", *2005 International Oil Spill Conference*, 9266-9269, Miami Beach, FL, 2005.

[Montreux Conv., 1937] "Convention Regarding the Regime of straits", *The American Journal of International Law*, **31**, no. 1, 1-18, 1937.

[Moore *et al*., 1999] Moore, D.R.J., Sample, B.E., Suter, G.W., Parkhurst, B.R., Scott, T.R., "A Probabilistic risk assessment of the effects of Methylmercury and PCBs on mink and Kingfishers along East Fork Poplar Creek, Oak Ridge, Tennessee, USA", *Environmental Toxicology and Chemistry*, **18**, no. 12, 2941-2953, 1999.

[Nicola, 1986] Nicola, V.F., "A single-server queue with mixed types of interruptions", *Acta Informatica*, **23**, no. 4, 465-86, 1986.

[Nitzov, 1998] Nitzov, B., *The Bosphorus: Oil Through Needle's Eye?*, Institute for Energy Economics and Policy, Sarkeys Energy Center of the University of Oklahoma, OK, 1998.

[Norman, 1973] Norman, R. J., *An Algorithm for the Scheduling of Vessels through Panama Canal*, M.S. Thesis, Operations Research Department, Naval Postgraduate School, 1973.

[NRC, 1975] Nuclear Regulatory Commission, *Reactor Safety Study: an Assessement of Accident Risks in US Commercial Nuclear Power Plants*, WASH-1400, NUREG-75/014, 1975.

[NRC, 1983] Nuclear Regulatory Commission, *PRA Procedures Guide*, US Nuclear Regulatory Commission NUREG/CR-2300, 1983.

Official Gazette, *Maritime Traffic Regulations for the Turkish straits and the Marmara Region*, 23515 regulation No: 98/11860, October 8, 1998.

[Oguzülgen, 1995] Oguzülgen, S., "The Importance of Pilotage Services in the Turkish straits for the Protection of Life, Property, and the Environment" in *Turkish straits: New Problems, New Solutions*, Foundation for Middle East and Balkan Studies, Istanbul, Turkey, 1995.

[Or and Kahraman, 2003] Or, I. and Kahraman, I., "A simulation study of the accident risk in the Istanbul Channel", *International Journal of Emergency Management*, **1**, no. 2, 110-124, 2003.

[Örs, 2005] Örs, H., "A stochastic approach to the modeling of the oil pollution", *Energy Sources*, **27**, no. 4, 387-392, 2005.

[Örs and Yılmaz, 2003] Örs, H. and Yılmaz, S.L., "Oil transport in the Turkish straits system: A simulation of contamination in the Istanbul Strait", *Energy Sources*, **25**, 11, 1043-1052, 2003.

[Otay and Özkan, 2003] Otay, E.N. and Özkan, S., "Stochastic Prediction of Maritime Accidents in the strait of Istanbul", *Proceedings of the 3rd International Conference on Oil Spills in the Mediterranean and Black Sea Regions*, 92-104, 2003.

[Özbaş, 2005] Özbaş, B., *Simulation of Maritime Transit Traffic in the Istanbul Channel*, M.S. Thesis, Department of Industrial Engineering, Boğaziçi University, Istanbul, Turkey, 2005.

[Palesano and Chandra, 1986] Palesano, J. and Chandra, J., "A machine interference problem with multiple types of failures", *International Journal of Production Research*, 24, no. 3, 567-82, 1986.

[Paté-Cornell, 1990] Paté-Cornell, M.E., "Organizational Aspects of Engineering System Safety: The Case of Offshore Platforms", *Science*, **250**, no. 4985, 1210-1217, 1990.

[Paté-Cornell and Fischbeck, 1993] Paté-Cornell, E. and Fischbeck, P., "P.R.A. as a management tool: organizational factors and risk-based priorities for the maintenance of the tiles of the space shuttle orbiter", *Reliability Engineering and System Safety*, **40**, 239-257, 1993.

[Petersen and Taylor, 1988] Petersen, E. R. and Taylor, A. J., "An Optimal Scheduling System for the Welland Canal", *Transportation Science*, **22**, no. 3, 173-185, 1988.

[Pravda and Lightner, 1966] Pravda, M.F., Lightner, R.G., "Conceptual Study of a Supercritical Reactor Plant for Merchant Ships", *Marine Technology*, **4**, 230-238, 1966.

[Psaraftis *et al*., 1998] Psaraftis, H.N., Panagakos, G., Desypris, N. and Ventikos, N., "Analysis of maritime transportation risk factors", *Proceedings of the 8th International Offshore and Polar Engineering Conference*, **4**, 477-483, Montreal, Canada, 1998.

[Rausand and Høyland, 2004] Rausand, M. and Høyland, A., *System Reliability Theory: Models, Statistical Methods, and Applications*, 2nd Edition, Wiley, 2004.

[Roeleven *et al*., 1995] Roeleven, D., Kok, M., Stipdonk, H.L. and De Vries, W.A., "Inland waterway transport: modelling the probability of accidents", *Safety Science*, **19**, no. 2-3, 191-202, 1995.

[Rogovin and Frampton, 1980] Regain, M. and Frampton, G.T., *Three Mile Island, a Report to the Commissioners and to the Public Government Printing Office*, 1980.

[Ross, 1980] Ross, S.M., *Introduction to Probability Models*, Academic Press, New York, NY, 1980.

[Roselli *et al*., 1994] Rosselli, A.T., Bronzini, M.S. and Weekly, D.A., "Computer simulation and capacity evaluation of Panama Canal alternatives", *28. International Navigation Congress*, Seville, Spain, 1994.

[Sadiq *et al*., 2003] Sadiq, R., Husain, T., Veitch, B., Bose, N., "Distribution of arsenic and copper in sediment pore water: an ecological risk assessment case study for offshore drilling waste discharges", *Risk Analysis*, **23**, no. 6, 1309-21, 2003.

[Slob, 1998] Slob, W., "Determination of risks on inland waterways", *Journal of Hazardous Materials*, **61**, no. 1-3, 363-370, 1998.

[Slob and Pieters, 1998] Slob, W., Pieters, M.N., "A probabilistic approach for deriving acceptable human intake limits and human health risks from toxicological studies: general framework", *Risk Analysis*, **18**, no. 6, 787-98, 1998.

[Steward *et al*., 1997] Stewart, M.G. and Melchers, R.E., *Probabilistic Risk Assessment of Engineering Systems*, Chapman & Hall, London, 1997

[Stiehl, 1977] Stiehl, G. L., "Prospects for Shipping Liquefied Natural Gas", *Marine Technology*, **14**, no. 4, 351-378, 1977.

[Szwed *et al*., 2006] Szwed, P., Rene Van Dorp, J., W.Merrick, J.R., Mazzuchi, T.A. and Singh, A., "A Bayesian Paired Comparison Approach for Relative Accident Probability Assessment with Covariate Information", *European Journal of Operations Research*, **169**, no. 1, 157-177, 2006.

[Talley, 1995a] Talley, W.K., "Safety investments and operating conditions: Determinants of accident passenger-vessel damage cost", *Southern Economic Journal*, **61**, 819-829, 1995.

[Talley, 1995b] Talley, W.K., "Vessel Damage Severity of Tanker Accidents", *Logistics and Transportation Review*, **31**, no. 3, 191-207, 1995.

[Talley, 1996] Talley, W.K., "Determinants of cargo damage risk and severity: The case of containership accidents", *Logistics and Transportation Review*, **32**, 377-388, 1996.

[Tan and Otay, 1998] Tan, B. and Otay, E., "A stochastic model of vessel casualties resulting from oil tanker traffic through narrow waterways", *12th European Simulation Multiconference*, 881-885, Manchester, UK, 1998.

[Tan and Otay, 1999] Tan, B. and Otay, E.N., "Modeling and analysis of vessel casualties resulting from tanker traffic through narrow waterways", *Naval Research Logistics*, **46**, no. 8, 871-892, 1999.

[Taylor *et al*., 2002] Taylor, C., Krings, A., Alves-Foss, J., "Risk Analysis and Probabilistic Survivability Assessment (RAPSA): An Assessment Approach for Power Substation Hardening", *Proc. ACM Workshop on Scientific Aspects of Cyber Terrorism*, 2002.

[Van der Tak and Spaans, 1976] Van der Tak, C. and Spaans, J.A., "Model to Calculate a Maritime Risk Criterium Number", *Navigation*, **23**, no. 4, 343-348, 1976.

[Van Dorp *et al*., 2001] Van Dorp, J.R., Merrick, J.R.W., Harrald, J.R., Mazzuchi, T.A. and Grabowski, M., "A risk management procedure for the Washington state ferries", *Risk Analysis*, **21**, no. 1, 127-142, 2001.

[Vesely *et al*., 1981] Vesely, W.E., Goldberg, F.F., Roberts, N.H. and Haasy, D.F., *The Fault Three Handbook*, US Nuclear Regulatory Commission, NUREG 0492, 1981.

[Vesper, 2006] Vesper, J.L., *Risk Assessment and Risk Management in the Pharmaceutical Industry: Clear and Simple*, PDA/DHI, 2006.

[Voortman et al., 2002] Voortman, G., van Gelder, P., Vrijling, J. K., "Risk-based design of large-scale flood defence systems", *28th International Conference on Coastal Engineering (ICCE 2002)*, 2373–2385, Cardiff, 2002.

[Wang and Rousch, 2000] Wang, J.X. and Rousch, M.L., *What every engineer should know about Risk Engineering and Management*, Marcel Dekker, 2000.

[Yudhbir and Iakovou, 2005] Yudhbir, L. and Iakovou, E., "A maritime oil spill risk assessment model", *2005 International Oil Spill Conference*, 4608-4613, Miami Beach, FL, 2005.

CURRICULUM VITA

ÖZGECAN S. ULUSÇU TÜTÜN

EDUCATION

1998-2002	UNIVERSITÉ GALATASARAY, Istanbul, TURKEY B.S., Industrial Engineering
2002-2004	RUTGERS UNIVERSITY, New Brunswick, NJ M.S., Industrial & Systems Engineering
2004-2008	RUTGERS UNIVERSITY, New Brunswick, NJ PhD, Industrial & Systems Engineering

EXPERIENCE

2003-2006	Department of Industrial and Systems Engineering, Rutgers University Teaching Assistant
2006-2007	Department of Industrial and Systems Engineering, Rutgers University Research Assistant
2005-2008	CAIT-DIMACS Laboratory for Port Security, Rutgers University Research Assistant

PUBLICATIONS

2002	Uluscu, O.S., La Proposition d'un modèle d'optimisation de la chaîne d'approvisionnement à multi échelon par la programmation linéaire (The Analysis of a Multi-Echelon Supply Chain Optimization Model using Linear Programming), Dissertation (B.S.), Université Galatasaray, Istanbul, TURKEY.
2005	Farahvash, P., O.S. Uluscu, T. Altiok and A. Santucci, VisioSim Portal: Interfacing Business Planning and Simulation Modeling, Research Paper, Department of Industrial and Systems Engineering, Rutgers University / US Army TACOM ARDEC, Picatinny Arsenal, NJ.

2007	Ulusçu, Ö. S., “Underwater Maritime Domain Awareness in the NY/NJ Harbor Complex”, Maritime Security Conference and Expo, New York, NY.
2007	Ulusçu, Ö. S., T. Altıok, “Waiting Time Approximation in Single-Class Queueing Systems with Multiple Types of Interruptions: Modeling Vessel Entrances at Waterways”, Research Paper, CAIT/DIMACS Laboratory for Port Security, Rutgers University, Piscataway, NJ.
2007	Ulusçu, Ö. S., T. Altıok, I. Or, B. Ozbas, A.O. Almaz, T. Yilmaz, “Transit Vessel Scheduling in the Istanbul Strait”, Research Paper, CAIT/DIMACS Laboratory for Port Security, Rutgers University, Piscataway, NJ.
2007	Özbaş, B., Or, İ., Altıok, T., Ö. S. Ulusçu, “A Risk Analysis Study of Maritime Traffic in the Strait of İstanbul”, Conference Program, 22nd European Conference on OR (EURO 2007), Prague, Czech Republic.
2008	Ulusçu, Ö. S., T. Altıok, “Waiting Time Approximation in Multi-Class Queueing Systems with Multiple Types of Interruptions: Modeling Vessel Entrances at Waterways”, Research Paper, CAIT/DIMACS Laboratory for Port Security, Rutgers University, Piscataway, NJ.